

***In Vitro* Exploration of Interactions
between Junctin and the Ryanodine
Receptor from Skeletal and Cardiac
Muscle**

by

Linwei Li

A thesis submitted for the degree of Doctor of Philosophy
of The Australian National University

January 2014

The John Curtin School of Medical Research
The Australian National University
Canberra
Australia



**Australian
National
University**

Statement

This thesis describes the results of research undertaken in the Muscle Research Group, Department of Molecular Bioscience, The John Curtin School of Medical Research, The Australian National University between August 2009 and January 2014. This study was supported by an Australian National University Postgraduate Research Scholarship, an Australian National University Supplementary Scholarship and an Australian National University Tuition Fee Sponsorship.

The result and analysis presented in this thesis are my own original work, accomplished under the supervision of Professor Angela Dulhunty and Assistant Professor Nicole Beard, except where otherwise acknowledged.

A handwritten signature in black ink, appearing to read 'Linwei Li', written in a cursive style.

Linwei Li

Muscle Research Group

Department of Molecular Bioscience

The John Curtin School of Medical Research

College of Medicine, Biology and Environment

The Australian National University

Acknowledgements

It is a great pleasure to express my gratitude to all those people who have supported me and make this thesis possible.

Firstly, I would like to express the deepest appreciation to the Chair of my supervisory panel, Professor Angela Dulhunty. I can't say thank you enough for her encouragement, supervision and support. Her guidance helped in all the time of research and writing the thesis. I am also heartily thankful to my co-supervisor, Assistant Professor Nicole Beard. Her good advice, support and friendship have been invaluable on both an academic and a personal level, for which I am highly grateful. Both of them have been and will always be an extraordinary influence in my life through their modesty, strong resilience, hard work, dedication and positive attitude towards life, not to mention their extensive and in depth knowledge in the field of muscle EC coupling. This growing-up experience with such strong role models became so treasurable, not only regarding research, but also in many other aspects of life. They have inspired me to become more active, independent and helped me realize the power of critical reasoning. Without their advice and understanding, the completion of this PhD would not have been possible. A special thank you goes to Angela, for her generous financial support with my medical expenses and the scholarship she kindly offered during the final stage of my study.

I would like to thank my advisor Professor Phil Board who has provided valuable comments for my project during panel meetings. I am also grateful to my ex-advisors Dr. Dan Liu and Dr. Shamaruh Mirza. I Thank Dan for combating the protein renaturing problem together with me and showing me so many experimental tricks, for encouraging and caring me, and for being a great friend. I also thank Shama for serving as my advisor during the later stages of my PhD, for showing me lab techniques and discussing with me experimental design, science as well as life in general. In addition, I would also like to thank Associate Professor Marco G. Casarotto for his advice on scrambled peptide design.

I would like to acknowledge the financial and academic support of the Australian National University, particularly in the award of a Postgraduate Research Scholarship and a Tuition Fee Sponsorship that provided the necessary financial support for the research. I also thank the John Curtin School of Medical Research for their support and assistance since the start of my PhD study, especially the ex-Safety Officer Kate Mckenzie and the HDR Coordinator Wendy Riley. Also a big thank you goes to Mr Robert Clements and Mr Luciano (Lou) Ciuffetelli, whose friendship made the life in JCSMR more enjoyable.

Many thanks to Suzy Pace and Joan Stivala for their enormous support in the lab, especially the SR vesicles and lipids they prepared which made this project possible. I thank Professor Esther

Gallant for helping me tackle the problems with the bilayers and taking efforts to solve my rig computer problem. I would like to extend huge, warm thanks to Suzy, my best friend in Australia. Words fail me to express my appreciation for her constant love, care and emotional support, for helping me get through the difficult times. I am extremely grateful for what she has done for me and the precious friendship. A special thank you also goes to Joan for her Linguistics lessons, the caring she provided and being a good friend.

I acknowledge the contribution to this project by Professor Esther Gallant (Lipid bilayer experiments), Suzy Pace (Ca^{2+} release spectrophotometric assay), Chris Thekkedam (Lipid bilayer experiments), and Umayal Narayanan (protein expression and purification, pull-down assays). I thank Dr. Yamuna Karuanssekara for her advice on primer design and help with full-length junctin purification. I also thank Dr. Lan Wei (Department of Pharmacology and Physiology, University of Rochester, New York, USA) for her valuable advice on junctin preparation over many emails despite her busy schedule during the early stage of the study. Here, I would like to extend my special big thank you to Umayal Narayanan. Her hard work, understanding and support made the late stage of thesis writing less difficult. Working together with her was such a great pleasure.

I am much indebted to Spencer Richardson and Joan Stivala for spending their precious time to edit my thesis. Thank you is just not enough to express my gratitude. I highly appreciate Robyn Rebbeck and Elize Wium for helping editing sections of my thesis.

There is no way to express how much it meant to me to have been a member of Muscle Research Group. I would like to thank all my current and previous fellow students and colleagues: Robyn, Elize, Hermia, Amy, Preeti, Maya, Spencer, Chris, Yamuna, Marie, Sally, Greg, Ruwani, Courtney, Alex, Amelina, Shama, Sadik, as well as Deepthi and Kaveenda from Molecular Genetics Group, for providing such a good atmosphere, for sharing the happy and hard moments and for their enormous support for the past four years. I would especially like to thank Robyn, Elize, Deepthi and Hermia, whose friendship I cherish so much.

My special appreciation goes to Dr. Jinglong Chen, who has always been so patient and provided so much valuable advice for my life. I would like to thank Dr. Spyros Zissimopoulos for encouraging and motivating me. I wish to thank my best friends in China, Ying Qian and Yongling Liu for their love, support and understanding. I would also like to extend warm thanks to my friends in Canberra: Guohua Xu, Shenglin Jin, Yuqi Wang, Jin Dai, and Jian Wang.

I am so grateful to Nick Laverty, the therapist of Pivotal Massage Clinic in Canberra. His expertise on physiotherapy helped me get through the hardest time of my PhD life. I can say without exaggeration that this thesis would not have been possible without his treatment. Here I

would like to thank my supervisor Angela again: it was her encouragement and support that made this all happen. I doubt that I will ever be able to convey my appreciation fully, but I owe them my eternal gratitude.

I would like to pay high regards to my family. I thank my Mum and Dad for striving hard to provide a good education for me and my siblings, for encouraging me to pursue my dreams, and for their unconditional love, tremendous support and encouragement. I could never express how grateful I am to my parents. My sister Nana, the best sister in the world, has been always thinking of me and supporting me, and has spent so much time and effort getting me medical supplies, with more than 4000 patches over the past two years to help me fight the disease. I cannot say thank you enough, my dear sister. I also thank my brother Linfeng and my sister-in-law Fangli for being supportive and sharing family stories. A huge thank you goes to my nephew Shaolin and niece Shaoting, whose sweet voices are a great joy to me and always cheer me up. I would like to thank Ben for his support and understanding for the last year, and for his encouragement despite the long distance between us.

Last but not least, I would like to remember and thank my grandma, whom I miss so much and dream of so often. She did not wait long enough to see me finish, but I know she is always with me and watching over me in the other world. Thanks Grandma!

Abstract

Muscle contraction is dependent on a large Ca^{2+} release from its intracellular Ca^{2+} store, the sarcoplasmic reticulum (SR), through ryanodine receptor Ca^{2+} release channels (RyRs). In the resting state, striated muscle requires a tight control of Ca^{2+} release through RyRs. Another SR bound protein, junctin, is thought to facilitate this. Located in both skeletal and cardiac muscle, junctin has a short N-terminal domain (Njun) and bulky, highly charged C-terminal domain (Cjun), that are exposed to the cytoplasm and SR lumen respectively. Although originally thought to function as a linker between the SR calcium binding protein (calsequestrin) and RyRs, recent studies suggest the junctin may have a more complex role in regulating RyR activity and SR Ca^{2+} handling. *In vitro* studies have shown that addition of full-length junctin (FLjun) to the luminal domain of RyR directly activates RyR in lipid bilayers. However, the molecular mechanism by which junctin regulates RyR activity has been unclear.

To explore the specific regions of junctin that regulate RyR, constructs corresponding to Njun, Cjun and FLjun were produced. Modified co-immunoprecipitation and affinity chromatography were employed to evaluate the direct interactions between junctin constructs and purified RyR. Both Cjun and Njun bound to the full-length RyRs. The effect of the junctin constructs on RyR1 (skeletal isoform) or RyR2 (cardiac isoform) activity was tested in lipid bilayer experiments with 1 mM luminal $[\text{Ca}^{2+}]$ to replicate resting conditions. As found previously, addition of FLjun to the luminal solution increased both RyR1 and RyR2 activity by ~2-3-fold. Curiously, luminal addition of Cjun strongly inhibited both RyR1 and RyR2, whereas cytoplasmic addition of Njun significantly increased RyR1 and RyR2 activity by ~5-6-fold. This was unexpected as the RyR-junctin interaction was assumed to occur only lumenally. Neither luminal addition of Njun nor cytoplasmic addition of the scrambled Njun sequence altered channel activity, suggesting a specific cytoplasmic effect of Njun. This suggestion was further substantiated as cytoplasmic Njun did not change the activity of native RyRs that retained endogenous junctin. Sequential addition of Njun to the cytoplasmic solution and Cjun to the luminal solution resulted in channel activity increasing by ~2-3-fold, as observed with luminal addition of FLjun. On the other hand, the RyR inhibition induced by luminal addition of Cjun was not altered by subsequent addition of Njun to the cytoplasmic solution.

The functional region of Cjun was localized to residues 85-106 that contain a KEKE motif, as luminal addition of a peptide corresponding to this region replicated the inhibitory effect of Cjun.

In conclusion, the study demonstrates that junctin regulates RyR1 and RyR2 via interactions in both the cytoplasm and SR lumen, the combined actions of Njun and Cjun indicate that the

novel cytoplasmic Njun-RyR interaction must be established before the luminal Cjun-RyR interaction to replicate the FLjun modulation of RyR1 and RyR2 activity.

Publications

Dulhunty AF, Wium E, **Li L**, Hanna AD, Mirza S, Talukder S, Ghazali NA, Beard NA (2012). Proteins within the intracellular calcium store determine cardiac RyR channel activity and cardiac output. *Clinical and Experimental Pharmacology and Physiology*, May;39(5):477-84

Selected Conference Abstracts

Australian Physiological Society

Li, L., Mirza, S., Beard N.A., Dulhunty, A.F.

In vitro characterization of interactions between junctin and ryanodine receptors
Geelong, Australia 12/2013.

Gage Conference on Ion Channels and Transporters

Li, L., Mirza, S., Beard N.A., Dulhunty, A.F.

In vitro exploration of cytoplasmic and luminal domain interactions between junctin and RyR1 or RyR2
Canberra, Australia 04/2013

Biophysical Society 57th Annual Meeting

Li, L., Mirza, S., Beard, N.A., Dulhunty, A.F.

A cytoplasmic interaction between junctin and RyRs with major consequences for RyR1 and RyR2 activity *in vitro*
Philadelphia, Pennsylvania, USA 02/2013

Biophysical Society 57th Annual Meeting

Mirza, S., Li, L., Beard, N.A., Dulhunty, A.F.

Different modes of interaction between junctin and ryanodine receptors
Philadelphia, Pennsylvania, USA 02/2013

Gordon Research Conference on Muscle Excitation-Contraction Coupling

Li, L., Beard N.A., Dulhunty, A.F.

In vitro characterization of interactions between junctin and ryanodine receptor (RyR1/ RyR2)
Les Diablerets, Switzerland 06/2012.

Gage Conference on Muscle

Li, L., Beard N.A., Dulhunty, A.F.

Characterization of interactions between junctin and ryanodine receptor (RyR1/RyR2) *in vitro*
Canberra, Australia, 04/2012.

Gage Conference on Ion Channels and Transporters

Li, L., Beard N.A., Dulhunty, A.F.

In vitro interactions between the C-terminus of junctin and RyR1/RyR2

Canberra, Australia 04/2011.

Gage Conference on Muscle

Wei, L., Wium, E., Li, L., Janczura, M., Dulhunty, A.F., Beard N.A.

Triadin and Junctin – not just luminal anchoring proteins

Canberra, Australia 04/2010

Abbreviations

[³ H]ryanodine	tritiated ryanodine
AEBSF	4-(2-Aminoethyl)-benzenesulfonyl fluoride hydrochloride
ADP	adenosine diphosphate
AMP	adenosine monophosphate
ATP	adenosine 5' triphosphate
APS	ammonium persulfate
BAPTA	1,2-bis(2-aminophenoxy)ethane-N,N,N',N'-tetra-acetic acid
BSA	bovine serum albumin
C	capacitance
CaM	calmodulin
CHAPS	3-[3-Cholamidopropyl]dimethylamino]-1-propane-sulfonate
CICR	Ca ²⁺ -induced Ca ²⁺ release
CRU	calcium release unit
CSQ	calsequestrin
DHPR	dihydropyridine receptor
DTT	dithiothreitol
EC coupling	excitation-contraction coupling
ECL	enhanced chemoluminescence
<i>E. coli</i>	<i>Escherichia coli</i>
EDTA	ethylenediaminetetraacetic acid
EGTA	ethylene glycol-bis(β-aminoethyl ether) N,N,N',N'-tetraacetic acid

FKBP	FK-506 binding protein
H	hour
HRC	Histidine-rich Ca^{2+} binding protein
HRP	horseradish peroxidase
I	current
I'	mean current
I_{max}	maximal current
I'_F	fractional mean current
IMAC	Immobilized Metal Affinity Chromatography
IP ₃ R	Inositol 1,4,5-trisphosphate receptor
IPTG	Isopropyl β -D-1-thiogalactopyranoside
JFM	junctional face membrane
jSR	junctional sarcoplasmic reticulum
kDa	kilodalton
Min	minute
MOPS	3-[N-Morpholino]propanesulfonic acid
MS	methane sulfonate
NCX	$\text{Na}^+/\text{Ca}^{2+}$ exchanger
OD	optimal density
PAGE	polyacrylamide gel electrophoresis
PBS	phosphate buffered saline
PC	phosphatidylcholine

PE	phosphatidylethanolamine
PEG	polyethylene glycol
PIPES	piperazine-N,N'-bis(2-ethanesulfonic acid)
PMSF	phenylmethylsulfonyl fluoride
P_o	open probability
PS	phosphatidylserine
PVDF	polyvinylidene difluoride
RyR	ryanodine receptor
SDS	sodium dodecyl sulfate
SDS-PAGE	sodium dodecyl sulfate polyacrylamide gel electrophoresis
SERCA	sarcoplasmic/endoplasmic reticulum Ca^{2+} ATPase
SOCE	store-operated Ca^{2+} entry
SR	sarcoplasmic reticulum
TA	the transmembrane assembly (of RyR)
TC	terminal cisternae
TEMED	N,N,N,N-Tetramethylethylenediamine
TES	N-Tris[hydroxymethyl]methyl-2-aminoethanesulfonic acid
T_c	mean closed time
τ_c	closed time constant
T_o	mean open time
τ_o	open time constant
TPBS	tween 20-supplemented phosphate-buffered saline

TRIS	tris-[hydroxymethyl]aminomethane
T-tubule	transverse tubule
V	voltage
VICR	voltage-induced Ca^{2+} release
WT	wild-type

Table of Contents

Chapter 1 Introduction and background.....	1
1.1 Overview of muscle tissue	1
1.2 Striated muscle and muscle fiber anatomy	2
1.2.1 Skeletal muscle	2
1.2.1.1 Skeletal muscle anatomy.....	2
1.2.1.2 Sarcoplasmic Reticulum (SR) and T (Transverse) –tubules in skeletal muscle fiber.....	5
1.2.2 Cardiac muscle.....	6
1.3 Major components and anatomy of the calcium release units (CRUs).....	8
1.4 Excitation contraction coupling	11
1.4.1 Overview.....	11
1.4.2 Mechanism of EC coupling.....	11
1.5 Sarcolemmal and SR Ca ²⁺ fluxes during muscle twitch	13
1.6 Ryanodine receptor Ca ²⁺ release channel (RyR).....	14
1.6.1 RyR genes, isoforms and distribution	15
1.6.2 RyR structure	16
1.6.2.1 Cytoplasmic assembly.....	17
1.6.2.2 Transmembrane assembly.....	18
1.6.3 Transmembrane segments and pore forming region	20
1.6.3.1 Transmembrane topology of RyR.....	20
1.6.3.2 Pore forming region	21
1.6.4 Ion selectivity and conductance	22
1.6.5 RyR regulation	25
1.6.5.1 RyR modulation by main regulatory ligands	25
1.6.5.2 RyR interaction with luminal proteins	31
1.7 CSQ.....	31
1.7.1 CSQ gene, isoforms	32
1.7.2 CSQ structure and Ca ²⁺ -binding properties.....	32
1.7.3 CSQ function	34
1.7.3.1 Changes in CSQ expression in genetic mice models and myocytes.....	34
1.7.3.2 CSQ polymorphism.....	38
1.7.3.3 Effects of CSQ on RyR channel activity revealed by lipid bilayers study	39
1.8 Triadin.....	40
1.8.1 Gene and isoform	41

1.8.2 Primary and secondary structure, KEKE motif	42
1.8.3 Post-translational modification	42
1.8.3.1 Disulfide bond formation	42
1.8.3.2 Glycosylation	43
1.8.3.3 Phosphorylation	43
1.8.4 Over-expression and down-regulation	44
1.8.4.1 Over-expression	44
1.8.4.2 Down-regulation	45
1.8.5 Protein-protein interactions	46
1.8.5.1 Triadin-DHPR	47
1.8.5.2 Triadin-RyR	47
1.8.5.3 Triadin-CSQ	48
1.8.5.4 Other protein-protein interactions (junctin, HRC)	49
1.9 Junctin	49
1.9.1 Junctin gene, structure, isoform	50
1.9.2 Junctin homology, KEKE motif	51
1.9.3 Junctin changes in the developing heart	52
1.9.4 Overexpression and down-regulation of junctin	52
1.9.4.1 Cardiac junctin modulation	52
1.9.4.2 Skeletal junctin ablation	54
1.9.5 Junctin and diseases	55
1.9.6 Junctin protein/protein interaction	56
1.9.6.1 Junctin and RyR (binding, regulation)	56
1.9.6.2 Junctin, CSQ, and triadin	58
1.9.6.3 Other interactions (possible interactions)	60
1.10 Project aims	61
Chapter 2 Materials and Methods	63
2.1 Materials	63
2.1.1 Reagents and Chemicals	63
2.1.2 Peptides synthesized	63
2.3 SR vesicle isolation and RyR purification	64
2.3.1 Isolation of skeletal and cardiac SR vesicles	64
2.3.1.1 Preparation of skeletal muscle RyR-enriched SR vesicle	64
2.3.1.2 Cardiac crude SR preparation	65
2.3.2 Purification of RyR1 and RyR2	66
2.4 Recombinant RyR1 and RyR2 preparation	67

2.4.1 RyR1 preparation	67
2.4.1.1 RyR1 plasmid construction	67
2.4.1.2 Expression and purification of recombinant RyR1 constructs	67
2.4.2 RyR2 preparation	68
2.4.2.1 RyR2 construct	68
2.4.2.2 Expression and purification of recombinant RyR2 mutant	68
2.5 Junctin purification	68
2.5.1 Endogenous junctin purification from rabbit skeletal muscle (SDS preparative gel electrophoresis)	69
2.5.2 Recombinant canine cardiac full-length junctin (FLjun)	70
2.5.2.1 Plasmid construction	70
2.5.2.2 Expression and purification of recombinant FLjun by IMAC (Immobilized metal affinity chromatography)	70
2.5.3 Recombinant canine cardiac junctin C-terminus (Cjun) with His-tag	71
2.5.3.1 Plasmid construction	71
2.5.3.2 Expression and purification of recombinant 6xHis-Cjun by IMAC	72
2.5.4 Recombinant canine cardiac junctin C-terminus (Cjun) without His-tag	72
2.5.4.1 Plasmid construction	73
2.5.4.2 Expression, purification and His-tag cleavage of recombinant Cjun	73
2.6 Electrophoresis and immunoblot	74
2.6.1 SDS-Polyacrylamide Gel Electrophoresis (PAGE)	74
2.6.2 Protein stains	74
2.6.2.1 Coomassie Brilliant Blue	74
2.6.2.2 Silver Stain	75
2.6.3 Gel drying	75
2.6.4 Immunoblot	75
2.6.4.1 PVDF membrane transfer	76
2.6.4.2 Immuno-detection	76
2.6.4.3 Visualization (SuperSignal Chemiluminescence)	76
2.6.5 Protein densitometry	77
2.7 Protein determination	77
2.7.1 BCA protein assay	77
2.7.2 Protein A280	77
2.8 Protein binding assay	78
2.8.1 Modified Co-Immunoprecipitation (Co-IP)	78
2.8.1.1 Co-IP precipitation of junctin by RyR	78
2.8.1.2 RyR precipitation by junctin co-IP	79

2.8.2 NeutrAvidin agarose affinity chromatography	79
2.9 Artificial Planar lipid bilayers	80
2.9.1 Overview of lipid bilayer system set up	80
2.9.2 Lipid bilayer formation and vesicle incorporation	81
2.9.3 Lipid bilayer experimental solutions	81
2.9.4 Channel recording.....	82
2.9.5 Single Channel analysis.....	83
2.10 Ca ²⁺ release from skeletal and cardiac SR vesicles	84
2.10.1 Njun/Cjun induced Ca ²⁺ release from SR vesicles	85
2.10.2 Ca ²⁺ release from SR vesicles pre-incubated with Njun/Cjun.....	86
2.10.3 Data analysis—calculation of rate of Ca ²⁺ release from SR vesicles	86
2.11 Statistics.....	87
Chapter 3 Full length junctin interacts with purified RyR1 and RyR2 channels	88
3.1 Introduction	88
3.2 Methods	89
3.2.1 Methods overview	89
3.2.2 SR vesicle isolation and RyR purification.....	89
3.2.3 Junctin purification.....	89
3.2.3.1 Endogenous junctin purification from rabbit skeletal muscle	89
3.2.3.2 Recombinant canine cardiac FLjun	90
3.2.4 Modified co-IP between FLjun and RyR1 and RyR2	90
3.2.5 Single channel recording and analysis.....	90
3.3 Results	91
3.3.1 General properties of RyR1 and RyR2.....	91
3.3.1.1 General observations	91
3.3.1.2 General RyR characteristics	92
3.3.1.3 Regulation of purified RyR1 and RyR2 by characterized ligands.....	94
3.3.2 Purification of full length junctin (FLjun).....	96
3.3.2.1 Endogenous junctin purification from muscle.....	96
3.3.2.2 Recombinant FLjun expression and purification.....	98
3.3.3 Physical interactions between FLjun and RyR1 and RyR2	100
3.3.4 Purified RyR1/2 regulation by FLjun (luminal interaction).....	101
3.3.4.1 The effect of FLjun on purified RyR1 or RyR2 activity	101
3.3.4.2 Changes in RyR1/RyR2 channel gating properties induced by FLjun re-association.	103
3.3.5 <i>Cis</i> FLjun does not alter purified RyR1 or RyR2 activity	107

3.4 Discussion	107
3.4.1 Muscle FLjun purification	108
3.4.2 Recombinant FLjun from <i>E.coli</i>	109
3.4.3 Luminal FLjun is a potent activator of purified RyR1 and RyR2	109
3.4.4 Limitations	111
3.4.5 Conclusion	111
Chapter 4 Modulation of RyR1/2 activity by the C-terminal domain of junctin	113
4.1 Introduction	113
4.2 Materials and Methods	113
4.2.1 Methods overview	113
4.2.2 SR vesicle isolation and RyR purification	114
4.2.3 Recombinant canine cardiac Cjun	114
4.2.4 Modified co-IP between Cjun and RyR1 and RyR2	114
4.2.5 Single channel recording and analysis	115
4.2.6 Ca ²⁺ release from skeletal and cardiac SR vesicles	115
4.2.6.1 Cjun induced Ca ²⁺ release from SR vesicles	115
4.2.6.2 Pre-incubation of SR vesicles with Cjun	115
4.3 Results	115
4.3.1 Expression and purification of Cjun	115
4.3.2 Physical interaction—Cjun binds to purified RyR1 and RyR2	116
4.3.3 Functional effect of Cjun on RyR1/2	117
4.3.3.1 The effect of luminal addition of Cjun on purified RyR1 or RyR2 activity	117
4.3.3.2 Cytoplasmic interaction between Cjun and RyR1/RyR2	122
4.4 Discussion	124
4.4.1 Cjun expression and purification	124
4.4.2 Cjun in the luminal solution is a potent inhibitor of purified RyR1 and RyR2 channels	129
4.4.3 The significance of cytoplasmic interaction of Cjun and the RyRs	130
4.4.4 Conclusion	130
Chapter 5 The N-terminal domain of junctin modulates RyR1 and RyR2 activity	131
5.1 Introduction	131
5.2 Materials and Methods	131
5.2.1 Methods overview	131
5.2.2 RyR preparation	132
5.2.3 Affinity chromatography between Njun peptide and RyR1 and RyR2	133

5.2.4 Single channel recording and analysis.....	133
5.2.5 Ca ²⁺ release from skeletal and cardiac SR vesicles	133
5.2.5.1 Njun induced Ca ²⁺ release from SR vesicles	133
5.2.5.2 Pre-incubation of SR vesicles with Njun.....	133
5.3 Results	134
5.3.1 Physical interaction between Njun and expressed RyR1 or RyR2	134
5.3.2 <i>Cis</i> Njun activates purified RyR1 and RyR2 activity	134
5.3.3 <i>Cis</i> scrambled Njun or <i>trans</i> Njun does not alter purified RyR1 or RyR2 activity ..	139
5.3.4 No effect of Njun on native RyR1 or RyR2	139
5.3.4.1 No effect of cytoplasmic addition of Njun on native RyR1/2 activity	140
5.3.4.2 Effect of Njun on Ca ²⁺ release from SR vesicles.....	141
5.3.5 Combined effects of Cjun and Njun on purified RyR1 and RyR2 channels	143
5.4 Discussion.....	149
5.4.1 Njun binds to the purified RyR.....	149
5.4.2 Cytoplasmic Njun modulates purified RyR1 and RyR2 channel activity	150
5.4.3 Njun plays a dominant role in FLjun regulation of the RyR	151
5.4.4 Conclusion.....	154

Chapter 6 Localization and characterization of a RyR interacting domain in junctin..155

6.1 Introduction	155
6.2 Materials and Methods	156
6.2.1 Methods overview	156
6.2.2 RyR preparation.....	156
6.2.3 Affinity chromatography	156
6.2.4 Single channel recording and analysis.....	156
6.3 Results	157
6.3.1 Identification of RyR1 binding residues in Cjun	157
6.3.1.1 Physical interaction between KEKE motif and RyR1/2	157
6.3.1.2 Functional effect of Jun _{KEKE} on purified RyR1 and RyR2 (luminal).....	158
6.4 Discussion.....	160
6.4.1 The KEKE motif of junctin binds to and regulates purified RyR	161
6.4.1.1 A RyR-binding site on junctin – the KEKE motif.....	161
6.4.1.2 KEKE motif exerts an inhibitory effect on purified RyR, similar to that seen in Cjun luminal effect.	161
6.4.1.3 Species-independence of junctin KEKE motif regulation of the RyRs	162
6.4.2 Rationale for using the KEKE motif peptide from different species	162
6.4.3 Limitations.....	163

6.4.4 Conclusion	163
Chapter 7 General Discussion.....	165
7.1 Distinct functional consequences of Njun and Cjun association with RyRs	166
7.1.1 The significance of Njun interaction with RyRs.....	166
7.1.2 Implication of Cjun as a channel inhibitor.....	167
7.2 Similar actions of junctin on RyR1 and RyR2.....	167
7.2.1 Implication of the similar actions in CSQ/junctin/RyR interaction	168
7.3 Implications of multiple interacting domains between RyRs and junctin	169
7.4 Interplay between triadin/junctin/CSQ/RyR in skeletal and cardiac muscle	170
7.5 Conclusion	173
7.6 Future directions	173
References.....	175

Chapter 1 Introduction and background

1.1 Overview of muscle tissue

Unless otherwise stated, the material in section 1.1 and 1.2 is sourced from (Marieb and Hoehn, 2007).

The cells of muscle tissues exhibit a unique functionality in their ability to contract. Muscle cells, or myocytes – and consequently, muscle tissues and whole muscles – can shorten to produce a net movement. Muscle tissues are classified as striated muscle or smooth muscle according to the organization of their cytoskeletal components and the gross cellular organization of the tissue. If the cytoskeletal components of the cells are arranged in a manner which produces striations – transverse stripes – visible under light microscopy, then the muscle tissue is classified as striated muscle. This striated appearance comes from the tissues' characteristic arrangement of actin and myosin filaments. Both skeletal and cardiac muscles exhibit this striated phenotype. Should the cytoskeletal components have a non-striated appearance, the muscle then is classified as non-striated or smooth muscle. Thus, muscle tissue can be described as being one of three different types:

- Skeletal muscles anchored by tendons (or by aponeuroses at a few locations) to bones, and are under conscious control, or are activated by reflex. Skeletal muscle is also called voluntary muscle, because it is the sole muscle type subject to conscious control. It is responsible for overall body mobility, including walking and running, as well as more subtle movements such as those that compose facial expressions etc. In addition, contraction of skeletal muscles also fulfils other functions, such as the maintenance of posture and the production of heat. Skeletal muscle contracts with high force and high speed; however, it fatigues easily and cannot sustain contraction for long periods of time. Skeletal muscle cells are long, multinucleated, cylindrical and heavily striated, and are normally referred to as fibers.
- Cardiac muscle is a specialized striated muscle found only in the heart and at the cardiac ends of the main blood vessels. It constitutes the bulk of the heart wall tissue. It is capable of long-lasting activity, and over a human lifespan may sustain more than two billion contractions without a pause. Unlike skeletal muscle fibers, the elongated cardiac cells, or cardiomyocytes, are short, branching cells and uninucleate (1-2) with light striations, and cannot be controlled consciously. Cardiac muscle contracts rhythmically and intrinsically (without external stimulation), providing the fundamental rhythm of the heartbeat, although neural controls may vary the heart rate for brief periods.

- Smooth muscle is found in the walls of blood vessels, in the intestine, and in the urinary and reproductive tracts. The long spindle-shaped cells have a single nucleus and associate to form muscle patterns appropriate to their function. For example, an annular arrangement in blood vessels, or a criss-cross network in the bladder. One of smooth muscle's key functions is to maintain the flow of fluids and foods along its hollow structures. The tissue type is referred to as smooth because it does not have the striations characteristic of other muscle types, and hence is smooth in appearance. Smooth muscle cannot be controlled consciously and thus acts involuntarily. Contractions of smooth muscle are slow, rhythmic and sustained. Because the main focus of this thesis is on striated muscle, further details of smooth muscle will not be discussed.

1.2 Striated muscle and muscle fiber anatomy

1.2.1 Skeletal muscle

1.2.1.1 Skeletal muscle anatomy

An individual skeletal muscle is considered an organ of the muscular system. Each muscle consists of skeletal muscle tissue, connective tissue, nerve tissue, and blood or vascular tissue. An individual skeletal muscle may be made up of hundreds, or even thousands, of muscle fibers bundled together and wrapped and held in position by connective tissue sheaths. These connective tissue coverings provide support and protection for the delicate cells and allow them to withstand the forces of contraction. Each individual muscle fiber is surrounded by a fine sheath of connective tissue, the endomysium. The endomysium-wrapped muscle fibers are collected into bundles, or fascicles, themselves covered by a layer of connective tissue or perimysium. Many bundles, or fasciculi, are wrapped in an "overcoat" of dense irregular connective tissue (epimysium) to form a whole muscle (Fig. 1-1).

Each skeletal muscle fiber (Fig. 1-1; and Fig. 1-2A), or myofiber, is a single cylindrical cell, long and narrow, and acts independently of its neighboring muscle fibers. Fiber diameters typically range between 10 to 100 μm , and they may be exceedingly long, with the longest myofibers of the thigh being up to 30 cm.

The cytoplasm of skeletal muscle fibers, the sarcoplasm, contains large amounts of glycosomes and myoglobin. Embedded in this sarcoplasm and running lengthwise through it are myofibrils (Fig. 1-2B), which are cylindrical bundles of contractile proteins. Each myofibril is ~ 1 to 2 μm in diameter. Muscle fibers usually contain hundreds to thousands of myofibrils that contain the contractile elements of the muscle cells. A surface lipid bilayer membrane, the sarcolemma (Fig. 1-2B; also see Fig. 1-3), encloses the sarcoplasm, multiple nuclei, and many mitochondria.

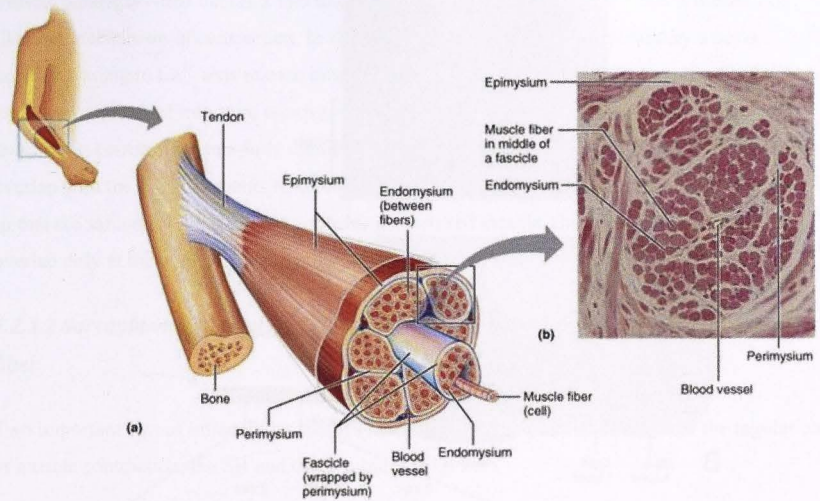


Figure 1-1 Skeletal muscle anatomy (Marieb and Hoehn, 2007).

As stated previously, skeletal muscle fibers appear striated (Fig. 1-2A). The striations consist of dark A bands and light I bands, repeating along the length of each fiber. Within each A band is a central light area, the H zone or H band, containing a central dark line, the M line. The I bands also have a midline interruption, a darker area called the Z disc or Z line. The region between adjacent Z lines is referred to as a sarcomere, each of which contains an A band flanked by half an I band (Fig. 1-2B&C). On average the 2 μm long sarcomere forms the basic contractile unit of a muscle fiber.

Located within sarcomeres are regularly arranged thin and thick filaments which give a myofibril its banding pattern (Fig. 1-2C&D). The thin filaments (7-8 nm thick) are made up mainly of the protein actin, complexed with troponin and tropomyosin. They extend from the I band into the A band, ending at the start of the H zone and are essentially inert and serve as “ratchets” upon which force can be exerted to drag together the Z discs. In vertebrate muscle, the thin filaments are arranged in hexagonal array on two Z discs: each sarcomere has a number of these arrays. Inside each hexagonal “cage” formed by the six thin filaments is a thick filament (Fig. 1-2E). The thick filaments (about 16 nm in diameter) contain primarily myosin and extend the entire length of the A band. They are connected to adjacent Z lines by very thin, elastic strands of titin. The thick filaments have long, fibrous tails and globular heads, the latter binding to actin in order to do the actual work of contraction. Their myosin heads also bind to ATP, which is the source of energy for muscle movement.

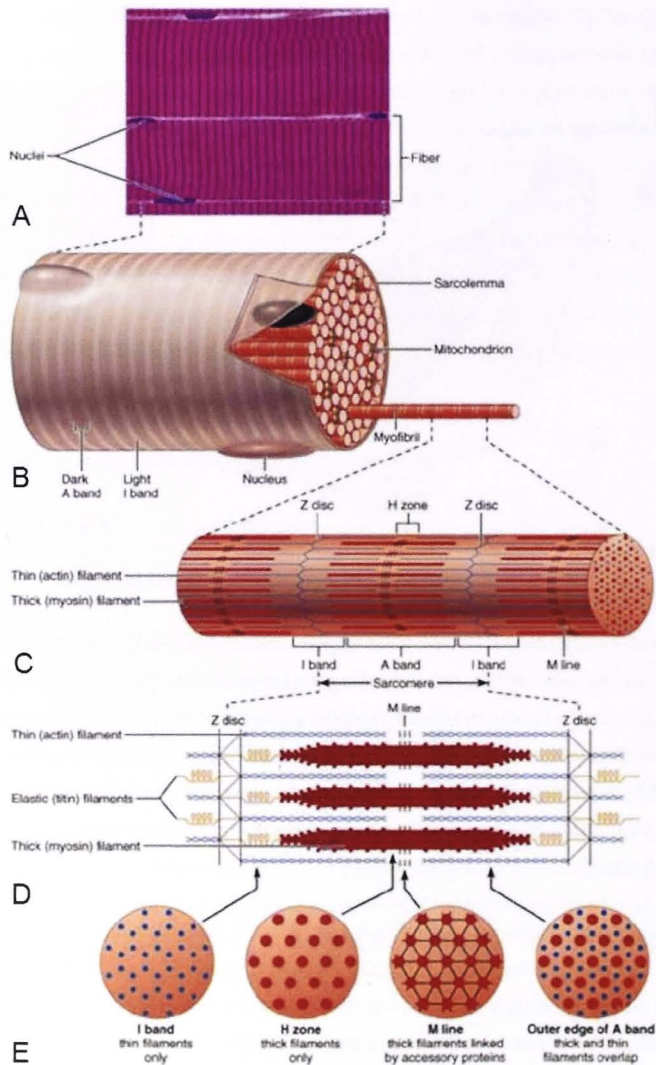


Figure 1-2 Microscopic anatomy of a skeletal muscle fiber. (A) Photomicrograph of portions of two isolated muscle fibers (700 \times). (B) Diagram of part of a muscle fiber showing the myofibrils. One myofibril extends from the cut end of the fiber. (C) A small portion of one myofibril enlarged to show the myofilaments responsible for the banding pattern. Each sarcomere extends from one Z disc to the next. (D) Enlargement of one sarcomere (sectioned lengthwise). Notice the myosin heads on the thick filaments. (E) Cross-sectional view of a sarcomere cut through in different areas. (Marieb and Hoehn, 2007)

Muscle contracts when the thick and thin filaments slide past each other – this is the sliding filament mechanism of contraction. In skeletal muscle, contraction is initiated by a nerve impulse leading to Ca^{2+} ions release into the myofibril. Binding of Ca^{2+} to troponin-C (TnC), the regulatory subunit of troponin, removes troponin's inhibitory effect on actin and myosin and thus allows contraction. In a fully contracted sarcomere the thick and thin filaments maximally overlap with the thick filaments reaching the Z line and the thin filaments reaching the M line, so that the sarcomere shortens. By contrast, in a relaxed muscle, the thick and thin filaments overlap only at the ends of the A band (Guyton and Hall, 2006).

1.2.1.2 Sarcoplasmic Reticulum (SR) and T (Transverse) -tubules in skeletal muscle fiber

Two important sets of intracellular tubules in skeletal muscle fibers participate in the regulation of muscle contraction, the SR and the T-tubules (Fig. 1-3).

The SR is a specialized endoplasmic reticulum, an entirely intracellular membrane bounded compartment which is not continuous with the sarcolemma. Most of these tubules run longitudinally along the myofibril and are thus termed longitudinal SR (ISR); these are important for Ca^{2+} sequestration, though not EC coupling. Other tubules form larger, perpendicular compartments at the A:I band junctions, called terminal cisternae or junctional SR (jSR). The main function of the SR in muscle is to regulate intracellular levels of ionic calcium by storing Ca^{2+} and releasing it to the myoplasm on demand. The terminal cisternae are the site of Ca^{2+} release from the SR and accommodate many crucial proteins and regulators of excitation-contraction (EC) coupling, including the ryanodine receptor (RyR) Ca^{2+} release channels. The SR in skeletal muscle is very highly organized. Except for the junctions between the SR and sarcolemma, the SR membrane appears fairly homogeneous (Bers, 2002).

At the junctions of the A and I bands, tube-like extensions of the sarcolemma called transverse-tubules or T-tubules enter the sarcoplasm and are aligned with the terminal cisternae of the SR. The lumen of the T-tubules is continuous with the extracellular space. They are termed “transverse” because they run perpendicular to the long axis of the fiber. The T-tubules branch extensively inside the sarcoplasm, which allows each sarcomere to be encircled by two T-tubules. The arrangement of the T-tubule network ensures that no part of the cytoplasm is more than $\sim 1 \mu\text{m}$ away from the nearest T-tubule, thus permitting the depolarization signal to propagate, virtually simultaneously, throughout the cell such that every myofibril in the muscle fiber contracts at the same time (Dulhunty, 2006). The T-tubules lie close to the ends of the terminal cisternae. This part of terminal cisternae membrane is termed the junctional face membrane (JFM). In skeletal muscle, most of the T-tubule membrane is involved in junctional, triadic complexes with the SR. The “triad” refers to the coupling of two SR terminal cisternae to

either side of a T-tubule (Fig. 1-3, right panel). Contained in the T-tubule are the voltage-sensitive dihydropyridine receptors (DHPRs), one of the key proteins involved in EC coupling, as well as many other proteins involved in the transmission of regulatory second messenger pathways (Brette and Orchard, 2003).

It is of physiological importance for EC coupling (see section 1.4) that the T-tubules are positioned close to the terminal cisternae of the SR, as this arrangement allows for physical and functional contact between DHPRs and RyRs. Thus, an action potential propagating along the sarcolemma activates DHPRs which cause RyRs calcium channels in the terminal cisternae to open, which in turn enables Ca^{2+} release from the SR into the cytoplasm and causes the intracellular $[Ca^{2+}]$ to increase.

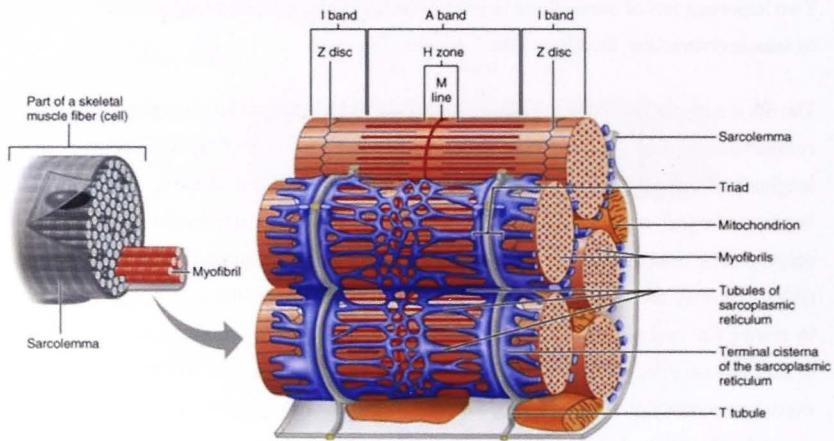


Figure 1-3 Schematic diagram of sarcoplasmic reticulum and T-tubular network of skeletal muscle (Marieb and Hoehn, 2007).

1.2.2 Cardiac muscle

Cardiac muscle, like skeletal muscle, appears striated and it too contracts via the sliding filament mechanism. However, in contrast to the long, cylindrical, and multinucleate skeletal muscle fibers, the cardiomyocytes (cardiac myocytes) are short, fat, branched, and interconnected. Each fiber contains one or at most two large, pale, centrally located nuclei (Fig. 1-4A). Cardiac myocytes are typically $< 20 \mu\text{m}$ in diameter, whereas the diameter of skeletal muscle fibers (section 1.2.1.1), can be up to $100 \mu\text{m}$.

Unlike skeletal muscle fibers, which are independent of one another both structurally and functionally, the plasma membranes of adjacent cardiac cells interlock at dark-staining junctions or intercalated discs (Fig. 1-4), thereby enabling adjacent myocytes to contract co-ordinately. These discs contain intermediate junctions, desmosomes, and gap junctions (Fig. 1-4B top right panel). The intermediate junctions and desmosomes are of central importance in the mechanical connection of one cell to the next, preventing adjacent cells from separating during contraction. Gap junctions are located predominantly on parts of the intercalated disk parallel to the long axis of the cell. They are low resistance electrical pathways that specifically allow action potentials to spread in the myocardium by permitting the passage of ions between cells, thereby transmitting depolarization across the entire heart. Because cardiac cells are electrically coupled by the gap junctions, the myocardium behaves as a single coordinated unit, or functional syncytium. This allows the chambers of the heart to contract and pump blood in a highly synchronous and coordinated manner (Guyton and Hall, 2006).

Approximately 25-35% of the volume of cardiac cells is occupied by large mitochondria, a much higher fraction than is found in skeletal muscle (~2%). This gives cardiac cells a high resistance to fatigue. Sarcomeres account for most of the remaining cell volume. The sarcomeres in cardiomyocytes have Z discs, A bands, and I bands similar to those found in skeletal muscle, reflecting the arrangement of the thick (myosin) and thin (actin) filaments (Fig. 1-4B bottom right panel). However, in contrast to skeletal muscle, the cardiac myofibrils vary considerably in diameter and branch extensively, accommodating abundant mitochondria between them. This produces a banding pattern less distinctive than that seen in skeletal muscle.

Notably, the system for delivering Ca^{2+} is less elaborate in cardiac muscle cells. In contrast to the extensive and well organized SR networks with large terminal cisternae (TC) abutting narrow T-tubules found in skeletal muscle, the SR systems in cardiac muscle are typically simpler, more sparse, and less rigid organized, with smaller TC at the cell surface and at junctions (Fig. 1-4B). Cardiac T-tubules are much wider (200 nm in heart vs. 30-40 nm in skeletal muscle) and fewer in number than in skeletal muscle. In contrast to skeletal muscle, T-tubules enter the cells once per sarcomere at the Z discs. The larger volume:surface ratio in cardiac muscle T-tubules allows a given ion flux across the membrane to produce smaller depletions and accumulations of ions. The T-tubule membrane is normally apposed to a single TC (forming a dyad; Fig. 1-4B bottom right panel), where the TC may wrap around the T-tubule. Peripheral couplings are also formed, in which a junction of the jSR is apposed to the surface sarcolemma. Occasionally a triad is present, but with a different appearance from the skeletal muscle triad due to the wide lumen of the T-tubule and narrower TC. Despite different architecture, in both skeletal and cardiac muscle, triads, dyads and peripheral couplings are broadly structurally and functionally equivalent. Collectively, these intracellular junctions are

termed EC coupling units, couplons or calcium release units (CRUs) (Franzini-Armstrong et al., 1998, 1999), and are the *loci* where the excitation-contraction (EC) coupling mechanism takes place (Schneider and Chandler, 1973). Additionally, special CRUs occur in the cardiac muscle, constituted by jSR domains bearing RyRs that are not associated with either exterior membranes (corbular or extended junctional SR, EjSR) (Franzini-Armstrong et al., 1999).

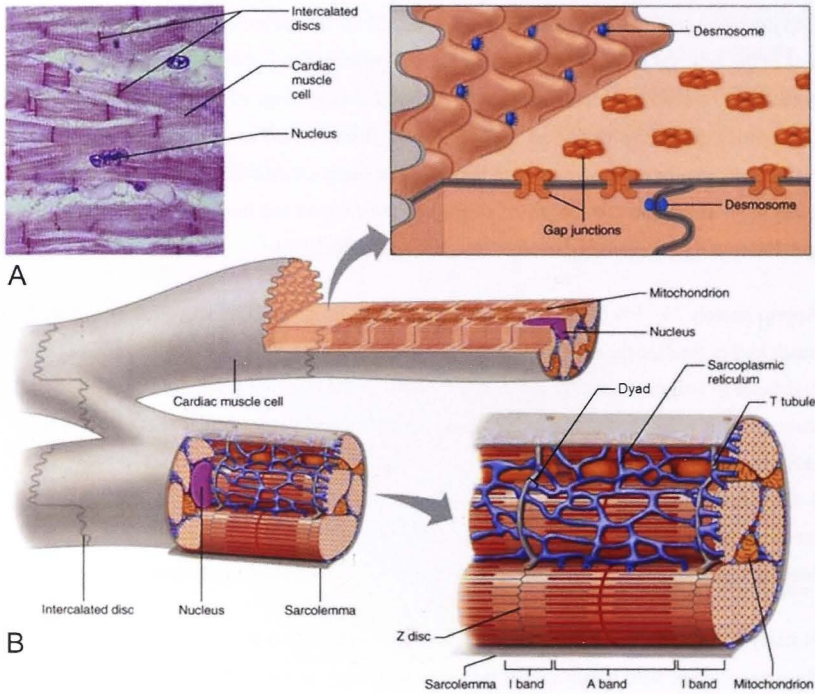


Figure 1-4 Microscopic anatomy of cardiac muscle. (A) Photomicrograph of cardiac muscle (700 \times). The dark-staining areas are intercalated discs, or junctions, between adjacent cells. (B) Cardiac cell relationships at the intercalated discs (bottom left) and relationships of T-tubules, SR and myofilaments (bottom right). (Marieb and Hoehn, 2007)

1.3 Major components and anatomy of the calcium release units (CRUs)

As mentioned in the previous section (1.2.2), calcium release units (CRUs) are constituted by specialized junctional domains of the SR and exterior membranes (with the exception of corbular SR described in section 1.2.2). The two associated domains are in turn separated from each other by the nonjunctional domains of the two compartments, which contain a different complement of proteins.

In both skeletal and cardiac muscle, CRUs are located mostly along the T tubule networks. The networks are located either in a single transverse fairly narrow band at the level of the Z line, or in two bands close by the Z line, positioned symmetrically distant from it (Franzini-Armstrong et al., 1999).

The two central elements of the CRUs essential to EC coupling are ryanodine receptors (RyRs, also see section 1.6) and dihydropyridine receptors (DHPRs). In muscle cells, both DHPRs and RyRs are strategically located within CRUs such that RyRs can receive a signal from the DHPRs. The grouping of DHPRs and RyRs (and other junctional SR proteins) forms a large functional signal transduction complex at the junction, a couplon, which may act in concert with other couplons during EC coupling (Sommer, 1998).

The Ca^{2+} release channels of the SR, the RyRs, were first observed as two rows of electron density occurring on the junctional face of cisternal, though not the longitudinal, SR membrane (Franzini-Armstrong, 1970). These densities project out from the SR towards the exterior membranes, forming large “feet” visible via electron microscopy (Inui et al., 1987a). These foot structures proved to have a 4-subunit structure, and have been subsequently identified as the cytoplasmic components of the homotetrameric RyR protein. The cytoplasmic domains of RyRs bridge the junctional gap (10-12 nm) separating the SR from the exterior membranes (Franzini-Armstrong and Nunzi, 1983; Franzini-Armstrong et al., 1999; Wagenknecht and Radermacher, 1997). The RyRs are packed in highly ordered arrays, with very similar inter-unit spacings (Block et al., 1988). In skeletal muscle, the RyR feet are arranged in a tetragonal disposition with an approximate center-to-center distance of 29 nm. In cardiac muscle, the RyR are arranged in regular intervals approximately equal to those of the skeletal muscle units (Sommer, 1998), but the precise parameters of their disposition are not known.

DHPRs are voltage-dependent, L-type Ca^{2+} channels located in the plasma membrane and T-tubules which sense depolarization. Each DHPR consists of four homologous ‘repeats’. In both skeletal and cardiac muscle cells, the action of DHPRs appears to trigger the release of intracellularly stored Ca^{2+} by promoting opening of nearby RyRs, via either direct allosteric or indirect chemical mechanisms (see section 1.4). In skeletal muscle, DHPRs have been identified with large intramembrane particles in junctional domains of the plasma membrane and T-tubules in isolated triads (Block et al., 1988; Takekura et al., 1994); a similar identification has been proposed for cardiac muscle (Sun et al., 1995). The disposition of DHPRs, however, is significantly different in cardiac and skeletal muscles.

In skeletal muscle, DHPRs are grouped into a diamond-shaped arrangement (a ‘tetrad’), or clusters of four DHPRs, located at the corners of hypothetical squares (Fig. 1-5C). The tetrads in turn are disposed in larger ordered arrays, which occur with a constant stoichiometry in

relation to the RyR tetramer such that one tetrad is associated with every other RyR (Fig. 1-5A&C). Such a regular pattern is only observed in skeletal muscles, and it constitutes the structural basis for the direct allosteric interactions between alternate RyRs and the DHPR tetrads (see section 1.4). In contrast to skeletal muscle, cardiac DHPRs within these junctional domains are much fewer in number and not organized in regular arrays of tetrads. A typical cardiac couplon may have about 100 RyRs and 10-25 DHPRs (Bers, 2001). In addition, although also being clustered in close proximity to RyRs, they are not disposed in a detectable ordered arrangements and thus do not appear to be specifically associated with the RyRs (Sun et al., 1995) (Fig. 1-5B&D). In mammalian cardiomyocytes, there appear to be 4-10 RyR per DHPR at each dyad, depending on species (Bers, 2001). This apparent difference in anatomy from skeletal muscle reflects the different activation mechanism applied in cardiac muscle. The DHPR-RyR interaction in these muscles is thought to be indirectly mediated by Ca^{2+} (see section 1.4).

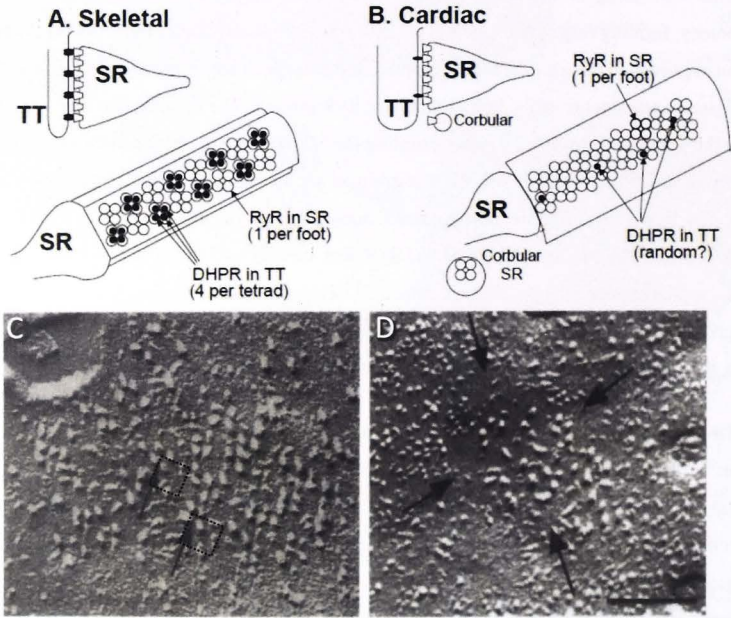


Figure 1-5 Comparison of DHPR and RyR arrangements in skeletal and cardiac muscles. (A)-(B) Diagram comparing the organizational differences between skeletal and cardiac T-tubule junctions. In the upper diagrams, trapezoids denote RyRs and filled ovals DHPRs. Note that DHPRs are sparse and less aligned in the heart (B). Image from (Bers, 2002). (C)-(D) Freeze-fracture electron micrographs of the surface membrane of developing mouse skeletal and cardiac muscle. DHPRs form arrays of tetrads (C, arrows point to individual tetrads), while in cardiac muscle DHPRs are randomly disposed (D). Image from (Franzini-Armstrong et al., 1998)

In addition to the two calcium channels (DHPRs and RyRs), CRUs contain numerous key regulatory proteins such as calmodulin, FK-506 binding proteins (FKPBs), and PKA; they also contain proteins located at the luminal SR surface (e.g. calsequestrin, triadin and junctin) that are associated with RyRs.

1.4 Excitation contraction coupling

1.4.1 Overview

In cardiac and skeletal muscle contraction occurs through a phenomenon known as excitation-contraction (EC) coupling. Broadly, EC coupling is defined as the process beginning with electrical excitation and ending in contraction of the muscle fiber. More narrowly, EC coupling is considered to be the process linking surface/T-tubule membrane depolarization to Ca^{2+} release from the SR – and subsequent activation of contractile proteins – which in turn triggers muscle contraction (reviewed in (Dulhunty, 2006)). The essential elements of this process are the ryanodine receptor (RyR, see section 1.3 and 1.6) and the surface voltage-activated L-type Ca^{2+} channel, the dihydropyridine receptor (DHPR, see section 1.3), both of which are located at the triad junctions. Failure in the expression of either protein leads to death at antenatal or neonatal stages.

Despite substantial differences between skeletal and cardiac muscle (discussed in section 1.4.2), the general scheme of E-C coupling is similar in both tissue types (Fig. 1-6). Electrical excitation of the surface membrane leads to an action potential which rapidly propagates as a wave of depolarization along the sarcolemma and down the T-tubules. At the triad junctions, the DHPR detects the depolarization and undergoes a conformational change (Rios and Brum, 1987; Schneider and Chandler, 1973), leading to a mechanical or chemical signal which activates the RyR on the closely opposed SR membrane. Ca^{2+} is then released from the SR into the cytosol, raising the cytoplasmic $[\text{Ca}^{2+}]$ from nM to μM levels, thereby facilitating binding of Ca^{2+} to troponin-C in sufficient quantities to activate contraction (Szent-Gyorgyi, 1975).

1.4.2 Mechanism of EC coupling

As mentioned previously, significant differences exist between the skeletal and cardiac EC coupling mechanisms. EC coupling in cardiac muscle depends not only on Ca^{2+} release from the SR, but also Ca^{2+} entry across the sarcolemma. Skeletal EC coupling, on the other hand, is dependent almost exclusively on Ca^{2+} released from the SR, with Ca^{2+} entry across the sarcolemma being quantitatively insignificant during a normal twitch (Bers, 2001).

In cardiac muscle, extracellular Ca^{2+} entry across the sarcolemma is an absolute requirement for EC coupling. The primary role of DHPRs in this muscle type is to function as a voltage-

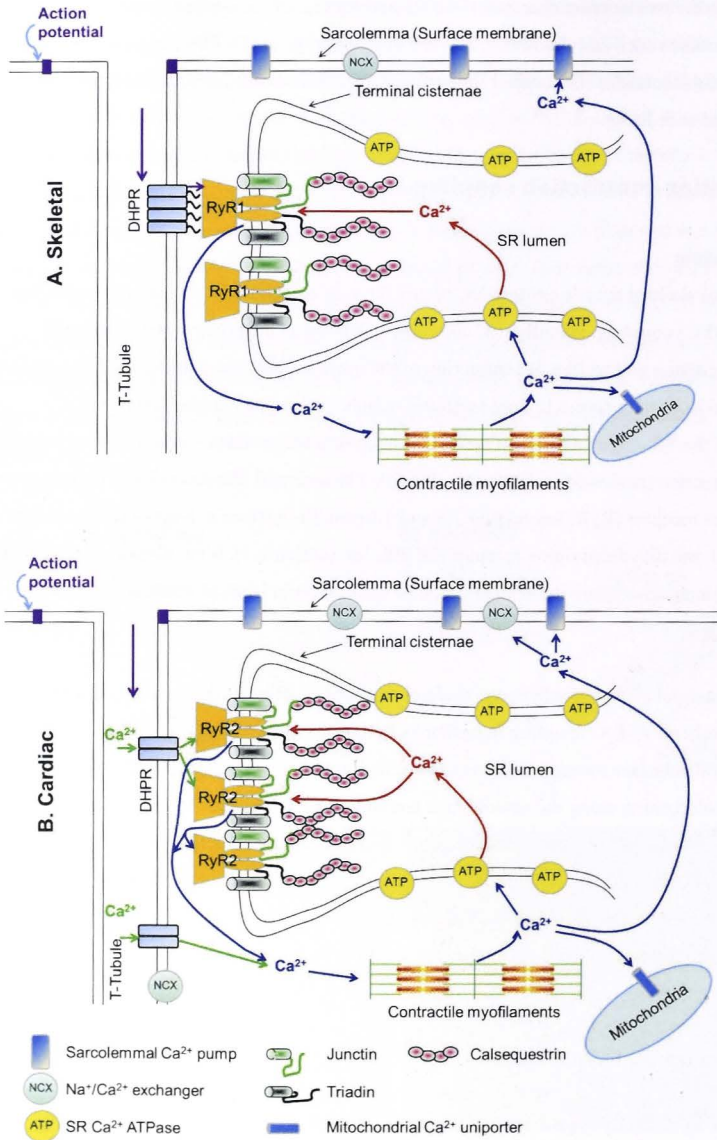


Figure 1-6 Scheme of skeletal and cardiac excitation-contraction (EC) coupling events. Electrical excitation at the sarcolemmal membrane activates the voltage-gated Ca^{2+} channel DHPR, leading to a mechanical (in skeletal muscle, **A**) or chemical signal (in cardiac muscle, **B**) which activates the RyR; the resultant Ca^{2+} release from the SR in turn activates contractile elements. The dark arrow indicates physical interaction between DHPR and RyR in skeletal muscle (**A**) while purple arrows indicate depolarization. Green, red and blue arrows indicate movement of Ca^{2+} during EC coupling (**A, B**). RyR1, skeletal RyR isoform; RyR2, cardiac RyR isoform (for detail, see section 1.6).

sensitive Ca^{2+} channel; correspondingly, the interaction between the DHPR and the RyR is chemical in nature. The action potentials, generated in the local pacemaker tissues, pass along the surface membrane and activate the DHPR in the T-tubule membrane. The DHPR opens rapidly, allowing the influx of extracellular Ca^{2+} . The Ca^{2+} entering the cell binds to and opens the RyR in the nearby SR membrane, which triggers a massive release of Ca^{2+} from the SR. This Ca^{2+} release from the SR activates adjacent RyRs, thus reinforcing Ca^{2+} release. This process is known as Ca^{2+} -induced Ca^{2+} release (CICR) (Fig. 1-6B). Notably, although CICR is the main mechanism in cardiac EC coupling, under some circumstances direct or indirect physical coupling between DHPRs and RyRs may also occur (Dulhunty and Pouliquin, 2003).

In vertebrate skeletal muscle, EC coupling is mediated by homologous proteins but employs a very different mechanism, involving a direct mechanical interaction between the DHPR and the RyR (Block et al., 1988). The action potential generated at the neuromuscular junction propagates over the surface membrane and into the T-tubule, which is far more extensive than in cardiac muscle (see section 1.2.1.2 and 1.2.2). The depolarization is detected by the voltage sensor, the DHPR, which is a different L-type channel isoform than in cardiac muscle. The DHPR undergoes a conformational change that is transmitted through direct physical interactions with the RyR1 in the SR membrane, leading to the RyR channel opening and subsequently a rapid release of Ca^{2+} . This process is termed voltage-induced Ca^{2+} release (VICR), or depolarization-induced Ca^{2+} release (Fig. 1-6A). However, it should be noted that CICR may be very important in recruiting the approximately 50% of RyRs which are not physically coupled to T-tubule tetrads (see section 1.3), the Ca^{2+} is from release through coupled RyRs not through DHPRs. Importantly, DHPRs only mediate a small, very slow influx of extracellular Ca^{2+} in skeletal muscle (Field et al., 1988; Lamb and Walsh, 1987; Tanabe et al., 1988). Notably, in invertebrate skeletal muscle and neonatal vertebrate skeletal muscle, EC coupling is more similar to that in cardiac muscle, requiring an influx of extracellular Ca^{2+} for full contraction.

1.5 Sarcolemmal and SR Ca^{2+} fluxes during muscle twitch

As previously described, the majority of the Ca^{2+} involved in the normal activation of skeletal muscle contraction is derived from the SR. The skeletal muscle DHPRs carry little Ca^{2+} current (Tanabe et al., 1988). During the cardiac action potential, Ca^{2+} enters the cell mainly through sarcolemmal L-type Ca^{2+} channels (DHPRs), which is critical in the activation of SR Ca^{2+} release (CICR), and also contributes to the activation of myofilaments and to the replenishment of the SR Ca^{2+} stores. However SR Ca^{2+} release in the heart is the major source of activator Ca^{2+} . In rabbit ventricular tissue, Ca^{2+} influx and SR Ca^{2+} release supply 25-30% and ~70% of the activating Ca^{2+} respectively (Bers, 2001).

Relaxation occurs with removal of Ca^{2+} from the cytoplasm, lowering intracellular $[\text{Ca}^{2+}]_i$ to the point that Ca^{2+} will dissociate from TnC. Four different Ca^{2+} transport mechanisms are involved in transport of Ca^{2+} out of the cytoplasm. Ca^{2+} can be: 1) pumped back into the SR via the SR Ca^{2+} ATPase (SERCA), which dominates during relaxation; 2) transported out of the cell by the sarcolemmal Ca^{2+} -ATPase pump (SLCP); 3) transported to the extracellular space by the sarcolemmal $\text{Na}^+/\text{Ca}^{2+}$ exchanger (NCX); or 4) translocated into mitochondria via the $\text{Na}^+/\text{Ca}^{2+}$ uniporter (Fig. 1-6; indicated by blue arrows). With respect to Ca^{2+} efflux from the cell, in skeletal muscle SLCP is the most effective pathway, with optimal activation at cytosolic $[\text{Ca}^{2+}]$ above $100 \mu\text{M}$; in cardiac muscle, the SLCP appears relatively unimportant. The NCX is the main mechanism of efflux in the heart during relaxation (diastole), but plays a less prominent role in skeletal muscle. Additionally, $\text{Na}^+/\text{Ca}^{2+}$ exchange can also mediate Ca^{2+} influx to a degree sufficient to activate cardiac cell contraction, but this likely does not occur under normal physiological conditions. The mitochondrial pathway contributes only fractionally (e.g. less than 1% in rabbit ventricle) to the removal of Ca^{2+} in both skeletal and cardiac muscles (Bers, 2001; Fieni et al., 2012).

Importantly, in order for a steady state to be achieved, the amount of Ca^{2+} -influx must be balanced with the amount of Ca^{2+} -efflux during the same contraction-relaxation cycle such that the cell does not experience a net gain or loss of Ca^{2+} .

1.6 Ryanodine receptor Ca^{2+} release channel (RyR)

The RyR is located in the membranes of internal Ca^{2+} storage organelles (Franzini-Armstrong and Protasi, 1997). It was first observed (although not specifically identified as an RyR) in skeletal muscle in the early 1970s, where it was visualized as amorphous material projecting from the SR membrane and joining the distal segment of the SR to the plasma (T-system) membrane - it was therefore referred to as the junctional foot protein (Franzini-Armstrong, 1970). The RyR received its name due to its specific affinity for a plant alkaloid, ryanodine (Fleischer et al., 1985; Inui et al., 1987b), which facilitated the purification and characterization of the protein. As the largest ion channel known to date, the RyR forms homotetrameric assemblies with a total molecular mass of ~ 2.2 MDa, with each monomer consisting of approximately 5000 residues (Inui et al., 1987b; Lai et al., 1988). The RyR is structurally related to the inositol 1,4,5-triphosphate receptor (IP_3R), and these together form the superfamily of intracellular Ca^{2+} release channels. The IP_3R resides mostly in the endoplasmic reticulum (ER) membrane of all cell types (Foskett et al., 2007), and is predominantly expressed in non-muscle cells (Berridge et al., 2000). The RyR and IP_3R proteins share considerable structural similarity and some sequence homologies, especially in the carboxyl-terminal sequences which form their channel pores and display approximately 40% homology. Together with IP_3R , RyR provides a regulated pathway for the release of stored Ca^{2+} during Ca^{2+} -

mediated signalling processes such as muscle contraction, fertilization, and cell proliferation (Berridge et al., 2000).

1.6.1 RyR genes, isoforms and distribution

There are three isoforms of RyR expressed in mammals: RyR1, RyR2, and RyR3, which are encoded by three different genes residing on separate chromosomes (Mattei et al., 1994). RyR1 was first identified and isolated from skeletal muscle (Takeshima et al., 1989; Zorzato et al., 1990), RyR2 was first detected in cardiac muscles (Nakai et al., 1990; Otsu et al., 1990), and RyR3 was originally identified in the brain, and hence often referred to as the brain isoform (Hakamata et al., 1992). RyR1 and RyR2 are also known as the skeletal and cardiac types respectively, based on the abundance and timing of their purification from various tissues. The RyR1 isoform is also expressed at low levels in cardiac muscle, smooth muscle, and in some parts of brain and many other tissues (Giannini et al., 1995; Lee et al., 2002; Nakai et al., 1990; Neylon et al., 1995; Vukcevic et al., 2010). RyR2 is also expressed at high levels in the brain and at low levels in other tissues (Furuichi et al., 1994; Giannini et al., 1995; Kuwajima et al., 1992; Lai et al., 1992; Nakanishi et al., 1992). In turn, RyR3 - the least understood of the RyR isoforms - seems to play its most prominent role during striated muscle development, and is ubiquitously distributed in smooth muscle and non-muscle cells (Furuichi et al., 1994; Giannini et al., 1995; Hakamata et al., 1992; Lai et al., 1992; Neylon et al., 1995; Ogawa et al., 2000), with small amounts also found in adult skeletal and cardiac muscles. In non-mammalian vertebrates, three isoforms, RyR α , RyR β and the cardiac type, are expressed, while only one isoform has been found in lower organisms, including nematodes, fruit flies, and lobsters (reviewed in (Lanner et al., 2010; Zissimopoulos and Lai, 2007)). RyR α and RyR β are highly homologous to mammalian RyR1 and RyR3 respectively (Ottini et al., 1996; Oyamada et al., 1994).

There is approximately 65% sequence homology across the three mammalian isoforms (Hakamata et al., 1992), with the highest rates of homology present at the carboxyl-terminal end. The largest degree of difference is found in three major regions of diversity, known as D1 (residues 4254-4631 in RyR1 and 4210-4562 in RyR2), D2 (residues 1342-1403 in RyR1 and 1852-1890 in RyR2), and D3 (residues 1872-1923 in RyR1 and 1852-1890 in RyR2). D1 is the most variable region, whereas D2 is absent altogether in RyR3. D1 is predicted to be functionally critical in the pore forming region (Zorzato et al., 1990), and mutations in D1 alter the Ca²⁺ and caffeine sensitivity of RyR1 (Du et al., 2000). D2 may be critical for the mechanical interactions between RyR1 and Ca_v1.1 (Perez et al., 2003), and D3 may contain Ca²⁺ dependent inactivation sites (Hayek et al., 1999). These three hyper-variable regions are thought to partially underlie the functional differences between the three isoforms.

1.6.2 RyR structure

High resolution structural information is essential to understand how ryanodine receptors function. However, it has so far not been possible to obtain RyR crystal structures due to the protein's massive size and the difficulty inherent in crystallizing integral membrane proteins. This is further compounded by the multiple modulators and the dynamic nature of the RyRs. However, progress in cryo-electron microscopy (cryo-EM) and single-particle three-dimensional reconstruction (3D cryo-EM) has made it possible to obtain low resolution structural architecture of these large proteins and to reveal some mechanisms of calcium release channel gating over the last two decades. Early cryo-EM studies of the structure of skeletal RyR were reported in the middle of the 1990s (Radermacher et al., 1994; Serysheva et al., 1995; Wagenknecht et al., 1989; Wagenknecht and Radermacher, 1995), albeit at modest resolution (20-40Å). Since 2005, more highly detailed structures of RyR1 at sub-nanometer resolution have emerged (Ludtke et al., 2005; Samso et al., 2009; Samso et al., 2005; Serysheva et al., 2008). Most cryo-EM studies have focused on RyR1 (Benacquista et al., 2000; Ludtke et al., 2005; Orlova et al., 1996; Radermacher et al., 1994; Radermacher et al., 1992; Samso et al., 2009; Samso et al., 2005; Serysheva et al., 2005; Serysheva et al., 2008; Serysheva et al., 1995; Serysheva et al., 1999), although some studies have been performed on RyR2 (Liu et al., 2002; Sharma et al., 1998) and RyR3 (Liu et al., 2001; Sharma et al., 2000); however, at much lower resolution than RyR1 structures. Further, the structure of RyR2 has been studied with comparative modeling and bioinformatics mapping techniques (Bauerova-Hlinkova et al., 2011; Bauerova-Hlinkova et al., 2010; Welch et al., 2004). Fourteen probable domains were revealed in the human RyR2 monomer via bioinformatics analysis in the study by Bauerova-Hlinkova et al. (2011), of which eight domains are located in the N-terminal region, three domains in the central region and three domains in the C-terminal part. A model of the N-terminal region of human RyR2 (residues 12-543) was constructed (Bauerova-Hlinkova et al., 2011) based on the structure of the homologous N-terminal region of rabbit RyR1 determined by Tung et al. (2010), and the first three N-terminal domains within this region have been verified to be able to behave as separate, independent protein units (Bauerova-Hlinkova et al., 2011; Bauerova-Hlinkova et al., 2010). Some small RyR segments have recently been obtained via x-ray crystallography (Amador et al., 2009; Lobo and Van Petegem, 2009; Tung et al., 2010). In general, the EM structures of all three isoforms are very similar, consistent with their high degree of sequence identity (~65%). Nevertheless, the small differences reveal the molecular basis of the specialized functional roles of each isoform.

Overall, the basic architecture of the RyRs has been described as resembling a mushroom, with a large 'cap' (corresponding to the cytoplasmic assembly, or CA) and a smaller transmembrane (TM) 'stalk' extending from the base of the cytoplasmic region into the SR lumen

(Radermacher et al., 1994; Serysheva et al., 1995). The structure of RyRs exhibits four-fold cyclic symmetry, reflecting its homotetrameric architecture. The cytoplasmic assembly, shaped like a square prism, has overall dimension of $\sim 275 \times 275 \times 100$ Å (Wagenknecht and Samso, 2002), and is composed of a series of interconnected tubular structures, which account for approximately 80% of the total protein mass. The transmembrane assembly has a square tapering prism shape with maximal dimensions of $115 \times 115 \times 60$ Å, and is localized to the carboxyl terminal of the protein. The transmembrane region is rotated by $\sim 38^\circ$ with respect to the cytoplasmic region (Radermacher et al., 1994; Serysheva et al., 1995; Wagenknecht et al., 1989). In addition, there is a space of 14 Å spanned by intra-assembly columns between the two structures (Orlova et al., 1996; Samso et al., 2009; Samso et al., 2005; Serysheva et al., 2005), which defines the transmembrane assembly boundaries.

1.6.2.1 Cytoplasmic assembly

The cytoplasmic assembly consists of several morphologically distinct segments: the ‘clamp’-shaped domains (C) at its periphery, the interconnecting ‘handle’ domains, and a ‘central rim’ that surrounds the central cavity of the cytoplasmic region (reviewed in (Capes et al., 2011; Lanner et al., 2010; Van Petegem, 2012), also see Fig. 1-7A). These segments have been further subdivided into 15 subregions per subunit (Serysheva et al., 2008), each likely corresponding to one or several protein folding domains, with an open arrangement allowing a substantial fraction of the cytoplasmic assembly volume to be available for interaction with the modulators that bind within the N-terminal regions of RyR. These subregions are indicated by identifying numbers (Samso et al., 2005; Serysheva et al., 2008) on the model depicted in Fig. 1-7, with the column region having been designated as subdomain 12. At sub-nanometer resolution, 36 α -helices and 7 β -sheets at various orientations have been resolved on the cytoplasmic region of each monomer (Serysheva et al., 2008); these appear interconnected and merge toward the center of the channel (Samso et al., 2005).

The ‘clamp’ domains, comprising subdomains 5-10, define the corners of the cytoplasmic assembly. They have been shown by higher resolution (~ 10 Å) cryo-EM to be formed by two separate structures: a flat tubular structure that loops around the outer corners of the square prism (domains 8a, 8 and 7) and a smaller elongated, tapering structure that extends toward its corner from the side of the square (domains 9-10). Two divergent areas were mapped in the clamps (Liu et al., 2004; Zhang et al., 2003). Seven α -helices and three β -sheets have been localized to this domain (Serysheva et al., 2008). This region exhibits major conformational changes during the opening and closing of the channel (Orlova et al., 1996; Samso et al., 2009; Sharma et al., 2000). In skeletal muscle, the ‘clamp’ region is most likely to interact with dihydropyridine receptors (Paolini et al., 2004), where it senses depolarization of the plasma membrane and controls RyR1 channel activity during excitation-contraction coupling.

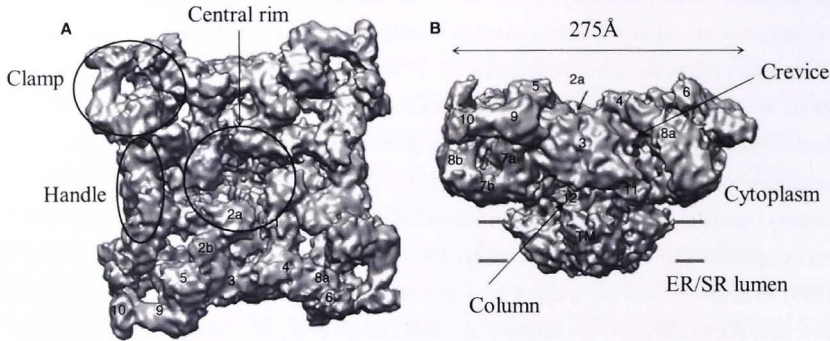


Figure 1-7 Cryo-EM reconstruction of RyR1 at 9.6 Å resolution (Electron Microscopy Data Bank entry 1275) (Serysheva et al., 2008). Two orientations are shown: (A) “top” view along the fourfold symmetry axis, looking from the cytoplasm toward the SR/ER; (B) “side” view showing the cytoplasmic and the transmembrane (TM) assembly/region. One of the “clamp” and “handle” structures and the “central rim” are indicated in (A). The numerals indicate the distinctive subregions. Figure modified and adapted from (Lanner et al., 2010).

The T-tubule facing surface of the RyR, structurally resembling a rhombus, is also formed of tubular structures, and is comprised of domains 2, 4, 5 and 6. It has been proposed that inter-domain interactions may occur among at least three separate bulks of mass in close proximity (pairs of domains: 2-4a', 5-6, 10-8a) (Samso et al., 2005).

The flat, slab-shaped ‘handle’ domains, formed by subdomains 3 and 4 (Lanner et al., 2010), where the FK506-binding proteins and calmodulin (CaM) binding sites are located, define the side of the cytoplasmic assembly. This region has been found to contain an expanded region of divergence (Samso and Wagenknecht, 1998), and a β 3 sheet has been mapped to subdomain 4, bridging the central rim with the clamp (Serysheva et al., 2008). A crevice (see Fig.1-7B), bounded by domains 3, 4, 8a and 8, extends to the T-tubule side from the SR side. Two more β -sheets have also been resolved in the central rim (subregions 1 and 2a) (Serysheva et al., 2008).

1.6.2.2 Transmembrane assembly

The square-shaped structure spanning the SR membrane, and the four high density column domains attached to it, together form the transmembrane assembly, or the ‘stem’ region of the ‘mushroom’ (Serysheva et al., 2005). The four columns which connect the cytoplasmic and the transmembrane domains were first observed in (Orlova et al., 1996), and were also reported in (Serysheva et al., 2005), but were not described in detail. At higher resolutions - ~ 10 Å (Samso et al., 2005) and 9.6 Å (Samso et al., 2009) - the columns’ structure and their movement upon gating have been studied more thoroughly. Formed from the SR-proximal part of the

cytoplasmic assembly, the ~ 14 Å columns span the gap and provide direct continuity between the cytoplasmic and transmembrane regions (Samso et al., 2005). A β -sheet has further been located in the column region (Serysheva et al., 2008). The four columns are together composed of four peripheral branches, which merge to define the external TA boundaries, and four inner branches of higher density located in the central region (Fig.1-8). These columns have been proposed to constitute an important component in orthograde RyR1 signaling between the protein's two major domains (Samso et al., 2005). The two columnar bundles converge into a ring of high density, possibly the ion gate. The structure of the columns has been further refined by the same group (Samso et al., 2009): the cytoplasmic "inner branches" stretch from the ion gate to the peripheral cytoplasmic domain, and the TM "inner helices" extend from the lumen to the ion gate. Three main constrictions along the four-fold axis are defined by the inner branches and inner helices: the cytosolic constriction defined by the distal enlargement of the inner branches; the ion gate defined by the meeting of the two bundles; and the opening to the SR lumen for the lowest constriction, formed by the pore helices in a region equivalent to the selectivity filter of the K^+ channels. Upon channel gating, a precise relocation of the two bundles results in an approximately 4 Å increase in the diameter of the ion gate, due to a converging of the conformational change in the cytoplasmic domains, underlying a long-range allosteric mechanism. A central cavity, or vestibule, four peripheral cavities, and the mouth of the presumed ion channel have also been defined (Fig.1-8B) (Samso et al., 2005).

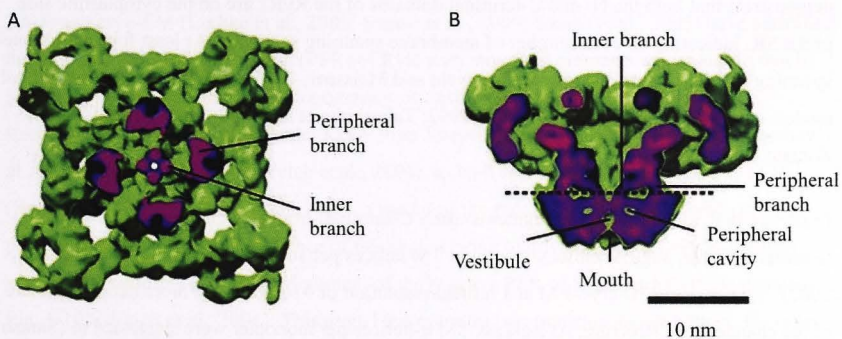


Figure 1-8 Internal structure of the columns and transmembrane region. (A) Section of RyR1 cut along the plane indicated by the dashed line in **B** seen from the SR lumen, the internal and peripheral regions of the columns are shown. (B) Slice across the side view showing the two branches of each column and basic architecture of transmembrane region. Figure modified and adapted from (Samso et al., 2005).

Compelling evidence suggests that the conduction pathways in the RyR channels are contained in the C-terminal part of the protein. The C-terminal 1000 residues of the RyR form a functional channel which binds to ryanodine with high affinity, preserves wild-type (WT) channel

conductance, and is activated by Ca^{2+} (Bhat et al., 1997; Treves et al., 2002; Wang et al., 1996); reviewed in (Dulhunty and Pouliquin, 2003).

1.6.3 Transmembrane segments and pore forming region

1.6.3.1 Transmembrane topology of RyR

The transmembrane topology of the RyR carboxyl-terminus is not yet fully understood, and several models have been proposed.

The number of transmembrane helices has been the subject of much debate, and the predicted number varies from between 4 to 12 (Brandt et al., 1992; Takeshima et al., 1989; Tunwell et al., 1996; Zorzato et al., 1990), with data for these predictions derived mostly from hydrophathy profiles. Two popular topological models for the transmembrane assembly of 4-TM (Takeshima et al., 1989) and 10-TM have been proposed (Zorzato et al., 1990) - the four segments of the 4-TM model correspond to M5, M6, M8 and M10 respectively of the 10-TM model. A third model suggests the existence of six transmembrane helices (6-TM), located in the carboxyl-terminal region of RyR1 (Brandt et al., 1992) and RyR2 (Tunwell et al., 1996).

Experiments using immunological techniques with site-directed antibodies (Grunwald and Meissner, 1995; Marty et al., 1994) in combination with proteolysis (Marty et al., 1994) demonstrate that both the N- and C-terminal domains of the RyR1 are on the cytoplasmic side of the SR, indicating an even number of membrane spanning segments. At least four membrane-spanning segments were suggested (Grunwald and Meissner, 1995), which is consistent with all models currently proposed (Brandt et al., 1992; Takeshima et al., 1989; Tunwell et al., 1996; Zorzato et al., 1990).

Experimentally determined TM segments using C-terminal-truncated channels fused with a C-terminal GFP tag, suggest either six or eight TM helices per subunit (Du et al., 2004; Du et al., 2002). Studies using 3D cryo-EM at a refined resolution of ~ 10 Å show a more detailed picture of the channel pore structure. At least six TM α -helices per monomer were suggested in (Samso et al., 2005); however, only five helix-like densities were identified by Ludtke et al. (2005) at similar resolution (9.6 Å). In a more recent study (Samso et al., 2009), the open and closed conformations of the channel have been compared, and three independent 3D reconstructions have been obtained, all of which suggest at least six transmembrane helices, supporting the previous study (Samso et al., 2005). The current predicted RyR membrane topology (RyR1 and RyR2) is depicted in Fig. 1-9.

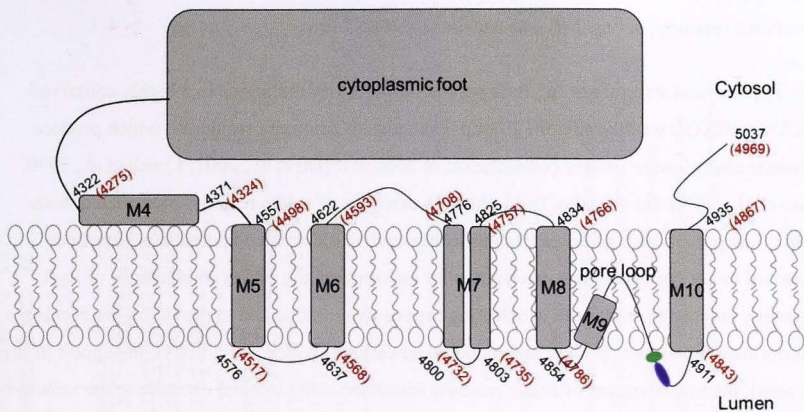


Figure 1-9 Membrane topology for ryanodine receptor 1 (RyR1) and 2 (RyR2). Coordinates given are for rabbit RyR1 (black) and rabbit RyR2 (red in brackets). The green oval denotes acidic residues contributing to a ring of negative charge at the mouth of the pore; the purple region denotes the GGGIGD selectivity filter. Figure modified from reviews by Zissimopoulos and Lai (2007) and Dulhunty et al. (2012).

1.6.3.2 Pore forming region

Both molecular modelling (Ramachandran et al., 2013; Ramachandran et al., 2009; Welch et al., 2004) and cryo-EM (Ludtke et al., 2005; Samsó et al., 2009; Samsó et al., 2005) have identified the probable pore-forming region (PFR) of RyR with structural elements equivalent to that of K^+ channels, with similar overall topography. By using the known X-ray crystal atomic structure of the bacterial K^+ channel KcsA from *Streptomyces lividans* as a template (Balshaw et al., 1999; Doyle et al., 1998; Welch et al., 2004), as well as the predicted structure of IP₃R (Balshaw et al., 1999; Zhao et al., 1999), a model of the putative PFR of RyR has been predicted, with the primary sequence of this region being highly conserved (>90% identity) across RyR isoforms (sequence alignment of the putative PFR of RyR1 and RyR2 is depicted in Fig. 1-10) (Welch et al., 2004). This model incorporates two transmembrane helices, the outer and inner helices, and the pore loop (P-loop) which links the two helices. The P-loop contains a pore helix and an amino acid motif (GGGIGD) similar to the selectivity filter motif (TVGYGD) of the KcsA channel, with a high density of negative charges exposed at both the luminal and cytosolic mouths of the pore. Fitting this structure to 4-TM and 12-TM model suggests that the M3 and M4 in the 4-TM model (Takehima et al., 1989) or the M8 and M10 helices in the 12-TM model (Zorzato et al., 1990) form the outer and inner helices respectively, and that the pore helix is formed by the M3-M4 luminal loop in 4-TM, or M9 in the 12-TM model. More recently, a slightly altered version of the model of PFR has been proposed by (Ramachandran et al., 2013) (Fig. 1-11). This model is based on homology modeling and cryo-EM data. Notably, the new

model adjusts the sequences of the six transmembrane segments (compare with the RyR membrane topology in Fig. 1-9) and includes the S4-S5 linker.

This hypothetical structure of the RyR pore is supported by mutations in a highly conserved GXRXGGGXGD motif within the P-loop – and also to adjoining residues – which produce dramatic alterations to unitary conductance, or abolish it (Du et al., 2001; Lynch et al., 1999; Zhao et al., 1999). On the other hand, the high densities of acidic residues identified at both ends of the pore, which give rise to significant negative electrostatic potentials, have been proposed to not only provide a mechanism for maximizing the cation conductance of RyR channels, but also to contribute to selecting cations over anions and to providing the necessary discrimination between divalent and monovalent cations (Welch et al., 2004). In support of this proposal, the neutralization of acidic residues identified at the luminal entrance to the selectivity filter in the RyR2 PFR model (ED4832AA, mutated residues highlighted in yellow in Fig. 1-10) results in substantial alterations to RyR2 ion handling and gating characteristics (Mead-Savery et al., 2009). Although the mutant channel discriminates between cations and anions, it no longer discriminates between divalent and monovalent cations and cation conductance is significantly altered, e.g., unitary K^+ conductance is reduced at low levels of K^+ activity but increases dramatically as activity is increased and shows little sign of saturation. In addition, the ED4832AA channel displays a higher open probability than that of the WT channel (Mead-Savery et al., 2009). Interestingly, the regulatory proteins triadin (section 1.8) and junctin (section 1.9) interact with this region, possibly through negatively charged residues located in the luminal end of the pore helix and the loop connecting the pore helix to the inner helix (Altschafel et al., 2011; Goonasekera et al., 2007; Lee et al., 2004). Indeed, three acidic residues (D4878, D4907 and E4908) in this region are critical for triadin binding to the RyR1 (Goonasekera et al., 2007; Lee et al., 2004).

As with RyR1 (see section 1.6.2.2), the putative PFR of RyR2 also forms a gated ion channel when incorporated into lipid bilayers, albeit with different gating and ion handling properties to those of the full-length RyR2 channel (Euden et al., 2013). This is not surprising, since the other domains of the full-length molecule would contribute to the structure of the PFR and the mechanisms governing function in the intact tetramer (Euden et al., 2013).

The diameter of the RyR (RyR1 and RyR2) pore has been estimated to be approximately 3.5-7 Å and the length approximately 10 Å (Orlova et al., 1996; Tinker and Williams, 1993, 1995; Tu et al., 1994a); reviewed in (Dulhunty and Pouliquin, 2003). The relative short, wide RyR channel pore would allow a high rate for Ca^{2+} flow down its concentration gradient, and hence to support its role as an effective Ca^{2+} -release channel (Williams et al., 2001).

1.6.4 Ion selectivity and conductance

	<u>Outer helix</u>	<u>Luminal</u>	<u>Pore helix</u>	
hRyR2	MGFKTLRILSSVTHNGK QLVLT VG LLAVVV LYTVVAFN FFRK FYNKS EDG D TPDMKCD			4805
rRyR2	MGFKTLRILSSVTHNGK QLVLT VG LLAVVV LYTVVAFN FFRK FYNKS EDG D TPDMKCD			4809
hRyR1	MGVKTLRILSSVTHNGK QLVMT VG LLAVVV LYTVVAFN FFRK FYNKS EDEDE TPDMKCD			4878
rRyR1	MGVKTLRILSSVTHNGK QLVMT VG LLAVVV LYTVVAFN FFRK FYNKS EDEDE TPDMKCD			4877
	** . ***** . ***** . ***** . ***** . ***** . ***** . ***** . ***** . ***** . *****			
	<u>GGIGD</u>			
	<u>Selectivity filter</u>		<u>Inner helix</u>	
hRyR2	DMLTCYMFHMYGV RAGGGIG DE I ED PAG DEYE IYRIIFDIT FFFFVIVILLAI I QGLII			4865
rRyR2	DMLTCYMFHMYGV RAGGGIG DE I ED PAG DEYE IYRIIFDIT FFFFVIVILLAI I QGLII			4869
hRyR1	DMMTCYLFHMYGV RAGGGIG DE I ED PAG DEYE LYRVVFDIT FFFFVIVILLAI I QGLII			4938
rRyR1	DMMTCYLFHMYGV RAGGGIG DE I ED PAG DEYE LYRVVFDIT FFFFVIVILLAI I QGLII			4937
	** . *** . ***** . ***** . ***** . ***** . ***** . ***** . ***** . ***** . *****			
	<u>Cytoplasmic remainder of the carboxy tail</u>			
hRyR2	DAFGELRDQQEQVKED M ETK FCIGINDYF DT VPHG FETH TL Q E H NLAN YLFF LMY LIN			4925
rRyR2	DAFGELRDQQEQVKED M ETK FCIGINDYF DT VPHG FETH TL Q E H NLAN YLFF LMY LIN			4929
hRyR1	DAFGELRDQQEQVKED M ETK FCIGIG SDY F DT VPHG FETH TL EE H N LAN YMFF LMY LIN			4998
rRyR1	DAFGELRDQQEQVKED M ETK FCIGIG SDY F DT VPHG FETH TL EE H N LAN YMFF LMY LIN			4997
	***** . ***** . ***** . ***** . ***** . ***** . ***** . ***** . ***** . ***** . *****			
	<u>remainder of the carboxy tail</u>			
hRyR2	KDETEHTGQ ESYVW KMY Q ERC WE FFPAG DCFRKQYED QLN			4965
rRyR2	KDETEHTGQ ESYVW KMY Q ERC WE FFPAG DCFRKQYED QLN			4969
hRyR1	KDETEHTGQ ESYVW KMY Q ERC WD FFPAG DCFRKQYED QLS			5038
rRyR1	KDETEHTGQ ESYVW KMY Q ERC WD FFPAG DCFRKQYED QLS			5037
	***** . ***** . ***** . ***** . ***** . ***** . ***** . ***** . ***** . ***** . *****			

Figure 1-10 Sequence alignment of the putative pore-forming region from human ryanodine receptors (hRyR) and rabbit ryanodine receptors (rRyR), with crucial residues or sequences highlighted (see legend). The corresponding residues RyR are highlighted according to (Welch et al., 2004). The letters coloured in blue denote predicted outer and inner helices in putative PFR; the letters coloured in orange denote putative pore helix; the underlined letters in black denote putative selectivity filter; the letters coloured in red or light green denote positively or negatively charged amino acids respectively in the cytosolic and luminal mouths of the pore; the letters highlighted in yellow denote mutated residues in study by Mead-Savery et al. (2009). The aligned residues are either identical (*), similar (:), weakly similar (.) or dissimilar. Alignment and similarity was determined using a CLUSTALW multiple sequence alignment (Combet et al., 2000).

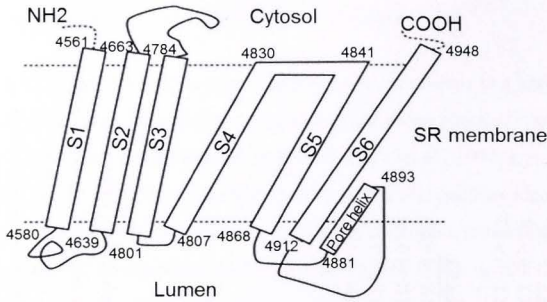


Figure 1-11 A revised model of the pore-forming region for RyR1, including four more transmembrane segment (S1-S4) and the S4-S5 linker. Figure modified and adapted from (Ramachandran et al., 2013). The boundaries of the TM helices are indicated.

The permeation properties of the RyR channel are similar across the RyR isoforms. The RyR ion channel is permeable to a wide range of divalent and monovalent cations, but shows very little discrimination between different monovalent cations and nearly no selectivity between various divalent cations. The RyR channel is moderately selective, between mono- and divalent cations (selectivity $\text{Ca}^{2+}/\text{K}^+ \sim 6.5$, $\text{Ca}^{2+}/\text{Na}^+ \sim 5$, $\text{Ca}^{2+}/\text{Tris}^+ \sim 14$, $\text{Ba}^{2+}/\text{K}^+ \sim 4.3$). However, it is highly selective for cations over anions, the latter having very limited permeability. Conversely, the channel displays very high levels of conductance for both divalent and monovalent cations (reviewed in (Dulhunty et al., 1996; Fill and Copello, 2002; Meissner, 1994; Williams, 1992). In symmetrical solutions containing a monovalent cation charge-carrying species, the slope conductance of the RyR channel is usually >500 pS, e.g. 700-800 pS for K^+ (250mM symmetric K^+), 550-600 pS for Na^+ (500mM symmetric Na^+), and ~ 525 pS for Cs^+ (250mM symmetric Cs^+). The conductance of RyR2 from sheep heart for monovalent cations (in the absence of any divalent cations) ranges from $723 \pm 9 - 215 \pm 3$ pS, with a sequence of $\text{K}^+ > \text{Rb}^+ = \text{NH}_4^+ > \text{Na}^+ = \text{Cs}^+ > \text{Li}^+$ and ~ 17.4 pS for Tris^+ (Lindsay and Williams, 1991). Organic tetra-alkylammonium (TAA) cations including tetramethylammonium (TMA^+), tetraethylammonium (TEA^+) and tetrapropylammonium (TPrA^+), which are all of similar dimensions to Tris^+ , do not permeate under similar conditions (Lindsay and Williams, 1991; Tinker et al., 1992a). In asymmetrical solutions containing a divalent cation as the main permeating species, the RyR channel displays a slope conductance of ~ 100 pS, e.g. 120 ± 30 pS for Ca^{2+} (50 mM luminal Ca^{2+} with 250 mM cytoplasmic K^+ or Na^+). The equivalent conductance sequence for divalent cations is $\text{Br}^{2+} > \text{Sr}^{2+} > \text{Ca}^{2+} > \text{Mg}^{2+}$, within the range $202 \pm 3 - 89 \pm 4$ pS (Tinker and Williams, 1992). The relatively high unit conductance of the RyR channel is fundamental to its physiological role of providing rapid release of Ca^{2+} into the cytosol upon excitation. The channel's apparent deficiency in cation discrimination may not be physiologically relevant, since the major driving force for translocation is the Ca^{2+} gradient across the SR membrane (Williams, 1992).

Both pH and temperature modify RyR channel conductance. A reduction of luminal pH from 7.4 to 6.8 produces a 27% decrease in single-channel Ca^{2+} conductance in both rabbit skeletal and canine cardiac RyR channels (Rousseau and Pinkos, 1990). With Ca^{2+} as the charge carrier, single-channel conductance drops with lowering the bathing solution temperature from 32 to 5 °C (Sitsapesan et al., 1991).

Multiple subconductance states of both native and purified RyR channels have also been resolved in single channel studies. In addition to a fully open state, three distinct conductance levels are seen at 25%, 50%, and 75% of maximum. It has been suggested that this may be related to either uncoordinated opening of conducting pores in each RyR subunit, or a single central pore presenting in several discrete conductance states within the tetramer (Liu et al., 1989; Smith et al., 1988); reviewed in (Dulhunty et al., 1996; Meissner, 1994). A 12-kDa or 12.6-kDa FKBP-binding protein (FKBP12 or FKBP12.6, respectively) is associated with the RyR protein with a stoichiometric relationship of four FKBP's per homotetramer (Jayaraman et al., 1992; Lam et al., 1995; Qi et al., 1998; Timerman et al., 1993; Timerman et al., 1996); reviewed in (MacMillan, 2013). Removal of FKBP12 increases the occurrence of subconductance opening in RyR1 (Ahern et al., 1994, 1997; Brillantes et al., 1994; Shou et al., 1998). FKBP12.6-deficient RyR2 channels display a similarly increased subconductance opening (Kaftan et al., 1996; Shou et al., 1998; Wehrens et al., 2003; Xiao et al., 1997). Therefore, FKBP's are proposed to be responsible for stabilizing inter-subunit coordination within the RyR and for the synchronization of the openings of these separate permeation states (Ahern et al., 1994; Brillantes et al., 1994; Ondrias et al., 1996). However, it should be noted that subconductance opening is not always observed upon FKBP's removal (Barg et al., 1997; Mayrleitner et al., 1994; Timerman et al., 1996), leading to controversy about FKBP's role in modifying RyR channel conductance.

1.6.5 RyR regulation

1.6.5.1 RyR modulation by main regulatory ligands

RyR is regulated by numerous physiological agents (e.g., Ca^{2+} , Mg^{2+} , and ATP), large organic proteins and enzymes, various cellular processes (e.g., phosphorylation, oxidation, etc.), and exogenous compounds (e.g., ryanodine, neomycin, caffeine, and ruthenium red). Among the endogenous effectors, Ca^{2+} , Mg^{2+} , and ATP are key regulators of RyR's (Laver, 2010). Currently, four types of Ca^{2+} sensing sites have been identified on RyR. Two Ca^{2+} -activation sites are located in the luminal and cytoplasmic domains of RyR, along with two inhibitory sites on the cytoplasmic domains (Laver, 2010). Magnesium is a potent RyR channel inhibitor, whereas ATP stimulates RyR activation by luminal and cytoplasmic Ca^{2+} . The function of these three major ligands of RyR is briefly reviewed below.

1.6.5.1.1 Cytoplasmic Ca²⁺

Ca²⁺ is the most important cationic modulator of RyR activity. In the absence of other regulatory ligands such as Mg²⁺ and ATP, the activity of RyR has a bell-shaped dependence on cytoplasmic Ca²⁺ (Bull and Marengo, 1993; Chen et al., 1997; Chu et al., 1993; Copello et al., 1997; Fabiato, 1985; Fill et al., 1990; Jeyakumar et al., 1998; Laver et al., 1995; Ma et al., 1988; O'Brien et al., 1995; Percival et al., 1994; Sitsapesan and Williams, 1995; Smith et al., 1988; Tripathy and Meissner, 1996). RyR channels are activated by a micromolar Ca²⁺ concentration range (1-10 μ M), with a threshold for channel activation at approximately 100 nM. Exposure to high Ca²⁺ concentration (500 μ M -10 mM) inhibits the channels. The biphasic behavior is proposed to be produced by two classes of Ca²⁺ binding sites on the cytoplasmic side of RyR, a high-affinity activation site (*A* site, \sim 1 μ M affinity with both RyR1 and RyR2) and a low-affinity inhibition site (*I1*-site, \sim 200 μ M affinity with RyR1 and 10 mM with RyR2) (Laver, 2007; Meissner et al., 1986; Meissner et al., 1997). More recently a high-affinity inactivation site on RyR2 (*I2*-site, \sim 1.2 μ M affinity) has also been identified (Laver, 2007). However, the precise locations of these sites have not yet been determined (Laver, 2010). In resting muscle, cytosolic [Ca²⁺] ranges from 100-150 nM (Bers, 2001; Lopez et al., 2000; Perez et al., 2005), and rises to micromolar levels during contraction (\sim 20 μ M in skeletal muscle (Hollingworth et al., 1996) and 1 μ M in cardiac myocytes (Bers, 2001)). Although cytosolic Ca²⁺ regulates RyR1 and RyR2 in a similar way, i.e., a biphasic response, the two isoforms have different sensitivities to Ca²⁺. One of the most important differences is that RyR1 is almost entirely inhibited by 1 mM Ca²⁺, whereas RyR2 is less sensitive to inhibition by high Ca²⁺. RyR3 responds to cytosolic Ca²⁺ in a fashion more similar to that of RyR2 than RyR1. The reported RyR2 and RyR3 half-maximal inhibiting Ca²⁺ concentrations range from 2 to >10 mM. Such high cytoplasmic Ca²⁺ concentrations are unlikely to occur in cells, even in microdomains, and thus the physiological role of this Ca²⁺ inhibition is unclear. RyR1 cannot be fully activated by Ca²⁺ alone; whereas for RyR2 and RyR3 are, almost maximally activated by Ca²⁺ alone at \sim 100 μ M (reviewed in (Zissimopoulos and Lai, 2007)). Another difference is that RyR1 is functionally heterogeneous to activating cytoplasmic Ca²⁺ levels, whereas RyR2 and RyR3 channels are more homogeneous in their responses to cytosolic Ca²⁺ (Chen et al., 1997; Chu et al., 1993; Copello et al., 1997; Fill and Copello, 2002; Jeyakumar et al., 1998; Laver et al., 1995; Ma, 1995; Percival et al., 1994); this may be due to the different redox states of the isoforms (Marengo et al., 1998; Zissimopoulos and Lai, 2007).

1.6.5.1.2 Luminal Ca²⁺

Consistent results have been obtained in Ca²⁺ release studies showing that Ca²⁺ release is enhanced with increasing luminal [Ca²⁺] but decreased when the Ca²⁺ store is depleted in both intact muscle cells and skinned muscle fibers (Donoso et al., 1995; Lamb et al., 2001;

Lukyanenko et al., 1999). This store-dependent Ca^{2+} release suggests a distinctive regulation mode of the RyR channel by luminal Ca^{2+} . In support of this hypothesis, single channel bilayer studies of RyRs demonstrate the responsiveness of RyR to alterations in luminal $[\text{Ca}^{2+}]$ although with some discrepancies between different studies (see below) (Lamb et al., 2001; Laver et al., 2004; Sitsapesan and Williams, 1994b, 1995; Xu and Meissner, 1998). The total concentration of Ca^{2+} in the SR is estimated to be ~ 20 mM (Fryer and Stephenson, 1996); however, most of Ca^{2+} in the SR is bound to luminal Ca^{2+} buffering protein CSQ and other Ca^{2+} binding proteins in the SR, resulting in a resting free $[\text{Ca}^{2+}]_{\text{SR}}$ of around 1 mM (Bers, 2004; Fryer and Stephenson, 1996; Shannon et al., 2003; Szegedi et al., 1999). It is the free rather than total luminal Ca^{2+} that determines many aspects of the Ca^{2+} store's operation and creates the large Ca^{2+} gradient between the SR lumen (1 mM) and the cytoplasm (0.1 to 10 μM) which ensures efficient Ca^{2+} release.

Activation of single RyR channels by luminal Ca^{2+} was first demonstrated by Sitsapesan and Williams (1994b) with lipid bilayer studies. Despite many similar studies having followed, the mechanism supporting luminal Ca^{2+} regulation of the RyR and the locations of the RyR- Ca^{2+} binding sites and/or sensors remains to be clarified. Although recent works by Qin et al. (2009) have presented evidence that luminal Ca^{2+} does not regulate the RyR1 channels, there is general agreement that channel activity is augmented when luminal $[\text{Ca}^{2+}]$ is increased. This may be attributed to an increased sensitivity of the RyR channel to cytosolic agonists such as cytosolic Ca^{2+} , ATP, and caffeine, and an alleviation of Mg^{2+} inhibition (Gyorke and Gyorke, 1998; Sitsapesan and Williams, 1997). However arguments remain about the mechanism of effects of luminal $[\text{Ca}^{2+}]$. Furthermore, different profiles of changes in RyR activity as a function of luminal $[\text{Ca}^{2+}]$ (from nM to mM), i.e. activation, inhibition and biphasic, have been observed (Beard et al., 2005; Ching et al., 2000; Gyorke and Gyorke, 1998; Gyorke et al., 2004a; Gyorke et al., 2002; Herrmann-Frank and Lehmann-Horn, 1996; Laver et al., 2004; Qin et al., 2008; Sitsapesan and Williams, 1995; Szegedi et al., 1999; Tripathy and Meissner, 1996; Wei et al., 2009a; Wei et al., 2006). Nevertheless, it should be noted that in these studies, the luminal protein/protein interactions and the RyR macromolecular complex have not been generally taken into consideration.

The regulation of RyRs by luminal Ca^{2+} has a complex dependence on membrane potential and luminal $[\text{Ca}^{2+}]$ (Laver, 2007; Xu and Meissner, 1998) indicating both Ca^{2+} -dependent activation and inhibition mechanism (Tripathy and Meissner, 1996). Two mechanisms for RyR modulation by luminal Ca^{2+} have been proposed. The "true luminal" hypothesis proposes that luminal regulation involves Ca^{2+} binding site(s) on the luminal side of the RyR (Sitsapesan and Williams, 1995), which is supported by the evidence that tryptic digestion of the luminal domains of the RyR2 abolished luminal Ca^{2+} -activation, presumably destroying the Ca^{2+} sensing

site (Ching et al., 2000). On the other hand, the “feed-through” mechanism involves luminal Ca^{2+} permeating the pore and binding to cytosolic Ca^{2+} site, namely *A* site (Herrmann-Frank and Lehmann-Horn, 1996; Laver et al., 2004; Tripathy and Meissner, 1996; Xu et al., 1996b). It appears that either mechanism can operate under different conditions (Laver, 2007; Laver et al., 2004). Three modes of action associated with Ca^{2+} sensors are proposed: a luminal activation site (*L*-site, 40–60 μM affinity with RyR2) (Laver, 2007; Laver and Honen, 2008), a cytoplasmic activation site (*A* site) and cytoplasmic inactivation *I2*-site (see section 1.6.5.1.1). It is proposed that luminal Ca^{2+} -activation is a multistep process. The initial Ca^{2+} binding to the *L* site triggers brief channel openings (~1 ms duration at rates of 1-10 s^{-1}), which allows luminal Ca^{2+} to access the *A*-site, producing up to 30-fold prolongation of openings; furthermore, the cytoplasmic Ca^{2+} -inactivation site (*I2*-site) causes a reduction in channel open durations at high levels of Ca^{2+} feed-through. In addition luminal Ca^{2+} has been shown to regulate Ca^{2+} release from RyRs by (a) modifying the *A*-site affinity for cytoplasmic Mg^{2+} through a noncompetitive and allosteric mechanism (Laver et al., 2004) and (b) potentiating the RyR2 gating in the presence of ATP, predominantly by binding to a luminal site with an affinity in the mM range (Tencerova et al., 2012).

It is also possible that luminal Ca^{2+} regulation is modulated by RyR accessory proteins. Multiple luminal Ca^{2+} sensors have been suggested: CSQ (section 1.7) is one of the candidates (Beard et al., 2005; Gyorke et al., 2004a; Wei, 2008; Wei et al., 2009a; Wei et al., 2006). Indeed, by suppressing Ca^{2+} “feed-through”, two luminal Ca^{2+} regulatory mechanisms have been identified in RyR2 (Qin et al., 2008). One is a RyR2-resident, CSQ2-independent luminal Ca^{2+} mechanism that modulates the maximal efficacy of cytosolic Ca^{2+} activation. However, it does not distinguish between luminal Ca^{2+} and Mg^{2+} , making the physiological relevance of this CSQ2-independent regulation uncertain. The other is a CSQ2-dependent luminal RyR2 Ca^{2+} regulation mechanism which does discriminate between luminal Ca^{2+} and Mg^{2+} . It has been suggested that this CSQ2-dependent mechanism alters the cytosolic Ca^{2+} sensitivity of the channel and the Ca^{2+} -dependent CSQ2-triadin interaction is likely the key luminal Ca^{2+} -sensing step (Qin et al., 2008). Furthermore, this second CSQ2-dependent mechanism is dependent on the presence or the absence of cytosolic Mg^{2+} and ATP (Chen et al., 2013) (see section 1.7.3.3). In addition, it has been shown by Qin et al. (2009) that CSQ-dependent luminal Ca^{2+} regulation of RyR2 lacks CSQ isoform specificity, as both CSQ1 and CSQ2 regulated RyR2 in a similar way (Qin et al., 2009). Curiously, in contrast to RyR2, no CSQ1-dependent luminal Ca^{2+} regulation of RyR1 channels was detected in the same study (Qin et al., 2009). Another accessory protein, junctin (section 1.9), is also implicated in this luminal Ca^{2+} -sensing process (Chen et al., 2013; Gyorke et al., 2004a; Wei et al., 2009a). A recent study by Altschafel et al. (2011) also suggests that junctin may affect the RyR2’s sensitivity to luminal Ca^{2+} . In general, more investigations are required to elucidate the precise mechanism of luminal Ca^{2+} regulation and luminal Ca^{2+} sensors.

In cardiac muscle, luminal Ca^{2+} also contributes to the initiation and termination of inter-RyR2 Ca^{2+} -induced Ca^{2+} release (Chen et al., 2013; Laver et al., 2013; Terentyev et al., 2002). In skeletal muscle, luminal Ca^{2+} modulates coupled gating of RyR1s (Laver et al., 2004; Porta et al., 2012).

1.6.5.1.3 Magnesium

As a potent inhibitor of RyRs, Mg^{2+} plays an important role in shaping both the cytosolic and luminal Ca^{2+} -dependence of RyR activity in the cell (Laver and Honen, 2008; Meissner and Henderson, 1987). In the cytoplasm, magnesium (9 mM) is buffered by ATP (~8 mM) so that the free $[\text{Mg}^{2+}]_{\text{cyto}}$ is ~1 mM (Godt and Maughan, 1988). The free $[\text{Mg}^{2+}]$ in the SR has not been directly determined but is predicted to be similar to that in cytoplasm and approximately half that of free $[\text{Ca}^{2+}]_{\text{SR}}$ (between 0.7 and 1.0 mM) (Laver and Honen, 2008). RyR1 is inhibited by >500 μM cytoplasmic Mg^{2+} and completely inactivated by millimolar concentrations (reviewed in (Zissimopoulos and Lai, 2007)). Thus, cytoplasmic Mg^{2+} inhibition is believed to be crucial for maintaining RyR1 in a closed resting state. In contrast, RyR2 and RyR3 are much less sensitive to Mg^{2+} inhibition than RyR1 (reviewed in (Zissimopoulos and Lai, 2007)). The mechanism by which Mg^{2+} inhibits the RyR channel activity is complicated. As yet, three forms of Mg^{2+} -inhibition have been identified which involve the binding of Mg^{2+} to the A-, L- and I1- Ca^{2+} sensing sites on the RyR. Mg^{2+} can inhibit RyRs by: (a) Mg^{2+} competing with Ca^{2+} for the activation site (A site) and acting as a RyR antagonist in the absence of Ca^{2+} (Laver et al., 2004); (b) Mg^{2+} binding to the low affinity inhibition site (I1-site) as a surrogate for Ca^{2+} , both (a) and (b) cause channel closure; and (c) a recently discovered luminal Mg^{2+} -inhibition mechanism, which involves Mg^{2+} displacing Ca^{2+} from the L-site and then Mg^{2+} flowing through the channel and binding to the A-site, thus terminating channel opening (Laver and Honen, 2008). The affinity of Mg^{2+} for A site is approximately 40-1000 fold lower than that of Ca^{2+} (Laver et al., 1997b; Meissner et al., 1986), while the affinities of I1- and L-sites for Mg^{2+} are identical to that for Ca^{2+} (I1-site: ~200 μM with RyR1 and ~10 mM with RyR2; L-site, ~40 μM with RyR2) (Laver et al., 1997a; Laver and Honen, 2008; Laver et al., 2004; Laver et al., 1995); the very low affinity for the I1-site in RyR2 also explains the low sensitivity of RyR2 to Mg^{2+} inhibition and accordingly, Mg^{2+} should play only a minor inhibitory role at physiological concentrations (~1 mM) in cardiac muscle. In contrast, intracellular Mg^{2+} (~1 mM) can exert a powerful inhibitory effect on RyR1 at rest. Consequently, in skeletal EC coupling, RyR1 cannot be activated simply by Ca^{2+} binding to the A site. Both luminal and cytoplasmic Mg^{2+} inhibition can be alleviated by increasing $[\text{Ca}^{2+}]_{\text{l}}$ or $[\text{Ca}^{2+}]_{\text{c}}$ (Laver and Honen, 2008). In addition in skeletal muscle, Mg^{2+} inhibition can be relieved by depolarization of the surface membrane (Lamb, 1993; Lamb and Stephenson, 1991). More recently, a study by Porta et al. (2012) has indicated that Mg^{2+} , together with ATP and high luminal $[\text{Ca}^{2+}]_{\text{l}}$, is required for the coupled

gating of RyR1s, and that ATP alone was not as effective as ATP/Mg²⁺ in allowing coupled gating.

1.6.5.1.4 Adenine nucleotides

Adenine nucleotides, including ATP, are major modulators of Ca²⁺ release channel function. Cytoplasmic ATP acts as both an energy source for muscle function and an effective RyR activator, both at rest and during EC coupling (Meissner et al., 1986; Rubtsov and Batrukova, 1997). At concentrations above 1 mM, ATP exerts its near-maximal action on the RyR. Other adenine nucleotides also enhance RyR channel activity but to a lesser extent, with a potency of AMP-PCP > cyclic-AMP (c-AMP) > ADP > AMP (Kermode et al., 1998; Laver et al., 2001; Meissner et al., 1986). In the cytoplasm, the resting concentration of ATP is around 6-8 mM, with most of the ATP existing in a Mg²⁺-bound form (Sonnleitner et al., 1997). The three RyR isoforms exhibit distinct patterns of modulation by ATP (Laver, 2010; Zucchi and Ronca-Testoni, 1997). Single channel experiments show that ATP's effect on RyR2 is less remarkable than its effect on RyR1s (Meissner and Henderson, 1987; Xu et al., 1996a); ryanodine binding assays confirm that ATP sensitivity is lower in cardiac muscle than in skeletal muscle (Michalak et al., 1988; Zimanyi and Pessah, 1991). In cardiac RyRs, ATP promotes channel activation by Ca²⁺ but cannot open the channel in the absence of Ca²⁺ (reviewed in (Laver, 2010)). Cardiac RyR activation by ATP is controlled by luminal Ca²⁺ levels: low [Ca²⁺]_{lum} (1 mM) enhance the affinity of RyR2 for ATP, but ATP does not activate the channel; at higher [Ca²⁺]_{lum} (8-53 mM, which is outside the physiological range encountered during normal Ca²⁺ cycling), the activation effect of ATP on RyR2 is markedly amplified without altering the affinity of RyR2 for ATP (Tencerova et al., 2012). In contrast, ATP augments skeletal RyR's activity in a Ca²⁺-independent manner and a combination of millimolar ATP and micromolar cytoplasmic Ca²⁺ elicits persistent channel activation (Meissner et al., 1986). ATP also enhances RyR3 channel activity and overcomes inhibition by millimolar Ca²⁺ (Chen et al., 1997; Manunta et al., 2000). The isoform-specific modulation by ATP partly underlies the varied characteristics of the Ca²⁺ release mechanisms found in different muscle types (reviewed in (Fill and Copello, 2002)). Several studies indicate that the activating effect of ATP occurs through direct binding to one or more sites on RyR1 that function cooperatively in the tetrameric channel (Hohenegger et al., 1995; Lai et al., 1988; Meissner, 1984). Covalent photo-reactive labeling demonstrates that three regions in RyR1 are involved in ATP-binding (Popova et al., 2012). These regions are widely separated in the primary structure of RyR1. The putative ATP-binding to conserved motifs within residues 427-1302 (fragment 8) provide a structural basis for the ATP binding pocket; and two other fragments 15 and 11 (residues 2402-2795 and 4476-5037 respectively) could either participate in the conformational arrangement of the same ATP binding pocket or constitute non-canonical ATP binding sites in RyR1 (Popova et al., 2012).

1.6.5.2 RyR interaction with luminal proteins

In all muscle types, RyR forms the center of a large multi-protein complex, including extracellular, cytoplasmic and SR luminal components linked by transmembrane entities, which together enable the RyR complex to sense the environment in each compartment (whether extracellular, cytoplasmic, or SR lumen) and to properly regulate intracellular Ca^{2+} release. Luminal proteins associated with RyR include calsequestrin (CSQ), the major luminal Ca^{2+} binding protein, and junctin and triadin, the anchoring proteins which link CSQ to RyR, and themselves modulate RyR activity, thereby playing a role in controlling Ca^{2+} release from the SR. The molecular interactions between CSQ, junctin, triadin, and RyR in the SR lumen may facilitate changes in Ca^{2+} release in response to alterations in SR Ca^{2+} load, and are believed to be of fundamental importance to Ca^{2+} homeostasis, as manipulation of the expression levels of any of the proteins can lead to massive adaptive changes. Additionally, several other Ca^{2+} binding proteins and small molecules are also present in the SR lumen and play a role in RyR regulation and Ca^{2+} homeostasis, e.g., histidine-rich Ca^{2+} binding (HRC) protein, sarcalumenin (SLM), junctate, JP-45, and CSQ-like proteins. Subsequent sections will focus on the major luminal regulators of both skeletal and cardiac RyR: CSQ, junctin and triadin.

1.7 CSQ

Calsequestrin, or CSQ, was first isolated from the SR of rabbit skeletal muscle in the early 1970s (Ikemoto et al., 1972; MacLennan and Wong, 1971; Meissner et al., 1973), and was identified as a major Ca^{2+} storage and buffering protein of approximately 400 residues with a molecular weight of ~44 kDa. This skeletal isoform of CSQ has since been referred to as CSQ1. A few years later, another CSQ isoform was identified in cardiac tissue (Campbell et al., 1983) and termed CSQ2. Structural studies have shown that CSQ is concentrated in the proximity of the SR junctional face on which RyR arrays can be found (Campbell et al., 1983; Saito et al., 1984), where it appears as an electron dense matrix in the SR lumen. Deep-etch electron microscopy reveals the presence of thin strands, or anchoring filaments – likely to be triadin and junctin – that seem to connect CSQ to the SR (Franzini-Armstrong et al., 1987). CSQ is by far the most abundant Ca^{2+} -binding protein in the SR of both skeletal and cardiac muscle. CSQ binds Ca^{2+} with a high capacity (40-50 mol Ca^{2+} mol⁻¹ CSQ) and either a low or moderate affinity ($K_d \sim 1$ mM) depending on the isoform under consideration (reviewed in (Beard et al., 2004)). The high storage capacity of CSQ allows SR-stored Ca^{2+} to reach levels of up to 20 mM while the free Ca^{2+} concentration remains sufficiently lower at ~1 mM. The stored Ca^{2+} enables frequent muscle contraction with minimal run-down in Ca^{2+} available for release and in tension – both being essential for the maintenance of movement.

CSQ is highly hydrophilic and acidic, with roughly 30% of its residues acidic, and a commensurate isoelectric point (pI) of ~3.75 (Slupsky et al., 1987). The carboxyl-terminal domain contains the highest surface negative charge density. An aspartate-rich region (residues 354-367 in rabbit CSQ1) at the C-terminus is the major Ca^{2+} binding motif of CSQ – and also interacts with “KEKE” motifs present in triadin and possibly junctin (see section 1.8 and 1.9), perhaps by forming a polar zipper-like structure (Kobayashi et al., 2000; Shin et al., 2000). It is therefore currently accepted that the C-terminus of CSQ constitutes the region which binds Ca^{2+} , triadin and/or junctin.

1.7.1 CSQ gene, isoforms

The two mammalian isoforms of CSQ1 and CSQ2 are encoded by two different genes (Fliegel et al., 1990; Scott et al., 1988). CSQ1 is the sole isoform found in fast-twitch skeletal muscle and the major isoform found in slow-twitch skeletal muscle, while CSQ2 is the only isoform expressed in the heart and a minor component in slow-twitch muscles (Fliegel et al., 1990; Lahat et al., 2001; Paolini et al., 2007; Scott et al., 1988). In addition, CSQ is expressed in smooth muscle, the cerebellum, and plant cells (Krause et al., 1989; Volpe et al., 1990; Volpe et al., 1994).

There is a high degree of sequence homology (from 74% to 98%) between the skeletal and cardiac CSQ in a number of different species (reviewed in (Beard et al., 2004), suggesting a structural similarity. One major difference between the two isoforms can be found in their C-terminal domains. Compared with skeletal isoform, the cardiac isoform has an extended C-terminus (residues 367-391), composed of 71% acidic residues. Curiously however, Ca^{2+} binding to CSQ2 is 50% lower than to CSQ1 and, as $[\text{Ca}^{2+}]$ increases from the nM to the mM range, CSQ2 undergoes fewer conformational changes than does CSQ1 (Cozens and Reithmeier, 1984; Ikemoto et al., 1972; Ikemoto et al., 1974; Ostwald et al., 1974; Park et al., 2004; Slupsky et al., 1987; Wei et al., 2009b). The difference in sequence between the two isoforms is very likely to underlie their differing behaviours, and this may in turn explain the isoform-specificity of CSQ's regulation of RyRs ((Wei et al., 2009b) and section 1.7.3.3).

1.7.2 CSQ structure and Ca^{2+} -binding properties

The crystal structure of CSQ1 derived from rabbit skeletal muscle was determined in the late 90s, at a resolution of 2.4 Å (Wang et al., 1998). The CSQ monomer is composed of three almost identical disk-like domains, each with a compact thioredoxin-like fold with four α -helices surrounding a β -sheet core which is stable in the presence of Ca^{2+} . Each domain is hydrophobic due to high aromatic amino acid content. However, a great number of acidic residues on the exterior domain surfaces ensure an overall electronegative potential. The three

domains are connected by short inter-domain loops, which also contain many acidic residues. The arrangement of these three domains of the CSQ monomer provide it with a characteristic acidic and hydrophilic center, which is important in allowing cation binding to CSQ which then neutralizes charge repulsion and stabilizes CSQ's conformation. The crystal structure of both canine and human cardiac CSQ has subsequently been found to be very similar to that of rabbit skeletal CSQ (Kim et al., 2007; Park et al., 2004).

In general, CSQ exists either as a monomer or as CSQ polymers with a wide range of molecular masses, depending on the local ionic strength and Ca^{2+} concentration (Kim et al., 2007; Park et al., 2004; Park et al., 2003). Increasing $[\text{Ca}^{2+}]$ promotes CSQ polymerization, which in turn further increases CSQ's Ca^{2+} -binding capacity (Wang et al., 1998); conversely, K^+ inhibits this process by inducing CSQ folding. Changes in pH may also be an important regulator of CSQ polymerization. A substantial amount of evidence shows radical changes in the structure of CSQ upon Ca^{2+} binding (reviewed in (Beard et al., 2004; Novak and Soukup, 2011)). Briefly, when Ca^{2+} is absent, CSQ is highly extended, with about 11% α -helical content in CSQ1 and ~3.5% α -helical content in CSQ2 (Cozens and Reithmeier, 1984; Ikemoto et al., 1972; Ikemoto et al., 1974; Ostwald et al., 1974). Ca^{2+} binding induces CSQ compaction, causing a loss of overall hydrophobicity with decreases in conformational asymmetry and increases in the protein α -helical content (20-35% in CSQ1 and 10.9% in CSQ2 at 1 mM Ca^{2+}) (Cozens and Reithmeier, 1984; Ikemoto et al., 1972; Ostwald et al., 1974). The polymer forms as more Ca^{2+} ions bind to CSQ. It is believed that the structural changes CSQ undergoes upon binding Ca^{2+} lead to a compact form which is required for high capacity Ca^{2+} binding (He et al., 1993). Moreover, Ca^{2+} binding to CSQ prevents other proteins from interacting with CSQ – for example, triadin and junctin – and further helps protect CSQ from proteolytic digestion (Mitchell et al., 1988; Ohnishi and Reithmeier, 1987).

Wang et al. (1998) predicted that two types of interactions are required for CSQ polymerization – front-to-front dimerization and then back-to-back packaging, which generate linear polymers. Deletion mutation studies confirm the involvement of both the N- and C-termini of the monomer in front-to-front and back-to-back interactions respectively (Bal et al., 2010; Gatti et al., 2001; Park et al., 2003). Furthermore, the front-to-front interaction occurs prior to back-to-back interaction as the N-terminal arm has fewer charged amino acid residues than the C-terminal tail and thus requires less cations to shield the acidic residues (Park et al., 2003). It was proposed that an increase in $[\text{Ca}^{2+}]$ to ~10 μM causes CSQ monomer compaction and further increases to between 10 μM and 1 mM lead to dimerization and thence polymerization (Beard et al., 2004). Studies by Wei *et al.* (Wei, 2008; Wei et al., 2009b) demonstrated that CSQ1 and CSQ2 are monomeric at 0.1-100 μM $[\text{Ca}^{2+}]$, and with a physiological $[\text{Ca}^{2+}]$ of 1 mM, CSQ1 is mostly polymerized while CSQ2 is still mostly monomeric/dimeric. Park et al. (2003) proposed

that regulation of $[Ca^{2+}]$ by CSQ involves an interplay between protein folding, Ca^{2+} binding, and CSQ polymerization. Additionally, the differences between the skeletal and cardiac CSQ's disposition in the jSR (Franzini-Armstrong, 2009) and functional domains has been suggested to be likely consequent to the ratio of CSQ to triadin and junctin. These authors also concluded that the clustering of CSQ in the junctional domain of SR required a specific interaction of CSQ with triadin and junctin, and further, that this interaction also defined the specific architecture of CSQ (Franzini-Armstrong, 2009). Recent results obtained both *in vivo* (living cell image analysis) and *in vitro* strongly suggest that the presence of junctin is required for depolymerization of CSQ upon Ca^{2+} depletion, and therefore that direct interactions between junctin and CSQ are necessary for CSQ-mediated control of $[Ca^{2+}]$ in SR (Lee et al., 2012).

1.7.3 CSQ function

A considerable body of evidence supports the concept that CSQ plays at least two different roles in skeletal and cardiac myocytes (reviewed in (Beard et al., 2004; Beard et al., 2009; Gyorke et al., 2009; Gyorke and Terentyev, 2008; Knollmann, 2009; Novak and Soukup, 2011)). This is mostly derived from experiments using knockouts and mutations which express different levels of CSQ isoforms, in addition to reconstitution into lipid bilayers. As a Ca^{2+} buffer in the SR lumen, CSQ supplies the bulk of Ca^{2+} and participates actively in muscle contraction by localizing Ca^{2+} near its points of release and regulating the amount of Ca^{2+} released through the RyR channel. At the same time, it helps keep the free Ca^{2+} concentration relatively low, thus allowing more efficient inward transport by the sarco/endoplasmic reticulum calcium ATPase (SERCA) pumps. On the other hand, CSQ serves as a modulator of SR Ca^{2+} release channel activity, either directly or via triadin/junctin, in a luminal Ca^{2+} -dependent manner, potentially by acting as luminal Ca^{2+} sensor for RyR. Whether this modulation is an essential component of EC coupling remains to be determined (Beard et al., 2005; Dulhunty et al., 2006; Gilchrist et al., 1992; Gyorke et al., 2004b; Terentyev et al., 2006; Terentyev et al., 2003; Toyoshima and Inesi, 2004). The impact of CSQ on RyR channel activity is still under debate as both activation and inhibition by CSQ have been reported, regardless of which CSQ isoform is under consideration (for more detail, see section 1.7.3.3).

1.7.3.1 Changes in CSQ expression in genetic mice models and myocytes

1.7.3.1.1 Overexpression

Transgenic mouse hearts expressing 10 to 20-fold higher levels of either canine or murine cardiac CSQ develop cardiac hypertrophy and heart failure, due to enlargement of ventricular myocytes, impairment of Ca^{2+} release from SR, and a decrease in Ca^{2+} spark frequency (Jones et al., 1998; Knollmann et al., 2000; Sato et al., 1998; Wang et al., 2000). A marked increase in the

SR Ca^{2+} content was observed in cardiac myocytes in these studies, consistent with the theory that SR Ca^{2+} storage capacity increases with CSQ2 overexpression. The reason for depressed Ca^{2+} transient and contractility may be explained by the excess CSQ2 binding more Ca^{2+} , leading to a reduction in free Ca^{2+} available in the SR for release. Furthermore the overexpression of CSQ results in a considerable widening of the jSR cisternae and an altered appearance of its contents, which become more finely granular and diffuse (Jones et al., 1998; Tijssens et al., 2003). This is ascribed to excess CSQ2 not binding to the membrane via triadin or junctin and therefore acquiring a more diffuse disposition (Franzini-Armstrong et al., 2005). In addition, chronic CSQ2 overexpression induces adaptation by altering the expression of other proteins. RyR, triadin, and junctin expression levels can be downregulated (Jones et al., 1998), while Ca^{2+} -ATPase and phospholamban can be increased (Sato et al., 1998). The changes make it difficult to attribute the changes in myocyte structure and function solely to CSQ2.

Two acute overexpression studies have been performed to minimize the impact of adaptive developmental responses in the whole animal (Miller et al., 2005; Terentyev et al., 2003). Overexpression of CSQ2 generated by adenovirus-mediated transfection of cardiomyocytes by a factor of $\sim 4 \times$ over 48-56 h resulted in proportional increases in the SR Ca^{2+} load, SR Ca^{2+} release, and a prolongation of the release phase. This suggested that the inactivation of RyR2 was delayed by the buffer action of CSQ2, although no specific inhibitory action of CSQ2 on RyR2 was observed (Terentyev et al., 2003). A limited increase in CSQ2 (~ 1.6 -fold) expression led again to an increase in SR Ca^{2+} levels, but reduced EC coupling (Miller et al., 2005). This latter result was observed in one transgenic mouse model (Jones et al., 1998; Sato et al., 1998), although not in others (Terentyev et al., 2003). While discrepancy exists among these various studies, in general, most of the results suggest an inhibitory effect of CSQ2 on RyR2 activity, and as a Ca^{2+} storage protein.

In contrast to CSQ2, overexpression of skeletal CSQ1 in cultured mouse C2C12 myotubes led to an enhancement in caffeine- and voltage-induced Ca^{2+} release, associated with an increase in the SR Ca^{2+} load (Shin et al., 2003). The differences between the skeletal and cardiac models may be due to specific Ca^{2+} signaling modulation by the skeletal and cardiac CSQ and RyR isoforms (Wei et al., 2009b). A profound depression of store-operated Ca^{2+} entry (SOCE) was also observed in the CSQ1 overexpression model, indicating the participation of CSQ1 in the regulation of SOCE in skeletal muscle; this CSQ-mediated inhibition of SOCE was attributed to the C-terminal aspartate-rich tail, since overexpression of CSQ1 without this region did not alter SOCE (Shin et al., 2003). Importantly, this aspartate-rich region is necessary for Ca^{2+} binding/CSQ polymerization, as well as for interacting with triadin and/or junctin (Shin et al., 2000). In agreement with the Shin study (Shin et al., 2003), CSQ1-knockdown skeletal muscle fibers exhibits significant elevation in SOCE (Zhao et al., 2010).

1.7.3.1.2 Down-regulation

Despite the important functions ascribed to CSQ, the genetic ablation of CSQ1, CSQ2, or both is not birth-lethal in mouse models. Initial evidence from null CSQ mutations in *C. elegans* wall muscles (which express a single CSQ isoform) (Cho et al., 2000) also suggests that CSQ is not essential for muscle function. Knollmann et al. (2006) characterized the first CSQ2 knockout mouse as a model for CPVT associated with CSQ mutations. CSQ2-null mice are viable and maintain relatively normal Ca^{2+} release, myocyte contractile function, and SR Ca^{2+} load under basal conditions, although they exhibit an increase in SR volume and a near absence of triadin-1 and junctin. So far, there is no consensus on the mechanism which compensates for CSQ-ablation, although SR Ca^{2+} storage capacity is preserved (Knollmann, 2009). One possibility is that changes in expression of other SR proteins such as triadin and junctin increase the SR Ca^{2+} content by affecting Ca^{2+} release through RyR2s. In support of this, homozygous CSQ2 nonsense mutations in humans do not alter contractile function (Postma et al., 2002). However, myocytes show significantly increased SR Ca^{2+} leak when exposed to isoproterenol, a drug used to induce CPVT (Knollmann, 2009; Knollmann et al., 2006). Loss of CSQ2 is thus suggested to contribute to an increased risk of triggered arrhythmia, but may paradoxically protect against reentrant-type arrhythmia (Kornyejev et al., 2012). Thus, it appears that CSQ2 is not essential for cardiac Ca^{2+} storage, but protects the heart against premature Ca^{2+} release and triggered arrhythmias. Together with triadin, CSQ2 seems important for the structural organization of the SR.

Considerable evidence has shown that $[\text{Ca}^{2+}]$ in the SR lumen regulates RyR (see section 1.6.5.1.2) and that the rate of SR Ca^{2+} leak is proportional to SR luminal $[\text{Ca}^{2+}]$ in a nonlinear fashion (Gyorke and Gyorke, 1998; Gyorke et al., 2002; Lukyanenko et al., 1996; Lukyanenko et al., 2001; Shannon et al., 2002; Terentyev et al., 2002). Ablation of CSQ2 results in a steeper relationship between SR Ca^{2+} leak and Ca^{2+} content in the SR, increasing the overall probability of spontaneous Ca^{2+} release at lower load levels (Dulhunty et al., 2012; Knollmann et al., 2006). Heterozygous CSQ2-KO mice with only a modest (~25%) reduction in CSQ2 also have a steeper SR Ca^{2+} content-SR Ca^{2+} leak relationship (Chopra et al., 2007; Chopra and Knollmann, 2009). Hearts lacking CSQ2 demonstrate a larger SR Ca^{2+} release triggered at the same free intra-SR Ca^{2+} concentration (Kornyejev et al., 2012). These results support a role for CSQ2 in luminal RyR2 regulation, which is in addition to its role in global SR Ca^{2+} buffering. However, it remains uncertain whether the loss of RyR2 regulation is due to the reduction in levels of CSQ2 itself or to changes in expression of proteins mediating CSQ2's binding to RyR2 channels, i.e., triadin and junctin (Gyorke et al., 2004a; Wei et al., 2009b). The greater Ca^{2+} release with lower luminal Ca^{2+} load following CSQ2 deletion or reduction may underlie the triggered beats in CSQ2-null myocytes, and the ventricular tachycardia observed *in vivo*

(Faggioni and Knollmann, 2012; Knollmann, 2009). Restoring CSQ2 in CSQ2-null mice by viral gene transfer restored normal levels of both triadin and junctin, rescued electrophysiological and ultrastructural abnormalities, and prevented life-threatening arrhythmias (Denegri et al., 2012)

Extensive work has also been done with CSQ1-null mice. The first knockout mouse lacking CSQ1 was generated and characterized in 2007 (Paolini et al., 2007). Under standard housing conditions, CSQ1-null mice are viable and fertile, capable of muscle contraction, and develop normally, in spite of muscle atrophy. However, there are changes in both the EC coupling apparatus and the intracellular Ca^{2+} flux in CSQ1-null mice; more evident in fast-twitch muscles (EDL) than slow-twitch muscles (soleus), likely because soleus expresses CSQ2. Lack of CSQ1 alters the ultrastructure by a) proliferation of SR junctional domains; b) reducing the size of SR terminal cisternae; c) increasing the density of Ca^{2+} -release channels (RyR); and d) increasing numbers of mitochondria. This demonstrates the importance of CSQ1 in the correct assembly of calcium release units (CRUs) and for the geometry of the SR in mature fast twitch fibers. In the knockout animals, twitch force is preserved; although characterized by a prolonged time course, reflecting slower Ca^{2+} re-uptake by the SR. CSQ1 knockout also leads to an increased SR Ca^{2+} depletion rate and the inability of muscles to sustain tension during a prolonged tetani. Thus, CSQ1 is indispensable for normal SR and CRU development and for the storage and release of appropriate amounts of SR Ca^{2+} . Contractile function in CSQ1-null mice under normal conditions may be due to adaptive changes in muscle structure and protein composition. It should be noted that in this study (Paolini et al., 2007), there was a relatively small reduction in electrically evoked Ca^{2+} transients and the total amount of releasable Ca^{2+} in the SR; similar unexpected findings were also reported in other skeletal studies (Royer et al., 2010; Wang et al., 2006) and in the cardiac field (Knollmann, 2009; Knollmann et al., 2006), suggesting that a means of Ca^{2+} storage unrelated to CSQ must play a key role in muscle – at least in the CSQ1-null animals. The experiments confirm the role of CSQ as a Ca^{2+} storage device, though this role may not be as critical as was previously thought.

Although CSQ1 ablation does not appear to impair motor activity under normal conditions, surprisingly, male CSQ1-null mice displayed a significantly increased incidence of spontaneous mortality and are susceptible to halothane- and heat-induced sudden death (Dainese et al., 2009), the phenotype of malignant hyperthermia (MH) and environmental heat stroke (EHS) in humans and animal models. Both this study and the work done by Royer et al. (2010) support the proposed role of CSQ1 as a luminal Ca^{2+} sensor that inhibits RyR-mediated SR Ca^{2+} release (Beard et al., 2002; Wei et al., 2006). The authors of these three articles argue that loss-of-function mutations in CSQ1 strongly enhanced MH and EHS susceptibility in mice, providing evidence that disruption in the regulation of RyR by CSQ1 represents a novel pathogenic

mechanism that underlies skeletal muscle (MH and EHS) diseases (Dainese et al., 2009; Protasi et al., 2011; Protasi et al., 2009), analogous to CSQ2 and CPVT.

These studies (Dainese et al., 2009; Paolini et al., 2007) indicate a perturbation in calcium handling in the cell. To address the nature of the calcium dysregulation, CSQ1-KO and CSQ1/CSQ2-null (i.e., CSQ-double KO, DKO) mice were generated and free $[Ca^{2+}]$ inside the SR of flexor digitorum brevis (FDB) was measured directly using a targetable ratiometric FRET-based calcium indicator (Canato et al., 2010). While no obvious difference in free SR $[Ca^{2+}]$ at rest was observed between WT, CSQ1-KO and CSQ-DKO fibers, ablation of CSQ (either CSQ1 alone or both CSQ1 and CSQ2) led to dramatic decrease in intraluminal free SR Ca^{2+} during electrical stimulation and a concomitant depletion of the SR Ca^{2+} store. In contrast, changes in the WT were small during sustained contraction, reflecting the potent buffering capabilities of CSQ.

Changes in CSQ1-null mice could be caused either by CSQ1 depletion or by adaptive changes that mask CSQ1 function. Reconstitution of CSQ1 in FDB fibers from CSQ1-null mice restored Ca^{2+} storage capacity and prevented SR depletion, showing that the SR Ca^{2+} storage ability and proper coordination of Ca^{2+} release and reuptake both require CSQ1. In addition, the terminal cisternae (TC) lumen was filled with electron dense matrix referable to CSQ, and its width was increased to that of WT fibers. The results support the crucial role of CSQ1 in both Ca^{2+} homeostasis and TC structure (Tomasi et al., 2012).

1.7.3.2 CSQ polymorphism

Catecholaminergic polymorphic ventricular tachycardia (CPVT) is an inherited arrhythmogenic condition. The disorder manifests at a young age and is characterised by syncope events, seizures, and sudden cardiac death following exercise or emotional stress, without any gross structural changes of the myocardium. The disease has been related to mutations in the cardiac RyR2, cardiac CSQ2 or triadin (Trisk 32) (Roux-Buisson et al., 2012), with RyR2 mutation being most commonly linked to this disease. CSQ2-linked CPVT accounts for 3-5% of all CPVT cases (Faggioni and Knollmann, 2012), and the mutations in CSQ are autosomal recessive. To date, 15 mutations in the CSQ2 gene have been associated with CPVT, including missense, nonsense, deletion, or frameshift mutations which may deplete CSQ2 in the SR (Faggioni and Knollmann, 2012). Various CSQ2 mutations likely act through at least two different mechanisms to induce arrhythmia: a) altering the Ca^{2+} storage and buffering function of CSQ2 and b) changing the way in which RyR2 is modulated by CSQ2, e.g., by affecting the interactions of CSQ2 with the RyR2 complex (Gyorke and Terentyev, 2008). Specifically, the CSQ2 D307H mutant prevented Ca^{2+} -dependent conformational changes, disrupted Ca^{2+}

binding to CSQ, and led to a failure of CSQ to bind normally to triadin and junctin (Houle et al., 2004).

CSQ1 gene polymorphisms have been associated with type 2 diabetes. The gene is encoded on chromosome 1q21, a region that has been linked to type 2 diabetes in diverse populations (Fu et al., 2004). More than ten single nucleotide polymorphisms (SNP) have been identified, each encoding a single missense, deletion, or insertion (Das et al., 2004). Increased CSQ expression and calcium binding was reported in diabetic rat skeletal muscle, although not in their cardiac muscle (Howarth et al., 2002). Therefore, CSQ1 may play a potential role in diabetic susceptibility.

1.7.3.3 Effects of CSQ on RyR channel activity revealed by lipid bilayers study

The direct effect of CSQ on the kinetics of RyR channel opening and closing has been evaluated in single channel lipid bilayer. However, the molecular interactions between CSQ2 and RyR2 are currently less well-characterized than those of CSQ1 and RyR1.

CSQ1 inhibits native RyR1 in complex with triadin and junctin: the inhibition depends on luminal $[Ca^{2+}]$ and is mediated through junctin, though not triadin. In contrast, purified RyR1 channels (lacking triadin and junctin) are activated by CSQ1 (Beard et al., 2005; Beard et al., 2002; Wei et al., 2009a; Wei et al., 2006). At a physiological luminal $[Ca^{2+}]$ of 1 mM, CSQ1 in its polymer conformation inhibits RyR1 opening. This inhibition is lost after a 2-3 min exposure to $\leq 100 \mu M Ca^{2+}$, as CSQ1 depolymerizes, leaving only non-functional monomers remaining associated with the anchoring protein, e.g., triadin and/or junctin. The immediate effect of lowering luminal Ca^{2+} is reduction in activity which is maintained until CSQ depolymerizes. In contrast, while RyR1 is CSQ1 regulated, lowering luminal $[Ca^{2+}]$ either does not alter or rapidly reduces activity. Thus the CSQ polymer prevents excess Ca^{2+} release by reducing RyR activity when luminal $[Ca^{2+}]$ is transiently depleted (Wei et al., 2006). Higher $[Ca^{2+}]$ (≥ 3 mM) exposure for 3-5 min also results in the loss of inhibition, as CSQ1 becomes super-compacted and dissociates from triadin and junctin (reviewed in (Beard et al., 2009)). In conclusion the luminal Ca^{2+} dependence of the regulatory effects of CSQ1 supports the notion that CSQ may serve as a luminal Ca^{2+} sensor for RyR1 in a manner facilitated by junctin. Curiously, no action of either CSQ1 or CSQ2 on RyR1 channels has also been reported (Qin et al., 2009). This finding led the authors to believe that the CSQ1 primarily serves as an intra-SR Ca^{2+} buffer in skeletal muscle and not as a RyR1 regulator (Qin et al., 2009). Clearly, CSQ1-dependent RyR1 regulation warrants further investigation.

The regulation of RyR2 by CSQ2 is more controversial. Gyorke et al. (2004a) found a similar inhibitory effect of CSQ2 on RyR2 associated with luminal triadin and junctin, although no

inhibition was evident with CSQ2 added to purified RyR2. The observed inhibition was Ca^{2+} -dependent, i.e., it occurred at low (20 μM) but not at high (5 mM) luminal Ca^{2+} levels (Gyorke et al., 2004a). The inhibition was proposed to be transmitted through triadin (Qin et al., 2008; Terentyev et al., 2007) and possibly junctin. The purification of RyR2 led to a loss of its ability to respond to luminal Ca^{2+} , while re-association with both CSQ2 and the anchoring proteins restored RyR2's responsiveness to luminal Ca^{2+} . The results suggested that CSQ2 may have a role as a luminal Ca^{2+} sensor for RyR2, as proposed for CSQ1/RyR1 described above. However, studies by two other independent groups found that CSQ2 activates CSQ2-stripped native RyR2 channels with both 1 mM and lower luminal $[\text{Ca}^{2+}]$ generally in the physiological range (Qin et al., 2009; Qin et al., 2008; Wei et al., 2008; Wei et al., 2009b). The apparent discrepancy could be due to the experimental conditions, e.g., purified or native RyR2, the luminal $[\text{Ca}^{2+}]$, the presence or absence of cytosolic Mg^{2+} and ATP, etc. The issue has been further addressed in a recent study (Chen et al., 2013). WT-CSQ2 action on RyR2 function was determined by cytosolic MgATP. When endogenous CSQ had been removed from RyR2, adding exogenous WT CSQ2 in the presence of cytosolic MgATP decreased channel activity and reduced activation by cytosolic Ca^{2+} . The reconstituted WT CSQ2-RyR2 complex was insensitive to luminal Ca^{2+} between 0.1 and 1 mM. Conversely, when cytosolic Mg^{2+} and ATP were absent, the addition of CSQ2 increased RyR2 opening, and the same change in luminal $[\text{Ca}^{2+}]$ significantly increased RyR2 activity (Qin et al., 2008). Thus, CSQ association/dissociation was suggested to be a prominent RyR2 regulatory event *in vivo*. The absence of a luminal Ca^{2+} response in the presence of both Mg^{2+} and ATP, questions the role of CSQ2 as luminal Ca^{2+} sensor as Mg^{2+} and ATP reflect cellular cytoplasmic environment. Nevertheless, the CSQ2-KO RyR2 (with a concomitantly profound reduction in triadin and junctin levels) resulted in enhanced cytosolic Ca^{2+} sensitivity, and the observation that adding back CSQ(WT) to KO RyR2 did not fully restore WT-like function is consistent with normal CSQ2-RyR2 functional interactions requiring a normal complement of triadin/junctin to be present.

It should be noted that recent experiments in this laboratory (Hanna, Beard and Dulhunty, submitted for publication) show that sheep RyR2 channels maintain usual luminal Ca^{2+} sensitivity in the presence of MgATP, provided the luminal and cytoplasmic solutions are redox buffered with GSG:GSSG.

1.8 Triadin

Triadin, an integral SR membrane protein, is believed to serve as a CSQ anchoring protein that retains CSQ close to the JFM and in close proximity to the RyR, and has also been suggested to play a role in modulating RyR activity, in mediating functional EC coupling, and in maintaining Ca^{2+} homeostasis (Goonasekera et al., 2007; Gyorke et al., 2004a; Ohkura et al., 1998; Wei et al., 2009a). Triadin is localized to the junctional SR in skeletal and cardiac muscle (Brandt et al.,

1993; Caswell et al., 1991; Guo and Campbell, 1995; Knudson et al., 1993). It directly binds to RyR, CSQ, and junctin, most likely through its C-terminus (Guo and Campbell, 1995; Guo et al., 1996a; Zhang et al., 1997).

1.8.1 Gene and isoform

Triadin was first identified as a highly enriched 95-kDa protein of the junctional SR in rabbit skeletal muscle (Brandt et al., 1990; Caswell et al., 1991; Kim et al., 1990b), named Trisk 95 (Marty et al., 2000). It was subsequently discovered that several shorter triadin isoforms with masses of 32, 49 and 51 kDa (Trisk 32, Trisk 49 and Trisk 51, respectively) are also present in skeletal muscle (Marty et al., 2000; Vassilopoulos et al., 2005). Trisk 95 and Trisk 51 are the major triadin isoforms in skeletal muscle, and are equally expressed in rabbit, rat and mouse skeletal muscle (Marty et al., 2009; Marty et al., 2000). Curiously, in human skeletal muscle, where Trisk 95 and Trisk 51 are present, Trisk 51 is the predominant isoform while Trisk 95 is either not detectable (Thevenon et al., 2003) or makes up only 40% of the total triadin content (Marty et al., 2009). Both Trisk 95 and Trisk 51 are localized within the triad junction and colocalize with the RyR, while Trisk 49 and Trisk 32 are found in different parts of the longitudinal SR, and are not associated with the RyR.

As in skeletal muscle, multiple triadin isoforms are expressed in cardiac muscle (Peng et al., 1994). Three cardiac triadin isoforms are found in rabbit heart: triadin 1, triadin 2 and triadin 3 (at 35 kDa, 40 kDa and 92 kDa respectively on SDS-PAGE) (Carl et al., 1995; Guo et al., 1996b). The three cardiac isoforms are also referred to as CT1 (triadin 1), CT2 (triadin2) and CT3 (triadin 3) (Guo et al., 1996b). CT1 is the predominant isoform, while CT2, CT3 are expressed at substantially lower levels in rabbit heart (Guo et al., 1996b). Only two of the cardiac triadin isoforms (CT1 and CT3) are found in canine cardiac muscle, with CT1 again the predominant isoform. CT2 was found to be a glycosylated form of CT1 (Kobayashi and Jones, 1999). Subsequent studies revealed that similar triadin expression patterns are also present in rabbit, pig, human, rat and mouse cardiac muscle, with CT1 consistently the predominant isoform, and CT2 being a glycosylated form of CT1 (Kobayashi and Jones, 1999).

All of the skeletal and cardiac isoforms of triadin are alternative spliced products of the same gene (Oddoux et al., 2009; Shen et al., 2007; Thevenon et al., 2003). Shorter triadin isoforms are truncated versions of the longest isoform, Trisk 95 (composed of 706 residues), but each has its own unique C-terminal tail. Interestingly, skeletal Trisk 32 is identical to the cardiac CT1 of mice and rats (Marty et al., 2009; Vassilopoulos et al., 2005); further, it migrates as a triplet on SDS-PAGE, suggesting that like CT1, it is susceptible to glycosylation. Trisk 32/CT1 is the only isoform expressed in both skeletal and cardiac muscle. However, it should be noted that unlike Trisk 32, which localizes in the longitudinal SR in skeletal muscle as previously

mentioned, CT1 localizes in the junctional SR and associate with RyR2 in the heart (Guo et al., 1996b; Vassilopoulos et al., 2005).

1.8.2 Primary and secondary structure, KEKE motif

The secondary structure of triadin has been assessed via hydrophobicity analysis and biochemical assays with antibodies against specific regions. There is a consensus that the protein contains a short cytoplasmic N-terminal domain (residues 1-47), a single membrane-spanning helix (residues 48-68), and a long C-terminal tail in the SR lumen (Guo et al., 1996b; Knudson et al., 1993; Taske et al., 1995). In fact, all triadin isoforms, both skeletal and cardiac, share identical sequences over the first 250-260 residues (Guo et al., 1996b; Hong et al., 2001; Knudson et al., 1993; Kobayashi and Jones, 1999; Taske et al., 1995; Vassilopoulos et al., 2005). This common region encompasses the short cytoplasmic N-terminal domain, the transmembrane segment, and the first part of the luminal domain. Therefore, it is expected that all triadin isoforms share the same single transmembrane domain structure, but contain C-terminal tails of varying lengths.

Triadin is basic and has a high density of charged amino acids in its luminal domain. In particular, Trisk 95 is abundant in charged amino acids (44.2%), with 46 more basic residues than acidic residues, giving triadin a pI of 10.18 (Knudson et al., 1993). Even CT1, a much shorter isoform, contains ~42.5% charged amino acids (Guo et al., 1996b). There are multiple clusters of charged amino acids in the luminal domain, with alternating positive and negative charge, enriched in Lys and Glu/Asp residues (Jones et al., 1995). These mixed charge clusters are named "KEKE motifs" (Realini et al., 1994) and may be responsible for its interactions with CSQ, junctin, RyR and the histidine-rich Ca^{2+} binding protein (HRC) (Jones et al., 1995; Kobayashi et al., 2000; Zhang et al., 1997). Indeed, one of KEKE motif (residues 200-232 in Trisk 95 or 210-224 in CT1) is found to be important for Trisk 95 binding to RyR, CSQ and possibly HRC (Kobayashi et al., 2000; Lee et al., 2001; Lee et al., 2004) (for more detail see section 1.8.5). However, it remains to be determined whether the three proteins (RyR, CSQ and HRC) compete for identical residues or whether they can be accommodated simultaneously.

1.8.3 Post-translational modification

1.8.3.1 Disulfide bond formation

Trisk 95 contains two cysteine residues in its luminal domain, Cys²⁷⁰ and Cys⁶⁷¹ (Knudson et al., 1993), which allow it to form a disulphide-linked oligomer. All other isoforms lack the C⁶⁷¹ residue (Guo et al., 1996b; Hong et al., 2001; Kobayashi and Jones, 1999; Marty et al., 2000; Vassilopoulos et al., 2005). The cysteines are likely to form disulfide bonds with cysteines on neighbouring Trisk 95 monomers i.e. Cys²⁷⁰ binds Cys²⁷⁰ and Cys⁶⁷¹ binds Cys⁶⁷¹ (Fan et al.,

1995). Mutating either cysteine to alanine reduces the total number of Trisk 95 polymers, indicating that disulfide bridging between both cysteines is required to fully enable Trisk 95 polymerization. Polymerization of triadin is predicted to help maintain the structural integrity of junctional couplings (Froemming et al., 1999). Moreover, different isoforms may also bind and polymerize with each other, demonstrated by co-immunoprecipitation of Trisk 95 and Trisk 51 (Vassilopoulos et al., 2010).

On the other hand, CT1/Trisk 32 has its unique divergent region at the C²⁷⁰ location in Trisk 95 (Guo et al., 1996b; Hong et al., 2001; Kobayashi and Jones, 1999). Therefore it does not contain cysteine residues and does not polymerize. Indeed, none of the cardiac isoforms form multimers via disulfide bonding (Guo et al., 1996), despite the fact that CT3 contains the Cys²⁷⁰ residue.

1.8.3.2 Glycosylation

Initial sequencing identified four potential N-linked glycosylation sites on Trisk 95, two cytoplasmic (Asp⁹ and Asp²¹) and two luminal (Asp⁷⁵ and Asp⁶²⁵) (Knudson et al., 1993). It has been suggested that residue Asp⁶²⁵ is more likely to be modified by post-translational processing, i.e. glycosylation (Knudson et al., 1993); this is confirmed by Fan et al. (1995). The migration of expressed rat Trisk 51, which does not contain the equivalent Asp⁶²⁵ of rabbit Trisk 95, as a double band on SDS-PAGE unless deglycosylated suggests the existence of other glycosylation sites common to both Trisk 95 and Trisk 51 (Marty et al., 2000).

Cardiac triadin isoforms are also naturally glycosylated. For example, canine CT1 is ~50% glycosylated; CT2 is the glycosylated form of CT1 (section 1.8.1); and CT3, upon endoglycosidase-H treatment, shows a 4 kDa decrease in molecular weight, suggesting it is also glycosylated (Kobayashi and Jones, 1999). The glycosylation site of CT1 is Asp⁷⁵ (Kobayashi and Jones, 1999). Both glycosylated and unglycosylated triadin are present in substantial amounts in the heart, however unglycosylated triadin degrades rapidly via proteasome-dependent pathways (Milstein et al., 2008). Although the significance of this rapid degradation remains to be investigated, it has been proposed that the glycosylation state of triadin may be important for maintaining triadin levels (Milstein et al., 2008).

1.8.3.3 Phosphorylation

There are multiple potential phosphorylation sites on Trisk 95 (Knudson et al., 1993), only two of which (residues 15 and 35) are cytoplasmic. Trisk 95 is a substrate for the endogenous calmodulin-dependent protein kinase II (CaMKII) which is associated with the junctional SR (Damiani et al., 1995). A consensus CaMKII target sequence RXXS/T is located between residues 34 and 37 (in the cytoplasmic N-terminal domain) of triadin, and Thr³⁷ is thought to be the phosphorylation site (Colpo et al., 2001). It has been proposed that triadin modulates RyR1

in a phosphorylation-dependent manner (Colpo et al., 2001), since Thr³⁷ inhibits RyR channel activity (Damiani et al., 1995) and RyR inhibition by CaMKII is due to triadin phosphorylation (Hain et al., 1995). However, the physiological significance of triadin phosphorylation still awaits further investigation.

1.8.4 Over-expression and down-regulation

1.8.4.1 Over-expression

In cardiac muscle, targeted CT1 overexpression in both isolated cells and animal models has yielded confounding results. Overexpression of CT1 in rat ventricular myocytes results in reduced I_{Ca} -induced Ca^{2+} transients amplitude but with widened and flattened voltage dependency (i.e., small I_{Ca} at low and high depolarizations triggers maximal Ca^{2+} transients, and increased susceptibility to arrhythmia, all accompanied by a lower SR Ca^{2+} content (Terentyev et al., 2005). Correspondingly, the channel activity of RyR2 isolated from CT1 overexpressing myocytes is a ~5-fold increase in P_o . Therefore, it appears that triadin enhances cardiac EC coupling by directly stimulating RyR2 (Terentyev et al., 2005). On the other hand, a negative role of triadin in cardiac EC coupling has also been suggested in mice overexpressing CT1, which display reduced contractility (Kirchhefer et al., 2004b; Kirchhefer et al., 2001). Triadin-null hearts exhibit a blunted contractile and Ca^{2+} handling response upon β -adrenergic stimulation and develop ventricular tachycardia (Kirchhefer et al., 2004b; Kirchhefer et al., 2007; Kirchhof et al., 2007). Further, the SR Ca^{2+} load is either reduced (Terentyev et al., 2005) or increased (Kirchhefer et al., 2004b; Kirchhefer et al., 2007). Some data suggest that triadin plays an inhibitory role in cardiac EC coupling. However, an increased Ca^{2+} spark amplitude (Kirchhefer et al., 2004b) and an increased [³H]ryanodine binding to RyR2 (Kirchhefer et al., 2001) from CT1 overexpressing cardiomyocytes suggest that RyR2 is more sensitized to activation when in the presence of excess triadin, in agreement with data from (Terentyev et al., 2005). Although the physiological role of triadin in the heart is not clearly revealed by these confounding results, it can be concluded that normal triadin levels are obligatory for the optimisation of normal SR Ca^{2+} handling, cardiac EC coupling, and contractile function.

In skeletal muscle, adenovirus mediated overexpression of Triske 95 or Trisk 51 in rat skeletal muscle primary culture shows that Trisk 95, not Trisk 51 overexpressing myotubes, significantly inhibits KCl depolarization-induced Ca^{2+} release (Rezgui et al., 2005). No alterations in the expression or co-localization of other key Ca^{2+} handling proteins were detected in the same study (Rezgui et al., 2005). These results suggest that triadin, and in particular Trisk 95, acts as a negative regulator of skeletal EC coupling (Rezgui et al., 2005). This is in contrast to enhanced cardiac EC coupling in CT1 overexpression (Terentyev et al., 2005). The reduced depolarization-induced Ca^{2+} release with Trisk 95 overexpression is also related to a reduction

in SOCE efficiency (Vassilopoulos et al., 2007). Recently overexpression of Trisk 95 in C2C12 and rat skeletal muscle cells decreased the amplitude and frequency of Ca^{2+} sparks and a depressed level of depolarization-induced Ca^{2+} transients (Fodor et al., 2008), supporting the idea that in skeletal muscle triadin plays a regulatory role in EC coupling. However, a myotube study by Goonasekera et al. (2007) has shown that disrupting the RyR1-triadin interaction impairs both Ca^{2+} release and skeletal EC coupling. Therefore, it seems that a moderate concentration of triadin is required to mediate EC coupling in normal skeletal muscle. However, results from these overexpression studies should be interpreted cautiously due to triadin's propensity for polymerization. In particular, triadin in high concentrations is more likely to self-aggregate, which may result in a reduction in overall free triadin able to associate with RyR.

1.8.4.2 Down-regulation

Triadin-null mice, void of all the triadin isoforms, have been developed (Oddoux et al., 2009; Shen et al., 2007). Homozygous triadin-null (*Trdn*^{-/-}) mice do not exhibit embryonic or birth lethality, and do not present any obvious functional phenotype (Oddoux et al., 2009; Shen et al., 2007). However, triadin-null skeletal muscles display a significant reduction in strength (Oddoux et al., 2009). No changes in the amplitude of KCl depolarization-induced Ca^{2+} transients were detected in triadin-null mice (Oddoux et al., 2009) or in shRNA mediated triadin-knockdown rat skeletal myotubes (Fodor et al., 2008). These findings challenge the idea that triadin plays a critical role in skeletal EC coupling as suggested in the overexpression models (1.8.4.1). However, significant reductions in the amplitude of electrical and KCl depolarization-induced Ca^{2+} transients have been shown in both adult skeletal muscle fibers and cultured myotubes in other triadin-null mouse models (Boncompagni et al., 2012; Eltit et al., 2011; Shen et al., 2007). Similarly, siRNA-mediated knockdown of triadin in C2C12 skeletal myotubes causes a decrease in KCl depolarization-induced Ca^{2+} transients (Wang et al., 2009), suggesting that triadin is likely to facilitate depolarization-induced Ca^{2+} release. The reason for the discrepancies between these studies remains unclear. A clear assessment of the functional alterations directly attributable to the loss of triadin is confounded by: 1) altered expression of other Ca^{2+} handling proteins (DHPR, RyR1/2, junctin, CSQ1/2, SERCA1, FKBP12, junctophilin-1 and junctophilin-2) during development in the transgenic mice (Boncompagni et al., 2012; Chopra and Knollmann, 2009; Oddoux et al., 2009; Shen et al., 2007); 2) remodelling of the junctional SR associated with loss of triadin (Boncompagni et al., 2012; Oddoux et al., 2009; Shen et al., 2007); and 3) different cell types being used, i.e. cultured myoblasts from neonatal animals versus adult muscle fibers, which may display different Ca^{2+} handling properties (Capote et al., 2005; Janowski et al., 2006; Marty et al., 2000; Vassilopoulos et al., 2005).

The functional consequences observed in triadin-null skeletal muscles, the alterations in CSQ expression, and the remodelling of the junctional SR were tied together in a recent study (Boncompagni et al., 2012). The reduced junctional SR volume and SR Ca^{2+} load were correlated with the decreased level of polymerized CSQ1 visualized as anchored to the junctional SR, which in turn is likely to influence EC coupling efficacy (Boncompagni et al., 2012). This suggested that triadin mainly serves as an anchoring or structural protein. In fact, the absence of periodic “anchors” that connect CSQ to the junctional SR membrane in triadin-null muscles (where junctin and CSQ are still present), could indicate that triadin is the anchor that retains CSQ, and thus indirectly maintains the structure of the junctional SR, which in turn supports EC coupling (Boncompagni et al., 2012). Supporting this line of reasoning, Oddoux et al. (2009) show a flattened and reduced volume of the junctional SR terminal cisternae and a loss of CSQ density associated with a lack of triadin. A reduction in the contacts between junctional and T-tubule membranes in cardiac muscle has also been observed (Chopra et al., 2009). Together these results all suggest a structural role for triadin. On the other hand, transient knockout of triadin in skeletal myotubes does not lead to changes in CSQ1 expression or SR Ca^{2+} load, but does result in a reduced level of KCl depolarization-induced Ca^{2+} release (Wang et al., 2009). Therefore, the effects of triadin deficiency cannot be fully attributed to loss of CSQ1 or to changes in the junctional SR volume.

Interestingly, although whole-cell patch clamp studies reveal almost normal bidirectional signalling in triadin-null myotubes, with no changes in DHPR Ca^{2+} current densities and voltage dependency, triadin-null cells display a moderate reduction in peak amplitude of voltage-evoked Ca^{2+} release, and therefore, reduced orthograde signalling between DHPR and RyR1 (Eltit et al., 2011). On the other hand, triadin-null myotubes exhibit significant alterations to overall Ca^{2+} homeostasis, likely driven in part by the disruption of the RyR1/FKBP12 interaction (Eltit et al., 2010). RyR1s from triadin-null mice exhibit lowered sensitivity for the binding of exogenous FKBP12 and a marked increase in subconductance activity (Eltit et al., 2010). Thus, loss of triadin may destabilize the RyR1-FKBP12 interaction. Addition of FKBP12 or FKBP12.6 to triadin-devoid RyR1s reduces the subconductance activity. Overexpression of FKBP12.6 almost completely reverses the effects of lack of triadin expression on Ca^{2+} homeostasis and fully restores depolarization-induced Ca^{2+} release to WT levels (Eltit et al., 2011). These findings suggest that the effects of triadin loss on the orthograde signal may be mediated by effects on the RyR1-FKBP12 interaction, supporting the idea that skeletal triadin is not directly involved in skeletal EC coupling. This also helps explain the functional consequences of triadin knock out which are not accounted for by CSQ loss and changes in junctional SR volume (Wang et al., 2009).

1.8.5 Protein-protein interactions

1.8.5.1 Triadin-DHPR

Early studies in skeletal muscle suggested that triadin binds to both DHPR and RyR and mediates functional couplings between the two during EC coupling (Brandt et al., 1990; Caswell et al., 1991; Kim et al., 1990b). However, a later study has failed to show any interaction between triadin and DHPR (Guo and Campbell, 1995), and no further evidence has been provided to either support or disprove direct structural or functional interactions between the two proteins. Moreover, with the elucidation of the topological structure of triadin, which presents only one short 46-residue N-terminal domain in the cytoplasm, it has become highly unlikely that the triadin-DHPR interaction occurs *in vivo*. The predicted cytoplasmic domain is too short to span the distance (120 Å) between the SR and T-tubule membranes and thereby facilitate a triadin-DHPR interaction (Knudson et al., 1993; Marty et al., 1995). Although it could be argued that the DHPR or its beta subunit might extend partially into the junction space, the veracity of an interaction with the DHPR is doubtful.

1.8.5.2 Triadin-RyR

Immunohistochemistry studies have localized most triadin isoforms at the junctional SR in the vicinity of RyRs, indicating the close association of the two proteins in both skeletal and cardiac muscles – with the notable exceptions of Trisk 32 and Trisk 49, which appear to be segregated to the longitudinal SR (Carl et al., 1995; Kim et al., 1990a; Knudson et al., 1993). The triadin-RyR interaction has been mostly investigated in the skeletal system. Indeed, direct triadin-RyR1 interactions have been confirmed in many studies (Caswell et al., 1991; Caswell et al., 1999; Groh et al., 1999; Guo and Campbell, 1995; Kim et al., 1990a); both cytoplasmic and luminal interactions between triadin and RyR have been reported.

1.8.5.2.1 Cytoplasmic interactions

A functional cytoplasmic triadin-RyR interaction has been suggested by several studies. Trisk 95 reduces [³H]ryanodine binding (which indirectly reflects P_o) to Trisk 95-null SR vesicles, and inhibits the activity of isolated RyR1s in lipid bilayers when added into the cytoplasmic solution (Ohkura et al., 1998). Correspondingly, a peptide comprising residues 18-46 of triadin inhibits channel activity (Groh et al., 1999). Despite the consistent functional studies, the nature of physical interactions between the cytoplasmic domains of the two proteins has proven elusive. An early study failed to find a cytoplasmic interaction between Trisk 95 and RyR1 (Guo and Campbell, 1995) or between the cytoplasmic regions of CT1 and RyR2 (Guo et al., 1996b) at 1 mM [Ca^{2+}]. On the other hand, Groh et al. (1999) found that a peptide corresponding to residues 18-46 of Trisk 95 interacts with RyR1 in a [Ca^{2+}]-dependent fashion, being strongest at low [Ca^{2+}] (1 mM EGTA) and inhibited by increasing [Ca^{2+}], was lost at 2 mM [Ca^{2+}]. Conversely,

Caswell et al. (1999) failed to detect binding between a Trisk 95 residues 2-49 peptide and RyR1, with a $[Ca^{2+}]$ of 100 μ M Ca^{2+} or in the presence 1 mM EGTA. These findings raise the question of whether the cytoplasmic interaction actually exists. Nevertheless, it is still plausible that the cytoplasmic RyR-triadin interaction may occur *in vivo* and potentially play a role in RyR regulation in response to changes in cytoplasmic Ca^{2+} .

1.8.5.2.2 Luminal interactions

Compelling evidence suggest that the luminal domain of triadin interacts with the RyR (Goonasekera et al., 2007; Guo and Campbell, 1995; Lee et al., 2006; Lee et al., 2004; Wium et al., 2012). Two modes of binding were proposed between the luminal domains of Trisk 95 and RyR1: 1) a low affinity ionic interaction between large, positively charged portions of Trisk 95 and negatively charged regions of RyR1; and 2) a specific high-affinity binding of a short relatively hydrophobic segment of triadin (residues 110-280 of Trisk 95) to RyR1 (Caswell et al., 1999). More recently, mutagenic analysis has revealed that the triadin-binding site of RyR1 may reside between the negatively charge residues Asp⁴⁸⁷⁸, Asp⁴⁹⁰⁷ and Glu⁴⁹⁰⁸ in the C-terminal intra-luminal loop of the RyR1 (Lee et al., 2004). Mutations of these residues either abolish (D4907A/E4908A; D4878A/D4907A/E4908A) or reduce (D4878A/D4907A) the triadin-RyR1 association (Goonasekera et al., 2007). Likewise, the corresponding RyR-binding site of triadin has been mapped to a charged cluster of KEKE residues (residues 200-232) within the luminal domain, which pattern of residues is known as a KEKE motif (Lee et al., 2004). This same KEKE motif is conserved across all of the skeletal and cardiac isoforms of triadin (Kobayashi et al., 2000; Lee et al., 2004; Wium et al., 2012).

Functional luminal triadin-RyR interactions have been extensively investigated. Luminal addition of purified skeletal or cardiac triadin to purified RyR1 or RyR2 fused into lipid bilayers increases channel activity (Gyorke et al., 2004a; Wei et al., 2009a) in a Ca^{2+} -independent manner (Gyorke et al., 2004a). The idea that triadin acts as a luminal activator of RyR *in vitro* is supported by the observation that [³H]ryanodine binding to purified WT RyR1s is significantly enhanced by the addition of purified skeletal triadin, indicating an increase in channel activity (Goonasekera et al., 2007). It has also been shown that disruption of the physical triadin-RyR1 association dramatically impairs electrically evoked Ca^{2+} transients, nearly ablating skeletal-type EC coupling without any noticeable effects on other RyR1 functions (Goonasekera et al., 2007; Lee et al., 2006). In summary, the current accumulated data from *in vitro* studies suggest that luminal triadin activates RyRs and plays an important role in ensuring fast and robust Ca^{2+} release during EC coupling in skeletal muscle.

1.8.5.3 Triadin-CSQ

Triadin directly interacts with CSQ (Guo and Campbell, 1995; Guo et al., 1996b; Zhang et al., 1997) and functions as a CSQ anchoring protein (Boncompagni et al., 2012). Binding interactions between triadin and CSQ occur in a Ca^{2+} -regulated fashion such that the interaction is enhanced when the Ca^{2+} concentration is decreased and is inhibited by an increase to millimolar $[\text{Ca}^{2+}]$ (Guo and Campbell, 1995; Kobayashi et al., 2000; Mitchell et al., 1988; Zhang et al., 1997). In addition, the triadin-CSQ interaction is independent of CSQ's phosphorylation status (Beard et al., 2008). The Asp-rich C terminus of CSQ (residues 354-367 in rabbit CSQ1) has been identified as responsible for binding to triadin in the skeletal system (Shin et al., 2000). Likewise, the CSQ binding domain of CT1 has been localized to a single KEKE motif at residues 200-224 (Kobayashi et al., 2000). The critical amino acids of triadin binding to CSQ are the even-numbered residues Lys²¹⁰, Lys²¹², Glu²¹⁴, Lys²¹⁶, Gly²¹⁸, Gln²²⁰, Lys²²² and Lys²²⁴. These residues are conserved within the KEKE motif across all triadin isoforms and species. Notably, the KEKE motif in triadin responsible for its binding to CSQ is the same motif that is critical for its binding to RyR (1.8.5.2.2). This may explain the inability of triadin to mediate signalling between CSQ1 and RyR1 (Wei et al., 2009a), as an inability of triadin to bind to both CSQ and RyR at the same time. On the other hand, triadin seems to be able to relay the inhibitory effect of CSQ2 to RyR2 either by itself or together with junctin (Gyorke et al., 2004a). Thus, it remains to be determined whether the same KEKE motif can accommodate RyR and CSQ simultaneously.

1.8.5.4 Other protein-protein interactions (junctin, HRC)

In addition to binding CSQ, triadin also directly interacts with other SR luminal proteins, such as junctin and the histidine-rich Ca^{2+} -binding protein (HRC) (Arvanitis et al., 2007; Glover et al., 2001; Lee et al., 2001; Zhang et al., 1997). Junctin is another CSQ anchoring protein, which has a similar structure to triadin and also contains multiple "KEKE" motifs (section 1.9, also see (Zhang et al., 1997)). In contrast to triadin's interaction with CSQ, the triadin-junctin interaction is Ca^{2+} -independent. The specific triadin-junctin interaction is predicted to occur at "KEKE" motifs, but the binding regions have not yet been located in either triadin or junctin (Zhang et al., 1997). Regardless, it is yet to be determined whether the triadin-junctin interaction occurs *in vivo* and whether this interaction plays any functional role. HRC is a Ca^{2+} -binding protein found in small amounts in the SR lumen. In both skeletal and cardiac muscles, it has been shown that HRC binds to triadin in a Ca^{2+} -sensitive manner through the same KEKE motif that is involved in triadin's binding to CSQ (Lee et al., 2001; Sacchetto et al., 2001; Sacchetto et al., 1999). This suggests that a binding competition to triadin may occur between HRC and CSQ. However, the existence of such a competitive binding *in vivo* remains to be investigated.

1.9 Junctin

1.9.1 Junctin gene, structure, isoform

Junctin, a 210-amino acid 26 kDa protein, was identified in the late 1980s as a major CSQ-binding protein, present in the junctional SR membranes of canine cardiac and skeletal muscle (Mitchell et al., 1988). Protein sequence and topological analysis shows that junctin is an integral SR transmembrane protein and shares a similar membrane topology and overall structure with triadin, containing a short cytoplasmic N-terminal tail (AAs 1-22), a single hydrophobic helix that spans the SR membrane (AAs 23-44), and a bulky, highly charged C-terminal tail (AAs 45-210) located in the SR lumen (Jones et al., 1995) (Fig. 1-12). It is localized to the jSR and is absent from other SR compartments, and comprises ~4.4% of the total jSR protein mass (Jones et al., 1995). Since its discovery, junctin has been thought to play a major role as a CSQ anchoring protein, keeping CSQ close to the junctional face membrane (JFM) and in close proximity to the RyR. This long-held view, however, is now being re-examined, and a more complex role for junctin has emerged. It has become apparent that the protein also plays a major role in regulating the Ca^{2+} release channel activity (reviewed in (Beard et al., 2009; Dulhunty et al., 2009; Fan et al., 2008; Pritchard and Kranias, 2009) and also (Altschafel et al., 2011)).

So far, junctin from four species (canine, human, rabbit, and mouse) has been cloned and characterized (Dinchuk et al., 2000; Jones et al., 1995; Lim et al., 2000; Wetzel et al., 2000). The protein is generally expressed as one gene product – i.e., one isoform – in skeletal and cardiac muscle, as well as in many other tissues. The expression density from highest to lowest is: fast skeletal muscle fiber, slow skeletal muscle fiber, and finally, cardiac muscle fiber (Dinchuk et al., 2000; Jones et al., 1995). Curiously, in human cardiac muscle, there are two alternatively spliced junctin isoforms. The second isoform is characterized by the inclusion of 15 amino acids at residue 55 (Lim et al., 2000). This additional isoform has not been confirmed in other species and its physiological and/or pathophysiological roles are as yet unknown.

Junctin is one of the alternative splicing variants of the locus aspartyl- β -hydroxylase ($\text{A}\beta\text{H}$)-J-J, which is located on human chromosome 8q12.1 and, through a complex pattern of alternative splicing can give rise to four distinct classes of proteins, including: (i) the non-catalytic product junctin, described in this section; (ii) aspartyl- β -hydroxylase, or Asph, a member of the alpha-ketoglutarate-dependent dioxygenase family; (iii) junctate, a moderate affinity, high capacity Ca^{2+} binding protein (Treves et al., 2000); and (iv) humbug, a truncated version of Asph, lacking its catalytic domain, and sharing with junctate a high capacity / moderate affinity Ca^{2+} binding domain (Dinchuk et al., 2000; Treves et al., 2009). Transcripts of junctin start from exon 1a under the control of the P2 promoter, the induction of which is controlled by the muscle specific transcription factor MEF-2 (Feriotto et al., 2005). Exon 2 encodes the transmembrane domain, and together with exon 3, is shared by all family members derived from the $\text{A}\beta\text{H}$ -J-J

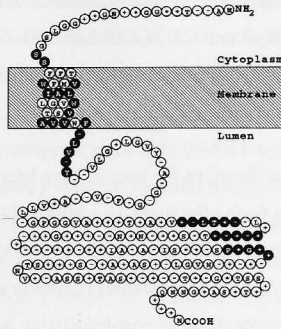


Figure 1-12 Topology of Junctin in the SR membrane. The N-terminal tail is located in the cytoplasm and the C-terminus end in the SR lumen. A single helix spanning the membrane connects the two domains. Positively and negatively charged amino acids are denoted by pluses and minuses, respectively. Taken from (Jones et al., 1995).

locus. The carboxyl-terminal portion of junctin results from the transcription of exons 4a and 5a, while all other products are generated via transcription of exons 4-24 and result in a variety of products of different sizes (Dinchuk et al., 2000; Feriotto et al., 2005; Treves et al., 2000).

1.9.2 Junctin homology, KEKE motif

Comparisons between human, rabbit, and canine junctin have revealed a significant sequence identity (>80%), and a ~90% homology across species (Lim et al., 2000; Wetzel et al., 2000). Specifically, there is striking homology (>97%) in the putative membrane spanning region and in the first 61 luminal residues; these same domains also exhibit a high degree of sequence homology with triadin (62% identity, (Jones et al., 1995)). An identity of ~86% was found in the N-terminal domains of human and canine junctin. The highly conserved amino-terminal region of the protein suggests that the transmembrane domain, the initial luminal portion, and possibly the N-terminal region may all play an important functional role and may contain the interaction sites for triadin, CSQ and RyR (Yazaki et al., 1990; Zhang et al., 2001). The C-terminal region, however, exhibits only 72 to 75% sequence homology (Wetzel et al., 2000). The intraluminal domain from human junctin contains minimal junctional SR targeting sequences (Rossi et al., 2013).

Like triadin, a remarkable feature of junctin is that it has a high density of charged residues (47.1%), with 17 more basic residues than acidic, and consequently, an estimated pI of 9.37. The cytoplasmic N-terminus contains 36.4% charged residues (8 of 22) with a calculated pI of 9.7. By comparison, the luminal segment is enriched in charged amino acids (54.8%) with a pI of 9.31. Junctin also contains multiple “KEKE” motifs throughout its luminal domain that are presumed to be involved in junctin’s interactions with CSQ, triadin and RyR (Jones et al., 1995;

Kobayashi et al., 2000; Zhang et al., 1997). There is evidence that multiple KEKE motifs are required for junctin's binding to RyR and CSQ (Altschafel et al., 2011; Kobayashi et al., 2000). Regardless, the precise regions in both junctin and its binding partners which interact have yet to be defined.

To date, no post-translational modifications for junctin have been reported. The protein contains no cysteine residues and does not form oligomers. In addition, junctin is not glycosylated, and contains no consensus glycosylation sites. However, the observation of junctin migrating as a closed spaced-doublet on SDS-PAGE in early studies (Costello et al., 1986; Jones et al., 1995) raised the possibility that partial proteolysis or post-translation modification may occur; further investigations are required to test this possibility.

1.9.3 Junctin changes in the developing heart

SR is less important in intracellular Ca^{2+} cycling in the neonatal mammalian heart than in adult heart. In the neonatal myocardium, Ca^{2+} influx and efflux via the sarcolemma is more important than the SR fluxes in regulating contraction-relaxation cycling. This is attributed to the poorly developed EC coupling machinery and the immaturity of SR function in neonates (Mahony, 1996; Page and Buecker, 1981). The maturation of SR Ca^{2+} cycling is closely correlated with an increase in SR Ca^{2+} cycling protein levels and their activity (Mahony, 1996; Moorman et al., 1995; Vetter et al., 1995). Junctin mRNA expression levels in foetal rabbit cardiac muscle are only ~16% of adult levels, but increase dramatically, to 40% at day one post-birth, and to 87% by day five. Adult levels of mRNA are then reached ~15 days post-birth (Wetzel et al., 2000), parallel to maturation of SR function 5-15 days post-birth (Miller et al., 1997). An age-dependent increase in junctin protein is observed in human and rat hearts (Jung et al., 2005). In agreement, a specific increase in the junctin content of the jSR is detected, along with structural maturation of the jSR, during the development of mice heart (Tijssens et al., 2003). Taken together, the progressive increase in junctin levels suggests that junctin may be involved in the maturation of the SR Ca^{2+} release mechanism, and also in establishing the functional EC coupling machinery in mammalian heart.

1.9.4 Overexpression and down-regulation of junctin

1.9.4.1 Cardiac junctin modulation

1.9.4.1.1 Junctin overexpression

The functional significance of junctin has been explored in the heart by the up-regulation or ablation of the protein. Mouse models with heart-specific overexpression of junctin consistently show depressed contractility and impaired muscle relaxation in association with a decreased SR

Ca²⁺ load (Hong et al., 2002; Kirchhefer et al., 2004a; Kirchhefer et al., 2006; Kirchhefer et al., 2003; Zhang et al., 2001). The diminished SR Ca²⁺ content is attributed to the potential role of junctin as a “placeholder” for Ca²⁺, competing alongside with luminal Ca²⁺ for the free binding sites on CSQ (Kirchhefer et al., 2006). Up-regulation of junctin in mice displayed a gene-dosage dependent effect on function. Transgenic mice with 29-fold higher levels of junctin in the myocardium exhibit severe cardiac hypertrophy, atrial fibrillation, fibrosis, increased L-type Ca²⁺ current density, and prolonged action potential duration, accompanied by heart failure and bradycardia (Hong et al., 2002). Mouse hearts with a 10-fold overexpression of junctin develop a modest impairment of relaxation, a lower Ca²⁺ transient amplitude, with unaltered contraction rate. These hearts are only mildly hypertrophic and showing no signs of fibrosis (Kirchhefer et al., 2003). Overexpressing myocytes demonstrate narrower jSR cisternae, a higher density of CSQ2 in the jSR, and the extension of jSR domains to non-junctional regions (Hong et al., 2002; Tijsskens et al., 2003; Zhang et al., 2001). This suggests that junctin may be involved in SR morphogenesis and in the assembly of the molecular components of the Ca²⁺ release machinery in jSR. However, chronic overexpression of junctin in these mice models leads to compensatory changes in other Ca²⁺ handling proteins: triadin and RyR levels are decreased (Hong et al., 2002; Kirchhefer et al., 2004a; Kirchhefer et al., 2003; Zhang et al., 2001), Na⁺/Ca²⁺ exchanger (NCX) expression is reduced, and the phosphorylation of RyR at residue 2809 increased by 64% (Kirchhefer et al., 2006). It is plausible that changes in these transgenic mouse models reflect secondary effects consequent to hypertrophy, alterations in the SR ultrastructure, and alterations of gene expression, all of which may prevent an assessment of alterations directly attributable to junctin. Acute adenoviral-mediated overexpression of junctin in adult rat cardiomyocytes shows that overexpression of junctin by either 2-fold (Gergs et al., 2007) or 1.6-fold (Fan et al., 2007) results in the depression of contractility, Ca²⁺ transient amplitude, and rates of contraction and relaxation, as well as a parallel decrease in SR Ca²⁺ load. There is no alteration of other Ca²⁺ handling protein levels, although a decrease in RyR2 was observed in the first study (Gergs et al., 2007). Conversely, neonatal rat cardiac myocytes overexpressing junctin do not show any alterations in either basal Ca²⁺ transients or SR Ca²⁺ content, this is likely due to the relatively moderate level of overexpression (Gergs et al., 2011).

1.9.4.1.2 Cardiac junctin ablation

Conversely, ablation of junctin in the heart produces an opposite effect. Acute downregulation of junctin by 40% in cardiomyocytes via adenoviral transference of antisense mRNA resulted in a significant increase in both fractional shortening and the rate of contraction and relaxation, as well as an increased Ca²⁺ transient peak and a faster Ca²⁺ decay, with no changes in other Ca²⁺-handling protein levels (Fan et al., 2007). Likewise, cardiomyocytes isolated from junctin-deficient mice demonstrated augmented Ca²⁺ transient and kinetics, along with enhanced

contractility and a parallel increase in SR Ca^{2+} load and elevated Ca^{2+} spark frequency indicative of increased SR leakage. *In vivo*, cardiac function in junctin-null mice is also enhanced (Yuan et al., 2007). Unlike junctin overexpression mouse models, junctin-KO mice do not experience any alterations in cardiac morphology or to any of the major Ca^{2+} cycling protein expression levels. An exception is a 70% increase in the NCX expression, accompanied by a concomitant elevation in current density, perhaps to compensate for the high luminal $[\text{Ca}^{2+}]$ (Yuan et al., 2007). Importantly, in the junctin-null mice, the changes in cardiac performance include delayed after-depolarization (DAD)-induced arrhythmias and an increased susceptibility to premature death during conditions of physiological stress. The increased incidence of DADs associated with aftercontractions in junctin-null cardiomyocytes has been attributed to aberrant RyR Ca^{2+} release in the absence of junctin (Yuan et al., 2007). Together with data from overexpression models, these results demonstrate an inverse relationship between junctin, cardiomyocyte SR Ca^{2+} content and contractile function, suggesting a negative regulatory role of junctin on RyR activity and further, the physiological importance of junctin in the maintenance of normal SR Ca^{2+} handling and cardiac performance.

A comprehensive study utilizing the junctin-KO mouse model of (Yuan et al., 2007) has revealed both novel mechanisms by which junctin controls the luminal Ca^{2+} sensitivity of RyR2 and the role junctin plays in cardiac dysfunction (Altschafel et al., 2011). Instead of a simple negative role for junctin as suggested in previous studies, this study demonstrates complex, luminal $[\text{Ca}^{2+}]$ -dependent effects of junctin depletion on intracellular Ca^{2+} homeostasis and RyR2 activity, and supports the notion that junctin deficiency contribute to arrhythmias under β -adrenergic stimulation or stress. Activator or inhibitor role of junctin are proposed under periods of prevalent parasympathetic or sympathetic activity, respectively. The maintenance of normal junctin expression levels is obligatory for optimal SR Ca^{2+} handling, and protects against cardiac arrhythmias (Altschafel et al., 2011). Indeed, in heterozygous junctin-deficient mice, the presence of only ~50% normal junctin levels is sufficient to prevent SR Ca^{2+} leakage, DAD-triggered arrhythmias, and premature death. At the same time there is enhanced cardiac contractility and SR Ca^{2+} content, as well as elevated NCX activity (Yuan et al., 2009). The absence of either junctin or junctin/triadin exacerbates the detrimental effects of ischemia/reperfusion injury by impairing contractile recovery and increasing cell death in the myocardium, suggesting important roles for these proteins in maintaining cardiac contractility and cell survival in response to such injuries (Cai et al., 2012).

1.9.4.2 Skeletal junctin ablation

The physiological role of junctin in Ca^{2+} release from skeletal muscle SR is less well characterized. To date, two skeletal junctin-null models have been examined. An early study reported that knocking down junctin (100% reduction) in skeletal muscle myotubes (C2C12)

resulted in significant impairment of K^+ -induced Ca^{2+} release consequent to a reduced SR Ca^{2+} store, accompanied by down-regulation of RyR1 and CSQ1 protein expression, although not their mRNA levels. There was no significant change in the resting cytosolic Ca^{2+} levels. These data indicate that lack of junctin may increase the rate of degradation of RyR1 and CSQ1, thus disrupting the macromolecular Ca^{2+} signalling complex (Wang et al., 2009). However, a more recent study with transgenic mice shows that ablation of junctin has only a very limited effect. There was no change in expression of other proteins in the Ca^{2+} release machinery, including RyR1 and CSQ1, in this model. There was also no change in jSR ultrastructure, although a slight change in the total jSR volume was detected. Furthermore, there was no significant alteration in E-C coupling, caffeine-induced Ca^{2+} release, or SR Ca^{2+} in the absence of junctin (Boncompagni et al., 2012). In contrast to (Wang et al., 2009), junctin depletion resulted in an elevated myoplasmic resting free $[Ca^{2+}]$ (Boncompagni et al., 2012). The reason for the disparity between these studies is unclear. Overall, the reductions in junctin levels, which resulted in severe deterioration of the heart's performance, showed only mild consequences in skeletal muscle. Curiously a severe pathology in junctin/triadin double-null muscles does support a role for junctin in regulation of Ca^{2+} homeostasis in skeletal muscle (Boncompagni et al., 2012).

It should be kept in mind that different targeting strategies in knocking out junctin may also cause variable alterations in the expression levels of other splice variants of the locus aspartyl- β -hydroxylase ($A\beta H$)-J-J – Asph, humbug and junctate (1.9.1) – possibly leading to some non-specific effects which may partly explain the discrepancies across different studies (Boncompagni et al., 2012).

1.9.5 Junctin and diseases

A role for junctin is suggested in cardiac and skeletal muscles pathologies.

In failing human hearts, junctin levels are decreased to almost undetectable levels (Gergs et al., 2007). At present, it remains unclear whether junctin down-regulation contributes to impaired SR Ca^{2+} handling, causing cardiac hypertrophy and heart failure, or whether it is compensatory to alleviate the deterioration of cardiac function. Based on transgenic studies, it was speculated that in failing hearts the reduced levels of junctin may compensate for lower SR- Ca^{2+} content arising from increased SR Ca^{2+} leak, or be an adaptation to chronic β -adrenergic stimulation. Reduction in junctin levels may therefore improve contractile function in heart failure states (Altschafel et al., 2011; Fan et al., 2007; Gergs et al., 2007; Yuan et al., 2009). In support of this idea, expression of junctin is significantly decreased in a transgenic mouse model of heart failure with cardiac-specific overexpression of the β_1 -adrenoceptor. Junctin levels declined with age and closely paralleled the development of cardiac hypertrophy and heart failure (Engelhardt

et al., 2001). This supports the notion that junctin expression attempts to compensate for dysregulation of SR Ca^{2+} -cycling in heart failure and plays an important role in normal cardiac function.

Another pathological condition related to junctin is diabetes-induced cardiac dysfunction, with consequent massive oxidative stress being particularly evident in heart tissues (Yildirim et al., 2013). There is markedly more junctin in diabetic cells: a luciferase reporter assay revealed that this up-regulation of junctin is effected by a down-regulation of miR-1 in the diabetic heart. Furthermore, the expression of junctin is closely associated with oxidative stress in the heart, since N-acetylcysteine (NAC)-treatment of diabetic rats prevents a junctin increase. This study suggests that junctin is actively involved in the development of diabetic cardiomyopathy.

So far, no mutations in junctin have been implicated in any human cases of CPVT. However, under high stress, junctin-KO mice exhibit a CPVT phenotype with enhanced $[\text{Ca}^{2+}]_i$ transients, DADs, aftercontractions, and triggered arrhythmias related to an increased probability of spontaneous SR Ca^{2+} release (Altschafel et al., 2011). The way in which junctin's absence leads to these clinical phenotypes is suggested to be similar to CPVT linked to RyR2 and CSQ2 mutations, where excessive RyR Ca^{2+} release during diastole is the primary cause of pathology (Priori and Chen, 2011). Thus, junctin ablation may alter RyR's Ca^{2+} sensitivity by impairing the physical interaction between the constituents of the protein complex – between CSQ and RyR – and thereby induce aberrant RyR openings (Dulhunty et al., 2012; Fan et al., 2008). Junctin ablation or mutations may mimic the etiology of CPVT by causing increased diastolic Ca^{2+} leak under β -adrenergic stimulation or stress conditions (Altschafel et al., 2011). However, a functional link between junctin and CPVT has yet to be clearly elucidated.

An association between junctin and skeletal myopathy has been indicated in a patient with mild myopathy characterized by the presence of hexagonally cross-linked tubular arrays in skeletal muscle fibers (Di Blasi et al., 2010). Immunohistochemistry has shown that the rod-like inclusions are positive for junctin (as well as CSQ and caveolin 3), suggesting an abnormal accumulation of the protein leading to rod formation, since protein crystals only rarely accumulate in tissues, usually as a consequence of an alteration in their synthesis, processing, or degradation. However, no mutations in the junctin encoding gene *Asph* were found in this case (Di Blasi et al., 2010).

1.9.6 Junctin protein/protein interaction

1.9.6.1 Junctin and RyR (binding, regulation)

As a key component of the RyR Ca^{2+} release complex, junctin has been found to interact with RyR directly in a Ca^{2+} -independent fashion (Zhang et al., 1997).

Notwithstanding the early discovery of the binding between junctin and RyR, the role of junctin in the regulation of the RyR is not well understood, and the respective binding sites on each protein are unknown. Most of our knowledge about functional effect of junctin on RyRs is derived from transgenic studies focusing on the cardiac system (section 1.9.4.1). The observations that junctin levels are inversely correlated with contractile function, and that junctin knockout or knockdown results in aberrant Ca^{2+} release, have suggested that junctin may act as a “brake” that inhibits RyR2 activity (Yuan et al., 2007). However, it is unclear whether this action is a direct effect of junctin per se on RyR2 activity, or an indirect effect whereby junctin serves as a transducer of CSQ signals.

In an *in vitro* lipid bilayer study Gyorke et al. (2004a) show that the inclusion of junctin to the luminal solution along with purified RyR2 enhances RyR channel activity in the presence of either 20 μM or 5 mM luminal $[\text{Ca}^{2+}]$, suggesting a positive role of junctin on RyR2 channel gating. However, the luminal $[\text{Ca}^{2+}]$ used was outside the range encountered during normal Ca^{2+} cycling (~ 0.1 to 1 mM) (Chen et al., 1996; Ginsburg et al., 1998) and reviewed in (Bers, 2002; Dulhunty et al., 2012). Nevertheless, the data suggest that junctin can modulate RyR activity. The discrepancy between this study and the transgenic studies may be due to different *in vitro* and *in vivo* conditions. It has been shown that junctin together with triadin can indirectly alter RyR2 activity via junctin- and/or triadin-CSQ interactions (Gyorke et al., 2004a). Similar results have been reported with junctin in skeletal muscle, with junctin having been shown to stimulate the activity of purified RyR1 in lipid bilayers, but also to inhibit channel activity when CSQ1 is added to the same luminal solution; the latter able to occur in the absence of triadin (Wei et al., 2009a).

A recent study revealed a novel mechanism by which junctin regulates RyR2 (Altschaffl et al., 2011). RyR2 channel activity from junctin-KO and WT cardiac SR implies that junctin has a luminal Ca^{2+} -dependent effect on RyR2. At low luminal Ca^{2+} (< 1 mM), junctin activates RyR2 channel (loss of junctin reduces RyR2 opening); conversely, at high luminal Ca^{2+} (> 1 mM), junctin inhibits the channels (RyR2 channels are more active in the absence of junctin). The crossover point occurs at ~ 1 mM luminal $[\text{Ca}^{2+}]$. Thus junctin may both attenuate and increase RyR2 activity depending on SR Ca^{2+} loads. However, the possibility that this dual effect may be related to regulation of RyR2 by CSQ2 cannot be excluded. Indeed, a steeper increase in RyR2 activity as a function of luminal $[\text{Ca}^{2+}]$ is also observed in the absence of CSQ2 (Dulhunty et al., 2012), that is similar to the effect observed in junctin-devoid RyR2 (above). Therefore, the precise way in which junctin regulates RyR2 channels remains to be clearly determined, as does junctin’s regulation of RyR1. The interactions between junctin and RyR1 or RyR2 are extensively investigated in the study reported in this thesis.

The opposing luminal Ca^{2+} -dependent effects of junctin on RyR2 (Altschafel et al., 2011) strongly suggests that multiple junctin-RyR2 interaction sites may exist. This is supported by experiments showing two domains of junctin bind to two different domains of the RyR2 (Altschafel et al., 2011). Luminal residues 47-77 of junctin bind specifically to RyR2 luminal M5-M6 linker (residues 4520-4553) (Fig. 1-9), while luminal residues 78-210 bind to the RyR2 pore loop (residues 4789-4846). The pore loop contains the pore helix and selectivity filter for the Ca^{2+} channel (Fig. 1-9, and also section 1.6.3.2), therefore this junctin binding site is a strategic location which influences the gating and conductance of the channel. Significantly, preliminary evidence from the Muscle Research Group indicates that the luminal domain of junctin binds to the pore loop of RyR1 which is equivalent to the pore loop region in RyR2. It is noteworthy that the same RyR1 pore loop region which binds junctin is also the single binding site for triadin, involving residues: D4907, E4908, and D4878 (Lee et al., 2004). Disrupting triadin's binding to RyR1 by mutating the three residues does not affect the ability of junctin to bind to RyR1, indicating that the binding site for junctin on this luminal loop may differ from that of triadin (Goonasekera et al., 2007) or that there are other junctin binding sites on the luminal domains of the protein.

There have been no studies of possible cytoplasmic interactions between junctin's N-terminal tail (Njun) and RyR1 or RyR2. The observations that cytoplasmic tail of skeletal triadin can bind to the cytoplasmic domain of RyR1 and inhibit the channel (Groh et al., 1999; Ohkura et al., 1998) raise the possibility that a cytoplasmic RyR/junctin interaction may exist. Some evidence suggests that the luminal part of junctin (which contains the bulk of the protein) interacts with the RyR (Zhang et al., 1997). The luminal domain of junctin is sufficient for binding with RyR2, and affinity binding assays have failed to detect a physical interaction between Njun and RyR2 (Zhang et al., 1997). However, this does not rule out the possibility of cytoplasmic interactions if the binding site on RyR of Njun is buried within the protein, or if binding between the cytoplasmic domains of the two proteins is weak (Dulhunty et al., 2012). The cytoplasmic regulation of RyR by Njun in both skeletal and cardiac muscle has been partially reviewed in (Dulhunty et al., 2012) and will be addressed in the Result chapters (see Chapter 5).

1.9.6.2 Junctin, CSQ, and triadin

1.9.6.2.1 Junctin and CSQ

The function originally proposed for junctin is as a linker connecting CSQ to the RyR, since junctin binds to ^{125}I -CSQ (Jones et al., 1995; Mitchell et al., 1988). Similar to the triadin-CSQ interaction, junctin-CSQ association was demonstrated to be Ca^{2+} -dependent, so that increasing $[\text{Ca}^{2+}]$ resulted in the gradual dissociation of junctin and CSQ. Junctin's CSQ-binding region

has been localized to its luminal domain (Zhang et al., 1997), with multiple binding sites on junctin indicated for junctin-CSQ association, since deletion of any one of several widely separated segments of the junctin luminal domain abolished CSQ2 binding (Kobayashi et al., 2000). *In vitro* binding assays have demonstrated a Ca^{2+} -dependent interaction between the carboxyl terminal portion of CSQ1 (aa 193-367) and junctin, with the Asp-rich region (354-367) at the CSQ1 C-terminus being believed to form at least part of this interaction site (Shin et al., 2000). Curiously, skeletal CSQ binding to junctin is affected by CSQ1 phosphorylation (threonine 353) (Beard et al., 2008). Only phosphorylated CSQ can bind to junctin at low Ca^{2+} (100nM, where CSQ1 exists as monomer). In contrast, the binding of triadin to CSQ is not influenced by CSQ's phosphorylation (Beard et al., 2008). Based on these observations, Beard and colleagues proposed that junctin's binding site on the CSQ C-terminus may differ from that of triadin, and further, that it may be formed at the monomer interface in CSQ multimers (Beard et al., 2008). Consistent with this proposal, a recent study revealed that a stoichiometric quantity of junctin is required for CSQ2 depolymerization upon Ca^{2+} depletion (Lee et al., 2012). FRET analysis revealed constant interactions between CSQ2 and junctin irrespective of the SR Ca^{2+} concentration, suggesting that junctin may be an essential component of the CSQ scaffold (Lee et al., 2012).

Although junctin's function as a CSQ anchoring protein is well recognized, the importance of this function has been recently challenged. Comparisons of mouse models lacking either triadin (Tdn-null), junctin (Jct-null) or both (Tdn/Jct-null) illustrate that the structural roles of triadin and junctin are not equivalent in skeletal muscle (Boncompagni et al., 2012). "Periodically disposed electron opaque densities (anchors)" that connect CSQ to the RyR-bearing jSR membrane were present in both WT and Jct-null muscles but absent in Tdn-null (with junctin and CSQ still present) muscles. This observation indicated that triadin is the major component of the CSQ-retention anchoring system, although a less dense anchor profile in Jct-null muscle does suggest some contribution of junctin to the structure. Nevertheless, the role of junctin mediating the link between CSQ and jSR membrane does seem of lesser importance than has been previously suggested – at least in skeletal muscle in these mouse models.

Lipid bilayer studies with reconstituted purified RyR1 reveal that the function of the junctin-CSQ1 interaction conveys CSQ1's inhibitory signal to RyR1, and that this function cannot be duplicated by triadin (Wei et al., 2009a). Results obtained with the cardiac isoforms indicate that junctin and triadin together mediate interactions of CSQ2 with RyR2 (Gyorke et al., 2004a; Wei et al., 2009b). However, the separate roles of the junctin-CSQ2 and triadin-CSQ2 interactions with RyR2 have yet to be established in the cardiac system.

1.9.6.2.2 Junctin and triadin

Interestingly, junctin also binds directly to triadin (Zhang et al., 1997). The interaction between junctin and triadin is Ca^{2+} -independent and has been suggested to stabilize a quaternary complex that anchors CSQ to the RyR, possibly through their KEKE motifs (Guo and Campbell, 1995; Zhang et al., 1997). However, it remains to be determined whether junctin and triadin bind to each other *in vivo*.

1.9.6.2.3 Interdependent expression among junctin, triadin and CSQ

Evidence from mouse transgenic models with either CSQ2 or triadin ablation suggests an interdependence of expression of the three jSR Ca^{2+} -handling proteins: junctin, triadin, and CSQ (Chopra and Knollmann, 2013; Knollmann, 2009). Both CSQ2-null and CSQ2 R33Q knock-in (with a 55% reduction in CSQ2-R33Q) mice exhibit a severe reduction in both triadin and junctin (Knollmann et al., 2006; Rizzi et al., 2008). Similarly, knockout of triadin causes the near-complete loss of CSQ2 and junctin (Chopra et al., 2009). These observations suggest the existence of a protein complex formed by the three proteins *in vivo*, consistent with *in vitro* studies. Notably, junctin levels are significantly more reduced as compared to triadin-1 and CSQ2 levels in all three models, indicating that junctin requires CSQ2 and triadin in order to maintain a stable conformation. Conversely, mice with gene-targeted ablation of junctin do not show any changes in CSQ2 and triadin expression (Altschafel et al., 2011; Yuan et al., 2007), implying that junctin itself may not be necessary for stability of the jSR protein expression.

1.9.6.3 Other interactions (possible interactions)

Junctin also binds to a 31 kDa protein and two CSQ-like proteins (~90 kDa) as shown in ^{125}I -junctin overlay assays (Zhang et al., 1997). The 31 kDa junctin-like protein (as described in (Jones et al., 1995)) was purified and identified to be an (ADP)ATP translocase (AAT) protein, a protein mainly expressed in mitochondria, which binds to junctin as well as to CSQ (Kagari et al., 1996; Yamaguchi et al., 1999; Yamaguchi and Kasai, 1998). It was suggested that CSQ, junctin, and AAT may form a protein complex in the terminal cisternae of the SR and play a role in regulating RyR and EC coupling (Kagari et al., 1996). In addition, the CSQ-junctin-AAT interaction might be related to the CRU-mitochondrion Ca^{2+} cross-talk (Shkryl and Shirokova, 2006). It has been shown that mitochondria are connected to the SR and in proximity of release sites (CRUs) via small strands or tethers (Boncompagni et al., 2009; Ogata and Yamasaki, 1987; Rossi et al., 2011). However, the physiological relevance and significance of this interaction still await further investigations, as does the nature of the potential interactions between junctin and the two CSQ-like proteins.

1.10 Project aims

For many years, junctin was considered to play a major role only in connecting CSQ to the RyR in skeletal and cardiac muscle, but it has been recognized as having a more complex role in recent years (detailed in section 1.9.4 and 1.9.6). Both *in vitro* and *in vivo* studies show a strong correlation between junctin and SR Ca^{2+} load, and junctin has been proposed to be very important for regulating RyR activity and SR Ca^{2+} handling. It is notable that junctin protein expression is significantly reduced in some models of heart failure, suggesting its involvement in the dysregulation of SR Ca^{2+} -cycling in failing heart (see section 1.9.5). To date, most of our knowledge about the effect of junctin on RyRs, particularly RyR2, is derived from transgenic studies (see section 1.9.6), which suggest junctin plays a role as either a RyR2 suppressor (Yuan et al., 2007) or as both an activator and inhibitor depending on SR Ca^{2+} levels (Altschafel et al., 2011). However, due to the confounding factors associated with changes in junctin expression in these studies, the specific physiological roles of junctin remain unclear. It is therefore, interesting to determine the direct regulatory effect of junctin on the RyR.

Despite the overall importance of junctin, there are only limited studies testing the direct effect of junctin on the RyR (see section 1.9.6.1). In contrast to the results of transgenic studies, *in vitro* lipid bilayer studies showed that junctin activates RyR2 when added to the luminal side of purified channels (Gyorke et al., 2004a), suggesting a positive role of junctin in regulating RyR2. However, the luminal Ca^{2+} concentrations used in these experiments – either 20 μM or 5 mM – differ from the physiological concentrations that might be expected during normal Ca^{2+} cycling (0.1-1.5 mM) (Chen et al., 1996; Ginsburg et al., 1998) and reviewed in (Bers, 2002; Dulhunty et al., 2012)). Thus, the role of junctin in regulating RyR2 has not been conclusively defined. Findings by others in the Muscle Research Group demonstrate that luminal addition of junctin under physiological Ca^{2+} concentrations directly enhances purified RyR1 channel activity (Wei et al., 2009a), although the specific mechanism behind this activation remains to be explored. Consequently, the work of this thesis had the following aims:

- 1) To investigate the specific role of junctin in regulating RyR2 activity at 1 mM luminal Ca^{2+} . To facilitate an accurate comparison, the effect of junctin on RyR1 has been re-addressed in this study. A second component of this aim was to investigate the precise mechanism by which junctin affects RyR1 and RyR2 activity. Experimental findings regarding this aim are presented in Chapter 3.
- 2) To identify the specific roles of junctin's cytoplasmic N-terminus (Njun) and luminal C-terminal domain (Cjun) on RyR regulation. The reported activation of purified RyR1 and RyR2 by junctin added to a luminal solution suggests that junctin activates RyR primarily via a luminal interaction. A cytoplasmic RyR-junctin interaction and its contribution to RyR regulation in conjunction with the luminal interaction have not

been previously explored. Therefore, this aims focused on exploring the respective roles of Njun and Cjun in modulating RyR activity. Complementary to this aim is an examination of how Cjun and Njun regulate RyR in concert. The full hypothesis and investigations of the second aim are detailed in Chapter 4 and 5.

- 3) To identify potential binding domains on junctin for RyR that are responsible for interaction between the two proteins. Multiple junctin-RyR interaction sites have been suggested (Altschafli et al., 2011; Dulhunty et al., 2012; Goonasekera et al., 2007). KEKE motifs have been proposed to facilitate protein-protein associations (Perutz, 1994; Realini and Rechsteiner, 1995; West et al., 2000), and junctin contains multiple KEKE motifs in its C-terminal domain (one “true” KEKE motif and two other KEKE-like motifs, defined in Chapter 6.1), which are presumed to participate in its interaction with RyR (Jones et al., 1995; Zhang et al., 1997). However, the role of KEKE motifs in the interaction between junctin and RyR remains unclear. Of particular interest to this study were the potential interactions between the “true” KEKE motif (residues 84-105) in junctin and RyR. Experimental findings with respect to this aim are presented in Chapter 6.

Chapter 2 Materials and Methods

2.1 Materials

2.1.1 Reagents and Chemicals

All materials used were of analytical grade. Acrylamide/Bis (37.5:1) solution, ammonium persulfate (APS), TEMED, Precision Plus Protein Dual Color standards, silver stain plus kit prep, cell dialysis membrane and Ni^{2+} -nitrilotriacetic acid agarose were purchased from Bio-Rad Laboratories, Inc. (N.S.W., Australia). Novex Dry ease large cellophane, Minimal Essential Medium (MEM) and Dulbecco's Modified Eagle Medium (DMEM) were obtained from Invitrogen Pty. Ltd (Mount Waverley, Australia). Tris, glycine and glycerol were from Bacto Laboratories Pty. Ltd. (N.S.W, Australia). The BCA protein assay kit, SuperSignal West Pico Chemiluminescent Substrate and PVDF membrane, NeutrAvidin-agarose and protein A/G plus agarose were from Thermo Fisher Scientific Inc. (Rockford, IL, USA). Fuji medical X-ray film was from Fujifilm Corporation (Tokyo, Japan). All stock solutions of phospholipids (phosphatidylethanolamine (PE), phosphatidylserine (PS) and phosphatidylcholine (PC)) were purchased from Avanti Polar lipids (Alabaster, USA). The monoclonal mouse anti-RyR 34C was obtained from Developmental Studies Hybridoma Bank, DSHB. A polyclonal anti-junctin antibody was raised against a junctin peptide (KLH-C-SKHTHSAKGNNQKRKN-OH, manufactured by GL Biochem, Shanghai, China) by IMVS Veterinary Services, Australia and purified. Precision StrepTactin-HRP conjugate for detecting biotinylated peptide was obtained from Bio-Rad Laboratories, Inc. (N.S.W., Australia). Anti-mouse, anti-rabbit IgG HRP secondary antibodies were from Santa Cruz (Santa Cruz, CA, USA). Nunc cell culture flasks were purchased from Thermo Fisher Scientific Inc. (Rockford, IL, USA) and petri dishes were from Bacto Laboratories Pty. Ltd. (N.S.W, Australia). Complete protease inhibitor cocktail tablets were obtained from F. Hoffmann-La Roche Ltd. (Roche Diagnostics, Germany). Isopropyl β -D-1-thiogalactopyranoside (IPTG) was from Astral Scientific (Caringbah, Australia). Lysozyme and MOPS were from Amresco (Solon, USA). All restriction-digestion enzymes were purchased from New England Biolabs (NEB). T4 DNA ligase was from Promega Corporation (Wisconsin, USA). All other chemicals were obtained from Sigma-Aldrich (Castle Hill, Australia). All PCR primers were synthesized by GeneWorks, Australia. Unless otherwise specified, all solutions and chemicals were dissolved or diluted in MilliQ-water, obtained from Milli-Q Advantage A10 ultrapure water purification system (Millipore Corporation, Billerica, USA). New Zealand white rabbits used to obtain skeletal muscle junctin were housed at the John Curtin School of Medical Research Animal House.

2.1.2 Peptides synthesized

Peptides were synthesized by the JCSMR Biomolecular Resource Facility using the 9-fluorenylmethyloxycarbonyl method on a CEM Microwave-assisted Peptide Synthesizer (CEM Corporation; Matthews, NC, USA). Synthesis was performed using Fmoc chemistry and solid phase peptide synthesis (SPPS) techniques. The N-terminus was protected by acetylation.

Njun: ¹MAEETKHGGHKNGRKGGLSQSS²²

Njun_{scrambled}: STGENKGHGLSGKHKSEGRAMG

Canine cardiac Jun_{KEKE} ⁸⁴KRRTKAKVKELT KEELKKEKEK¹⁰⁵

For affinity chromatography a biotin tag was conjugated to the N-terminal end of Njun,

Njun_{scrambled}, canine cardiac Jun_{KEKE} peptides.

The rabbit skeletal Jun_{KEKE} peptide, ⁸⁶KRRTKAKVKELIKEELKKGKEK¹⁰⁷, was manufactured by GL Biochem (Shanghai) Ltd (Shanghai, China).

All peptides were purified using high performance liquid chromatography (HPLC) (SHIMADZU, Japan) and purity was determined using mass spectroscopy (MALDI TOF/OFTTM Model 4800, Applied Biosystems, USA).

1 mg/ml stock peptides were prepared either in distilled water or relevant buffer depending on the down-stream application, snap frozen and stored in 10 µl aliquots at -20 or -70 °C. The precise concentration of the peptide solutions were confirmed by BCA assay method (see section 2.7.1).

2.3 SR vesicle isolation and RyR purification

The experimental procedures of SR vesicle isolation and RyR1/RyR2 purification were undertaken by Mrs. Suzy Pace and Mrs. Joan Stivala (Muscle Research Group, John Curtin School of Medical Research, Australian National University, Canberra, Australia). All steps were performed at 4 °C.

2.3.1 Isolation of skeletal and cardiac SR vesicles

2.3.1.1 Preparation of skeletal muscle RyR-enriched SR vesicle

For native skeletal SR vesicles, back and leg muscles (predominantly fast twitch skeletal muscle) were removed from New Zealand white rabbits, and SR vesicles were prepared using the methods of (Saito et al., 1984) with minor changes (Ahern et al., 1994). The skeletal muscle was removed and rinsed immediately in phosphate buffered saline (PBS), which contains 137

mM NaCl, 7 mM Na₂HPO₄, 2.56 mM NaH₂PO₄, and 2 mM EGTA(*ethylene glycol-bis[β-aminoethyl ether]N,N,N',N'-tetraacetic acid*), pH 7.4. Excess fat was removed, the muscle tissue was then diced and snap-frozen in 50 g aliquots in liquid nitrogen and stored at -70 °C until required.

The diced muscle tissue was snap frozen. During preparation of SR vesicles, 100 g tissue was homogenized in a Waring blender (Waring Products Div., Connecticut, USA) for 4 × 15 s on high speed in a homogenizing buffer consisting of 5 mM imidazole, 300 mM sucrose, pH 7.4 and a cocktail of protease inhibitors (1 mM benzamide, 0.5 mM PMSF, 3 μM anti-calpain I, 3 μM anti-calpain II, 2.3 μM leupeptin and 1.46 μM pepstatin A). In all cases, pH was adjusted using a TPS digital pH meter (Bacto Laboratories; Lane Cove, Australia). The homogenate was centrifuged at 11,000 × g for 20 min in a Beckman J2-21 centrifuge, JA-14 rotor (Beckman Instruments, Gladesville, Australia). The pellet was resuspended in the homogenizing buffer, followed by another homogenization and centrifugation as described above. The resultant supernatant was then filtered through four layers of cotton gauze and centrifuged at 110,000 × g in a Beckman Coulter Optima XE-100 ultracentrifuge, Ti-45 rotor for 1-2 h.

The pellet, containing crude SR, was collected and resuspended in 42 ml homogenising buffer in a Dounce Teflon homogeniser (Edwards Instrument Company; Narellan, Australia). Eight ml of homogenized vesicles was loaded onto a discontinuous sucrose density gradient comprising of 4 ml of 45%, 7 ml of 38%, 7 ml of 34%, 7 ml of 32% and 4 ml of 27% (w:v) sucrose layers. Sucrose solutions were prepared in a SR diluting buffer containing 20 mM imidazole, pH 7.4 and a cocktail of protease inhibitors as described above.

The sucrose gradient was centrifuged at 72,000 × g overnight in a SW28 rotor (Beckman L8-70 Ultracentrifuge, Beckman Instruments, Australia) at 4 °C to allow the sub-fractionation of crude SR vesicles. The bands at the 34-38% (band 3) and 38-45% (band 4) were collected and diluted with at least two volumes of diluting buffer. Finally, the diluted fractions were centrifuged at 125,000 × g in a Beckman Ti-45 rotor at 4 °C for 1 h (Beckman L8-70 Ultracentrifuge, Beckman Instruments, Australia). The final pellet was resuspended in 1 ml homogenizing buffer and protease inhibitor cocktail, divided into 15 μl aliquots, snap frozen and stored at -70 °C.

2.3.1.2 Cardiac crude SR preparation

Cardiac crude SR was prepared as described by Chamberlain and Fleischer (1988) with adjustment. Sheep hearts were collected in ice cold phosphate buffered saline (PBS, contents see 2.3.1.1) with 2 mM EGTA and then rinsed several times to remove blood. Fat was trimmed from the ventricles and the auricles removed. The ventricles were cut to small pieces in Petri dishes in homogenizing buffer containing 0.29 M sucrose, 10 mM imidazole, 0.5 mM DTT and

3 mM NaN₃, pH 6.9, and homogenized in a Waring blender 3 x 10 s on high. The homogenates were centrifuged at 9,700 x g in a Sorvall SS-34 rotor for 20 min. The resultant supernatant was filtered through four layers of cotton gauze, followed by a further high speed centrifugation in a Beckman Ti-45 rotor for 2 h at 104,537 x g. The pellet was then resuspended in 60 ml of Solution A (homogenizing buffer with 0.65 M KCl, plus standard protease inhibitor cocktail: 1 mM benzamide, 0.7 mM PMSF, 2.3 μM leupeptin (1 μg/ml) and 1.46 μM pepstatin A (1 μg/ml), in a Potter homogenizer (Edwards Instrument Company; Narellan, Australia). The homogenate was set on ice for 30 min and centrifuged at 4,350 x g for 10 min in Beckman JA-20 rotor, to remove insolubles. The supernatant was then centrifuged at 257,090 x g in a Beckman Ti-70 rotor for 100 min. The crude SR pellet was finally suspended in 15 ml of Solution A, snap frozen in 15 μl or 1 ml aliquots and stored at -70 °C or in liquid nitrogen.

2.3.2 Purification of RyR1 and RyR2

RyR1 and RyR2 were purified from rabbit skeletal SR and sheep cardiac SR respectively using the same procedure according to (Lee et al., 1994) and (Laver et al., 1995) with minor modifications. RyR was purified from solubilized SR vesicles using a discontinuous sucrose gradient. Gradient and solubilization solutions contained 25 mM Na-PIPES (piperazine-N,N'-bis (2-ethanesulfonic acid)), 1 M NaCl, 1 mM DTT (dithiothreitol), 0.5% (w/v) CHAPS, 0.25% (w/v) L- α -phosphatidylcholine (Avanti), 100 μM EGTA, 92 μM CaCl₂, 500 μM AMP, pH 7.4 and protease inhibitors recommended by the provider (Roche 'Complete' tablet). Sucrose gradients were made of four 7.5 ml layers (5%, 10%, 15% and 20% (w/v) sucrose), and kept for at least 4 h before use. A mixture of 10 mg of SR vesicles were solubilized on ice for 0.5-1 h in solubilization solution at a final protein concentration of 2.5 mg/ml, where the vesicles were homogenized for 1 min every 10 min using a glass Potter homogenizer (Kontes Glass Company; Vineland, New Jersey, USA) during incubation. The insoluble membrane fragments were removed by centrifugation at 163,200 x g for 20 min (Beckman rotor TLA 100.3). Supernatant containing the solubilized SR (4 ml) was loaded on to the continuous 5-20% sucrose gradient and centrifuged overnight (14-16 h) at 71,935 x g in a Beckman SW28 rotor. Fractions (2 ml) were then collected, and RyR-enriched fractions were identified on silver-stained SDS/PAGE and immunoblot. Selected fractions containing purified RyR1/RyR2 were sequentially concentrated ~10-fold using a Vivaspin 2 concentrator (Sartorius Stedim Biotech; Bohemia, USA), snap frozen in 15 μl aliquots and stored at -70 °C. Protein concentration was determined by DC protein assay (Lowry assay) (Bio-Rad). The purified RyRs were routinely checked with immunoblot using anti-CSQ, anti-triadin and anti-junctin antibody to ensure there was no contamination by those regulatory proteins (Fig. 2-1).

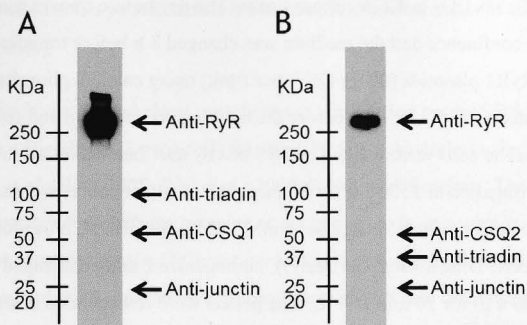


Figure 2-1 Purification of skeletal RyR1 and cardiac RyR2. (A) Immunoblot of purified RyR1 (~0.35 μ g) from rabbit skeletal SR vesicles using anti-RyR 34C, anti-triadin (IIG12 for skeletal isoform), anti-CSQ1 (VIIIID21) and anti-junctin antibodies. (B) Immunoblot of purified RyR2 (~0.5 μ g) from sheep cardiac SR vesicles using anti-RyR 34C, anti-CSQ2, anti-triadin (E18 for cardiac isoform) and anti-junctin antibodies. (A) and (B) confirmed the presence and the purity of RyR1 and RyR2 respectively (no CSQ, triadin and junctin contamination). The position of the molecular weight markers are shown to the left of the lanes.

2.4 Recombinant RyR1 and RyR2 preparation

2.4.1 RyR1 preparation

2.4.1.1 RyR1 plasmid construction

The construction of RyR1 plasmids (GFL) was undertaken by Dr. Shamaruh Mirza (Canberra, Australia).

A HindIII restriction enzyme site was introduced by PCR upstream of the initiation codon of rabbit RyR1 cDNA; forward and reverse primers were 5' - AAG CTT ACA CCA TGG GTG ACG GAG G and 5' - GGC CGT CGA CAG GTG CAG GTA respectively. Amplification conditions were denaturation 92 °C 30 s, annealing 55 °C 30 s, extension 72 °C 45 s, with a total of 35 cycles. The PCR amplified HindIII_{polylinker}/SallI546 fragment was ligated into HindIII/Sall sites of the polylinker of the pEGFP-C1 to form the GHS construct. Subsequently the SallI546/Sall_{polylinker} from the pTZ full length RyR cDNA (kindly supplied by Dr. Francesco Zorzato, Department of Biomedicine and Anesthesiology, Basel University Hospital, Hebelstrasse, Basel, Switzerland; (Zorzato F, 1990)) was removed and cloned in-frame into GHS to form GFL (RyR tagged at the 5'-end with EGFP).

2.4.1.2 Expression and purification of recombinant RyR1 constructs

HEK293 cells were grown in MEM (Minimal Essential Medium) (Invitrogen, Mount Waverley, Australia) with 10% FCS, 0.1% PSN (Penicillin G+ Streptomycin Sulphate+ Neomycin

Sulphate), at 37 °C, 5% CO₂ in T175 culture flasks. The day before transfection, cells were plated out at 50% confluence and the medium was changed 3 h before transfection. Cells were transfected with RyR1 plasmids (80 µg DNA per flask) using calcium phosphate precipitation. Cells were incubated at 37 °C for 24 h before the medium was changed and for another 24 h before harvesting. The cells were washed in PBS briefly and then harvested in cold PBS followed by centrifugation at 1500 x g for 20 min. The resultant pellets were suspended in sucrose-imidazole buffer (300 mM sucrose, 5 mM imidazole, pH 7.4, plus protease inhibitor cocktail tablet (Roche Diagnostics, Germany)), homogenized, and centrifuged in an Eppendorf centrifuge (~11600 x g) for 20 min at 4 °C. The pellets were resuspended in sucrose buffer and re-homogenised. After ultra-centrifugation at 91943 x g for 2 h at 4 °C in a Beckman TLA120.2 rotor, the pellets were homogenised using potter homogenizer with 100 strokes and resuspended in sucrose-imidazole buffer. The homogenates were snap-frozen and stored at -70 °C.

2.4.2 RyR2 preparation

2.4.2.1 RyR2 construct

Recombinant RyR2 in stable, inducible HEK293 cell lines was obtained from collaborator Dr. Magdolna Varsanyi (Institut für Physiologische Chemie, Ruhr-Universität, Bochum, Germany). For generation of the stable, inducible HEK293 cell lines, please refer to (Koop et al., 2008).

2.4.2.2 Expression and purification of recombinant RyR2 mutant

The stable, inducible HEK293 cell lines were grown in DMEM (Dulbecco's Modified Eagle Medium) high glucose with sodium pyruvate (Invitrogen, USA), with 10% FBS, 1% PS (100U Penicillin G, and 100 µg/ml Streptomycin Sulphate), 2 mM L-glutamine, 0.1 mM non-essential amino acids, and 50 µg/ml Hygromycin B, at 37 °C, 5% CO₂ in Nunc cell culture flasks. Before inducing expression, cells were split into media without Hygromycin B and incubated at 37 °C for 24-48 h. Expression was induced by incubating cells in media with 1µg/ml tetracycline and without Hygromycin B for another 24-48 h as described previously (Kong et al., 2007; Koop et al., 2008). After harvesting cells, the cell pellets were homogenized the same way as for RyR1 constructs described in section 2.4.1.2. Briefly, when cells reached full confluency, they were collected in PBS and centrifuged at 1500 x g for 20 min, the resultant pellets were then suspended in sucrose-imidazole buffer (for buffer content see above, section 2.4.1.2), homogenized and centrifuged (11600 x g). The pellets were resuspended in sucrose-imidazole buffer and re-homogenised. After ultra-centrifugation (91943 x g), the pellets were homogenised and resuspended in sucrose-imidazole buffer. The homogenates were snap-frozen at 15 µl aliquots and stored at -70 °C until required.

2.5 Junctin purification

2.5.1 Endogenous junctin purification from rabbit skeletal muscle (SDS preparative gel electrophoresis)

Isolation of junctin from rabbit skeletal muscle tissue was carried out by SDS preparative gel electrophoresis in a Bio-Rad 491 prep cell (Bio-Rad; N.S.W., Australia) using the procedure described in Wei *et al.* (Wei, 2008; Wei et al., 2009a) with modifications. The Bio-Rad 491 prep cell is an apparatus for purifying proteins or nucleic acids from complex mixtures by continuous-elution electrophoresis. Different percentages of resolving and stacking gels were used. The resolving gel was prepared on a casting stand in a 28 mm diameter gel assembly tube at a 6.5 cm height, containing 12% acrylamide/bis (37.5:1), 0.375 M Tris-HCl (pH 8.8), 0.025% ammonium persulphate (APS), and 0.025% *N,N,N,N*-Tetramethylethylenediamine (TEMED). A stacking gel of double the sample volume was prepared and contained 4% acrylamide/bis (37.5:1), 0.125 M Tris-HCl (pH 6.8), 0.05% (APS), and 0.1% TEMED.

To isolate junctin, skeletal crude SR vesicles (see section 2.3.1.1) were solubilized in 1%/0.5% CHAPS/PC, 1mM DTT, 1M NaCl, 20mM MOPS, and 200 μ M EGTA pH 7.4 plus protease inhibitors, with homogenization on ice for 1 h. Solubilized SR vesicles were then centrifuged at 135,000 x g for 15 min in a Beckman TLA 100.3 rotor to remove insoluble membrane fragments. The supernatant was diluted 2:1 with a sample buffer containing 188 mM Tris-HCl, pH 6.8, 30% glycerol, 6% SDS, 0.06% bromophenol blue, and 15% β -mercaptoethanol and boiled for 5min before being loaded onto the preparative gel.

The electrophoresis was run at a constant current of 40 mA in a denaturing buffer containing 25 mM Tris, 191 mM glycine, 0.1% SDS, pH 8.3. Fractions were collected when the tracking dye started to migrate out of the gel, approximately 4 h after the electrophoresis started. Two ml fractions were collected at a flow rate of 1ml/min using a Model EP-1 Econo peristaltic Pump (Bio-Rad; N.S.W., Australia) and a BioLogic BioFraction collector (Bio-Rad; N.S.W., Australia). Eighty fractions were collected and analyzed by mini SDS-PAGE followed by coomassie blue stain or silver stain and immunoblot (using anti-junctin antibody) to locate junctin.

To re-nature the junctin protein purified from the denaturing system (SDS), detergent exchange was used by replacing the denaturing buffer with a non-denaturing buffer to induce protein refolding. Junctin was firstly co-precipitated from fractions by adding potassium chloride (KCl) (Carraro et al., 1991; Wei, 2008) to a final concentration of 400 mM, incubating at room temperature for 20 min with gentle agitation. The fractions were then centrifuged in an eppendorf centrifuge (~15,800 x g) for 15 min. The precipitated protein was eluted and re-folded by detergent exchange in a buffer containing 0.2% Triton X-100, 20 mM MOPS, 150 mM KCl, and 200 μ M EGTA, pH 7.4 plus protease inhibitors, and incubating at room

temperature for 1 h. The mixture was then centrifuged as above for 10 min to remove SDS-KCl precipitates. Dissolved protein remained in the supernatant, which was diluted at least 20-fold to remove residual Triton X-100 (the concentration of Triton X-100 was reduced to disrupt protein-detergent micelles) by washing samples 4 times in MOPS buffer (20 mM MOPS, 150 mM NaCl, pH 7.4 with protease inhibitors), using Millipore's Amicon Ultra-4 centrifugal filter devices following the manufacture's instruction (Millipore corporation). During the final wash, the purified junctin was concentrated to 0.2-0.4 mg/ml and stored at -70 °C until required.

2.5.2 Recombinant canine cardiac full-length junctin (FLjun)

2.5.2.1 Plasmid construction

The construction of 6×His-FLjun plasmid was undertaken by Dr Shama Mirza (Canberra, Australia).

Recombinant full-length canine junctin in the pBlueScript II SK vector (Jones et al., 1995) was sub-cloned into a pET15b.ep (modified) vector using forward and reverse PCR primers 5'-GGG GGG CAT ATG GCT GAA GAG ACA AAG and 5'-CGG GAT CCT CAG TTC TTC TTC TTC respectively. Amplification conditions were denaturation 95 °C 30 s, annealing 56 °C 30 s, extension 72 °C 36 s, total 30 cycles. The PCR amplified NdeI/BamHI_{polylinker} was digested by NdeI and BamHI and subsequently subcloned into the NdeI/BamHI sites of the polylinker of the pET15b.ep (modified) vector, downstream and in-frame with a poly-histidine-tag. FLjun-pET15b.ep (modified) was formed by digesting the pET15b.ep (mod) plasmid and PCR amplified FLjun fragment with NdeI/BamHI following with gel-purifying the DNA fragments and ligating for 45 min at room temperature. Constructs were verified by sequencing (JCSMR Biomolecular Resource Facility).

2.5.2.2 Expression and purification of recombinant FLjun by IMAC (Immobilized metal affinity chromatography)

The majority of this work was conducted by Miss Umayal Narayanan (Muscle Research Group, John Curtin School of Medical Research, Australian National University, Canberra, Australia) under my supervision. All steps were carried out at 4 °C unless otherwise noted.

The FLjun-pET15b.ep (mod) plasmid was transformed into *E. coli* BL21(DE3) and FLjun was expressed as a His fusion protein in *E. coli*. A single colony was inoculated into 5 ml of Luria-Bertani (LB) broth supplemented with 125 µg/ml ampicillin at 37 °C overnight. The culture was transferred to a larger volume of fresh LB broth (1:100 dilution) supplemented with 125 µg/ml ampicillin, incubated at 37 °C with agitation until A600 was between 0.6 and 0.8. Protein expression was induced by adding isopropyl-β-D-thiogalactoside (IPTG) to a final

concentration of 0.6 mM, and incubation was continued for another 3-4 h at 37 °C. The bacterial cells were centrifuged (5,000 x g, 20 min at 4 °C). Cell pellets were either used immediately for FLjun purification or frozen at -20 °C until required.

The cell pellets were resuspended in cold PBS (137 mM NaCl, 7 mM Na₂HPO₄, 2.56 mM NaH₂PO₄, pH 7.4) plus 1% Triton X-100, 5% glycerol and protease inhibitor cocktail tablet (Roche Diagnostics, Germany). Then the cells were lysed in 0.5 mg/ml lysozyme for 20 min on ice followed with sonication using Branson Sonifier S-250A Analog Ultrasonic Cell Disruptor/Homogenizer (Branson Ultrasonics Corporation, Danbury, Connecticut, USA) for a complete disruption of the cell membrane. The lysate was centrifuged at 15,000 x g for 25 min at 4 °C twice in a SS-34 rotor (Sorvall) to remove any unbroken cells and debris. The cleared supernatant was again centrifuged at 150,000 x g for 45 min at 4 °C either in a TLA100.3 or Ti70 rotor (Beckman ultra). The resultant supernatant which contains solubilized FLjun was then incubated with Ni²⁺-nitrilotriacetic acid (NTA) agarose (Bio Rad) (with 25 mM imidazole) at 4 °C for 2 h, allowing the poly His-fusion protein to attach to the matrix. Following incubation, the FLjun-poly His-Ni²⁺-NTA agarose complex was washed in cold Buffer A (50 mM NaH₂PO₄, 300 mM NaCl, pH 8.0 with 1% Triton X-100, 5% glycerol and 25-35 mM imidazole) and the fusion protein was finally eluted with Ni elution buffer (50 mM NaH₂PO₄, 300 mM NaCl, 250 mM imidazole, pH 8.0 with 1% Triton X-100 and 5% glycerol). The protein was concentrated and dialyzed against MOPS buffer (20 mM MOPS, pH 7.4, 150 mM NaCl plus 0.2% Triton X-100 and 5% glycerol). Triton X-100 was removed using Bio-Beads SM-2 adsorbents (Bio-Rad; N.S.W., Australia) that were degassed before usage according to manufacturer's instructions. Purified FLjun from above steps was then incubated with the prepared adsorbents at room temperature for 1 h and 45 min followed by centrifugation in an eppendorf centrifuge (~1000 x g for 3 min). The supernatant that contains purified FLjun but not Triton X-100 was concentrated using Millipore's Amicon Ultra-4 centrifugal filter devices following the manufacture's instruction (Millipore corporation) (~0.2 mg/ml). Final sample was snap-frozen and stored at -70 °C until required.

NB. The methods for recombinant canine cardiac FLjun purification are novel and were developed and optimized by me as a part of this project.

2.5.3 Recombinant canine cardiac junctin C-terminus (Cjun) with His-tag

2.5.3.1 Plasmid construction

Construction of the 6×His-Cjun plasmid was conducted by Dr Dan Liu (Molecular Genetics Group, John Curtin School of Medical Research, Australian National University, Canberra, Australia.)

Luminal junctin (Cjun) corresponding to junctin aa46-210 was made using forward and reverse PCR primers 5'-CGG AAT TCC TTG TTG ATT ATG AAG AAG TT and 5'-CGG GAT CCT CAG TTC TTC CTC TTC TGG T respectively, from full length junctin in the pBlueScript II SK vector (Jones et al., 1995). Amplification conditions were denaturation 95 °C 30 s, annealing 52 °C 30 s, extension 72 °C 40 s, total 30 cycles. The PCR amplified EcoRI136/BamHI_{polylinker} fragment was ligated into EcoRI/BamHI sites of the polylinker of the pGADT7 to form the Cjun-pGADT7 construct. Subsequently this construct was digested by NdeI and BamHI and subcloned into the NdeI and BamHI sites of the polylinker of the pET15b.ep (modified) vector, downstream and in-frame with a poly-histidine-tag, to form Cjun-pET15b.ep (mod) by digesting the plasmids pET15b.ep and pGADT7-Cjun with NdeI/BamHI following with gel-purifying the DNA fragments and ligating overnight at 4 °C. Constructs were verified by sequencing (JCSMR Biomolecular Resource Facility).

2.5.3.2 Expression and purification of recombinant 6xHis-Cjun by IMAC

The Cjun-pET15b.ep (mod) plasmid was transformed into *E. coli* BL21(DE3) and Cjun was expressed as a His fusion protein in *E. coli*. A single colony was inoculated into 5 ml of LB broth supplemented with 125 µg/ml ampicillin at 37 °C overnight. The culture was transferred to a larger volume of fresh LB broth (1:100 dilution) supplemented with 125 µg/ml ampicillin, incubated at 37 °C with agitation until A600 was between 0.6 and 0.8. Protein expression was induced by adding isopropyl-β-D-thiogalactoside (IPTG) to a final concentration of 0.6 mM, and incubation was continued for another 3-4 h at 37 °C. The bacterial cells were centrifuged (5,000 x g, 20 min at 4 °C). Cell pellets were either used immediately for Cjun purification or frozen at -20 °C until required.

The cell pellets were resuspended in cold PBS plus protease inhibitor cocktail tablet (Roche Diagnostics, Germany) and lysed in lysozyme (0.5 mg/ml) for 20 min on ice followed with a FRENCH Pressure cell (1000 psi) for cell membrane disruption. The lysate was centrifuged at 100,000 x g for 40 min at 4 °C either in a TLA100.3 or Ti70 rotor (Beckman ultra). The supernatant which contains Cjun was then incubated with Ni²⁺-NTA agarose (Bio Rad) (1ml of 50% slurry was used for 500 ml bacteria culture) at 4 °C for 2.5 h followed with wash in cold Buffer A (50 mM NaH₂PO₄, 300 mM NaCl, pH 8.0 with 10-20 mM imidazole) to remove non-specific bindings, the fusion protein was eluted with Ni elution buffer (50 mM NaH₂PO₄, 300 mM NaCl, 500 mM imidazole, pH 8.0). The protein was concentrated and the buffer was exchanged with MOPS buffer (20 mM MOPS, pH 7.4, 150 mM NaCl) using Millipore's Amicon Ultra-4 centrifugal filter devices (Millipore corporation). Purified 6xHis-Cjun (~0.5 mg/ml) was snap-frozen and stored at -70 °C.

2.5.4 Recombinant canine cardiac junctin C-terminus (Cjun) without His-tag

2.5.4.1 Plasmid construction

To ensure there is no non-specific interaction between poly His-tag and RyRs, pHUE system was employed (Baker et al., 2005; Catanzariti et al., 2004b), as this system enables the His-tag to be cleaved from Cjun by using a catalytic fragment of the deubiquitylating enzyme (ubiquitin-specific protease) mouse Usp2cc, which was also fused to a poly-histidine tag (see section 2.5.4.2). Cjun was made using forward and reversed PCR primers 5'-GACCCGCGGTGGACTTGTTGATTATGAAG and 5'-CGAAGCTTTCAGTTCTTCCTCTTC respectively, from Cjun-pET15b.ep (mod) vector, see section 2.5.3.1. Amplification conditions were denaturation 95 °C 1 min, annealing 50 °C 1 min, extension 72 °C 1 min for a total of 28 cycles. The PCR amplified SacII/HindIII_{polylinker} fragment was digested by KspI (KspI and SacII recognize the same restriction site) and HindIII and subsequently subcloned into the SacII and HindIII sites of the polylinker of the pHUE vector, downstream and in-frame with a poly-histidine-tagged ubiquitin. Cjun-pHUE was formed by digesting the plasmid pHUE and PCR amplified Cjun fragment with KspI/HindIII following with gel-purifying the DNA fragments and ligating overnight at 4 °C.

After ligation, the products were then transformed to DH5a competent cells. Several colonies were picked to plate out, and inoculated in 5 ml LB+Amp. Plasmid has been extracted with miniprep kit (Qiagen) followed by digesting with *KspI/HindIII*. The digested plasmids were then run on a 1% agarose gel. Those with right size band (~500 bp) were regarded as positive colonies, which were further verified by sequencing (JCSMR Biomolecular Resource Facility).

2.5.4.2 Expression, purification and His-tag cleavage of recombinant Cjun

The Cjun-pHUE plasmid was transformed in *E.coli* strain BL21(DE3) and Cjun was expressed as a poly His-ubiquitin fusion protein in *E.coli* colonies in the same way as for Cjun-pET15b.ep described in section 2.5.3.2. Briefly, a single colony was grown in LB broth supplemented with 125 µg/ml ampicillin at 37 °C overnight and then transferred to a larger volume of LB broth (1:100 dilution) with ampicillin, incubated at 37 °C to an optical density of 0.6-0.8 at 600 nm. Protein expression was induced by 0.6 mM IPTG for 3-4 h at 37 °C before bacteria were collected by centrifugation (5,000 x g, 20 min at 4 °C). Cell pellets were either used immediately for Cjun purification or frozen at -20 °C until required.

Recombinant protein was purified in a similar way as for 6xHis-Cjun (section 2.5.3.2). The cell pellets were resuspended in cold PBS plus protease inhibitors and lysed by using lysozyme followed with a FRENCH Pressure cell (1000 psi). After centrifugation at 100,000 x g for 40 min at 4 °C, the recombinant Cjun was purified from the clear lysate by affinity chromatography

using Ni²⁺-NTA agarose and finally eluted in Ni elution buffer (for buffer content see section 2.5.3.2).

After purification, the 6xHis-ubiquitin tag used for the affinity chromatography was subsequently cleaved by digestion with Usp2cc, in the presence of 1mM DTT at 25 °C for 3 h. As the Usp2cc was also fused to a poly-histidine tag, this protein was obtained and purified using a similar method of *E. coli* expression and IMAC as described in Catanzariti et al. (2004a). The excised 6xHis-ubiquitin tag and Usp2cc were then removed by incubating the digested recombinant protein with Ni-NTA agarose at 4 °C for 2 h. The resin was then spun down at 453 x g for 10 min, the supernatant, containing purified Cjun, was washed, concentrated in MOPS buffer (20 mM MOPS, 150 mM NaCl, pH 7.4) (~0.6 mg/ml) using Amicon concentrators and stored at -70 °C until required. This strategy provides recombinant Cjun without any additional residues.

2.6 Electrophoresis and immunoblot

2.6.1 SDS-Polyacrylamide Gel Electrophoresis (PAGE)

Denaturing SDS-PAGE was performed to analyze and visualize the proteins using a Bio-Rad Mini-PROTEAN[®] Tetra Cell system according to the method of Laemmli (1970). 0.75 mm thick mini Tris-Glycine gels of various polyacrylamide percentages, including 7%, 10%, 12%, as well as 4-15%, 5-17% gradient gels, were used according to the molecular weight of the analyzed proteins. Running gels were composed of an appropriate percentage of acrylamide-bis (37.5:1 v/v), 0.1% SDS, 0.375 M Tris-HCl (pH 8.8), 0.05% APS and 0.2% TEMED in MilliQ-water. A stacking gel, the top 1.5 cm of the 7.0 cm gel, was normally composed of 3 or 4% acrylamide-bis (37.5:1 v/v), 0.1% SDS, 0.125 M Tris-HCl (pH 6.8), 0.1% APS and 0.2% TEMED in MilliQ-water. Protein samples were mixed with a 4 x sample buffer containing 250 mM Tris-HCl (pH 6.8), 40% glycerol, 10% SDS, 20% mercaptoethanol and 0.1% bromophenol blue. Gels were run at 200 V constant voltage on a Bio-Rad power pac 200/300 (Bio-Rad; N.S.W., Australia) for approximately 60 min in electrophoresis buffer, composed of 25 mM, 191 mM Glycine and 0.1% SDS, pH 8.3.

Bio-Rad Precision Plus Protein Dual Color standards (Bio-Rad; N.S.W., Australia) were used as protein standards unless otherwise noted.

2.6.2 Protein stains

2.6.2.1 Coomassie Brilliant Blue

Protein bands were visualized by staining gels with Coomassie blue stain, containing 0.1% coomassie brilliant blue, 40% ethanol and 10% glacial acetic acid, for at least 1 h with gentle agitation. Excess staining of gel background was then removed by destaining gels using a destaining solution composed of 20% ethanol and 5% acetic acid. The spent destain solution was periodically exchanged with fresh destain until the background are completely destained. The gels were either stored in MilliQ-water and photographed or dried as described in section 2.6.3.

2.6.2.2 Silver Stain

Silver staining is a highly sensitive method for detecting proteins in polyacrylamide slab gels, and is 10-50 folds more sensitive than Coomassie brilliant blue R-250 for proteins (detection is ~ 0.1 ng/mm²). A Silver Stain Plus kit was used according to manufacturer's instructions (Bio-Rad; N.S.W., Australia). After gel electrophoresis, the gel was placed in a Fixative Enhancer solution containing 50% methanol, 10% acetic acid and 10% fixative enhancer concentrate for 20 min with gentle agitation. The fixing step renders the protein molecules in the gel insoluble and prevents them from diffusion. Substances such as ions, denaturant, or detergents that interfere with silver staining are removed during this step. After fixing, the gel was then rinsed 2 x 10 min in MilliQ-water followed by developing in staining solution, containing 5% silver complex solution (contains NH₄NO₃ and AgNO₃), 5% reduction moderator solution (contains tungstosilicic acid), 5% image development reagent (contains formaldehyde), and 2.5% (w/v) development accelerator reagent (contains Na₂CO₃). Under mildly acidic conditions, silver ions are prevented from being reduced and thus can react with proteins. Upon addition of formaldehyde, the silver ions are reduced to metallic silver at high pH (Na₂CO₃ renders the development solution alkaline). The gel was developed for about 15 min until desired staining is achieved, which was stopped by placing the gel in 5% acetic acid for a minimum of 15 min. after stopping the reaction, the gel was washed in MilliQ-water for 5 min and dried or photographed.

2.6.3 Gel drying

A gel drying apparatus (Invitrogen, USA) was used for preserving gels. After extensive washes in MilliQ-water, gels were equilibrated in a dehydrating buffer (2% glycerol, 20% ethanol) for at least 20 min. Two sheets of cellophane were soaked in dehydrating buffer for 1 min. The equilibrated gels were then sandwiched between the two cellophane sheets, which again were sandwiched between drying frames for 12-36 h. The dried gels were documented by digital imaging on a flat bed scanner.

2.6.4 Immunoblot

2.6.4.1 PVDF membrane transfer

Immunoblot analysis was performed as described previously (Towbin et al., 1979). SDS-PAGE was performed as described in 2.6.1. Following electrophoresis, the gel was transferred to a transblot cassette (Bio-Rad) overlaid with a 0.45 μm PVDF membrane and sandwiched between layers of fiber pads plus filter paper. The PVDF membrane was prepared soaking in methanol for 1 min, in MilliQ-water for 5 min and finally equilibrating in transfer buffer, containing 37 mM Tris, 140 mM glycine and 20% methanol for at least 10 min. The final cassette was clamped and placed in a transblot tank and proteins were electrophoretically transferred at 35 V for 1 h, then at 100 V for 2 h in transfer buffer using a Bio-Rad Power Pac HC (Bio-Rad; N.S.W., Australia).

2.6.4.2 Immuno-detection

After protein transferred, the blot was immersed in 5% (w/v) skim milk dissolved in PBS (to block non-specific binding) for 1 h at room temperature. With respect to multiple protein bands detection, as the bands required different probes, the membrane was cut according to molecular weight as indicated by prestained protein standards. After a brief wash with TPBS (0.05% Tween-20 in PBS), the membrane was then incubated in primary antibody (containing antibody in TPBS with appropriate dilution) with rotation overnight at 4°C. The membrane was washed extensively in TPBS (6 \times 5 min) and then exposed to a horseradish peroxidase (HRP) labelled secondary antibody (1:6000 of anti-mouse, anti-rabbit in TPBS) for 1-2 h at room temperature with rotation. Following washing with 5 \times 5 min TPBS and 1 \times 5 min PBS, the blot was finally visualized (for visualization of multiple protein bands, the cut membranes were reassembled in the same cassette for exposure). For detection of biotin bound peptide, the membrane was blocked in 5% milk overnight at 4 °C at first, followed with 5 \times 5 min of wash with TPBS and then exposed to StrepTactin (1:5000 in TPBS) for 1-2 h at room temperature (and washed as listed above) and visualized.

2.6.4.3 Visualization (SuperSignal Chemiluminescence)

After antibody exposure, the membrane was exposed to SuperSignal West Pico Chemiluminescent Substrate (Thermo Fisher Scientific) according to company's instructions. Briefly, the working solution was prepared by mixing equal parts of the Stable Peroxide Solution and the Luminol/Enhancer Solution. The blot was then incubated with working solution for 5 min. After being removed from working solution, the blot was placed in a plastic membrane protector (plastic wrap) and then a film cassette with the protein side facing up. In a darkroom, the membrane was exposed to Fuji Super RX medical X-ray film (Fujifilm Corporation, Japan) for seconds to minutes, exposure time varied to achieve optimal results.

The film was then developed by submerging in Kodak Readymatic dental Developer (Carestream Helath; Rochester, USA) (1min) and Kodak Readymatic dental Fixer (1min) with shaking sequentially, and finally washed in water and air dried.

2.6.5 Protein densitometry

Protein bands density (either stained gels or x-ray films from Immunoblot) was quantified by Quantity One 1-D Analysis software (Gel Doc XR) (Bio-Rad; N.S.W., Australia). The background was removed by subtracting the density of a section directly underneath the protein band from the density of the protein band.

2.7 Protein determination

2.7.1 BCA protein assay

Protein concentration was determined by using a Pierce BCA protein assay kit according to manufacturer's instruction. The assay was conducted in a 96 well flat bottom IWAKI-ELISA/assay plate (Asahi Techno Glass Corporation). Working Reagent (WR) was firstly prepared by mixing 50 parts BCA Reagent A with 1 part Reagent B (Reagent A:B, 50:1). Protein standards were prepared by weighing out BSA and dissolving it in solution the same as protein sample solution. Ten μl of sample solution and protein standards of 0.125, 0.25, 0.375, 0.5, 0.75, 1, 1.5 and 2 mg/ml (BSA) were added in triplicate to the wells, followed by 10 μl of protein samples in duplicates or triplicates. 200 μl WR was added to each well, and the plate was covered with parafilm (Pechiney Plastic Packaging, Inc. Chicago, USA) and mixed thoroughly for 30 s on a titertek plate shaker (Flow laboratories; North Ryde, Australia). After incubating at 37 °C for 30 min, the plate was cooled to room temperature; the absorbance was measured at 562 nm (reference wavelength: 750 nm) using a EL8000 Universal Microplate reader (BioTek Instruments, Inc. Winooski, Vermont, USA). Sample protein concentrations were determined by using the standard curve generated by the KCjunior software (BioTek Instruments, Inc. Winooski, Vermont, USA).

2.7.2 Protein A280

When a rapid estimation of protein concentration was required, spectrophotometric determination of absorbance at 280 nm (A280) was used. Absorbance was measured on a Nanodrop ND-1000 spectrophotometer (Thermo Fisher Scientific). This method is applicable to purified proteins that contain tryptophan (Trp, W), tyrosine (Tyr, Y) residues or cysteine (Cys, C)-cysteine disulphide bonds and exhibit absorbance at 280 nm.

The protein concentration was calculated according to Beer's Law:

$$c = A / \epsilon b$$

Where c is the molar concentration of the analyzed protein solution (moles/liter or molarity (M)); A , the absorbance value; ϵ , the molar absorption coefficient ($M^{-1}cm^{-1}$) and b , the path length (cm). At 280 nm, the value of the molar absorption coefficient, i.e. ϵ , was approximated by the following equation:

$$\epsilon = (nW \times 5500) + (nY \times 1490) + (nC \times 125)$$

Where n is the number of each residue.

2.8 Protein binding assay

2.8.1 Modified Co-Immunoprecipitation (Co-IP)

To investigate protein-protein interactions between FLjun or recombinant Cjun and purified RyR1/RyR2 isolated from skeletal/cardiac muscle, a modified co-immunoprecipitation (co-IP) (Beard et al., 2008) was performed using the Pierce Co-Immunoprecipitation (Co-IP) kit (Thermo Fisher Scientific) according to manufacturer's instructions with modifications. For each experiment, 20 μ l of protein A/G plus agarose was prepared by washing with 200 μ l of 1 x coupling buffer (containing 0.01 M sodium phosphate, 0.15 M NaCl, pH 7.2) followed with centrifugation to remove the supernatant. The wash step was repeated twice. The control agarose (Thermo Fisher Scientific) was prepared the same way as for protein A/G plus agarose. All centrifuge steps were 1000 x g for 1 min at room temperature in this experiment.

To eliminate non-specific binding of RyR or junctin to protein A/G agarose, 10 μ g of purified RyR or junctin was diluted in IP/Lysis buffer, composed of 0.025 M Tris, 0.15 M NaCl, 0.001 M EDTA, 1% NP-40, 5% glycerol, pH 7.4, to 0.1 mg/ml and then pre-cleared by incubating with 100 μ l of prepared control agarose with rotation for 2 h at 4 °C. The mixtures were centrifuged and the supernatant was removed and used in the subsequent co-IP assay.

2.8.1.1 Co-IP precipitation of junctin by RyR

For junctin precipitation by RyR co-IP, anti-RyR 34C antibody, which recognizes both RyR1 and RyR2, was used. Ten μ g of 34C anti-RyR antibody was adjusted to 100 μ l with 1 x coupling buffer, and then associated with protein A/G plus agarose by rotating for 1h at room temperature. Any unbound antibody was removed with three repeats of a wash step with 1 x coupling buffer followed by centrifugation and then removing the supernatant.

The resultant protein A/G resin-antibody was incubated with 3% BSA (prepared in $1 \times$ coupling buffer) with rotation for 1 h at room temperature to block the agarose resin, followed by centrifugation to remove supernatant. Pre-cleared purified RyR (methods see above) was then added to the antibody bound agarose and incubated with rotation at 4°C overnight. Following incubation, the samples were spun down and the supernatant was removed. Any RyR protein not bound to the antibody was removed by washing three times in cold IP/lysis buffer ($2 \times 200 \mu\text{l}$ plus $1 \times 100 \mu\text{l}$). The protein A/G-antibody-RyR complex was finally incubated with pre-cleared Cjun with rotation for 2 h at room temperature followed by three washes with cold IP/lysis buffer as above to remove unbound protein. The pre-cleared Cjun was also incubated with protein A/G agarose alone as control. Immunoprecipitated samples were eluted from the beads by incubating at 65°C for 10 min in the standard Laemmli sample buffer (Laemmli, 1970), separated on SDS-PAGE (see section 2.6.1), transferred to immobilon membranes (section 2.6.4) and immunoprobed (using anti-RyR 34C or anti-junctin antibody) to identify proteins bound to the protein A/G plus agarose.

2.8.1.2 RyR precipitation by junctin co-IP

The reverse assay was also performed, with anti-junctin first bound to protein A/G sepharose, then coupled with pre-cleared FLjun or Cjun, then incubated with pre-cleared purified RyR1 or RyR2 and processed as described above (section 2.8.1.1).

2.8.2 NeutrAvidin agarose affinity chromatography

Binding of peptides (i.e., Njun, Njun_{scrambled} or Jun_{KEKEamine}) to protein constructs (e.g. recombinant RyR1 or RyR2) could not be determined by using co-IP, as the peptides seemed to intrinsically bind to the protein A/G sepharose (section 2.8.1), with pre-clearing unable to resolve the problem (data not shown). Therefore, NeutrAvidin agarose affinity chromatography was employed. All centrifuge steps were $1000 \times g$ for 3 min at room temperature in this experiment.

To prepare neutravidin-agarose (Thermo Fisher Scientific), $500 \mu\text{l}$ of PBS was added to $100 \mu\text{l}$ of neutravidin-agarose 50% slurry, which were subsequently centrifuged and the supernatant was removed. The wash step was repeated twice and the resultant pellets were resuspended in $50 \mu\text{l}$ binding/wash buffer (PBS + 0.1% SDS) to obtain a 50% slurry. One hundred μg of biotinylated peptide (diluted to $1 \mu\text{g}/\mu\text{l}$ with binding/wash buffer) were added to $100 \mu\text{l}$ of 50% prepared agarose slurry and then incubated with rotation at room temperature for 2.5 h. The supernatant was removed after centrifugation. The unbound peptide was removed with five repeats of a wash step protocol which involved resuspending the pellets in $500 \mu\text{l}$ of binding/wash buffer followed by centrifugation and then supernatant removed.

Ninety μg (for each experiment) of recombinant RyR1 or RyR2 were diluted in binding buffer (PBS + 0.1% SDS + protein inhibitors: AEBSF (Sigma-Aldrich, USA) or Protease Inhibitor Cocktail (Roche Diagnostics, Germany)) and pre-cleared by incubating with 100 μl of control agarose resin for 2 h at room temperature to eliminate any RyR that may bind to neutravidin-agarose. Pre-cleared supernatant were then incubated with NeutrAvidin-agarose-bound biotinylated normal peptide or scrambled peptide or with NeutrAvidin-agarose alone overnight at 4 $^{\circ}\text{C}$. Following incubation, the NeutrAvidin agarose-complex was centrifuged and the supernatant was removed. Any protein that had not bound to the peptide was removed with five times of a *wash step protocol* (above). Bound proteins were eluted from the beads by incubating at 65 $^{\circ}\text{C}$ for 10 min in 15 μl of Laemmli sample buffer. The eluted protein in the supernatant were then run on SDS-PAGE (see section 2.6.1), transferred to immobilon for immunoblot (see section 2.6.4), using anti-RyR 34C antibody to detect recombinant RyR1 or RyR2 and StreptActin-HRP conjugate to detect biotinylated peptide.

2.9 Artificial Planar lipid bilayers

2.9.1 Overview of lipid bilayer system set up

Single channel recording was performed according to (Hamilton 1989) with some modifications (Laver, 2001). The planar lipid bilayer was set up with a Derlin cup (Caillac Plastics; Seaford, Australia) being fitted into a Teflon chamber, so that the chamber was divided into two compartments. The Derlin cup contains a 150-200 μm aperture across which a lipid bilayer was painted. The aperture was viewed using a light microscope (Olympus; Tokyo, Japan) at 40 x magnification and illuminated with a fiber optic light (Narishige scientific instrument lab; Tokyo, Japan). Stock solutions were added directly into both compartments before the lipid film was painted across the aperture. Electrical connection between the solutions and an Axopatch 200B Integrating Patch clamp (Axon Instruments, Foster City, CA, USA) or a Warner BC-525 Bilayer clamp amplifier (Warner Instruments, Hamden, USA) was established via silver chloride (AgCl) coated silver electrodes through a CV 203BV head stage (Axon instruments, USA). Both electrodes were inserted into salt agar bridges (2% (w/v) agar powder in 250 mM CsCl) to reduce junction potentials on AgCl electrodes.

The compartment to which the SR vesicles were added is known as the *cis* chamber and was voltage clamped at +40 or -40mV under all conditions. The opposing compartment, referred to as the *trans* chamber, was grounded. The potentials are expressed according to standard physiological convention as $V_{cis} - V_{trans}$. The current/signal was filtered at 1 kHz with a low pass 8-pole Bessel filter integrated in the Axopatch 200B and displayed using the in-house Continuous analog/digital conversion program 1.0 (BLM1), and recorded at a bandwidth of 5 kHz. The parameters give a sampling interval of 200 μs , i.e. one point every 200 μs . The entire

setup, both chambers and head stage, was housed in a grounded Faraday cage with a sliding front to reduce electrical and vibrational noise.

2.9.2 Lipid bilayer formation and vesicle incorporation

The artificial lipid was a mixture composed of phosphatidylethanolamine (PE), phosphatidylserine (PS) and phosphatidylcholine (PC) at a ratio of 5:3:2 (v/v). Once mixed, the chloroform in which the lipids were stored was evaporated under nitrogen gas. The dried lipids were then redissolved in a hydrophobic solvent *n*-decane at a final concentration of 45-50 mg/ml. The bilayer was formed by applying the lipid to the aperture in the Derlin cup using a flame polished glass rod. A thick lipid film was initially produced after painting the lipids with two monolayers across the aperture and the solvent *n*-decane trapped in between. During bilayer formation, the compressive force of solutions on both sides of the lipid and lipid tail aggregation facilitate the drainage of solvent away from the two monolayers such that the bilayer can be formed (Laver, 2001). The initial lipid film can reflect light strongly whereas the field where a bilayer forms becomes dark thus allowing observing the bilayer formation under a microscope. This process can occur either spontaneously or by applying a gentle pressure using a glass rod to the edge of the film thus helping *n*-decane removal. SR vesicle was normally added after a bilayer with an optimal thickness being achieved for better incorporation. The thickness of the membrane was monitored by observing the capacitance changes of the bilayer through applying 1V/s triangular ramp via a ramp generator (JCSMR workshop, ANU; Canberra, Australia). An increase in bilayer capacitance denotes the thinning of the lipid bilayer, which is indicated by the responsiveness of the amplitude of the current to the applied voltage ramp ($C=I/(dV/dt)$).

SR vesicles containing ion channels were added to the *cis* solution (to a final concentration of 1-50 $\mu\text{g/ml}$ depending on vesicles being used with vigorous stirring. Vesicle incorporation was promoted by i) an osmotic potential gradient created by 250 mM *cis* cesium ions (Cs^+) versus 50 mM *trans* Cs^+ (see section 2.9.3); ii) a high *cis* $[\text{Ca}^{2+}]$ (minimum 1mM) (Laver, 2001; Miller and Racker, 1976). Once channel gets incorporated into the bilayer, which can sometimes be detected as an increase in conductance of the bilayer membrane or appearance of channel openings, *cis* $[\text{Ca}^{2+}]$ was adjusted to 1 μM or 100 nM in RyR1 and to 1 μM in RyR2 to prevent further vesicle incorporation. Two mM ATP (buffered to a pH 7.4 by 10 mM TES) was added to activate RyRs in some cases. In general, channels incorporated in such a way that their cytoplasmic surface faces the *cis* chamber, while the luminal side faces the *trans* solution (Miller & Racker, 1976; Sitsapesan & Williams, 1994). In this study, the orientation of RyR channel incorporation was confirmed by the characteristic response of RyR to its agonists (ATP and Ca^{2+}) or antagonist (ruthenium red).

2.9.3 Lipid bilayer experimental solutions

All solutions were adjusted to a pH of 7.4 with CsOH or HCl using a digital pH meter (TPS Pty. Ltd, Brisbane, Australia) and made using MilliQ-water. The solutions used in lipid bilayer experiments were either stored at 4 °C (*cis* and *trans* solutions and ruthenium red) or at -20 °C (BAPTA, ATP). The incorporation solutions were *cis* (cytoplasmic) containing: 230 mM CsCH₃O₃S (CsMS), 20 mM CsCl, 1 mM CaCl₂ and 10 mM TES, pH 7.4 and a *trans* (luminal) solution containing: 30 mM CsCH₃O₃S, 20 mM CsCl, 1 mM CaCl₂ and 10 mM TES (pH 7.4). The fast Ca²⁺ chelator 1,2-bis (2-aminophenoxy)ethane-N,N,N,N-tetraacetic acid (BAPTA) was used to adjust the free [Ca²⁺] in the solution. The amount of BAPTA required was calculated using the in-house program Bound and Determined (BAD) (Brooks and Storey, 1992). The purity of BAPTA and free [Ca²⁺] in the solution was determined by a Radiometer Analytical ISE25Ca Ca²⁺ electrode (Villeurbanne Cedex, France Radiometer Analytical SAS, Villeurbanne, France).

In bilayer experiments, Cs⁺ was chosen as the current carrier instead of Ca²⁺ for multiple reasons: a) for RyR, the conductance of Cs⁺ is significantly higher than that of Ca²⁺, leading to a 5-fold increase in signal to noise ratio (Sitsapesan and Williams, 1994a); b) compared with Ca²⁺, Cs⁺ has a much weaker regulatory effect on RyR (Laver et al., 1995); c) Cs⁺ can block SR K⁺ channels effectively, which ensures that the current signals recorded was RyR activity but not K⁺ channel activity (Cukierman et al., 1985). CH₃O₃S⁻ was used as the major anion; this is to prevent current through anion channels, e.g. SR Cl⁻ channels due to their low permeability to CH₃O₃S⁻ (Laver et al., 1995).

2.9.4 Channel recording

Channel activity was recorded using the BLM1 program with Axopatch 200 Amplifier (Axon Instruments, Foster City, CA, USA). After channel incorporation, the recording commenced and the following changes were made to standard solutions: 200 mM CsMS was added to the *trans* chamber to achieve symmetrical solutions (with respect to [Cs⁺], [Cl⁻] and [CH₃O₃S⁻]), so that there was no ionic gradient across the bilayer; the *cis* [Ca²⁺] was adjusted to 1 μM (by the addition of 1.32 mM BAPTA) or 100 nM (by the addition of 4.25 mM BAPTA), 2 mM ATP was added to *cis* solution in some control conditions. The effect of junctin constructs addition in this study was not affected by the presence of absence of ATP; therefore, channel data with ATP and without ATP were pooled and included in calculation of average channel activity. There was no change in pH with the addition of BAPTA, ATP or CaCl₂ to the solutions. The solution was stirred for 20-30 s after the addition of substances to ensure equilibration. Bilayer potential is expressed as $V_{cis} - V_{trans}$. Therefore when a voltage of +40 mV was applied, $V_{applied} = V_{cis} - V_{trans} = 40 - 0$, current would flow from *cis* to *trans* chamber, while with -40 mV current would flow from *trans* to *cis* chamber. The bilayer potential was changed between +40 mV and -40 mV every 30 s. Currents were recorded continuously throughout the experiments with a

minimum of 5 min for control activity. Junctin constructs were added into either *cis* or *trans* chamber as designated to desired concentrations and channel activity was recorded for about 10 min in most cases. Additional recordings were carried out after the addition of 20 μM ruthenium red, an RyR-specific antagonist, to the *cis* chamber at the end to further confirm channel was a RyR (Ma, 1993).

Details of each individual experimental procedure are given in results chapters. All channel experiments were conducted at 23 ± 2 $^{\circ}\text{C}$

2.9.5 Single Channel analysis

Single channel parameters were obtained from an in-house program, Channel 2 (developed by P.W. Gage and M. Smith, John Curtin School of Medical Research; Canberra, Australia). Channel parameters were measured from 90 s of channel activity at each potential, before and after the addition of junctin protein/peptide. The following parameters were determined: open probability (P_o), fractional mean current (I'_F), mean open time (T_o), and mean closed times (T_c). The above parameters are defined by the following equations:

$$\text{Open probability } (P_o) = \frac{T_{open}}{T_{time}} \quad \text{[Equation 2.1]}$$

$$\text{Fractional Mean Current } (I'_F) = \frac{I'}{I_{max}} \quad \text{[Equation 2.2]}$$

$$\text{Mean open time } (T_o) = \frac{T_{open}}{n} \quad \text{[Equation 2.3]}$$

$$\text{Mean closed time } (T_c) = \frac{T_{closed}}{n} \quad \text{[Equation 2.4]}$$

Where T_{open} is the total channel open time; T_{closed} is the total channel closed time; T_{time} , the total duration of analyzed record; n , the number of channel opening events; I' , mean current, an average of all data points during a recording period and I_{max} , maximal current of the analyzed record.

In this study, RyR activity was quantified by assessing open probability (P_o) in two ways, either the probability that the channel would be open at any one time, as T_{open}/T_{time} (equation 2.1), where threshold level for channel opening was set at $\sim 20\%$ of the maximum single channel conductance, and the closed threshold was placed above baseline noise or halfway in between open threshold and baseline in order to exclude baseline noise. P_o was also approximated by the average current as a function of the maximum current, i.e. I'_F (equation 2.2). I'_F is approximately equal to the P_o measured by threshold discrimination when most of channel openings are to the maximum conductance. It has been shown that P_o and I'_F values obtained from a single channel record from a predominantly active channel are very similar (Beard et al.,

2008). P_o is the most accurate measure of RyR channel activity when only one channel is active in a bilayer, whereas I'_F most accurately quantifies RyR activity when multiple channels are active. Since I'_F is approximately equal to P_o (Beard et al., 2008), all channel activity (measures either as I'_F or P_o) is expressed as P_o . Slow fluctuations in the baseline current were corrected using an in-house correction program Baseline (written by Dr D.R. Laver, University of Newcastle, Australia). In this study, data from +40 mV and -40 mV were pooled and included in calculation of average channel activity as there was no significant difference between each potential.

In addition, a more detailed analysis of the effect of the FLjun, Cjun and Njun on purified RyR1 or RyR2 channel activity was derived from the statistics of amplitudes and durations (i.e. open and closed dwell-times, the time constant distributions) according to (Sigworth and Sine, 1987; Tae et al., 2011). To obtain the frequency distribution of dwell times, the data of open and closed times were grouped into bins that are equally spaced on a log scale, and the square root of the relative frequency of events ($P^{1/2}$) was plotted against the logarithm of the open (open circles) or closed times (filled circles) in milliseconds. The open and closed times were fitted with three exponential components in both RyR isoforms, and the appropriate fit was determined using least square analysis. In this study, 1-10 ms were assigned to τ_{O1} or τ_{C1} , 10-50 ms to τ_{O2} or τ_{C2} , and 50-500 ms to τ_{O3} or τ_{C3} . An example was shown in Fig. 2-2.

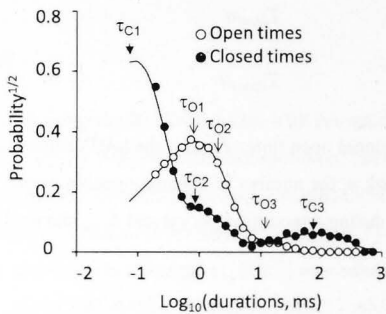


Figure 2-2 A probability (the square root) distribution of open (open circles) and closed (filled circles) dwell-times. Exponential open and closed time constants were determined. Example is shown from a simulated, single channel recording, figure adapted and modified from (Laver, 2001). The arrows indicate individual open time constants (τ_{O1} , τ_{O2} , and τ_{O3}) and individual closed time constants (τ_{C1} , τ_{C2} , and τ_{C3}). The solid lines are theoretical probability functions.

2.10 Ca^{2+} release from skeletal and cardiac SR vesicles

Part of this work (Ca²⁺ release assay with Cjun) was undertaken by Mrs. Suzy Pace (Muscle Research Group, John Curtin School of Medical Research, Australian National University, Canberra, Australia.)

A Cary 1E UV-Visible spectrophotometer (Varian, Sydney, Australia) was used to monitor Ca²⁺ release from populations of intact SR vesicles at 710 nm, using the Ca²⁺ indicator antipyrilazo III (Dulhunty et al., 1999; Hanna et al., 2011; Jalilian et al., 2008). It should be noted that the native RyR-containing SR vesicles used in this assay were prepared from either skeletal or heart muscle following well established procedures analogous to previously published methods (Chamberlain and Fleischer, 1988; Saito et al., 1984); for details, see section 2.3.1). These vesicles have been shown to retain morphologically well-preserved junctional feet (RyR) structures projecting out of the vesicles, with similar orientation to feet observed in micrographs of intact fibers (Saito et al., 1984). Therefore, the SR vesicles were expected to be of the same “polarity” (i.e., the cytoplasmic domains of the RyRs facing outside the vesicles). In addition, as the natural consequence of the structure of the RyR-containing microsomal vesicle, the RyR channels was always inserted in the bilayer with its cytoplasmic domain exposed to the *cis* chamber when the vesicles were added to the *cis* solution (Tu et al., 1994b). Therefore, the response of RyR in SR vesicles to the constructs tested (Cjun/Njun) here was assumed to reflect the interaction between Cjun/Njun and the cytoplasmic domain of RyR. Changes in absorbance as a function of time were observed using the Kinetics program (Varian, Sydney, Australia). The temperature was maintained at 25 °C for all experiments unless otherwise stated and the cuvette solution was magnetically stirred throughout the experiment. Calibration curves were obtained by measuring optical density changes with addition of four consecutive 12.5 μM (50 μM in total) CaCl₂ to the cuvette solution at the start of each day (Eager and Dulhunty, 1999). The calibration curve was not affected by Njun, Cjun, caffeine, or ruthenium red. Changes in absorbance as a function of time were observed using the Kinetics program (Varian, Sydney, Australia). The extravesicular [Ca²⁺] could be calculated by measuring the change in absorbance that occurs with addition of known amount of Ca²⁺ using the following equation, which was used to determine the rate of Ca²⁺ release in each experiment (Chu et al., 1988).

$$\text{Ca}^{2+} \text{ Calibration} = \frac{50 \text{ nmol Ca}^{2+}}{\Delta \text{ absorbance}} \quad [\text{Equation 2.5}]$$

2.10.1 Njun/Cjun induced Ca²⁺ release from SR vesicles

SR vesicles (for skeletal vesicles—50 μg/ml; for cardiac vesicles—100 μg/ml) were added to a cuvette to a total volume of 2 ml containing 100 mM KH₂PO₄, 0.5 mM antipyrilazo III, 1 mM Na₂ATP, and 4 mM MgCl₂. The addition of Na₂ATP and MgCl₂ (MgATP) activated the SERCA pump leading to an uptake of extravesicular Ca²⁺. After equilibration of the solution (1

min for skeletal vesicles and 3 min for cardiac vesicles), the SR was loaded with four additions of $7.5 \mu\text{M}$ CaCl_2 . One min (skeletal)/ 3 min (cardiac) equilibration time was allowed between each Ca^{2+} addition. Thapsigargin (300 nM for skeletal SR vesicles and $2.25 \mu\text{M}$ for cardiac SR vesicles) was then added to block the SERCA to prevent Ca^{2+} uptake during the experiment (Sagara and Inesi, 1991), so that Ca^{2+} release could be specifically measured. Njun/Cjun ($5 \mu\text{M}$) was added 30 s after thapsigargin to examine the ability of high concentrations of Njun/Cjun to immediately stimulate Ca^{2+} release by measuring the optical density. Ruthenium red ($5 \mu\text{M}$) was then added to confirm that Ca^{2+} release was through the RyR, which caused a flatline of the optical density. The flatline indicated that Ca^{2+} was not being released or taken up by the SR vesicles and that both the RyR and the SERCA pump were blocked. Finally Ca^{2+} ionophore (A23187) ($1.5 \mu\text{g/ml}$) was added to release any Ca^{2+} remaining in the SR into the extravesicular space. The rate of Ca^{2+} release induced by Njun/Cjun was calculated (see section 2.10.3) and the results were compared to control experiments where either MilliQ-water (where Njun peptide was dissolved) or MOPS buffer (20 mM MOPS, 150 mM NaCl, pH 7.4) (where Cjun was dissolved) was used in place of Njun/Cjun to obtain a baseline leak of Ca^{2+} from the SR, in the presence of SERCA pump being blocked by thapsigargin.

2.10.2 Ca^{2+} release from SR vesicles pre-incubated with Njun/Cjun

SR vesicles ($50 \mu\text{g/ml}$ for skeletal vesicles and $100 \mu\text{g/ml}$ for cardiac vesicles) were incubated with Njun/Cjun ($5 \mu\text{M}$) (or with MilliQ-water/MOPS buffer alone for control experiments) for 30 min on ice prior to their addition to the cuvette solution (see section 2.10.1 for the composition of the solution). The concentration of Njun or vehicle buffer in the cuvette was adjusted to the incubation concentration, and the vesicles were loaded with Ca^{2+} in the usual way (see section 2.10.1). Following inhibition of SERCA with thapsigargin (300 nM for skeletal SR vesicles and $2.25 \mu\text{M}$ for cardiac SR vesicles), Ca^{2+} release was stimulated with either 0.5 mM (skeletal) or 5 mM (cardiac) caffeine and the rate of caffeine-induced Ca^{2+} release measured following incubation in either: buffer plus Njun/Cjun, or buffer plus MilliQ-water/MOPS buffer. The experiment was completed with the addition of ruthenium red and Ca^{2+} ionophore A23187 as in section 2.10.1. The results with Njun/Cjun were compared to control experiments where vesicles were pre-incubated with MilliQ-water/MOPS buffer in place of Njun/Cjun. The amount of Ca^{2+} loaded into the SR was not altered by incubation of SR vesicles with Njun, Cjun or control buffer.

2.10.3 Data analysis—calculation of rate of Ca^{2+} release from SR vesicles

Ca^{2+} release rate was determined by measuring the rate of change in optical density immediately following stimulation of Ca^{2+} release. The initial release rate was the most rapid Ca^{2+} release per unit time (Olson et al., 2000). The rate of Ca^{2+} release was determined by drawing a tangent line

to the initial release data, the slope of which was measured by the Kinetics program. The slope of the curve measured was used in the following equation (equation 2.6) to calculate the slope of Ca^{2+} release (Chu et al., 1988):

$$\text{Slope of } \text{Ca}^{2+} \text{ release} = \frac{\Delta \text{ absorbance}}{\text{time (min)}} \quad [\text{Equation 2.6}]$$

This value, together with the value obtained for the Ca^{2+} calibration (equation 2.5), the rate of Ca^{2+} release in nmol Ca^{2+} /mg protein/min was calculated with the following equation:

$$\text{Rate of } \text{Ca}^{2+} \text{ release} = \frac{\text{slope of } \text{Ca}^{2+} \text{ release / uptake} \times \text{Ca}^{2+} \text{ calibration}}{\text{protein (mg)}} \quad [\text{Equation 2.7}]$$

2.11 Statistics

Average data are given as mean \pm SEM. Statistical significance between control and test values was evaluated using paired or unpaired Student's *t*-test or ANOVA (analysis of variance) as appropriate. To reduce effects of variability in control parameters, data with junctin constructs (J) are expressed relative to control (C), (e.g., $\log_{10}X_J - \log_{10}X_C$, $X=P_o$, T_o , T_c , rate of Ca^{2+} release, etc). Numbers of observations (*n*) are given in tables and figure legends. A *P* value <0.05 was considered to be significant.

Chapter 3 Full length junctin interacts with purified RyR1 and RyR2 channels

3.1 Introduction

As detailed in Chapter 1 (section 1.7-1.9), proteins associated with the RyR in the SR lumen including CSQ, triadin and junctin, play a role in modulating Ca^{2+} release through the RyR. In recent years, their importance in both the regulation of Ca^{2+} store and Ca^{2+} release from the RyR has been increasingly recognized. The main focus of this chapter is on direct regulation of isolated RyR1 and RyR2 ion channel activity by junctin.

As discussed in Chapter 1.9, most of our knowledge about the functional effect of junctin on RyR2s is derived from transgenic studies, which suggest that junctin suppresses RyR2 activity (Yuan et al., 2007) or acts as both an activator and inhibitor depending on SR Ca^{2+} load (Altschafel et al., 2011). However, it remains unclear whether this action is a direct effect of junctin on RyR2 activity or an indirect effect through CSQ, since changes in junctin expression may influence interactions between CSQ2 and RyR2, thus functional changes may be due to alterations in CSQ regulation of RyRs rather than junctin effects per se (Yuan et al., 2007). Even in a study carefully carried out by Altschafel et al. (2011), where CSQ2 was mostly excluded from junctin-KO and WT cardiac SR in lipid bilayer studies, the possibility that the effects may be related to altered RyR2 regulation by CSQ2 and altered triadin interactions cannot be entirely excluded. Therefore, the direct regulatory effect of junctin on the RyR2 remained to be clearly elucidated.

In contrast to the results in the transgenic studies, *in vitro* lipid bilayer studies showed that addition of junctin to the luminal side of purified RyR2 (Gyorke et al., 2004a) in lipid bilayers evoked significant channel activation, indicating a positive effect of junctin on RyR2 activity. Nevertheless, it is worth noting that the luminal $[\text{Ca}^{2+}]$ used in the Gyorke study (20 μM or 5 mM) do not include the physiological concentrations between 0.1 and 1.5 mM. Hence, the role of junctin in modulating RyR2 activity still remains elusive. Due to the physiological importance of junctin in the maintenance of normal SR Ca^{2+} handling and cardiac function suggested from transgenic studies, it is important to determine the molecular interactions between junctin and the RyR2 at a more physiological Ca^{2+} concentration, i.e. 1 mM luminal $[\text{Ca}^{2+}]$.

So far, the first and the only study to look at the direct effects of junctin on the skeletal RyR channel elegantly carried out by others in the Muscle Research Group revealed that the junctin added to luminal side of purified RyR1 evoked significant channel activation with physiological cytoplasmic and luminal Ca^{2+} concentrations (Wei et al., 2009a), indicating that junctin may

thus activate the channels in skeletal muscle. Nevertheless, the precise way by which junctin modulates RyR1 remained unclear. This problem will be discussed in the following chapters (Chapter 4 and 5).

As mentioned in Chapter 1.9.1, junctin contains a single membrane spanning domain, a short cytoplasmic N-terminal tail and a longer C-terminal tail in the SR lumen. In this chapter, junctin will be investigated as a whole, i.e. full length junctin (FLjun). The body of work described in this chapter has defined the overall interaction between FLjun and the RyRs.

Aim:

The primary aim of the experiments described in this chapter was to characterize the functional effects of junctin on purified RyR2 at resting luminal $[Ca^{2+}]$ (1 mM). The direct effect of junctin on purified RyR1 activity was also tested for comparison. A second component of this aim was to investigate the precise mechanism by which junctin regulates RyR1 and RyR2 activity. An additional aim was to develop a method to generate the full length recombinant junctin to overcome the low yield problem sometimes encountered during muscle junctin purification.

3.2 Methods

3.2.1 Methods overview

Junctin was first purified from rabbit skeletal muscle for the investigation of its interaction with the RyR1 and RyR2. The one isoform of junctin is expressed in both the skeletal and cardiac systems. In addition, recombinant FLjun was expressed and purified from *E.coli*. Modified co-immunoprecipitation (co-IP) was carried out to evaluate the physical interaction between FLjun and purified RyR1 or RyR2. Single channel recording in lipid bilayers was employed to explore the direct functional effect of luminal junctin on RyR1 or RyR2 channel activity at resting Ca^{2+} (1mM). A control experiment was also carried out to determine whether junctin in the cytoplasm affected the RyR activity.

3.2.2 SR vesicle isolation and RyR purification

As detailed in section 2.3.1, skeletal SR vesicles were prepared from rabbit skeletal muscle and sheep heart respectively. Skeletal RyR1 and cardiac RyR2 were solubilized and purified from skeletal and cardiac SR vesicles respectively as described in section 2.3.2.

3.2.3 Junctin purification

3.2.3.1 Endogenous junctin purification from rabbit skeletal muscle

Skeletal junctin was purified using SDS preparative gel electrophoresis from rabbit skeletal muscle tissue as detailed in section 2.5.1. In brief, the crude SR vesicles were solubilized by 1% CHAPS to remove insoluble membrane fragments. Solubilized SR was separated by a 12% preparative gel electrophoresis for junctin purification. Fractions containing the band with a molecular mass of ~25 kDa (normally in fractions 45-60), analyzed by analytical mini SDS-PAGE, were precipitated by 400 mM KCl, redissolved in Triton X-100 and washed and concentrated.

3.2.3.2 Recombinant canine cardiac FLjun

Due to difficulty in reproducing results with preparative gel electrophoresis from rabbit skeletal muscle, recombinant FLjun was expressed and purified from *E.coli* (detailed in section 2.5.2). Recombinant FLjun was obtained by subcloning canine cardiac muscle junctin cDNA and expression in *E.coli* as a poly-histidine (6×His) fusion protein. Maximum yield of recombinant protein was achieved by expressing the protein for 4 h at 37 °C following induction with 0.6 mM IPTG. The fusion protein was purified using Ni²⁺-nitrilotriacetic acid agarose matrix by IMAC under native conditions with 1% Triton X-100. 6×His-FLjun was coupled to the affinity matrix after incubating protein supernatant with the agarose. Any unbound proteins were removed by extensively washing the beads. The fusion protein was eluted against 500 mM imidazole elution buffer. Triton X-100 contained in the eluted sample was subsequently removed using Bio-Beads SM-2 adsorbents.

3.2.4 Modified co-IP between FLjun and RyR1 and RyR2

Direct binding between skeletal FLjun and the RyR1 and RyR2 was assessed using a modified co-IP. The assay was performed in two ways: 1) co-IP precipitation of RyR1 (n=3) or RyR2 (n=3) by FLjun, 2) FLjun precipitated by RyR1 (n=3) or RyR2 (n=3) co-IP as described in section 2.8.1. To eliminate non-specific binding between the protein and the matrix, a) both purified FLjun and RyR1 or RyR2 were pre-cleared in 100 µl control agarose resin and b) the protein A/G agarose-antibody complex was blocked with 3% BSA to occupy any possible binding sites on the resin. The final RyR/junctin-antibody-protein A/G agarose complex was subjected to extensive washing to remove any unbound proteins, and then eluted by incubating at 65 °C for 10 min in Laemmli sample buffer and tested with SDS-PAGE and immunoblot. Anti-RyR 34C and anti-junctin antibody were used to probe RyR1/RyR2 and FLjun respectively.

3.2.5 Single channel recording and analysis

Single RyR channel recordings were carried out and analyzed as described in section 2.9. Stable control activity was recorded for a minimum of 5 min before adding FLjun, alternating between +40 and -40 mV every 30 s.

RyR is well known for the large variation between the activity of individual channels, possibly due to differences between the degree of phosphorylation, nitrosylation, or oxidation of the channels (Copello et al., 1997; Marengo et al., 1998). To reduce effects of variability in control parameters (P_{oc}), data with FLjun are expressed relative to control, i.e. the difference between the $\log_{10} X_C$ and $\log_{10} X_I$ ($X = P_o, T_o, T_c$) for each channel (e.g., $\log_{10} P_{oi} - \log_{10} P_{oc}$). The fractional mean current (I'_F) was measured in the recordings where multiple channels incorporated (see section 2.9.5 and below section 3.3.1.1). When I'_F under test conditions is normalized to control I'_F , it is approximately equal to relative P_o (Beard et al., 2008). All channel activity (measured either as I'_F or P_o) is expressed as P_o both in this chapter and the following chapters.

3.3 Results

3.3.1 General properties of RyR1 and RyR2

3.3.1.1 General observations

Following lipid bilayer formation, purified RyR1s or RyR2 was added to the *cis* chamber. The incorporation of the RyRs generally occurred from 3 min up to more than 15 min after their addition. Channel incorporation was usually indicated by a step increase in bilayer conductance, or the appearance of channel openings. If incorporation did not occur after 20 min following vesicle addition, more vesicles (~10-25 $\mu\text{g/ml}$) were added to the *cis* chamber. If there was still no incorporation after another 20 min, the chambers were washed, the solutions were replaced and the procedure was repeated.

After an initial fusion event, 200 mM $\text{CsCH}_3\text{O}_3\text{S}$ was added to the *trans* chamber to bring *trans* $[\text{Cs}^+]$ to 250 mM, therefore equilibrating the $[\text{Cs}^+]$ in the chambers to prevent further fusion; $[\text{Ca}^{2+}]$ in the *cis* chamber was adjusted to 1 μM in most cases with *trans* $[\text{Ca}^{2+}]$ being a constant 1 mM; 2 mM ATP was added to the *cis* chamber in some cases (see Methods, section 2.9.4).

Multiple channels often incorporated into the bilayer, regardless of the RyR isoform being used. The number of channels incorporating into an artificial lipid bilayer varies and the activity also varies between one channel opening and more than one channel being active. Fig. 3-1 shows recordings with up to 4 channels (for both RyR1 and RyR2) opening simultaneously. The presence of multiple active channels in the bilayer does not alter the overall response of RyR1 or RyR2 to RyR modulators, e.g. Ca^{2+} , ATP, ruthenium red. The activity of multiple channel bilayers was measured as mean current (see section 2.9.5 for detail), with data presented as

fractional mean current I'_F (average current/maximal channel amplitude) which is approximately equal to P_o .

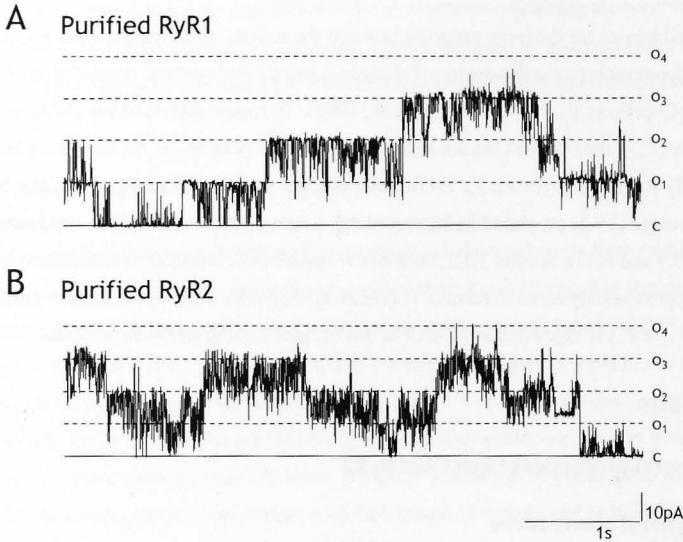


Figure 3-1 Multiple channel incorporation into lipid bilayers. Five second recordings of multiple RyR1 (A) and RyR2 (B) activity at +40 mV are shown. Multiple channel openings are upward from zero current (c, solid line) to maximum open conductance (o₁, one channel open, o₂, o₃ and o₄ simultaneous opening of two, three or four channels).

3.3.1.2 General RyR characteristics

3.3.1.2.1 Purified RyR1 and RyR2 channel conductance

Channel identity in lipid bilayers was confirmed by evaluating the voltage-dependence of channel activity and its conductance as well as its response to ligands (section 3.3.1.3). The maximum current amplitudes of a single RyR (both RyR1 and RyR2) were very similar at +40 and -40 mV under control conditions (1 μM *cis* $[\text{Ca}^{2+}]$ and 1 mM *trans* $[\text{Ca}^{2+}]$; Fig. 3-2A&B). A current-voltage curve was constructed using the maximum current obtained from Fig. 3-2A&B, showing the linear current-voltage relationship through zero (Fig. 3-2C&D) as previously reported for RyR1 and RyR2 channels (Lai et al., 1988; Laver et al., 1995; Liu et al., 1989).

The maximum ion channel conductance (G) depends on 1) the maximum current through the channel (I); 2) the voltage across the bilayer (V); 3) the ion charges on either side of the lipid bilayer. Due to the symmetric $[\text{Cs}^+]$ (250/250 mM) set for control conditions, the reversal

potential for Cs^+ (E_{Cs}) fell at 0 mV. Therefore, the conductance of a channel can be calculated using the following equation:

$$G_{\text{max}} = I_{\text{max}}/V \quad \text{[Equation 3.1]}$$

Where G_{max} is the maximal conductance at a particular voltage (S), I_{max} is the maximal current at a particular voltage (A), and V is the voltage across the lipid bilayer (V).

The average maximal single channel conductance at +40 mV was 281.8 ± 14.5 pS or 288.1 ± 10.7 pS at -40 mV for purified RyR1 channels ($n=16$). Purified RyR2 displayed a maximal single channel conductance of 269.6 ± 15.77 pS at +40 mV and 263.7 ± 14.3 pS at -40 mV ($n=12$). These results demonstrate an approximately equal channel conductance at both +40 mV and -40 mV under control conditions. The average of these conductance values is 284.8 ± 9.1 pS for RyR1 and 266.6 ± 10.5 for RyR2 under conditions with $1 \mu\text{M}$ *cis* [Ca^{2+}] and 1mM *trans* [Ca^{2+}]. These observations are similar to values previously reported for RyR1 and RyR2 conductance under identical experimental conditions with 250 – 300 pS (Dulhunty et al., 2001a), and are in agreement with literature on RyR1 (Lai et al., 1988; Liu et al., 1989; Meissner, 1994) and RyR2 (Laver et al., 1995; Tinker et al., 1992b) conductance which varies between 200 – 525 pS. As mentioned in Chapter 1.6.4, channel conductance was expected to be ~ 525 pS under equal 250 mM [Cs^+] in the *cis* and *trans* chambers (Laver et al., 1995; Tinker et al., 1992b), so much higher than the values reported in this study. However, it should be noted that those high values were obtained either in the absence of divalent cations (e.g., Ca^{2+}) (Tinker et al., 1992b) or with very low free cytoplasmic and luminal [Ca^{2+}] at $100 \mu\text{M}$ (Laver et al., 1995). As detailed in Chapter 1.6.4, RyR favours the passage of divalent as opposed to monovalent cations, e.g., the relative permeability of Ca^{2+} with respect to Cs^+ ($P_{\text{Ca}}/P_{\text{Cs}}$) has been reported within the range 13 – 30 (Laver et al., 1995); and Ca^{2+} has a much lower conductance through the RyRs with ~ 100 pS conductance at $\sim 50 \text{mM}$ *trans* [Ca^{2+}] (Smith et al., 1986; Tinker and Williams, 1992). As such it is expected that millimolar *trans* Ca^{2+} in our system would compete with Cs^+ for passing through the pore of RyR channels, therefore lowering the conductance recorded (Chu et al., 1993). This is exemplified in Fig. 3-3A&B, where reducing *cis* Ca^{2+} from 1mM to $1 \mu\text{M}$ resulted in a slight increase in both RyR1 and RyR2 channel conductance. There have been no reports that any experimental compounds used in this study influence RyR conductance. No changes in RyR1 or RyR2 conductance with the addition of junctin constructs used were observed during this project.

In addition to channel conductance, the identification of RyR channels in lipid bilayers was also determined by their responses to cytoplasmic regulators, including cytoplasmic Ca^{2+} , ATP and ruthenium red as described in the following section (section 3.3.1.3). This also determined whether the channel incorporated with the correct orientation.

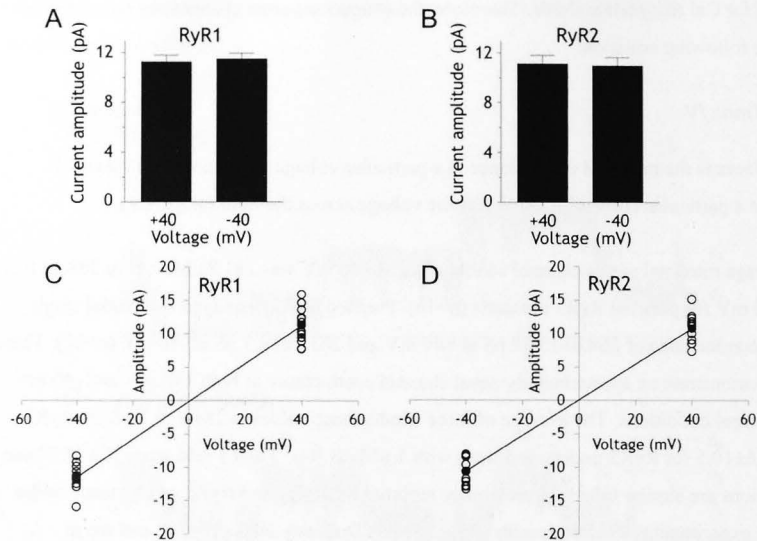


Figure 3-2 Current – voltage relationship for purified RyR1 and RyR2 channels at +40 and -40 mV. (A)-(B) Maximum single current amplitude was measured at +40mV and -40mV for RyR1 (A) and RyR2 (B) under control conditions where ionic strength was symmetrical (250/250 mM Cs⁺), *cis* [Ca²⁺] was 1 μ M and *trans* [Ca²⁺] was 1 mM. n = 16 channel records for RyR1 and n=13 for RyR2. (C)-(D) The linear fit (solid line) is based on the mean values (filled black circles) for the scatter of single current amplitude (open circles) at each voltage analyzed.

3.3.1.3 Regulation of purified RyR1 and RyR2 by characterized ligands

3.3.1.3.1 Cytoplasmic Ca²⁺

As mentioned previously (Chapter 1.6.5.1.1), cytoplasmic Ca²⁺ is an important modulator of RyR activity. It either inhibits or enhances channel activity in skeletal and cardiac muscle depending on Ca²⁺ concentration. Micromolar cytoplasmic Ca²⁺ (1-10 μ M) activates the channels, with a threshold for channel activation at approximately 100 nM; while higher Ca²⁺ concentrations (500 μ M-10 mM) inhibit the channels. Although cytoplasmic Ca²⁺ has a biphasic effect on both RyR1 and RyR2 activity, RyR2 is at least 10-fold less sensitive to cytoplasmic [Ca²⁺] inhibition than the RyR1 (Laver et al., 1995). RyR1 is almost entirely inhibited by 1 mM Ca²⁺ (Fill et al., 1990), whereas RyR2 is maximally activated (Chu et al., 1993; Laver et al., 1997a; Laver et al., 1995) (see Fig. 3-3A&B top traces). Following RyR incorporation, the *cis* [Ca²⁺] was reduced from 1 mM to 1 μ M with the addition of the Ca²⁺ chelator BAPTA to the *cis* solution (section 2.9.4). The reduction in *cis* [Ca²⁺] increased RyR1 channel open probability (P_o) by 3.29 \pm 1.19-fold. In contrast, RyR2 activity was reduced to submaximal levels shortly after lowering *cis* [Ca²⁺] (Fig. 3-3C). These changes in activity occurred at both +40 mV and -

40 mV and stabilized within 1-2 min, thus confirming the cytoplasmic orientation of the channel and its identity as RyR1 or RyR2. These observations agree with previous reports on the response of RyR1 and RyR2 to *cis* $[Ca^{2+}]$ (Chu et al., 1993; Laver et al., 1997a; Laver et al., 1995; Meissner et al., 1986).

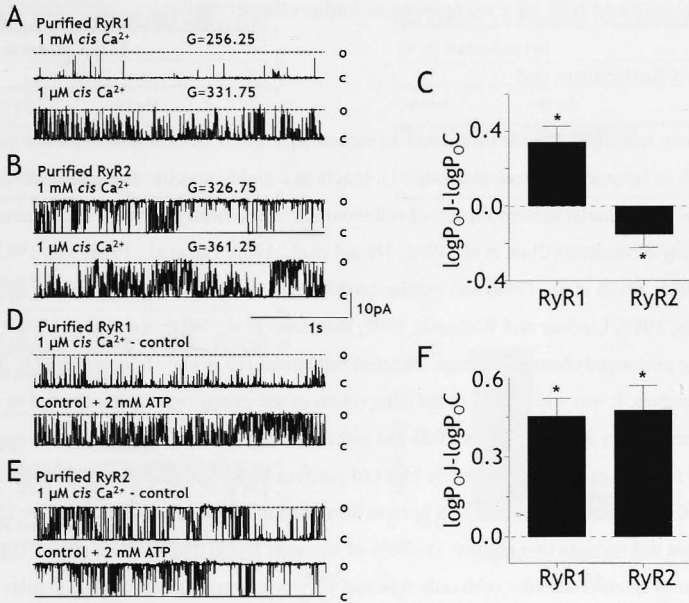


Figure 3-3 RyR regulation by *cis* Ca^{2+} and ATP. (A), (B), (D) & (E) Records of 3 s of single channel activity at +40 mV. Single channel opening is upward, from zero current (continuous line, c) to maximum open channel conductance (broken line, o). *Trans* $[Ca^{2+}]$ was 1 mM. (A) & (B) The response of RyR1 (A) and RyR2 (B) to altered *cis* Ca^{2+} ; $[Ca^{2+}]$ was decreased from 1 mM (upper trace in each panel, used for incorporation), to 1 μ M (lower trace) by the addition of BAPTA. (C) Average data (n=15 for RyR1 and n=9 for RyR2) from both +40 mV and -40 mV for relative open probability ($\log P_{oJ} - \log P_{oC}$) from channels in A & B. (D) & (E) Following RyR1 (D) and RyR2 (E) incorporation and control recording (upper trace in each panel), 2 mM ATP was added to the *cis* chamber, activating the channel (lower trace). (F) Average data (n=11 for RyR1 and n=9 for RyR2) for relative open probability ($\log P_{oJ} - \log P_{oC}$) from channels in D & E. Asterisks (*) indicate average values significantly different from the control (P<0.05 Student's paired *t*-test).

3.3.1.3.2 ATP

ATP in the cytoplasm is a potent RyR1 activator (Smith et al., 1986). It is believed that ATP potentiates channel activity in two ways, either by binding directly to the RyR (Laver et al., 2001; Meissner et al., 1986), or by facilitating RyR phosphorylation through hydrolysis (Dulhunty et al., 2001b). Two mM ATP was added to the *cis* chamber in the presence of 1 μ M

cis Ca²⁺ to increase channel activity. This also determines the identity and orientation of the channel incorporated into the lipid bilayers. The addition of ATP led to a significant increase in channel activity (3.24±0.61-fold and 3.67±0.92-fold increase in average P_o in RyR1 and RyR2 respectively) at both +40 mV and -40 mV (Fig. 3-3D-F). The activation occurred within 1-2 min after ATP addition, suggesting the correct RyR incorporation. Channels that could not be activated by 2 mM ATP were excluded from further channel analysis.

3.3.1.3.3 Ruthenium red

Ruthenium red, also known as ammoniated ruthenium oxychloride, is an inorganic polycationic dye with an intense red colour (Luft, 1971). It acts as a highly specific antagonist of RyR Ca²⁺ channels. Micromolar concentrations of ruthenium red specifically decrease the channel open probability of skeletal (Chen et al., 1992; Hymel et al., 1988; Lai et al., 1988; Ma, 1993; Smith et al., 1985; Smith et al., 1988) and cardiac (Ashley and Williams, 1990; Holmberg and Williams, 1989; Lindsay and Williams, 1991; Rousseau et al., 1986; Xu et al., 1999) RyRs by inducing prolonged channel closings. Because ruthenium red is known to irreversibly block RyR channels, it was added only at the completion of the experiment, and was used to confirm the channel was a RyR. Addition of 20 µM ruthenium red to the *cis* chamber at the end of channel recordings almost completely blocked purified RyR1 opening to levels close to zero at both +40 and -40 mV (Fig. 3-4A). In comparison, the inhibition of purified RyR2 by 20 µM ruthenium red fell into two groups: 1) ~20% of channels tested displayed an almost complete abolition of channel activity, with only rare and very brief openings remaining, similar to that observed for purified RyR1 (Fig. 3-4B); 2) the activity of ~80% purified RyR2 channels was found to be less sensitive to ruthenium red inhibition than purified RyR1 (Fig. 3-4C). These findings are consistent with previous observations with purified cardiac RyR Ca²⁺ channel inhibition induced by ruthenium red (Anderson et al., 1989; Lindsay and Williams, 1991). Analysis of a random sample of activity from a channel falling into the second category (Fig. 3-4C) suggested an average of ~85% decrease in RyR2 channel open probability (Fig. 3-4D). Blockage by ruthenium red occurred within 1-3 min of its addition to the *cis* chamber for both RyR1 and RyR2 channel types.

3.3.2 Purification of full length junctin (FLjun)

3.3.2.1 Endogenous junctin purification from muscle

Purified junctin from rabbit skeletal muscle using SDS preparative gel electrophoresis (section 2.5.1 and 3.2.3.1) resolved as a homogenous protein band at ~25 kDa on SDS-PAGE (Fig. 3-5A lane 2). The 25 kDa protein was confirmed to be junctin by immunoblot using polyclonal anti-junctin antibody (Fig. 3-5B). Purified junctin was also immunoprobed by anti-triadin and anti-

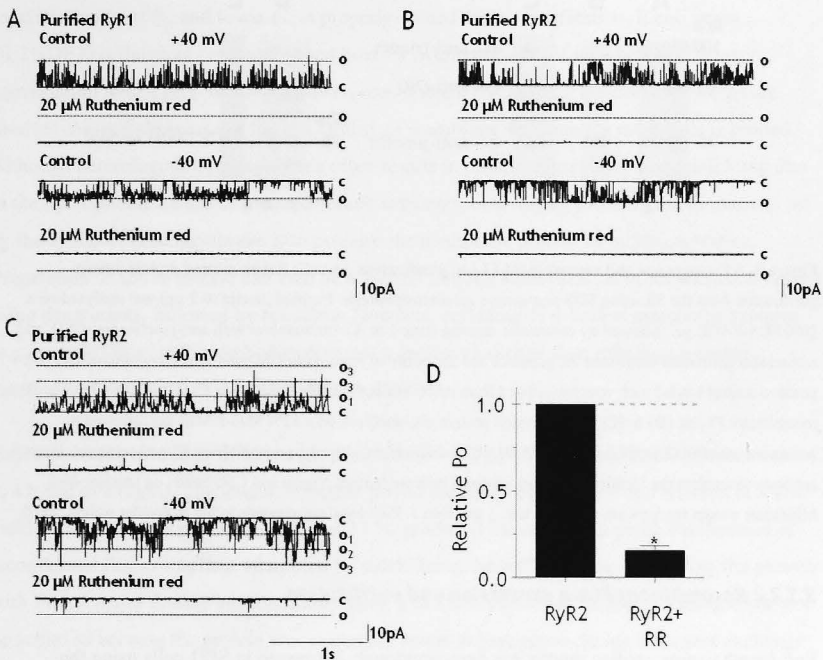


Figure 3-4 RyR responses to ruthenium red. (A-C) Three second records of single channel activity at both +40 mV and -40 mV. Channels are opening upward from zero current (continuous line, c) to maximum open conductance (broken line, o or o₁, one channel open, o₂ and o₃ simultaneous opening of two or three channels) at +40 mV and downward at -40 mV. Channels were recorded in the presence of 1 μ M *cis* Ca²⁺ and 1 mM *trans* Ca²⁺. (A) Changes in RyR1 activity with the addition of 20 μ M ruthenium red to *cis* chamber. (B) & (C) RyR2 responses to *cis* ruthenium red fell into two groups: 1) channel activity almost totally abolished by ruthenium red (B); 2) channel remains opening but to a much lesser extent (C). (D) Average data (n=12) from both +40 mV and -40 mV for RyR2 relative open probability (P_o) from channels in C. Asterisks (*) indicate average values significantly different from the control ($P < 0.05$ Student's paired *t*-test). Overall, ruthenium red blocked both RyR1 and RyR2 channels at both potentials (second and bottom traces in each panel).

CSQ antibodies to establish protein purity. No detectable CSQ or triadin was found in the purified junctin sample (Fig. 3-5B).

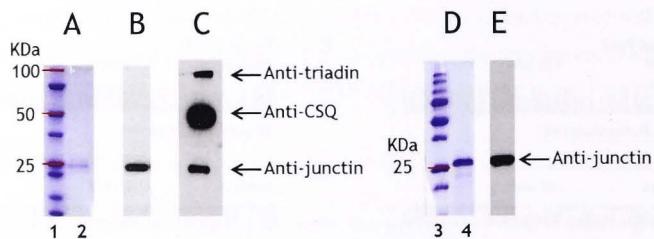


Figure 3- 5 Endogenous and recombinant FLjun purification. (A)-(C) Rabbit skeletal muscle junctin purification from the SR using SDS preparative gel electrophoresis. Purified junctin (0.2 μ g) was analyzed on a 10% SDS-PAGE gel followed by coomassie staining (lane 2 in A). Immunoblot with anti-junctin, anti-CSQ, and anti-triadin antibodies confirmed the presence and the purity of junctin (no CSQ and triadin contamination) (B); positive control loaded with vesicles isolated from rabbit skeletal muscle is shown in C. (D)-(E) Purification of recombinant FLjun. (D) 6 \times His-FLjun fusion protein was analyzed on a 12% SDS-PAGE gel followed by coomassie staining (2 μ g FLjun, lane 4 in D). (E) Immunoblot (with \sim 1 μ g recombinant FLjun) using anti-junctin antibody to confirm the identity of junctin. Arrows indicate junctin, triadin and CSQ bands on immune-blot. Molecular weight markers are shown in lane 1 and lane 3. Pink band corresponds to the molecular weight noted.

3.3.2.2 Recombinant FLjun expression and purification

Full length canine cardiac junctin has been previously expressed in Sf21 cells using the BaculoGold System (Gyorke et al., 2004a; Zhang et al., 1997). The final protein was solubilized in detergent-containing solutions, either with 0.1% Triton X-100 (Zhang et al., 1997) or 1% CHAPS (Gyorke et al., 2004a). Recombinant protein production using the Baculovirus-insect cells (e.g. Sf21 cells) system allows almost all the post-translational modifications required for biological activity. However, it is worth noting that the post-translational modifications occurring with this system differs from those in mammalian cells (Sridhar et al., 1994). In addition expression in insect cells is very time-consuming (Sridhar et al., 1994), with the time from transfection to harvest being typically 3-4 weeks. Also, the expression level can be variable and the cost is relatively high compared to some other expression systems (e.g. bacteria and yeast systems). In comparison, although bacteria *E. coli* cells lack the ability to perform certain eukaryotic post-translational modifications, such as glycosylation, *E. coli* is still the preferred host for recombinant protein expression (Yin et al., 2007). As the quickest method developed so far, the use of *E. coli* is well documented for its advantages of low cost, easy transformation and fermentation, high protein yields and scalability. To date, there have been no reports of FLjun expression in *E. coli* system, presumably due to inherent difficulties in integral

membrane protein expression and purification. In this study, recombinant FLjun was successfully expressed and purified from *E. coli* strain BL21(DE3).

As mentioned, integral membrane proteins such as junctin are notoriously difficult to express, to solubilize and purify, and to maintain properly-folded during purification. *E. coli* strain BL21(DE3) is the most commonly used host for overexpression of membrane proteins, in combination with a pET vector. However, one inherent issue is that membrane proteins are inserted into membranes, and the availability of membrane structures in most cells is limited. Although heterologous overexpression often results in protein aggregation and misfolding due to the hydrophobic nature of transmembrane segments, one way of avoiding the limitations set by the availability of membrane is to produce the membrane protein as inclusion bodies. Preparation of active protein can then be achieved through solubilization of the inclusion bodies using denaturants, followed by refolding. However, refolding of α -helical membrane proteins (e.g., junctin) from inclusion bodies presents a greater challenge than refolding β -barrel membrane proteins (Bannwarth and Schulz, 2003).

Expression was trialed at different temperatures (37 °C, 25 °C, 18 °C) and for different times (2, 3, 4 h and overnight). The longer induction period increased degradation and resulted in a low yield. A relatively short period (3-4 h) at 37 °C produced the maximum yield. Purification of recombinant FLjun was then attempted by solubilizing the cell pellets and purifying the protein with IMAC under denaturing conditions using 8 M Urea. However, further refolding could not be achieved because the protein was extremely prone to precipitate during detergent exchange (from 8 M Urea to different percentages of CHAPS or CHAPS/PC). The problem was overcome by solubilizing and purifying the protein under native conditions using 1% Triton X-100. Although the resultant yield of junctin was relatively lower than that using the denaturing protocol because Triton X-100 is less potent than Urea in protein solubilization, the output was still satisfactorily high, and was far above that from muscle junctin purification.

An additional problem with this procedure was the presence of high amount of Triton X-100 (1%), which posed a challenge for lipid bilayer experiments because Triton X-100 would destabilize the artificial membrane. Therefore, it was necessary to remove Triton X-100 from the final product. This could not be achieved by diluting and washing the protein as done with muscle junctin buffer exchange (see Methods, section 2.5.1). This was because at least a 100-fold dilution would have been required to disrupt the protein-detergent micelles, as Triton X-100 has a low critical micelle concentration (~0.01-0.015%, w/v) (Tiller et al., 1984). This would have been time-consuming and substantial amounts of protein would have been lost during washing and concentrating steps. Therefore Bio-Beads SM-2 non-polar polystyrene adsorbents were used for Triton X-100 removal (Holloway, 1973). The incubation conditions for SM-2 adsorbent and protein solution were optimized (i.e., 1 h and 45 min at room

temperature) in order to remove any residual Triton X-100 and minimize loss of the membrane protein since it could be adsorbed onto SM-2 as well. Using this method, a final sample without detergent was obtained. One point was noted during the protein storage, which may be worthwhile mentioning for purifying other membrane proteins: undesirable aggregation of the protein in the presence of 1% Triton X-100 was visible as a precipitate when the protein was kept at 4 °C for an extended period (~36-48 h). Therefore, the whole procedure should be conducted with an intermediate delay of no longer than 36 h at 4 °C, especially when the protein concentration is high. Alternatively, the sample can be stored at -20 °C if a relatively long stopping point is needed.

The purified recombinant FLjun sample was evaluated by SDS-PAGE and identified using immunoblot (Fig. 3-5D&E). A purity of over 90% was routinely achieved.

3.3.3 Physical interactions between FLjun and RyR1 and RyR2

Purified skeletal FLjun binding to RyR1 and recombinant canine FLjun binding to RyR2 have been previously reported (Goonasekera et al., 2007; Zhang et al., 1997). In this study, to re-confirm the binding of skeletal FLjun to the RyR1 and examine its ability to bind to RyR2, a modified co-IP was conducted as described in section 2.8.1 and 3.2.4. The final eluted proteins were assessed using SDS-PAGE and immunoblot. The presence of the RyR1 or RyR2 (the protein band above 250 kDa) and junctin (~25 kDa) detected by anti-RyR 34C (recognizing both RyR1 and RyR2) and anti-junctin antibody) (Fig. 3-6 lane 1&2) confirmed that the eluted proteins were junctin and the RyR. Control experiments were performed using protein A/G agarose alone (i.e. in the absence of antibody). No detectable RyR1, RyR2 (Fig. 3-6 lane 3&4) or FLJun (Fig. 3-6 lane 5) was bound to the protein A/G agarose in the absence of antibody. The binding was therefore due to the interaction between junctin and the RyR. The ability of purified FLjun to interact with RyR also indicated that the refolded junctin, purified using SDS

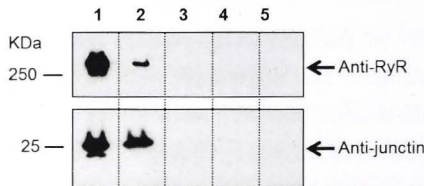


Figure 3-6 Interactions of the purified FLjun with purified RyR1 or RyR2. Immunoblot of the eluted proteins from FLjun/RyR co-IP using monoclonal anti-RyR 34C and polyclonal anti-junctin antibodies, confirming the direct physical interaction between purified skeletal FLjun and RyR1 (lane 1, n=3) or RyR2 (lane 2, n=4). Protein A/G agarose alone did not bind to either RyR1 (lane 3), RyR2 (lane 4) or FLjun (lane 5). The protein molecular weight makers are shown to the left of the immune-blot.

preparative gel electrophoresis, retained its functional characteristics. This result is consistent with previous studies (Goonasekera et al., 2007; Wei et al., 2009a).

It should be noted that the difference in the intensity between RyR1 and RyR2 bands (Fig. 3-6 lane 1&2, upper bands) was mainly due to the anti-RyR 34C antibody used, which has a higher sensitivity in detecting RyR1 than in detecting RyR2 (exemplified in Fig. 2-1, Chapter 2). This also applies to the results obtained with Cjun (Chapter 4, Fig. 4-2), Njun (Chapter 5, Fig. 5-2) and Jun_{KEKE} (Chapter 6, Fig. 6-1).

3.3.4 Purified RyR1/2 regulation by FLjun (luminal interaction)

3.3.4.1 The effect of FLjun on purified RyR1 or RyR2 activity

The result from protein complex immunoprecipitation demonstrates that purified FLjun is able to associate with both the purified skeletal and cardiac RyR. Previous studies with single channel recording have shown that the addition of junctin to the luminal solution in bilayers enhanced the purified RyR1 (Wei et al., 2009a) and RyR2 (Gyorke et al., 2004a) channel opening, indicating a positive role of junctin on RyR channel gating. However, in the latter study (Gyorke et al., 2004a), the $[Ca^{2+}]$ of *trans* solution, which represents luminal side of SR, was either too low at 20 μ M or too high at 5 mM to reflect the physiological range of $[Ca^{2+}]_{SR}$ (0.1~1.5 mM, (Chen et al., 1996; Ginsburg et al., 1998) and reviewed in (Bers, 2002; Dulhunty et al., 2012)) in the heart. To investigate the functional consequences of the physical interactions between FLjun and the RyR2 at resting luminal $[Ca^{2+}]$ (1 mM), lipid bilayer experiments were conducted. The regulation of purified RyR1 by FLjun was re-examined in this study both to: a) compare with the FLjun effect on cardiac RyR2 (this study); and b) confirm the activating effect of FLjun on skeletal RyR1 observed by Wei et al. (2009a). Purified RyR1 or RyR2 channels were incorporated into lipid bilayers using standard *cis* and *trans* solutions (see section 2.9.3 for the composition of these solutions). Channel activity was recorded under symmetrical (Ca^{2+}) conditions (section 2.9.4) in the presence of a *trans* $[Ca^{2+}]$ of 1 mM. The *cis* $[Ca^{2+}]$ in this experiment was 1 μ M for RyR2, and 1 μ M or 100 nM for RyR1 (adjusted by the addition of BAPTA); 2mM ATP was added to *cis* solution in some cases (section 2.9.4). In control experiments, the addition of vehicle solutions lacking active compounds (e.g. FLjun, Cjun, Njun or Jun_{KEKE}), did not lead to changes in channel activity (Fig. 3-7 and 3-8; also see (Wei, 2008)). Therefore, the changes in channel activity shown in all figures in this thesis were specific changes in response to the addition of proteins or peptides (in this chapter the addition of FLjun). Five μ g/ml (213 nM) FLjun was added to the luminal side of RyR1 or RyR2, i.e., *trans* chamber. This concentration was selected as it was similar to the concentration used in previous studies (Gyorke et al., 2004a; Wei et al., 2009a), and it has been previously shown in this laboratory to induce a maximal increase in RyR1 channel activity (Wei et al., 2009a).

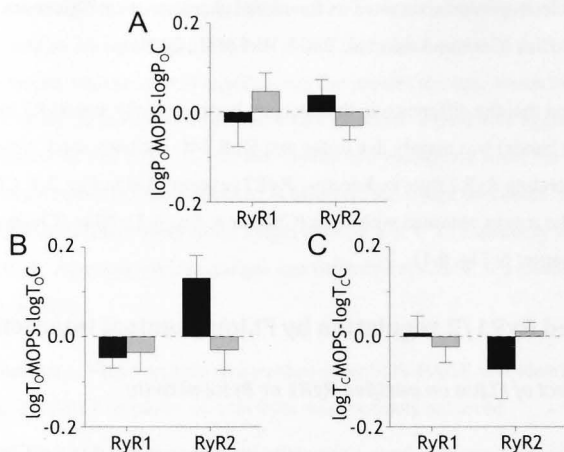


Figure 3-7 MOPS buffer (20 mM MOPS, 150 mM NaCl, pH 7.4; for FLjun in this chapter and Cjun in Chapter 4) alone has no effect on purified RyRs channel activity. (A)-(C) average data for relative open probability ($\log P_{oJ} - \log P_{oC}$, A), mean open time ($\log T_{oJ} - \log T_{oC}$, B) and mean closed time ($\log T_{cJ} - \log T_{cC}$, C). No significant differences found before and after MOPS buffer addition to either the *trans* (black bins) or *cis* (light grey bins) solution ($P > 0.05$ Student's *t*-test, paired, $n = 4-6$ for RyR1 and $n = 5-8$ for RyR2).

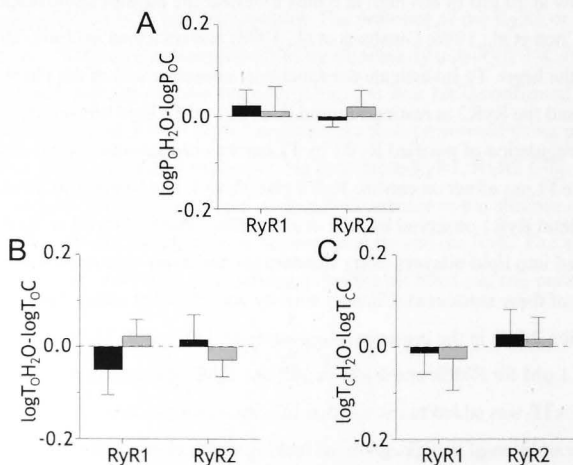


Figure 3-8 MilliQ-water (for Njun, Njun_{scrambled} in Chapter 5 and Jun_{KEKE} in Chapter 6) alone does not alter purified RyRs channel activity. (A)-(C) average data for relative open probability ($\log P_{oJ} - \log P_{oC}$, A), mean open time ($\log T_{oJ} - \log T_{oC}$, B) and mean closed time ($\log T_{cJ} - \log T_{cC}$, C). No significant differences found before and after MilliQ-water addition to either the *trans* (black bins) or *cis* (light grey bins) solution ($P > 0.05$ Student's *t*-test, paired, $n = 4-6$ for RyR1 and $n = 5-6$ for RyR2).

The presence of FLjun (muscle isolated) in the *trans* chamber bathing the luminal side of the channels induced a significant increase in both purified RyR1 and RyR2 channel open probability (P_o) (Fig. 3-9A&B). The open probability increased 1.86±0.14-fold in RyR1 and 2.81±0.44-fold in RyR2 (Fig. 3-9C). Average P_o rose from 0.12±0.03 to 0.21±0.04 for RyR1 and from 0.27±0.05 to 0.59±0.07 for RyR2. The results indicate that junctin is a potent luminal activator of both RyR1 and RyR2. The ability of FLjun to enhance RyR1 channel opening is consistent with that found in a previous study (Wei et al., 2009a).

3.3.4.2 Changes in RyR1/RyR2 channel gating properties induced by FLjun re-association.

To explore further the effect of FLjun on RyR1 and RyR2, single channel activity was analyzed in a subset of recordings where only one channel opening was recorded and changes in open and closed time underlying the changes in P_o were examined. The results show that after FLjun association with the RyRs, there was an average 2.23±0.64-fold and 2.11±0.36-fold increase in T_o for RyR1 and RyR2 respectively (Fig. 3-9D). The mean channel closed times were reduced by FLjun with an average ~2-fold reduction in RyR1 (to 0.56±0.06% of control level) and ~3-fold decrease in RyR2 (to 0.35±0.04% of control) (Fig. 3-9E). The increase in open probability induced by FLjun was therefore due to an increase in the mean open time (T_o) and a decrease in mean closed time (T_c) of both RyR1 and RyR2 channels.

The effects of FLjun on the RyR1 and RyR2 gating were further explored by examining the effects of FLjun on the distribution of open and closed times, the changes in which underlie the increase in mean open time and decrease in mean closed time. The best exponential fit to both open and closed time distributions in control channel activity was obtained using three time constants in both RyR1 and in RyR2 channels (shown in Fig. 3-10 and Table 3-1). The average open time constants in RyR1 channels were $\tau_{o1} = 3.3 \pm 0.16$ ms; $\tau_{o2} = 16.5 \pm 0.48$ ms; $\tau_{o3} = 151.1 \pm 3.36$ ms and average closed time constants $\tau_{c1} = 3.4 \pm 0.18$ ms; $\tau_{c2} = 21.49 \pm 0.78$ ms; $\tau_{c3} = 233.4 \pm 3.71$ ms (Fig. 3-10A&B). The time constant values after addition of FLjun did not change significantly, but there were significant differences in distribution of events between the time constants. With channel openings, 57±8.2% of openings fell into τ_{o1} before, and 43±6.6% after, addition of FLjun. Conversely, there were 2.6±1.4% of openings in τ_{o3} before and 14.0±5.2% after, adding FLjun. There was a trend towards an increase in the number of events in τ_{o2} with 37±5.8% before and 42±6.1% after FLjun, although the difference was not significant. With the dwell times in the closed state, the fraction of events falling into τ_{c2} and τ_{c3} were reduced significantly from 10±2.8% before, to 6.0±1.8% and 42±3.7% to 38±4.6% after adding FLjun respectively. There was however, an increase in the shortest time constant from 48±6.3% to 54±5.7%.

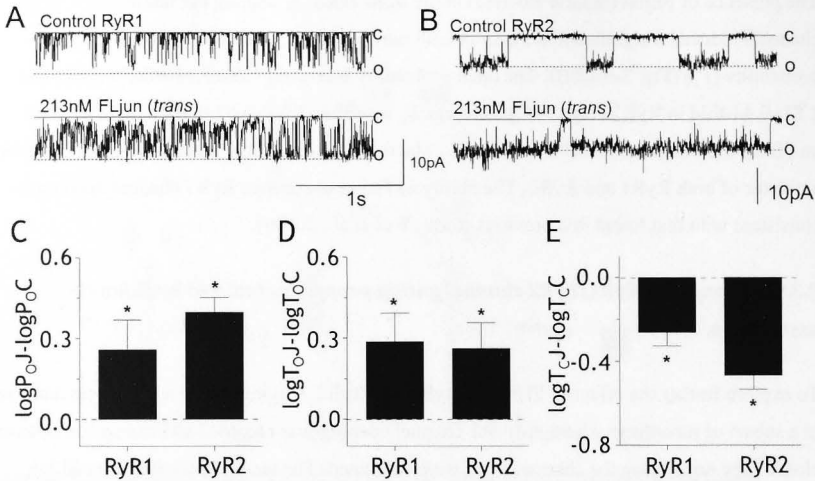


Figure 3-9 Addition of FLjun to the luminal side of purified RyRs activates channels at 1 mM *trans* Ca²⁺. (A)-(B) Records of 3 s of single channel activity at -40 mV. Single channel opening is downward, from zero current (continuous line, c) to maximum open channel conductance (broken line, o). The upper trace in each panel shows control purified RyR activity and the lower trace shows activity after luminal addition of 213 nM (5 μ g/ml) FLjun to RyR1 (A) or RyR2 (B). (C)-(E) Average pooled data from both +40 mV and -40 mV for relative open probability ($\log P_{oJ} - \log P_{oC}$), mean open time ($\log T_{oJ} - \log T_{oC}$) and mean closed time ($\log T_{cJ} - \log T_{cC}$), showing channel activation after adding FLjun. Asterisks (*) indicate average values significantly different from the control ($P < 0.05$ Student's paired *t*-test, $n = 6-10$ for RyR1 and $n = 13-14$ for RyR2).

The open and closed time constants for control RyR2 activity were remarkably similar to those determined for RyR1 channels. The average open time constants for RyR1 were $\tau_{O1} = 3.7 \pm 0.27$ ms; $\tau_{O2} = 18.5 \pm 0.95$ ms; $\tau_{O3} = 130.8 \pm 12.82$ ms and average closed time constants $\tau_{C1} = 3.4 \pm 0.19$ ms; $\tau_{C2} = 21.9 \pm 1.37$ ms; $\tau_{C3} = 190.4 \pm 12.51$ ms (Fig. 3-10C&D). The consequence of FLjun addition to the luminal solution was also similar to that seen in RyR1, with RyR2 activity also showing an increase in the number of openings events in τ_{O3} and a decrease τ_{O1} (Fig. 3-10A&C). Likewise, there was also a reduction in long closures (in τ_{C3}) (Fig. 3-10B&D; Table 3-1, row 11-12). Taken together, no alteration in the time constant values was induced by FLjun, but there was a significant re-distribution of events with an increase in long open events in τ_{O3} (with fewer events in τ_{O1}), and a decrease in long closures in τ_{C3} (with more events in τ_{C1}).

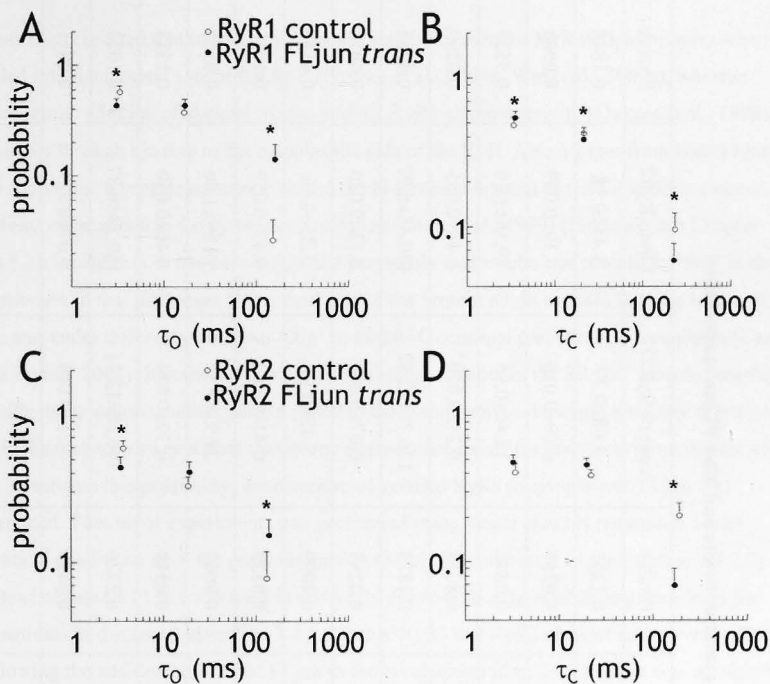


Figure 3-10 Effects of 213 nM FLjun (*trans*) on average open (A&C) and closed (B&D) time constants and fraction of events in each time constant of purified RyRs. The probability of events falling into each time constant is plotted against the time constant in ms (open time or closed time). Time constants are shown for control data (open circles) and 213 nM FLjun (filled circles) for RyR1 (A&B) or RyR2 (C&D). Vertical bars indicate the SEM for event probability. Horizontal bars indicating the SEM for the time constant are contained within the symbols. Asterisks (*) indicate significant differences between control data and with 213 nM FLjun ($P < 0.05$ student's *t*-test, paired, $n = 8$ for RyR1 and $n = 13$ for RyR2).

Table 3-1 A summary of the open and closed time constants before and after FLjun reassociation

	control(RyR1)	Fljun+RyR1	P value	control(RyR2)	Fljun+RyR2	P value
τ_{O1}	3.32±0.16	3.06±0.12	0.1262	3.68±0.27	3.44±0.18	0.1848
P1	0.57±0.082	0.43±0.066	0.0255	0.59±0.076	0.39±0.069	0.0060
τ_{O2}	16.52±0.48	16.89±0.48	0.6845	18.46±0.95	19.36±1.20	0.5527
P2	0.37±0.058	0.42±0.061	0.8079	0.33±0.050	0.48±0.055	0.0299
τ_{O3}	151.11±3.36	159.38±4.22	0.1873	130.77±12.82	130.45±6.97	0.4083
P3	0.03±0.014	0.14±0.052	0.0255	0.07±0.040	0.13±0.030	0.0078
τ_{C1}	3.43±0.18	3.56±0.07	0.4099	3.42±0.19	3.25±0.16	0.4649
P1	0.48±0.063	0.54±0.057	0.0139	0.41±0.062	0.47±0.059	0.1055
τ_{C2}	21.49±0.78	21.41±0.47	0.9067	21.92±1.37	19.69±1.06	0.0553
P2	0.42±0.037	0.38±0.046	0.0319	0.39±0.034	0.46±0.050	0.1333
τ_{C3}	233.38±3.71	226.25±4.40	0.2326	190.38±12.51	169.23±9.37	0.1023
P3	0.10±0.028	0.06±0.018	0.0499	0.21±0.046	0.07±0.021	0.0011
n	8	8		13	13	

P1, P2 and P3 denote probability. P value <0.05 are in bold, denoting significant difference from control value.

3.3.5 *Cis* FLjun does not alter purified RyR1 or RyR2 activity

Experiments in this section were conducted by Mr Chris Thekkedam (Muscle Research Group, John Curtin School of Medical Research, Australian National University, Canberra, Australia).

It has been reported that triadin enhances the activity of isolated RyR in lipid bilayers when added into the luminal side of the RyR (Gyorke et al., 2004a; Wei et al., 2009a), whereas cytoplasmic addition of skeletal triadin inhibits RyR1 channel activity (Ohkura et al., 1998), probably through binding to the cytoplasmic side of the RyR. Also a paper from Isabel Marty's lab shows that a peptide corresponding to the N-terminal domain of triadin inhibits channel activity when added to the cytoplasmic solution (Groh et al., 1999) (for detail, see Chapter 1.8.5.2). In addition, it has been suggested previously that triadin can potentially 'flip' in the membrane so that the longer C-terminal part of the protein might at times face the lumen of the SR, and under different conditions 'flip' so that its C-terminal part faces the cytoplasm (Caswell and Brandt, 2002). Junctin is a homologous protein to triadin in the SR Ca^{2+} release complex, raising the question whether junctin added to the cytoplasmic side would have any effect on RyR channel activity or if dual membrane organization exists for junctin as proposed for triadin. To investigate this possibility, the response of purified RyRs to cytoplasmic FLjun was examined. This set of experiments was performed using single channel recordings under identical conditions as in the previous section (3.3.4). Recombinant FLjun (section 3.3.2.2) instead of muscle FLjun was used in this study due to difficulty in obtaining muscle FLjun sometimes as discussed in section 3.4.1. Neither RyR1 nor RyR2 channel activity was affected following the addition of 213 nM FLjun to the *cis* chamber (Fig. 3-11). There was no significant change in channel open probability (P_o) (Fig. 3-11C). This was reflected by a lack of changes in channel T_o and T_c (Fig. 3-11D&E). These findings were similar to the observation by Gyorke et al. (2004a) that addition of FLjun to the cytoplasmic side did not alter purified RyR2 activity, although they used different conditions (i.e., 20 μM or 5 mM *trans* $[\text{Ca}^{2+}]$ used in the Gyorke study instead of 1 mM). The results demonstrate that FLjun can only regulate the RyR when added to the luminal side.

3.4 Discussion

Previous studies have shown that the FLjun is able to bind to the RyR2 (Zhang et al., 1997) and that it can directly modulate both skeletal and cardiac RyR activity (Altschafli et al., 2011; Gyorke et al., 2004a; Wei et al., 2009a). However the regulation of RyR2 by junctin per se in the presence of a resting luminal Ca^{2+} concentration of 1 mM remained to be clearly defined (for detail, see section 1.9.6.1 and section 3.1). This study investigated the direct effect of junctin on both purified RyR isoforms. The results presented in this chapter show for the first

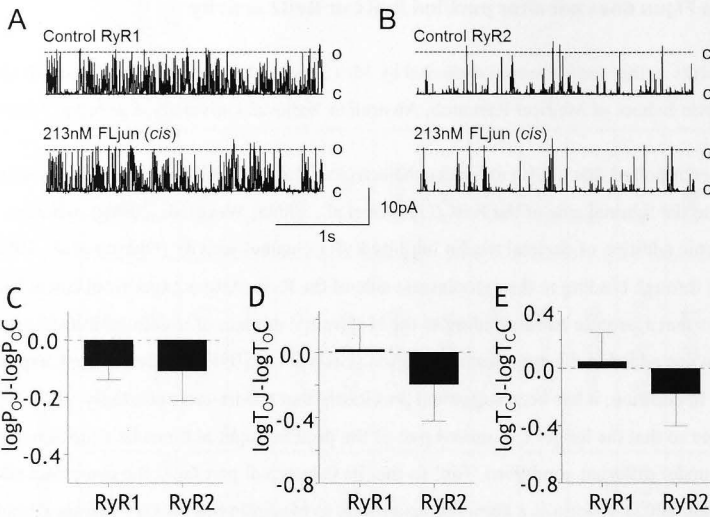


Figure 3-11 Addition of FLjun to *cis* side of purified RyRs does not alter channel activity. (A)-(B) Records of 3 s of single channel activity at -40 mV. Single channel opening is downward from zero current (continuous line, c) to maximum open conductance (broken line, o). The upper trace in each panel shows control activity and the lower trace shows activity after adding 213 nM FLjun to the cytoplasmic solution bathing RyR1 (A) or RyR2 (B). (C)-(E) average data for relative open probability ($\log P_{oJ} - \log P_{oC}$, C), mean open time ($\log T_{oJ} - \log T_{oC}$, D) and mean closed time ($\log T_{cJ} - \log T_{cC}$, E). No significant differences found with FLjun before and after protein addition ($P > 0.05$ student *t*-test, paired, $n=14$ for RyR1 and $n=12$ for RyR2).

time that in the presence of a physiological luminal $[Ca^{2+}]$ (1 mM *trans* Ca^{2+}), FLjun added to luminal solution enhances cardiac RyR channel activity by promoting long channel openings and reducing channel closures. Similar activating effects were observed with skeletal RyR exposed to luminal FLjun, which is consistent with a previous study by Wei et al. (2009a).

3.4.1 Muscle FLjun purification

A protocol modified from (Wei, 2008; Wei et al., 2009a) was employed to isolate junctin from skeletal muscle tissue. The one step preparative gel electrophoresis technique yielded similar separation results to those obtained previously (Wei, 2008; Wei et al., 2009a). In addition, a re-nature step with KCl precipitation and detergent exchange resulted in a similar ~80% protein recovery (Wei, 2008; Wei et al., 2009a). Sometimes however this method yielded very low amounts of junctin. In this case, multiple isolation experiments were required in order to obtain enough protein for downstream experiments. As this was labour- and time-consuming, a method for the expression and purification of FLjun was developed.

3.4.2 Recombinant FLjun from *E.coli*

In recombinant FLjun, the hexahistidine tag (6xHis-tag) on the N-terminal end of FLjun had to be removed. This tag is composed of 24 amino acids (¹RRYTMGSSHHHHHSSGLVPRGSH²⁴). It is not necessary to remove the His-tag for most applications. It was also shown in this study that this tag seems not to cause an effect on regulation of RyRs by the hydrophilic C-terminal domain of junctin (Cjun) (Chapter 4, Fig. 4-3). However, the His-tag attached here may present a problem in affecting membrane insertion via the N-terminal domain of junctin that is likely to occur in single channel lipid bilayer studies. To address this issue, tag removal through thrombin cleavage is underway (conducted by Miss Umayal Narayanan, Muscle Research Group, John Curtin School of Medical Research, Australian National University, Canberra, Australia), prior to Triton X-100 removal procedure. Currently, 60-70% cleavage efficiency has been achieved but this is still not ideal (data not shown). More trial experiments will be necessary to attain maximum recovery of the cleaved protein. Alternatively, it may be worth considering placing the tags on the C-terminal end of the protein to reduce such risk. Another approach is to re-clone FLjun into pHUE vector as for Cjun (Methods, section 2.5.4), although the effectiveness of Usp2cc to cleave the 6xHis-ubiquitin tag in the presence of detergent remains to be determined (Baker et al., 2005). However, due to time constraints this part of work was not performed. This can be investigated in the future. It is important now to examine the luminal interactions of expressed FLjun (without extra residues) with the RyRs.

3.4.3 Luminal FLjun is a potent activator of purified RyR1 and RyR2

In this chapter the physical interaction between FLjun and purified RyR1 and RyR2 has been examined. The modified co-IP assay showed a robust physical association between FLjun and the RyRs (Fig. 3-6). This replicates the interaction seen between endogenous junctin from rabbit skeletal muscle and expressed WT RyR1 (Goonasekera et al., 2007) as well as canine cardiac junctin and the RyR2 (Zhang et al., 1997). In order to determine the functional consequence of the physical interaction, single channel experiments were subsequently conducted and the effect of FLjun on channel activity was monitored at 1 mM luminal [Ca²⁺], which is maintained under resting conditions in striated muscle (Chen et al., 1996; Fryer and Stephenson, 1996). Addition of FLjun to luminal solution produced a significant increase in channel open probability in both purified RyR isoforms, reflecting an increased channel activity. The enhanced RyR1 activity induced by luminal FLjun is in agreement with previous findings in this laboratory (Wei et al., 2009a). These results also confirmed that the FLjun purified through preparative electrophoresis (described in section 2.5.1 and 3.2.3.1) retained its functional properties, i.e. the effect on RyR1 channel activity.

Strong activation of purified RyR2 channels was also observed upon luminal addition of FLjun under the same conditions, i.e., 1 mM *trans* $[Ca^{2+}]$, suggesting that junctin is a RyR2 activator in cardiac muscle. This is similar to the increased RyR2 activity seen after adding recombinant canine cardiac FLjun to the *trans* chamber at 20 μ M and 5 mM luminal Ca^{2+} concentrations in a previous report (Gyorke et al., 2004a). The similar observations in the present study and the study by Gyorke et al. (2004a), to some extent, indicate that the effect of luminal FLjun on RyR2 activity might be independent of luminal $[Ca^{2+}]$. However, a complex regulation of RyR2 by junctin has been recently demonstrated in a junctin-KO study (Altschafel et al., 2011). The activity of RyR2 from junctin-KO and WT cardiac SR was monitored in parallel studies. The results suggest a dual effect of junctin on RyR2 activity depending on luminal Ca^{2+} . Briefly, junctin appears to activate RyR2 at low luminal Ca^{2+} (<1 mM) and inhibit the channel when luminal Ca^{2+} is high (>1 mM) with the crossover point at \sim 1 mM luminal Ca^{2+} (for more detail, see Chapter 1.9.6.1). This result differs from the activation seen in this study using 1 mM luminal Ca^{2+} . The reason for this discrepancy is not clear and warrants further study. Nevertheless, it is worth noting that it is possible that the dual effect observed in (Altschafel et al., 2011) may be related to regulation of RyR2 by CSQ2 or other luminal proteins in the absence of junctin. Also, species-dependent differences and the effects of experimental conditions on the interactions between the cardiac isoforms of the proteins remain to be clarified.

Notably, the finding that FLjun functions as a RyR2 channel activator was in contrast to a negative regulatory role of junctin indicated in most transgenic studies reported (Fan et al., 2008; Fan et al., 2007; Kirchhefer et al., 2006; Yuan et al., 2007) (for more detail, refer to Chapter 1.9.4.1). However, this is not surprising since the conditions in which junctin exerts its effects on RyR2 activity are very likely to be different in the current study compared to the transgenic studies. Compensatory changes in expression of other proteins as well as in the cardiac T-tubule/SR junction also have an impact on Ca^{2+} handling (Franzini-Armstrong et al., 2005; Kirchhefer et al., 2003). These complex changes would obscure the physiological alterations that could be directly attributed to junctin removal. In addition, there is a strong possibility that the suggested inhibitory effect of junctin in these studies may be due to an indirect effect of junctin relaying CSQ2 signal to RyR2, rather than a direct effect of junctin per se. The effect of Cjun on the RyRs may also play a role in the overall changes in these transgenic studies (for data on Cjun effect, see Chapter 4).

In this study, the increase in P_o of both RyR isoforms induced by luminal FLjun was attributed to a prolonged mean open time (T_o) and an abbreviated mean closed time (T_c) (Fig. 3-9D&E). In particular, a \sim 2-fold increase in T_o and \sim 2-fold decrease in T_c in RyR1 channels were similar to changes previously reported (Wei et al., 2009a), which showed an equivalent \sim 2-fold increase in T_o , although the reduction in T_c was relatively higher (\sim 3.5-fold). Further examination revealed

that in both RyR channel types, changes in mean open and closed times were not due to changes in open and closed time constants, since there were no significant alterations in the time constant values (Fig. 3-10 and Table 3-1). Instead, a significant re-distribution of events was observed upon FLjun addition. It appears that FLjun promotes channel openings by increasing long open events and reducing the number of opening events in the shortest open time constant τ_{O1} . The briefer mean closed times could be attributed to decrease in events in long closures in τ_{C3} . Notably, the three open and closed time constants in RyR1 and RyR2 channels were remarkably similar.

It has been suggested that in single channel recordings, junctin added to the *trans* chamber is very likely to insert into the bilayer in its normal orientation, i.e., the N-terminal tail facing the cytoplasmic solution and the C-terminal domain lumenally (Wei et al., 2009a). Such an insertion of FLjun was further suggested in the current study, as both Njun applied to the *cis* solution and FLjun to the *trans* solution were shown to activate the channel (For data on Njun regulation of the RyR, see Chapter 5). To ensure the specificity of such luminal FLjun-RyR interaction, control experiments were performed by adding FLjun to the *cis* solution. In this case, junctin would be expected to insert in the opposite way with its N-terminus facing the luminal solution. This was consistent with the fact that cytoplasmic FLjun (recombinant) did not influence the activity of either RyR1 or RyR2 channels (Fig. 3-11), although this may require further confirmation (see section 3.4.2, due to possible effects of the presence of 6×His-tag). A previous study indeed suggests that addition of FLjun to the *cis* side had no effect on purified RyR2 channel activity (Gyorke et al., 2004a). Therefore, the data strongly suggest that the FLjun can only activate the RyRs when added lumenally.

3.4.4 Limitations

Ideally, the specificity of the luminal effect of FLjun on RyR activity should be examined. This could be explored by repeating the experiments with native RyR1 and RyR2 by adding FLjun to the luminal solution, as the native RyRs should already be bound and regulated by endogenous junctin. One would expect that adding exogenous FLjun to the *trans* side would not bind or induce any changes in RyR activity if the effect of FLjun (*trans*) is specific. However, due to time constraints, the experiments could not be conducted. This could be investigated in the future.

3.4.5 Conclusion

Taken together, the results presented in this chapter provide the first evidence of the sole effect of junctin on purified cardiac RyRs in the absence of other proteins at a physiological luminal Ca^{2+} concentration of 1 mM. The functional regulation of the RyR1 and RyR2 by FLjun

provides a data base for the remainder of this thesis in which the molecular components of FLjun activation were investigated.

Chapter 4 Modulation of RyR1/2 activity by the C-terminal domain of junctin

4.1 Introduction

The role of full-length junctin (FLjun) as an activator of both the RyR1 and RyR2 channels at resting (1 mM) luminal $[Ca^{2+}]$ has been addressed in Chapter 3. As previously mentioned (Chapter 1.9.1), the majority (~78.6%) of junctin (FLjun) is contained in its luminal C-terminal domain (Cjun). There is a long-held view that the major effect of FLjun on RyR depends on luminal interactions between the two proteins since the luminal domain of junctin binds to RyR2, and this has led to the proposal that in intact muscle junctin interacts with RyR from the luminal surface of the SR membrane (Zhang et al., 1997). This was supported in a study investigating binding regions on interacting domains of junctin and RyR2 (Altschafel et al., 2011). However that study focused only on Cjun with other segments (e.g. N-terminal domain) not being considered (Altschafel et al., 2011). More recently, Rossi et al. (2013) showed that the intraluminal domain of junctin, i.e., Cjun, contains minimal junctional SR targeting sequences. Together, these studies indicate that the presence of Cjun is probably sufficient both to localize junctin to the junctional SR and to allow junctin to interact with RyR, CSQ and triadin. If this were the case, one would expect Cjun added to the luminal solution to impose a similar effect on RyR channel activity to that seen with FLjun, i.e., an activation. As yet, there have not been any reports on the effects of Cjun skeletal and cardiac RyRs exclusively. Therefore, the direct effects of Cjun on regulating RyR1 and RyR2 were considered here.

Aim:

The aim of the work presented in this chapter was to determine (a) the direct physical interactions between Cjun and the RyRs, and (b) the potential regulatory effects of Cjun and purified RyR1 and RyR2 channel activity.

4.2 Materials and Methods

4.2.1 Methods overview

Recombinant Cjun was engineered in the study in this chapter. The Cjun protein was expressed and purified from *E.coli* to examine its ability to bind and interact with RyR1 and RyR2. The physical association between Cjun and the purified RyRs was examined using modified co-IP. Functional regulation of both purified RyR isoforms by Cjun was explored using single channel techniques under physiological luminal $[Ca^{2+}]$ (1 mM). Control experiments were also

performed to assess whether Cjun in the cytoplasm affects RyRs activity, both lipid bilayer studies and Ca^{2+} release spectrophotometric assay were performed in this case.

4.2.2 SR vesicle isolation and RyR purification

Purified skeletal and cardiac RyRs as well as crude SR vesicles used in the experiments in this chapter were obtained using the methods described in section 2.3.

4.2.3 Recombinant canine cardiac Cjun

Cjun was expressed and purified from *E.coli* as detailed in section 2.5.3 and 2.5.4. In brief, recombinant Cjun was obtained by subcloning canine cardiac muscle junctin cDNA corresponding to junctin aa46-210 and expressed in *E.coli* either as a poly-histidine (6×His) fusion (for Cjun sub-cloned into pET15b.ep vector) or poly His-ubiquitin (6×His-ub) fusion (for Cjun in pHUE vector) protein. Maximum yield of recombinant protein was achieved by expressing the protein for 4 h at 37 °C following induction with 0.6 mM IPTG. After lysozyme solubilization of the bacteria, the cell membranes were ruptured and the contents of the cell were released with a cell disruption bomb (Nitrogen decompression). The fusion protein was purified using Ni^{2+} -nitrilotriacetic acid agarose matrix by IMAC under native conditions. 6×His-Cjun or 6×His-ub-Cjun was coupled to the affinity matrix after incubating the protein supernatant with the agarose. Any unbound proteins were removed by extensive washing of the beads. The fusion protein was eluted against 500 mM imidazole elution buffer. For Cjun cloned in pET15b.ep vector, the 6×His tag was still attached to the N-terminal of Cjun; for Cjun in pHUE vector, the 6×His-ub was removed by Usp2cc cleavage. Purified recombinant Cjun (either with tag or without) was washed against a standard wash/exchange buffer and concentrated.

4.2.4 Modified co-IP between Cjun and RyR1 and RyR2

The modified co-IP assay was carried out to investigate the direct binding of recombinant Cjun to the purified RyR1 or RyR2 in the same way as for FLjun (see Method, section 2.8.1 or Chapter 3, section 3.2.4). Recombinant GST fusion Cjun protein binding to cardiac RyR2 has been previously reported (Zhang et al., 1997). In this study, both Cjun with 6×His tag and Cjun alone were tested to check their interaction with RyR1 or RyR2. Co-IP was conducted in two ways, either Cjun precipitated by RyR1 (n=3) or RyR2 (n=3) co-IP or co-IP precipitation of RyR1 (n=4) or RyR2 (n=4) by Cjun. After extensive washing to remove the unbound proteins, the final resultant complex (RyR/Cjun-antibody-protein A/G agarose) was incubated with Laemmli sample buffer at 65 °C for 10 min to elute the proteins and tested with SDS-PAGE and immunoblot.

4.2.5 Single channel recording and analysis

Single RyR channel recording was undertaken and analyzed as described in section 2.9. Cjun was added to either the *trans* or *cis* chamber to assess its effect on RyR channel activity.

4.2.6 Ca²⁺ release from skeletal and cardiac SR vesicles

4.2.6.1 Cjun induced Ca²⁺ release from SR vesicles

Cjun-induced Ca²⁺ release from SR vesicles was tested as described in section 2.10.1. The SR vesicles were first loaded with Ca²⁺, then exposed to thapsigargin to block SERCA to prevent Ca²⁺ uptake during the experiment (Hanna et al., 2011; Jalilian et al., 2008; Sagara and Inesi, 1991). Cjun (5 μM) was added 30 s after thapsigargin to examine its ability to immediately stimulate Ca²⁺ release by measuring the optical density. This concentration of 5 μM was chosen because the effects of compounds often require higher concentrations to affect SR Ca²⁺ release, than those needed to alter RyR activity in bilayers (Dulhunty et al., 1999). The rate of Ca²⁺ release induced by Cjun was calculated (section 2.10.3) and the results were compared to control experiments where MOPS buffer (20 mM MOPS, 150 mM NaCl, pH 7.4, where Cjun was dissolved) was used in place of Cjun.

4.2.6.2 Pre-incubation of SR vesicles with Cjun

Ca²⁺ release from SR vesicles pre-incubated with Cjun was assessed as detailed in section 2.10.2. In brief, the SR vesicles were exposed to 5 μM Cjun for ~30 min prior to thapsigargin addition (20 min pre-incubation plus 10 min during Ca²⁺ loading), to provide sufficient time for RyR-Cjun interaction, if there were any, to be fully established. In these experiments, caffeine was used to stimulate Ca²⁺ release and the effect of pre-incubation with Cjun on caffeine-induced Ca²⁺ release was measured. The rate of caffeine-induced Ca²⁺ release was compared to control experiments in which the vesicles were pre-incubated with MOPS. The rate of Ca²⁺ release was calculated in the same way as describe in section 2.10.3.

4.3 Results

4.3.1 Expression and purification of Cjun

Recombinant Cjun (either with 6×His-tag or without tag) purification was analyzed by SDS-PAGE and identified using immunoblot (Fig. 4-1). A purity of over 95% was achieved in both cases.

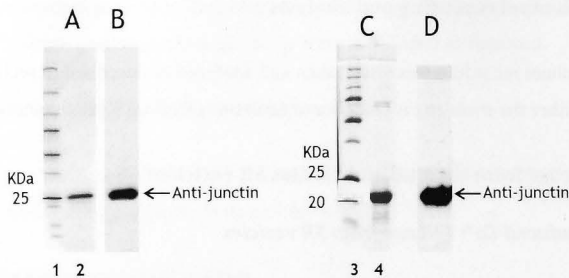


Figure 4-1 Recombinantly expressed and purified Cjun. (A)-(B) Recombinant 6×His-Cjun using pET15b.ep (mod.) vector. The fusion protein (~0.5 μg) was analyzed on a 10% SDS-PAGE gel followed by coomassie staining (lane 2 in A) and immunoblot (B). (C)-(D) Recombinant Cjun utilizing pHUE vector. Cjun (~5 μg) was analyzed on a 12% SDS-PAGE gel followed by coomassie staining (lane 4 in C) and immunoblot (D). The 6×His-ub tag was cleaved with ubiquitin protease Usp2cc and removed by re-binding to the Ni-NAT resin. Immunoblot using anti-junctin antibody confirmed the identity of Cjun obtained from both pET15b.ep (mod.) and pHUE vectors. Molecular weight markers are shown in lane 1 and lane 3 respectively. Pink band corresponds to the molecular weight noted.

4.3.2 Physical interaction—Cjun binds to purified RyR1 and RyR2

The interaction between Cjun protein and the RyR was examined using modified co-IP and was visualized using SDS-PAGE and immunoblot (section 2.8.1 and 4.2.4) (Fig. 4-2). Immunoblot of the RyR/Cjun-antibody complex probing with anti-RyR 34C and anti-junctin antibodies confirmed that the eluted proteins were Cjun and the RyR (Fig. 4-2 lane 5-8). Control experiments were performed in the absence of antibody with no detectable RyR1 or RyR2 shown (Fig. 4-2 lane 1&2). Nor did 6xHis-Cjun or Cjun (no tag) bind to protein A/G agarose (Fig. 4-2 lane 3&4). The co-IP results clearly demonstrated that both 6×His-Cjun and Cjun (no tag) were able to bind directly to the purified skeletal RyR1 and cardiac RyR2.

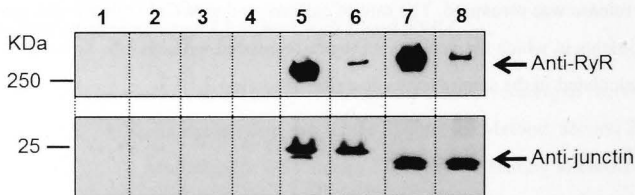


Figure 4-2 Binding of Cjun to purified RyR1 and RyR2. Immunoblot of the eluted proteins from Cjun/RyR co-IP using monoclonal anti-RyR 34C and polyclonal anti-junctin antibodies, confirming the association of purified RyR1 and RyR2 with Cjun (with His-tag) (lane 5 and 6 respectively, n=3 for RyR1, n=4 for RyR2). Some co-IP experiments were also performed with Cjun (without His-tag) and purified RyR1 and RyR2 with similar results (lane 7 and 8 for RyR1 and RyR2 respectively), confirmed in 2 repeats. Protein A/G agarose alone did not bind to either RyR1 (lane 1) or RyR2 (lane 2), nor did it bind to 6×His-Cjun (lane 3) or Cjun (no tag) (lane 4). Molecular weights to the left of lanes.

4.3.3 Functional effect of Cjun on RyR1/2

The ability of Cjun to modify RyR channel activity was examined using single channel recordings and Ca^{2+} release assays. Purified RyR1 or RyR2 was incorporated into lipid bilayers using standard incorporating solutions (for composition of these solutions see section 2.9.3) and channel activity was recorded under symmetrical (Cs^+) conditions (section 2.9.4), *trans* [Ca^{2+}] was maintained at 1mM under all conditions. Cjun (213 nM) was added either to the luminal side or the cytoplasmic side of RyR1 or RyR2 accordingly.

4.3.3.1 The effect of luminal addition of Cjun on purified RyR1 or RyR2 activity

In this experiment, 213 nM Cjun (with 6xHis-tag) was added to the luminal (*trans*) side of the purified RyRs. It was expected that the luminal addition of Cjun would activate RyRs in the same way as FLjun since the major effect of FLjun has been assumed to be due to an interaction between the proteins within the lumen of the SR. In contrast, Cjun induced a significant inhibition of both RyR1 and RyR2 channel activity after its addition to the luminal solution. Channel P_o in RyR1 fell to 0.68 ± 0.17 of control and in RyR2 fell to 0.48 ± 0.06 of control (Fig. 4-3A-C; P_o from 0.085 ± 0.04 to 0.037 ± 0.016 in RyR1, and from 0.348 ± 0.026 to 0.174 ± 0.031 in RyR2). To exclude the possibility of any non-specific interaction between 6xHis-tag and luminal RyR, identical experiments were carried out with the recombinant Cjun (without any tag). Adding Cjun (no tag) to the luminal side produced a significant decrease in the open probability in both channel types (Fig. 4-3C, cross-hatched bins), P_o fell to 0.38 ± 0.07 of control in RyR1 (from 0.44 ± 0.07 to 0.19 ± 0.06) and to 0.37 ± 0.07 in RyR2 (from 0.246 ± 0.055 to 0.084 ± 0.014), similar to the effect of luminal 6xHis-Cjun on purified RyRs. The similarity of the response of purified RyR1 and RyR2 to 6xHis-Cjun and Cjun (no tag) suggests that the inhibitory effect was due to the luminal interaction between Cjun and the RyR, but not the 6xHis-tag. No apparent changes in channel activity were observed when adding Cjun to luminal side of native RyR1 ($n=1$) or RyR2 ($n=2$) (data not shown).

Further examination of the effect of Cjun on RyR1 and RyR2 channel activity revealed that the decrease in channel activity was due to an abbreviation of average mean open times and prolonged mean closed times (Fig. 4-3D&E, black bins). After luminal addition of Cjun (6xHis-Cjun), the mean channel open time was reduced with an average ~2-fold reduction in RyR1 (to 0.48 ± 0.06 of control) and ~1.4-fold reduction in RyR2 (to 0.70 ± 0.09). In contrast, there was an average 8.18 \pm 2.20-fold and 5.74 \pm 2.03-fold increase in mean closed times for RyR1 and RyR2 respectively (Fig. 4-3D&E, black bins). Analysis of data obtained with luminal addition of Cjun (no tag) to purified RyRs showed a similar change in T_o and T_c (T_o : to 0.64 ± 0.15 of control in RyR1 and 0.49 ± 0.04 in RyR2; T_c : 2.98 \pm 0.79-fold increase in RyR1 and 3.8 \pm 0.53 increase in RyR2) (Fig. 4-3D&E, cross-hatched bins).

The changes in RyR channel gating in this set of experiment was also accompanied by corresponding changes in time constant distributions (Fig. 4-4; Table 4-1). As can be seen with FLjun (see Chapter 3.3.4.2), three open time constants and three closed time constants were used with both RyR1 and RyR2 channel activity to obtain the best exponential fit. The average open time constants in RyR1 channels were $\tau_{O1} = 2.9 \pm 0.12$ ms; $\tau_{O2} = 16.7 \pm 0.19$ ms; $\tau_{O3} = 165.0 \pm 1.78$ ms and average closed time constants $\tau_{C1} = 3.1 \pm 0.16$ ms; $\tau_{C2} = 22.6 \pm 0.37$ ms; $\tau_{C3} = 235.3 \pm 2.51$ ms. Addition of Cjun did not induce significant changes in the time constant values, but the number of events falling into these time constants was significantly different. With the dwell times in the open state, 79 \pm 2.5% of openings fell into τ_{O1} before, and 87 \pm 3.8% after, Cjun addition. Conversely, the fraction of events in τ_{O2} were 20 \pm 2.3% before and 13 \pm 3.7% after adding Cjun. In addition, there was a trend towards a reduction in the number of events falling into τ_{O3} with 0.5 \pm 0.21% before and 0.2 \pm 0.16% after Cjun, although the difference was not significant. With channel closings, the number of events in τ_{C2} was decreased significantly from 42 \pm 2.5% before, to 34 \pm 3.4% after, adding Cjun. By contrast, 16 \pm 2.4% of closings fell into τ_{C3} before, and 31 \pm 6.4% after, the addition of Cjun. There was also a significant decrease in the number of events in the shortest closed time constant from 42 \pm 4.5% to 34 \pm 5.6% after Cjun addition (Fig. 4-4A&B).

The open and closed time constant values for RyR2 activity were again similar before and after luminal addition of Cjun, and were also similar to those determined for RyR1 channels. The average open time constants for RyR2 channels were $\tau_{O1} = 2.5 \pm 0.11$ ms; $\tau_{O2} = 15.5 \pm 0.17$ ms; $\tau_{O3} = 144.2 \pm 2.17$ ms and average closed time constants $\tau_{C1} = 4.1 \pm 0.14$ ms; $\tau_{C2} = 22.4 \pm 0.26$ ms; $\tau_{C3} = 257.1 \pm 2.16$ ms. Cjun addition to the luminal solution produced similar effects to those seen in RyR1. There was an increase in the number of opening events in τ_{O1} (from 62 \pm 8.9% to 75 \pm 6.4%) and a decrease in the longest closures τ_{O3} (from 2.0 \pm 0.7% to 0.6 \pm 0.19%). A \sim 1.5-fold reduction in events occurring within τ_{O2} was also observed (from 36 \pm 8.4% to 24 \pm 6.3%), although the difference was not statistically significant. With the number of closed events, after adding Cjun, RyR2 activity showed a \sim 2.4-fold increase in long closures (in τ_{C3} , from 8.5 \pm 2.5% to 22 \pm 6.2%) with no significant changes in τ_{C1} and τ_{C2} . As with FLjun (see Chapter 3.3.4.2), there was no difference between effects of Cjun on RyR1 and RyR2 (Fig. 4-4, Table 4-1).

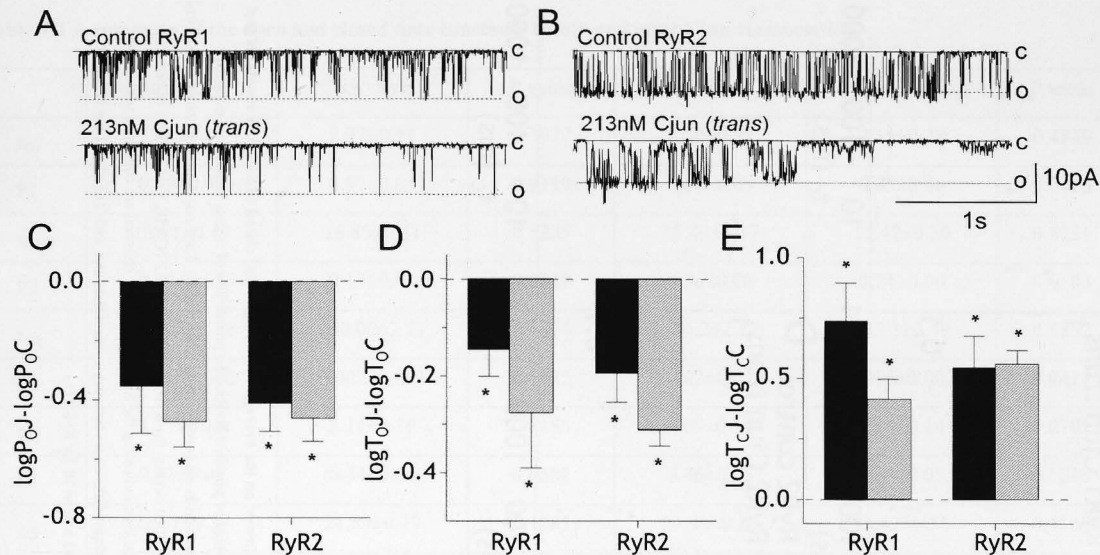


Figure 4-3 Luminal addition of Cjun inhibits purified RyR channel activity at 1 mM *trans* Ca²⁺. (A)-(B) Records of 3 s of single channel activity at -40 mV. Single channel opening is downward from zero current (c, continuous line) to maximum open conductance (o, broken lines). The top recording in each panel shows control channel activity and the lower trace shows activity in the same channel after addition of 213 nM FLjun to the luminal solution bathing RyR1 (A) and RyR2 (B). (C)-(E) Average pooled data from both potentials for relative open probability ($\log P_o J - \log P_o C$, C), mean open time ($\log T_o J - \log T_o C$, D), and mean closed time ($\log T_c J - \log T_c C$, E) for RyR1 and RyR2. Data are shown for effects of the Cjun (with 6×His-tag, Methods section 2.5.3 and 4.2.3) on the luminal side of RyR1 (n=9-12) and RyR2 (n=11-17) (filled bins). Some experiments were also performed with luminal addition of Cjun (without His-tag, Methods section 2.5.4 and 4.2.3) with similar results in RyR1 (n=7-8) and RyR2 (n=6) (cross-hatched bins). The asterisk (*) indicates average values significantly different from the control ($P < 0.05$ Student's *t*-test, paired).

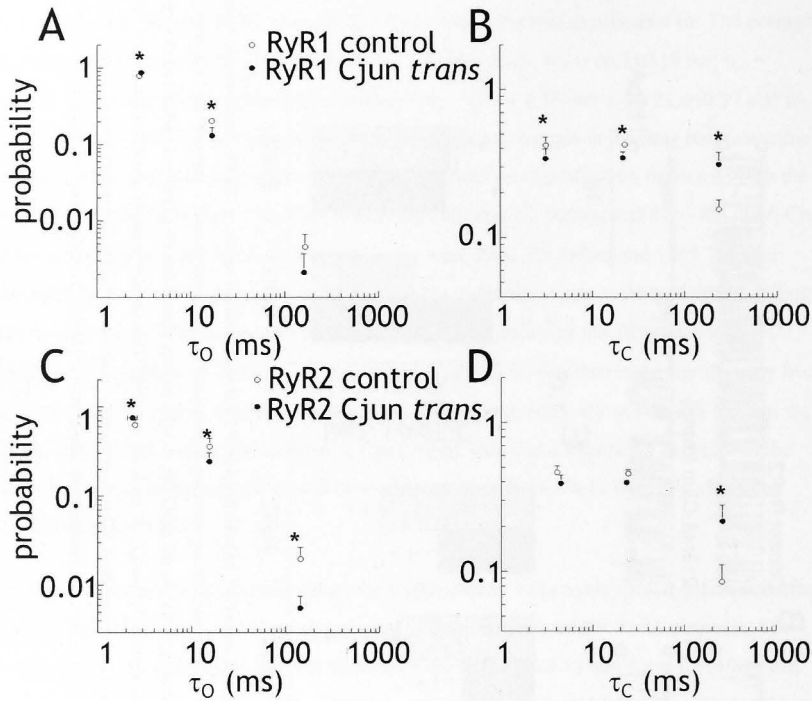


Figure 4-4 Effects of 213 nM Cjun (*trans*) on the average open (A&C) and closed (B&D) time constants and fraction of events in each time constant of purified RyRs. The probability of events falling into each time constant is plotted against the time constant in ms (open time or closed time). Time constants are shown for control data (open circles) and 213 nM Cjun (filled circles) for RyR1 (A&B) or RyR2 (C&D). Vertical bars indicate the SEM for event probability. Horizontal bars indicating the SEM for the time constant are contained within the symbols. Asterisks (*) indicate significant differences between control data and with 213 nM FLjun ($P < 0.05$ Student's *t*-test, paired, $n=12$ for RyR1 and $n=10$ for RyR2).

Table 4-1 A summary of the open and closed time constants before and after Cjun reassociation

	control(RyR1)	Cjun+RyR1	P value	control(RyR2)	Cjun+RyR2	P value
τ_{O1}	2.85±0.12	2.97±0.14	0.3927	2.50±0.11	2.35±0.28	0.4839
P1	0.79±0.02	0.87±0.04	0.0219	0.62±0.09	0.75±0.06	0.0428
τ_{O2}	16.71±0.19	16.85±0.31	0.5205	15.49±0.17	15.42±0.30	0.8251
P2	0.20±0.02	0.13±0.04	0.0229	0.36±0.08	0.24±0.06	0.0503
τ_{O3}	165.04±1.78	160.00±2.21	0.1474	144.2±2.17	143.1±2.40	0.1852
P3	0.005±0.002	0.002±0.001	0.1175	0.02±0.01	0.006±0.002	0.0421
τ_{C1}	3.13±0.16	3.11±0.16	0.8166	4.09±0.14	4.48±0.14	0.0701
P1	0.42±0.05	0.34±0.06	0.0382	0.46±0.05	0.39±0.05	0.1536
τ_{C2}	22.61±0.37	21.89±0.39	0.1585	24.40±0.26	23.42±0.55	0.1162
P2	0.42±0.02	0.34±0.03	0.0343	0.45±0.03	0.39±0.02	0.1915
τ_{C3}	235.33±2.51	236.17±1.47	0.7599	257.10±2.16	260.80±3.06	0.1354
P3	0.16±0.02	0.31±0.06	0.0118	0.09±0.03	0.22±0.06	0.0130
n	12	12		10	10	

P1, P2 and P3 denote probability. P value <0.05 are in bold, denoting significant difference from control value.

4.3.3.2 Cytoplasmic interaction between Cjun and RyR1/RyR2

4.3.3.2.1 Cytoplasmic addition of Cjun causes weak inhibition of both purified RyR1 and RyR2 channel activity

The cytoplasmic effect of Cjun on purified RyRs was also determined. The experiment conditions and the concentration of added Cjun (213 nM) were the same as in the previous section. Unlike *cis* FLjun (see Chapter 3.3.5), the addition of Cjun to the cytoplasmic (*cis*) solution produced a significant decrease in both purified RyR1 and RyR2 channel activity (Fig. 4-5). The average relative P_o values (calculated for individual channels) was 0.72 ± 0.06 and 0.82 ± 0.05 in RyR1 and RyR2 respectively (Fig. 4-5C, black bins; control P_o was reduced from 0.38 ± 0.08 to 0.28 ± 0.07 in RyR1 and from 0.37 ± 0.04 to 0.27 ± 0.03 in RyR2). But the reduction was significantly less than that seen when adding Cjun to the luminal side (Fig. 4-5C, cross-hatched bins).

The channel gating properties, mean open time and mean closed time (T_o and T_c) were examined as well for this series of experiments. The results suggest that the average decrease in RyR1 channel open probability with *cis* Cjun could be attributed to a significant increase in mean closed time (~2.6-fold increase); there was no significant change in T_o when Cjun was added. For RyR2, the reduction in channel activity was primarily due to a significant prolongation of T_c (~1.5-fold increase) with a trend towards lower T_o values with (Fig. 4-5D&E, black bins). Again, changes in T_o and T_c induced by cytoplasmic Cjun was smaller than those caused by luminal Cjun.

The weak inhibition induced by Cjun *cis* may be due to Cjun acting directly at a cytoplasmic domain of the RyRs, or in a luminal microdomain that is also available from the *cis* chamber. An alternative possibility is that Cjun may cross the membrane and access the luminal domain to act as luminal Cjun, although this is less likely due to the high density of charged residues that it contains (for detail, see Chapter 1.9.2). Nevertheless, if this were the case, one would expect that the effect of Cjun addition to either chamber be eliminated or at least reduced if it was added first to the opposite solution. To examine these possibilities, Cjun was either applied first to luminal side and then to cytoplasmic solution (Fig. 4-6A&B), or in the reverse order (Fig. 4-6C&D). (NB. Part of this work was performed by Prof. Esther Gallant from Muscle Research Group, John Curtin School of Medical Research, Australian National University, Canberra, Australia). In both cases, the strong inhibition with luminal addition and weak inhibition with cytoplasmic addition were maintained irrespective of which side had Cjun added first (Fig. 4-6). These observations indicate that the altered RyR activity by *cis* Cjun was through Cjun acting on a cytoplasmic site. In the following sections (section 4.3.3.2.2 and 4.3.3.2.3), further investigations were carried out to determine the specificity of this cytoplasmic effect of Cjun.

4.3.3.2.2 Effect of Cjun (*cis*) on native RyR1 and RyR2 channel activity

Similar experiments were repeated with native RyR1 and RyR2 by adding Cjun to the cytoplasmic solution to determine the specificity of this cytoplasmic effect. Since the native RyRs already contain endogenous junctin, one would expect that if some junctin was inserted into the membrane with its C-terminus facing the *cis* side, and if the C-tail binding was specific, then adding exogenous Cjun to the *cis* side could not bind or induce any changes in RyR activity. Interestingly, in these experiments, native RyR1 and RyR2 were shown to respond differentially to cytoplasmic Cjun, which was inconsistent with the RyR isoform independent actions of FLjun (Chapter 3), Cjun (this Chapter), Njun (Chapter 5) and Jun_{KEKE} (Chapter 6) seen in all other experiments. Addition of Cjun to cytoplasmic solution again induced a small reduction in native RyR2 channel activity (Fig. 4-7C 4th black bin), similar to its effect on purified RyR2 channels (Fig. 4-7C 3rd cross-hatch bin), suggesting the non-physiological nature of the cytoplasmic Cjun-RyR2 interaction as endogenous Cjun would presumably already be bound to sites that it had occupied *in vivo*. Curiously, there was no effect of Cjun on native RyR1 channels in bilayers, in contrast to its inhibitory effect on purified RyR1 (Fig. 4-7C 1st two bins).

4.3.3.2.3 No effect of Cjun on Ca²⁺ release from SR vesicles

The cytoplasmic effect of Cjun on native RyRs was further explored by examining its effects on Ca²⁺ release from intact SR vesicles. Investigations into this interaction were undertaken by Mrs. Suzy Pace (Muscle Research Group, John Curtin School of Medical Research, Australian National University, Canberra, Australia). In contrast to single channel studies, the Ca²⁺ release assay with intact SR vesicles provided a more intact system. The assay was conducted in two ways as described in section 2.10 and 4.2.6.

In one case, Ca²⁺ release was stimulated by addition of Cjun to a solution containing RyR1 or RyR2 channels in SR vesicles (section 2.10.1 and 4.2.6.1). In control experiments, MOPS buffer was used. The rates of Ca²⁺ release immediately after Cjun in MOPS buffer addition were measured and compared with the rate with MOPS buffer alone. Similar to the failure of *cis* Cjun to affect native RyR1 channels in lipid bilayers, Cjun did not cause a significant change in the rate of Ca²⁺ release from RyR1-containing vesicles (Fig. 4-8 1st black bin; from 97.92±1.99 in the absence of Cjun in control experiment to 87.28±11.73 nmol Ca²⁺/mg protein/min). On the other hand, Cjun also had no significant effect on Ca²⁺ release from SR vesicles containing RyR2 (from 5.95±1.29 (control) to 4.24±1.43 nmol Ca²⁺/mg protein/min), in contrast to its inhibition of native RyR2 channels in bilayers, although there was a trend towards a reduced rate of Ca²⁺ release (Fig. 4-8 2nd black bin).

In the second case, the vesicles were pre-incubated with Cjun for 20 min prior to the experiments. Caffeine was used to stimulate Ca^{2+} release. The rate of caffeine-induced Ca^{2+} release from vesicles pre-incubated with Cjun was compared to control experiments in which the vesicles were pre-incubated with MOPS buffer. No overall changes were observed in the rate of caffeine-induced Ca^{2+} release from vesicles containing either RyR1 or RyR2 after pre-incubation with Cjun (Fig. 4-8 light grey bins; from a control of 229.54 ± 40.50 to 278.13 ± 33.27 (with Cjun) nmol Ca^{2+} /mg protein/min in RyR1, and from 56.25 ± 3.87 (control) to 51.63 ± 3.35 nmol Ca^{2+} /mg protein/min in RyR2). This was again in contrast to the negative effect of Cjun on native RyR2 channel activity in bilayers but consistent with its lack of an effect on native RyR1 channels.

Taken together, the inconsistent results obtained with native RyRs (section 4.3.3.2.2 and 4.3.3.2.3) question the significance of the cytoplasmic effect of Cjun.

4.4 Discussion

In this chapter, the physical interaction and functional regulation of the purified RyR1 and RyR2 by junctin's luminal domain, Cjun, were extensively investigated at a resting luminal $[\text{Ca}^{2+}]$ of 1 mM. Cjun expressed and purified from *E.coli* was re-associated with purified RyRs in the absence of other junctin segments and FLjun. For the first time, the effects of Cjun have been characterized on single RyR1 and RyR2 channels and Cjun was shown to regulate purified RyRs. The unexpected finding was that purified RyRs are inhibited by luminal Cjun, in contrast to the activation by luminal FLjun. The novel results presented in this chapter challenge the long-held assumption that FLjun regulates RyRs simply through its C-terminal domain and suggest a more complex mechanism for FLjun regulation of RyRs.

4.4.1 Cjun expression and purification

Topology analysis has revealed the C-terminal, luminal domain of junctin (Cjun) encompasses amino acids 45-210 (Jones et al., 1995). In an early study (Zhang et al., 1997), GST-fused Cjun protein (canine cardiac isoform, residues 46-210) was found to be only poorly expressed in *E.coli*. This was possibly due to the vector being improperly selected or to potential Cjun degradation during expression. Recently, also using *E.coli*, Lee et al. (2012) were able to express 6xHis-tagged mouse junctin. This construct however, only contained residues 68-207, corresponding to canine junctin residues 66-210, i.e., without the initial luminal part (residues 45-65). For this reason, a protocol for expression of Cjun of its full sequence was developed. In this study, the issue of poor expression of full length Cjun observed in (Zhang et al., 1997) was resolved by constructing canine Cjun (residues 46-210) as 6xHis-fusion protein using a modified pET15b.ep vector, and *E. coli* strain BL21(DE3) as a host for the expression (for

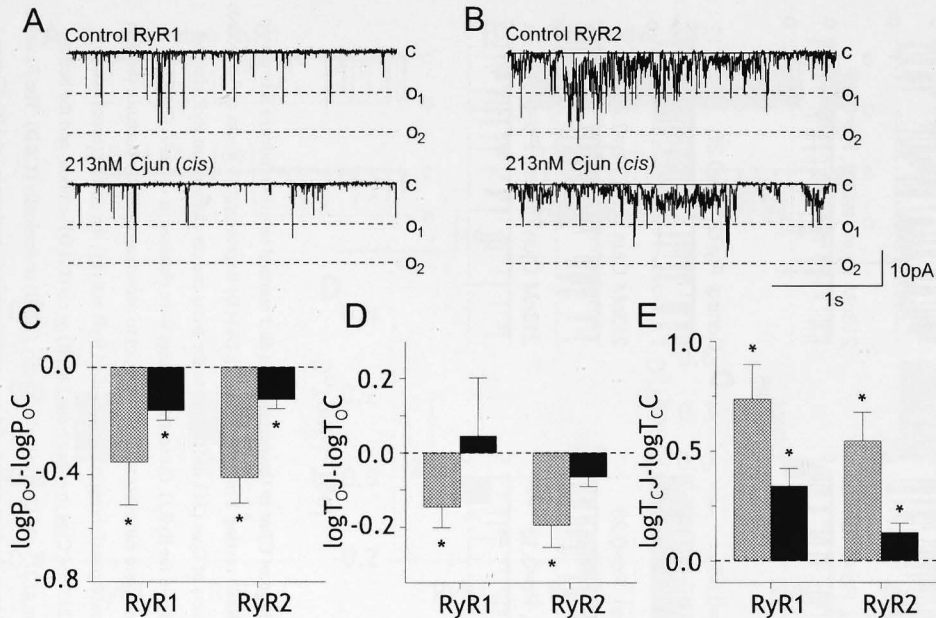


Figure 4-5 Weak inhibition of purified RyR channel activity by cytoplasmic addition of Cjun. (A)-(B) Records of 3 s of single channel activity at -40 mV. Single channel opening is downward from zero current (continuous line, c) to maximum open conductance (broken lines, o_1 , o_2). Top traces in each panel show purified RyR control activity and the lower traces show activity in the same channel after addition of 213 nM Cjun to the cytoplasmic solution bathing RyR1 (A) and RyR2 (B). (C)-(E) Average data for relative open probability ($\log P_{oJ} - \log P_{oC}$, C), mean open time ($\log T_{oJ} - \log T_{oC}$, D), and mean closed time ($\log T_{cJ} - \log T_{cC}$, E) from both potentials, before and after adding Cjun cytoplasmically (black bins) (Cjun (luminal addition) data are from previous figures and included for comparison, cross-hatched bins). Asterisks (*) indicate significant differences between control data and with 213 nM Cjun *cis* ($P < 0.05$ Student's *t*-test, paired, $n = 10-12$ for RyR1 and $n = 17-27$ for RyR2).

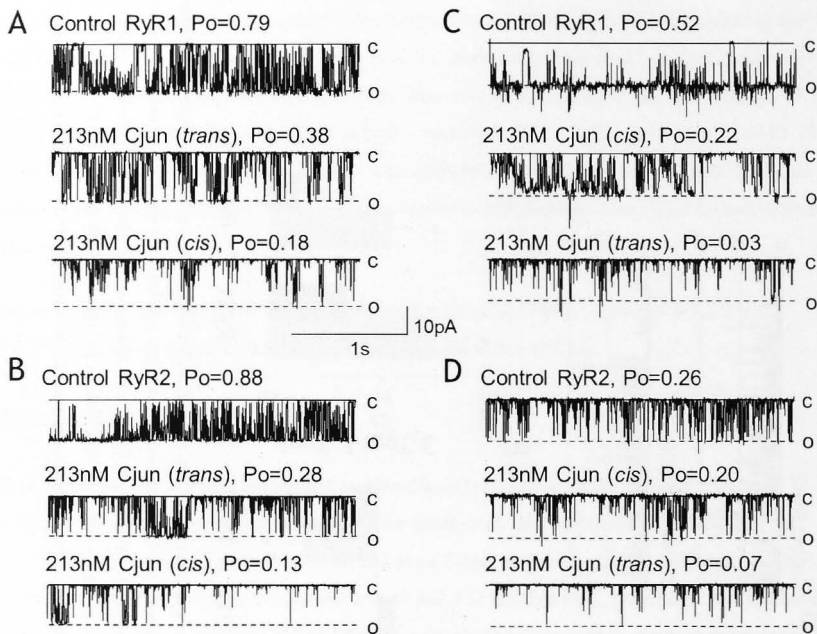


Figure 4-6 Sequential addition of Cjun to the cytoplasmic and luminal solution induces a two-step inhibition of purified RyRs at resting 1 mM $[Ca^{2+}]_i$. (A)-(D) Representative traces of 3 s records illustrating the additive effects of Cjun (213 nM) added to the *trans* and *cis* chamber on RyR channel activity ($n=3$ for RyR1 and $n=6$ for RyR2). Current recordings were obtained at -40 mV. Channel openings are downward from zero current (continuous line, c) to maximum open conductance (broken line, o). The top record in each panel shows control purified RyR activity, the middle record was obtained after first adding 213 nM Cjun to either *trans* (A&B) or *cis* (C&D) solution, and the bottom record after second addition of 213 nM Cjun cytoplasmically (A&B) or lumenally (C&D). The P_o value measured for each channel trace is given on top of the current records. Cytoplasmic (*cis*) $[Ca^{2+}]_i$ was 1 μ M under all conditions.

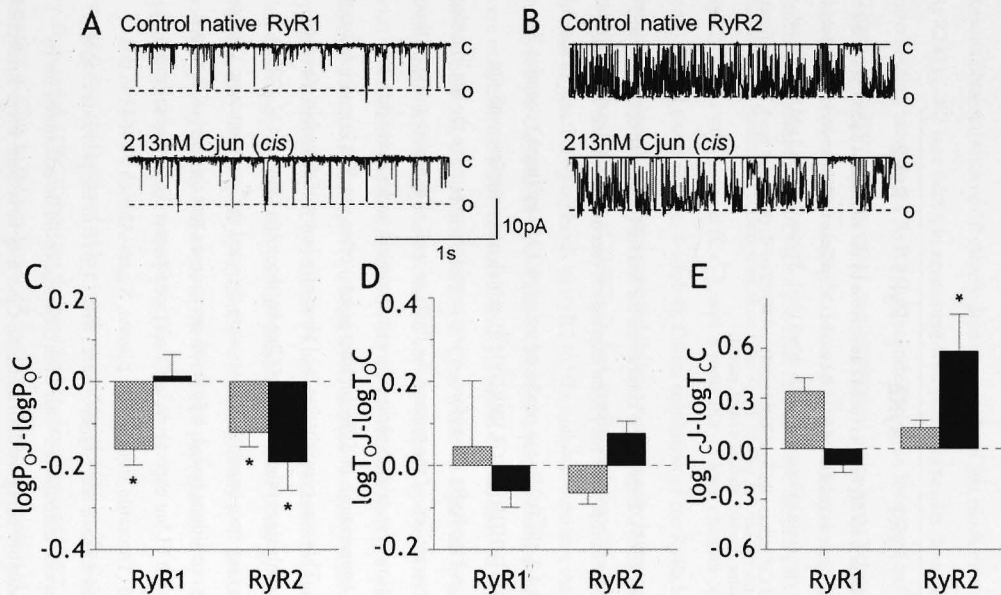


Figure 4-7 Addition of 213 nM Cjun (cis) to native RyRs containing endogenous junctin causes different effect on RyR1 and RyR2 channel activity. (A)-(B) Records of 3 s of single channel activity at -40 mV. Single channel opening is downward from zero current (continuous line, c) to maximum open conductance (broken line, o). The upper trace in each panel shows control activity and the lower trace shows activity after adding 213 nM Cjun to the cytoplasmic solution bathing RyR1 (A) or RyR2 (B). (C)-(E) average data for relative open probability ($\log P_{oJ} - \log P_{oC}$, C), mean open time ($\log T_{oJ} - \log T_{oC}$, D) and mean closed time ($\log T_{cJ} - \log T_{cC}$, E), determined for individual channel for RyR1 (n=6) and RyR2 (n=7-8). No significant differences in native RyR1 activity found with Cjun before and after protein addition ($P > 0.05$ Student *t*-test, paired), whereas a small reduction in RyR2 channel activity was observed upon Cjun addition ($P < 0.05$, Student's *t*-test, paired). Cjun (cytoplasmic addition) to purified RyRs data from Fig. 4-5 are included for comparison (cross-hatched bins).

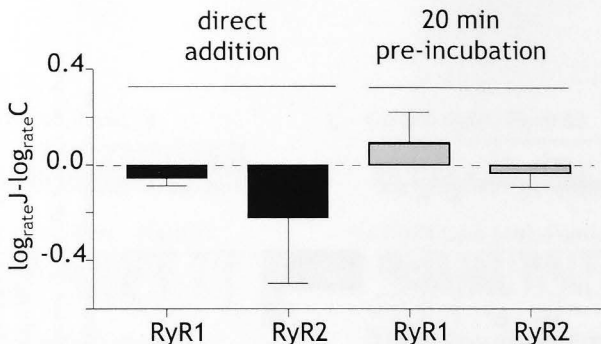


Figure 4-8 The rate of Ca^{2+} release from SR vesicles remain unaffected by the addition of $5 \mu\text{M}$ Cjun to the extravesicular solution. Adding Cjun produced no effect in the rate of Ca^{2+} release from either skeletal ($n=4$) or cardiac ($n=3$) SR through RyRs containing endogenous junctin (black bins). Preincubation in $5 \mu\text{M}$ Cjun did not alter the rate of caffeine induced Ca^{2+} release through RyR1 ($n=4$) and RyR2 ($n=3$) (light grey bins). No significant difference found from control value ($P>0.05$ Student's *t*-test, paired).

detail, see Methods, section 2.5.3). Expression conditions for 6xHis-Cjun were optimized at 37°C for 4 h, which was similar to that used for FLjun expression (section 2.5.2 and 3.3.2.2).

As mentioned in section 3.4.2, the 6xHis-tag produced using pET15b.ep (mod.) contains 24 amino acids ($^1\text{RRYTMGSSHHHHHHSSGLVPRGSH}^{24}$), which may interfere with the interaction between Cjun and the RyRs. Therefore, it was necessary to remove the tag in order to exclude any potential interactions of the tag and the RyRs as well as to ensure the specificity of Cjun-RyR interaction. However, trial experiments with thrombin under many different conditions (e.g., different temperatures at different time points) often resulted in multiple bands monitored by SDS-PAGE. This was possibly due to: 1) low efficiency of thrombin cleavage used here; 2) potential proteolysis at other site(s) of Cjun by thrombin (Jenny et al., 2003), although no thrombin cleavage sites currently known were detected in Cjun sequence; 3) protein self-degradation under the conditions tested. It is worth mentioning that this part of the work was done before recombinant FLjun expression in *E.coli* (see Chapter 3), thrombin from different sources was used (Thrombin from bovine plasma, Sigma-Aldrich #T4648 in this chapter and Thrombin CleanCleave Kit, Sigma-Aldrich #RECOMT in the previous chapter). Therefore, the low success rate encountered with Cjun cleavage could be accounted for by lower grade (less pure) thrombin being used. In addition, Cjun may have been more susceptible to degradation in normal MOPS buffer than FLjun in a buffer containing detergent and glycerol. Multiple bands also occurred in control experiments incubating Cjun alone under the same conditions as Cjun/Thrombin. In order to combat these problems, an in-house pHUE vector was employed (Methods, section 2.5.4, also see (Baker et al., 2005; Catanzariti et al., 2004b)). This expression system is fairly robust and has been shown to be effective and applicable to a wide

range of protein expression (Catanzariti et al., 2004b). Cjun protein (without His-tag residues) of over 95% purity was achieved using this method (Fig. 4-1C&D). This once again proves the effectiveness and efficiency of the pHUE-based *E.coli* expression system.

4.4.2 Cjun in the luminal solution is a potent inhibitor of purified RyR1 and RyR2 channels

Results obtained with co-IP clearly demonstrate that Cjun binds directly to purified cardiac RyR2 (Fig. 4-2 lane 6&8), in agreement with previous results from other assays showing the *in vitro* binding between the RyR2 and recombinant Cjun fused to a 6xHis tag and a GST tag (Zhang et al., 1997). As expected, similar physical interactions between Cjun and purified skeletal RyR1 were detected (Fig. 4-2 lane 5&7). Lipid bilayer experiments revealed the functional consequences of such a physical link between the proteins. For the first time, Cjun added to the luminal solution was shown to elicit strong inhibition on both purified RyR1 and RyR2 using 1 mM luminal $[Ca^{2+}]$, with a reduction in long channel openings and encouraging long channel closures (Fig. 4-3&4-4). Direct regulation of the RyRs by luminal Cjun was not unexpected since it has been suggested that junctin primarily interacts with the RyRs via the luminal domain (Zhang et al., 1997). In fact, the findings that Cjun, but not the N-terminal domain of junctin (Njun) binds to RyR2 led the authors to believe that junctin must interact with the RyR from the luminal side of the SR in intact muscle (Zhang et al., 1997). Overall, if this were true, then the effect of junctin on RyR would depend only on luminal interactions between the two proteins, i.e. luminal addition of Cjun would be expected to activate RyRs as FLjun does. However, the suppressed channel activity induced by Cjun was in complete contrast to what we expected and also contrasts with the general concepts. Despite the failure to detect the physical association between Njun and RyR2 in a previous report (Zhang et al., 1997), the opposite actions exhibited by luminal FLjun and Cjun presented in the previous chapter and this chapter strongly indicate that junctin N-terminus residing in the cytoplasm, or transmembrane residues, may interact with cytoplasmic or transmembrane RyR domains. These interactions potentially play an important role in the overall FLjun regulation of the RyRs. In fact, Njun does appear to have an effect on the RyRs (see Chapter 5).

Few previous studies have addressed the specific role of Cjun. To date, in addition to the study by Zhang et al. (1997), showing the binding between Cjun and RyR2 as mentioned above, the targeting of Cjun to the junctional SR has been examined (Rossi et al., 2013). Expression of deletion mutants of junctin in primary myoblast demonstrated that Cjun alone is targeted to the junctional SR membrane, though a correct link between Cjun and the RyR, CSQ or triadin remains questionable (Rossi et al., 2013). There have been no investigations of the functional consequence of such targeting. However, it would be intriguing to see if Cjun could impose a similar inhibitory effect on the RyRs or Ca^{2+} release *in vivo* in transgenic mice or *in vitro* in

myotubes or cardiomyocytes, where colocalization of Cjun and RyR as well as CSQ or triadin could be determined. However, due to time and technical constraints, this work could not be performed.

4.4.3 The significance of cytoplasmic interaction of Cjun and the RyRs

Whether the inhibition of purified RyR1 and RyR2 observed with cytoplasmic Cjun has any physiological significance remains questionable (Fig. 4-5 black bins). Experiments with sequential addition of Cjun to *cis* and *trans* solutions indicate *cis* Cjun alters channel activity by acting on a cytoplasmic site of the RyR (Fig. 4-6). Nevertheless, trypsin digestion of SR vesicles indicates that the C-terminal domain of junctin is largely located inside the SR (Jones et al., 1995). That Cjun has a similar inhibitory effect on native RyR2s containing endogenous junctin suggests the cytoplasmic binding site for Cjun is not occupied by endogenous junctin and thus may not be physiological. Curiously, Cjun caused no changes in the rate of Ca^{2+} release from SR vesicles containing RyR2. Also curiously, addition of cytoplasmic Cjun did not alter native RyR1 activity or Ca^{2+} release from RyR1-containing vesicles. These results are inconsistent with the isoform independent actions of all other junctin constructs on RyR, also raising the question of the specificity of the cytoplasmic Cjun-RyR interaction. The likely non-specificity of this interaction is further supported by the observation that the junctin KEKE motif peptide failed to replicate the action on the cytoplasmic domain of the purified RyRs, whereas the same peptide reproduced the inhibitory effect on channel activity seen when Cjun was added luminally (Chapter 6). FLjun also had an effect on the luminal side but no effect on the cytoplasmic side of purified RyRs (Chapter 3). Consequently, it seems doubtful that a cytoplasmic Cjun-RyR interaction occurs physiologically. That said, it is not impossible that the C-terminal part of junctin would be exposed to the cytoplasm during targeting to junctional SR or during development and that under these circumstances the activity of the RyR is influenced by the interaction.

4.4.4 Conclusion

The results presented in this chapter provide novel information on the regulation of the RyR1 and RyR2 by the luminal, C-terminal domain of junctin, Cjun. For the first time, it has been demonstrated that Cjun plays an inhibitory role in regulating RyR channel activity, which is in marked contrast to the activating role of FLjun. Potential regulation of the RyR by the N-terminal or transmembrane domain of junctin may underlie the difference between FLjun and Cjun effects. Therefore, in the next chapter, a study of the interaction between Njun and purified RyR1 and RyR2 is described.

Chapter 5 The N-terminal domain of junctin modulates RyR1 and RyR2 activity

5.1 Introduction

In Chapter 3, FLjun was established as a RyR channel activator; while in chapter 4, contrary to expectations, Cjun was shown to be a potent channel inhibitor. The activating effect of FLjun and the inhibiting effect of Cjun raise the question of whether the short N-terminal tail of junctin (Njun) might have a functional role even though a previous study failed to show a physical interaction between Njun and RyR2 (Zhang et al., 1997). This possibility is supported by the observation that the cytoplasmic domain of skeletal triadin, which is structurally similar to junctin, can bind to the cytoplasmic domain of RyR1 and inhibit the channel (Groh et al., 1999; Ohkura et al., 1998). However, there have been no reports addressing the effects of cytoplasmic regulation of the RyR by N-terminal junctin. Therefore, the direct effects of Njun on RyR1 and RyR2 were investigated.

Aim:

The aim of the experiments detailed in this chapter was to determine: 1) the physical interactions between Njun and the RyRs; 2) the influence of Njun alone on purified RyR activity; and 3) the contribution of cytoplasmic junctin-RyR interaction to RyR regulation in conjunction with the luminal interaction.

5.2 Materials and Methods

5.2.1 Methods overview

Affinity chromatography was employed to evaluate the direct binding between Njun and the RyRs. Single channel recordings in lipid bilayers were used to explore the functional regulation of both purified RyR isoforms by cytoplasmic Njun, as well as to examine the combined action of Njun and Cjun. Recombinant RyR1 and RyR2 were expressed and purified from HEK293 cells in order to investigate their physical association with Njun (for explanations for using expressed RyRs rather than purified muscle RyRs see section 5.2.3). An Njun peptide, corresponding to the first 22 residues of canine cardiac junctin, was synthesized and tested for its ability to bind and interact with both RyR1 and RyR2. It should be noted that the N-terminal domain of junctin contains 36.4% charged residues (8 of 22) with an overall positive charge (a calculated pI of 9.7) (Table 5-1, row 1; also see (Jones et al., 1995)). Therefore it was possible the Njun peptide may interact in a non-specific manner with the RyRs which have excess negative charge (Takeshima et al., 1989). To explore this possibility, several control

experiments were conducted (section 5.3.4) to evaluate the specificity of Njun's physical binding with and functional effect on the RyRs. Further, lipid bilayer experiments were performed with native RyRs in conjunction with a Ca^{2+} release spectrophotometric assay with the aim of assessing the physiological relevance of the cytoplasmic Njun-RyR interaction examined in this study.

Table 5-1 Peptides used in this study

Name	Description	Sequence
Njun	Junctin N-terminus	¹ MAEETKHGGHKNGRKGGLSGSS ²²
Njun _{scrambled}	A scrambled Njun peptide used as a negative control	STGENKKGHGLSGKHKSEGRAMG

Blue and red indicate negatively and positively charged residues respectively.

5.2.2 RyR preparation

RyR1 and RyR2 used for affinity chromatography described in section 5.3.1 were expressed and purified from HEK293 cells as detailed in section 2.4. Recombinant RyR expression in HEK293 cells was achieved either using calcium phosphate precipitation (for RyR1) or tetracycline induction (for RyR2). After harvesting, the cell pellets were homogenized in sucrose-imidazole buffer. RyR expression was verified by subjecting the cell homogenate to SDS-PAGE followed by immunoblot. The presence of RyR1 and RyR2 (the protein band above 250 kDa, Fig. 5-1 lane 2 and lane 4 respectively) as detected by anti-RyR 34C antibody confirmed that the expressed proteins were RyR1 and RyR2.

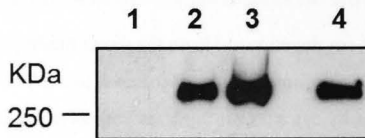


Figure 5-1 Expression of recombinant RyR1 and RyR2. Film exposed to a immunoblot membrane probed for RyR1 and RyR2 is shown. The membrane has been probed with anti-RyR1 34C antibody to confirm expression of RyR1 and RyR2. Immuno-detected proteins at > 250 kDa indicate the presence of RyRs. Lane 1 was loaded with vesicles from native HEK293 cells without transfection as a negative control. Lane 2 was loaded with vesicles from HEK293 cells after recombinant RyR1 DNA transfection and expression. Lane 3 was loaded with RyR-enriched SR vesicles isolated from rabbit skeletal muscle as a positive control. Lane 4 was loaded with vesicles from stable, inducible HEK293 cell lines after recombinant RyR2 expression induction. Protein markers are shown to the left of the blot.

For single channel experiments, the RyRs were obtained as described in section 2.3: skeletal and cardiac SR vesicles were obtained from rabbit skeletal muscle and sheep heart respectively as described in section 2.3.1; RyR1 and RyR2 were solubilized and purified from SR as detailed in section 2.3.2.

5.2.3 Affinity chromatography between Njun peptide and RyR1 and RyR2

To determine the direct binding of the Njun peptide to recombinant RyR1 or RyR2, NeutrAvidin agarose affinity chromatography was performed as described in section 2.8.2. RyRs purified from muscle were also tested for their binding to Njun, but they seemed to intrinsically bind to the agarose beads, with pre-clearing unable to resolve this problem (data not shown). This was likely due to the purification procedure leading to the exposure of residues which are normally buried in the RyR and which may contain binding sites for the agarose. Therefore, solely recombinant RyR1s and RyR2s were used for this experiment. Pre-cleared recombinant RyR1 or RyR2 was incubated with NeutrAvidin agarose-bound Njun peptide. After washing away unbound RyR, the NeutrAvidin agarose attachments were eluted, subjected to SDS-PAGE and probed for the presence of Njun and RyR using StrepTactin-HRP conjugate and anti-RyR 34C antibodies respectively. The protein bands were visualized as described in section 2.6.4.3 and density was quantified using the Quantity One as described in section 2.6.5.

5.2.4 Single channel recording and analysis

Lipid bilayer experiments were carried out and analyzed as described in section 2.9. Skeletal or cardiac SR vesicles, purified RyR1 or RyR2 preparations were used and the junctin peptide (Njun or Njun_{scrambled}) was added to RyRs reconstituted in artificial lipid bilayers.

5.2.5 Ca²⁺ release from skeletal and cardiac SR vesicles

5.2.5.1 Njun induced Ca²⁺ release from SR vesicles

Njun-induced Ca²⁺ release from SR vesicles were examined as described in section 2.10.1. In brief, following loading the SR vesicles with Ca²⁺ and thapsigargin addition to block SERCA (Hanna et al., 2011; Jalilian et al., 2008), 5 μM (for consistency with experiments in Chapter 4, section 4.2.6.1) Njun peptide was added 30 s after thapsigargin to determine whether it would induce Ca²⁺ release. In control experiments, MilliQ-water was added and the rate of Ca²⁺ release after addition of Njun in MilliQ-water was compared with the rate with MilliQ-water alone. The rate of Ca²⁺ release was calculated as described in section 2.10.3.

5.2.5.2 Pre-incubation of SR vesicles with Njun

Ca²⁺ release from SR vesicles pre-incubated with Njun was assessed as detailed in section 2.10.2. In short, vesicles were exposed to 5 μM Njun for ~20 min before Ca²⁺ loading and then thapsigargin addition. Following thapsigargin, Ca²⁺ release was stimulated by caffeine (0.5 mM and 5 mM for skeletal and cardiac SR vesicles respectively). The rate of caffeine-induced Ca²⁺ release after pre-incubation with Njun was compared to control experiments in which the vesicles were pre-incubated with MilliQ-water.

5.3 Results

5.3.1 Physical interaction between Njun and expressed RyR1 or RyR2

Part of this work was conducted by Miss Umayal Narayanan (Muscle Research Group, John Curtin School of Medical Research, Australian National University, Canberra, Australia) under my supervision.

A substantial amount of RyR1 or RyR2 was bound to Njun, with the presence of the RyR1 or RyR2 seen as a band above 250 kDa (Fig. 5-2A lane 2&5, top bands) and the peptide band seen at ~10 kDa (Fig. 5-2A lane 2&5, bottom bands). A control experiment was performed using biotinylated Njun_{scrambled} peptide coupled NeutrAvidin agarose or the agarose alone (i.e. in the absence of peptides). No detectable RyR1 or RyR2 bound to the NeutrAvidin agarose in the absence of the biotinylated peptides (Fig. 5-2A lane 1&4). Some RyRs were precipitated by Njun_{scrambled} peptide, but to a lesser extent than seen with normal (non-scrambled) Njun (~25% of that precipitated by Njun) (Fig. 5-2A lane 3&6 and Fig. 5-2B). Taken together with the results below showing that the Njun_{scrambled} peptide had no effect on channel activity (see section 5.3.3), it is likely that the scrambled peptide binding was non-specific. Given that neither RyR1 nor RyR2 bind to the NeutrAvidin agarose and there is much less binding to the Njun_{scrambled} peptide, this suggests that Njun is able to associate specifically with the RyRs. As mentioned previously, this was unexpected, as it has been assumed that interactions between RyR and junctin occurred only between the luminal domains of the two proteins, since the study by Zhang et al. (1997) failed to detect an interaction between GST-fused Njun and RyR2.

5.3.2 *Cis* Njun activates purified RyR1 and RyR2 activity

The functional consequences of a direct interaction between Njun and purified RyR1 and RyR2 were examined with single channel recording, using standard *cis* and *trans* solutions with 1 μM Ca²⁺ in the *cis* chamber and 1 mM Ca²⁺ in the *trans* chamber (for methods and solution composition see section 2.9.2-2.9.4). 213 nM Njun was added to the cytoplasmic (*cis*) solution following channel fusion with the bilayer and several minutes of recording of control channel activity.

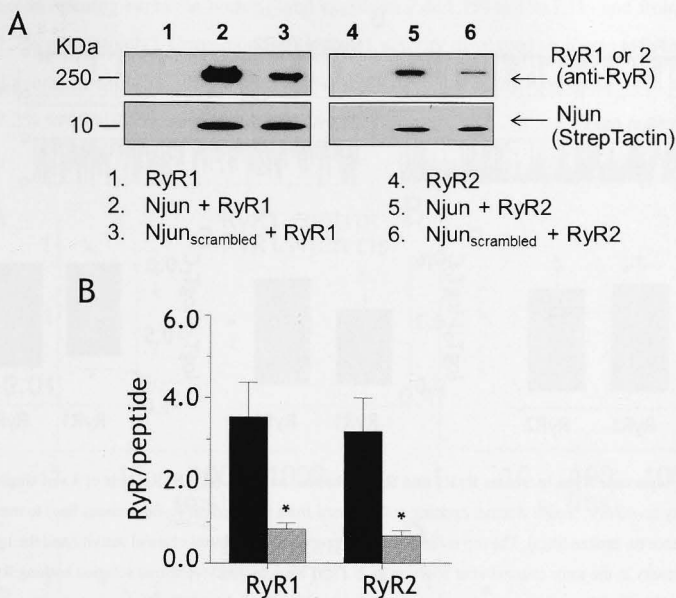


Figure 5-2 Binding of the junctin N-terminal tail (Njun) peptide to RyR1 and RyR2. (A) Immunoblot showing the association of recombinant RyR1 and RyR2 with the biotinylated Njun peptide coupled to NeutrAvidin agarose (Lane 2 and 5). The upper half of the membrane was probed with anti-RyR 34C antibody, and the lower half was probed with Streptactin-HRP conjugate to identify the biotin tagged peptides. NeutrAvidin-agarose alone did not bind to either RyR1 (lane 1) or RyR2 (lane 4). The Njun_{scrambled} peptide bound to RyR1 (lane 3) and RyR2 (lane 6), but to a lesser extent than that seen with Njun. Molecular weights to the left of lanes. **(B)** Average of RyR1 or RyR2 band density relative to peptide (Njun, black bins; Njun_{scrambled}, light grey bins) band density. The asterisk (*) indicates average values significantly different from Njun ($P < 0.05$ student's *t*-test, paired, $n=8$ for RyR1 and $n=7$ for RyR2).

Contrary to our expectations, the addition of Njun to the *cis* chamber elicited a dramatic increase in the activity of purified RyR2 and RyR1 channels (Fig. 5-3). The open probability increased 5.0 \pm 1.0-fold in RyR1 and 6.9 \pm 2.4-fold in RyR2 (Fig. 5-3C). Average P_o rose from 0.021 \pm 0.01 to 0.125 \pm 0.06 for RyR1 and from 0.103 \pm 0.03 to 0.263 \pm 0.04 for RyR2. It is notable that the increase in open probability induced by *cis* Njun was significantly greater than the increase produced by FLjun added to the luminal solution (see Chapter 3.3.4.1 and Fig. 3-9C). Interestingly, a time delay was often observed before full Njun activation was established: 2.2 \pm 0.7 min in RyR1 ($n=12$) and 3.4 \pm 1.1 min in RyR2 channels ($n=12$) respectively. This implies the binding site on cytoplasmic domain of RyR for Njun was not easily accessible, although faster activation did occur in some experiments (6 out of 24). Overall, the results show that Njun is a potent activator of both RyR1 and RyR2.

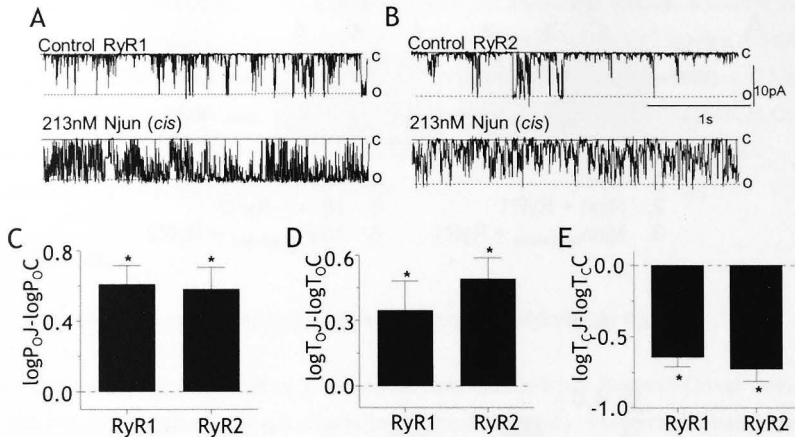


Figure 5-3 Cytoplasmic Njun increases RyR1 and RyR2 channel activity. (A)-(B) Records of 3 s of single channel activity at -40 mV. Single channel opening is downward from zero current (c, continuous line) to maximum open conductance (o, broken lines). The top recording in each panel shows control channel activity and the lower trace shows activity in the same channel after addition of 213 nM Njun to the cytoplasmic solution bathing RyR1 (A) and RyR2 (B). (C)-(E) Average data for relative open probability ($\log P_{oJ} - \log P_{oC}$, C), mean open time ($\log T_{oJ} - \log T_{oC}$, D), and mean closed time ($\log T_{cJ} - \log T_{cC}$, E) for RyR1 and RyR2. Data were pooled at both potentials before and after the addition of Njun. The asterisk (*) indicates average values significantly different from the control ($P < 0.05$ Student's *t*-test, paired, $n = 9$ for RyR1 and $n = 14$ for RyR2).

Further analysis revealed that the changes in RyR channel activity following Njun addition to the cytoplasmic solution was due to corresponding changes in mean open times and mean closed times. These changes followed a similar pattern to that seen after adding FLjun to the luminal solution, but to a greater extent (Fig. 5-3D&E, for comparison, see Chapter 3.3.4.2 and Fig. 3-9D&E). After cytoplasmic Njun association, RyR1 displayed a 3.32 ± 1.27 -fold increase in mean open times and a ~ 4 -fold (to 0.24 ± 0.03) decrease in mean closed times. Similarly, there was a significant increase in mean open times (4.02 ± 0.02 -fold) and reduction in mean closed times (~ 6 -fold, to 0.16 ± 0.53) in RyR2.

The changes in mean open and closed times were due to an alteration of the open and closed time distributions. Three time constants achieved the best exponential fit to both open and closed time distributions in both RyR1 and RyR2 channels (shown in Fig. 5-4A-D and Table 5-2). The open and closed time constant values for RyR1 activity were similar before and after cytoplasmic addition of Njun. The average open time constants in RyR1 channels were $\tau_{01} = 2.1 \pm 0.17$ ms; $\tau_{02} = 17.0 \pm 0.84$ ms; $\tau_{03} = 149.1 \pm 1.93$ ms and average closed time constants $\tau_{c1} = 3.4 \pm 0.20$ ms; $\tau_{c2} = 22.2 \pm 0.87$ ms; $\tau_{c3} = 245.2 \pm 5.67$ ms. After the addition of Njun, the number of opening events in τ_{01} fell from $97 \pm 1.2\%$ to $78 \pm 8.6\%$. In contrast, there was a ~ 10 -fold

increase in opening events in both τ_{O2} and τ_{O3} (from $2.4 \pm 1.1\%$ to $19 \pm 7.1\%$ and from $0.3 \pm 0.15\%$ to $3 \pm 1.7\%$ respectively). Correspondingly, RyR1 activity displayed an increase in the number of closed events in τ_{C1} ($15 \pm 7.0\%$ to $39 \pm 12.4\%$) and a decrease in the long closures in τ_{C3} (from $57 \pm 12.2\%$ to $30 \pm 10.5\%$) (Fig. 5-4A&B).

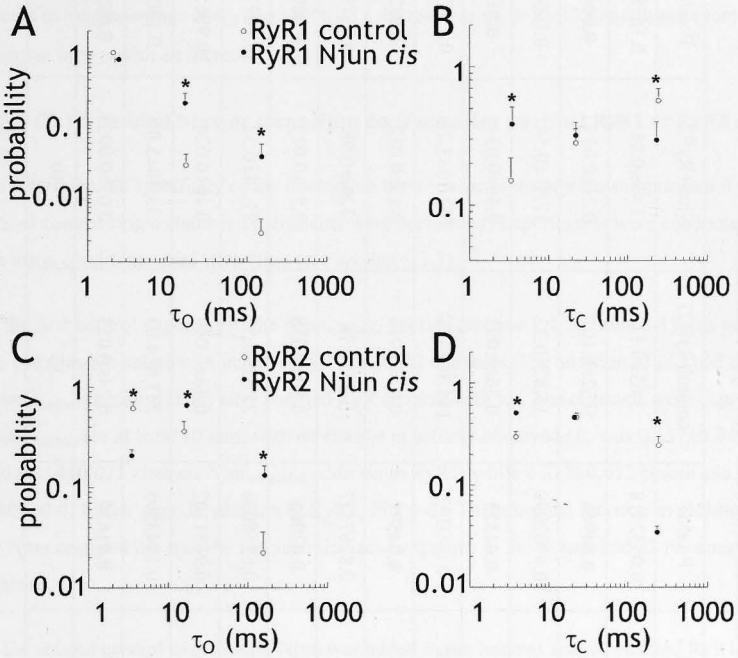


Figure 5-4 Effects of 213 nM Njun (*cis*) on the average open (A&C) and closed (B&D) time constants of purified RyRs. The probability of events falling into each time constant is plotted against the time constant in ms (open time or closed time). Time constants are shown for control data (open circles) and 213 nM Njun (filled circles) for RyR1 (A&B) or RyR2 (C&D). Vertical bars indicate the SEM for event probability. Horizontal bars indicating the SEM for the time constant are contained within the symbols. Asterisks (*) indicate significant differences between control data and with 213 nM Njun ($P < 0.05$ student's *t*-test, paired, $n = 9$ for RyR1 and $n = 10$ for RyR2).

Similar open and closed time constants were determined for RyR2 channels as those for RyR1 (Fig. 5-4C&D; Table 5-2). Again, there were no significant alterations of the time constant values after Njun addition. The average open time constants for RyR2 channels were $\tau_{O1} = 3.6 \pm 0.11$ ms; $\tau_{O2} = 15.8 \pm 0.32$ ms; $\tau_{O3} = 154.3 \pm 3.12$ ms and the average closed time constants were $\tau_{C1} = 3.9 \pm 0.18$ ms; $\tau_{C2} = 22.5 \pm 0.57$ ms; $\tau_{C3} = 243.8 \pm 4.03$ ms. The fraction of events falling into the long open time constants increased significantly in RyR2 (from $36 \pm 9.2\%$ to $66 \pm 3.3\%$ for τ_{O2} and from $2.2 \pm 1.4\%$ to $13 \pm 3.2\%$ for τ_{O3}) (Fig. 5-4C) after adding Njun. Conversely, events occurring within the shortest open time constant were reduced significantly (~3-fold

Table 5-2 A summary of the open and closed time constants before and after Njun reassociation

	control(RyR1)	Njun+RyR1	P value	control(RyR2)	Njun+RyR2	P value
τ_{O1}	2.08±0.17	2.44±0.25	0.0532418	3.63±0.11	3.49±0.08	0.167851
P1	0.97±0.012	0.78±0.086	0.04946	0.62±0.101	0.21±0.031	0.0045
τ_{O2}	17.04±0.84	16.63±0.58	0.4702099	15.82±0.32	17.01±0.54	0.10666
P2	0.02±0.011	0.19±0.071	0.04323	0.36±0.092	0.66±0.033	0.016
τ_{O3}	149.10±1.93	152.11±1.59	0.090252	154.30±3.12	162.10±3.28	0.118738
P3	0.003±0.0015	0.03±0.017	0.04597	0.02±0.014	0.13±0.032	0.0128
τ_{C1}	3.37±0.20	3.48±0.15	0.8267577	3.85±0.18	3.86±0.08	0.957996
P1	0.15±0.070	0.39±0.124	0.02066	0.30±0.038	0.51±0.025	0.0005
τ_{C2}	22.20±0.87	22.19±0.68	0.6558036	22.53±0.57	21.14±0.32	0.107736
P2	0.28±0.076	0.32±0.076	0.9151102	0.46±0.049	0.46±0.024	0.986526
τ_{C3}	245.20±5.67	232.56±6.97	0.1848895	243.8±4.03	233.30±5.05	0.10018
P3	0.57±0.122	0.30±0.105	0.01639	0.24±0.053	0.03±0.005	0.0031
n	9	9		10	10	

P1, P2 and P3 denote probability. P value <0.05 are in bold, denoting significant difference from control value.

reduction, from $62 \pm 10.1\%$ to $21 \pm 3.1\%$). The changes in the dwell times in the closed state after Njun addition were again similar to those seen in RyR1, with RyR2 activity also showing an increase in the number of events falling into τ_{C1} (from $30 \pm 3.8\%$ to $51 \pm 2.5\%$) and a decrease in τ_{C3} (from $24 \pm 5.3\%$ to $3 \pm 0.5\%$) (Fig. 5-4D). Altogether, Njun addition to the cytoplasmic solution did not alter the time constants but led to a dramatic re-distribution of events with more events in long openings in τ_{O2} and τ_{O3} (with a decrease in τ_{O1} in RyR2), and fewer events in long closures in τ_{C3} (with an increase in τ_{C1}).

5.3.3 *Cis* scrambled Njun or *trans* Njun does not alter purified RyR1 or RyR2 activity

To determine the specificity of the interaction between the Njun peptide and purified RyRs, two sets of control single channel experiments were performed. Experiments were conducted under the same conditions used with Njun (see section 5.3.3).

In the first control experiment, the Njun_{scrambled} peptide (section 2.1.2; Table 5-1) was added to the cytoplasmic solution of purified RyR1 or RyR2 channels. The addition of 213 nM *cis* Njun_{scrambled} peptide did not alter purified RyR channel activity. The channels were exposed to Njun_{scrambled} for at least 10 min, with no change in activity observed (P_o was 0.137 ± 0.043 before and 0.114 ± 0.031 after *cis* Njun_{scrambled} addition in RyR1, while 0.317 ± 0.012 before and 0.306 ± 0.011 after peptide addition in RyR2; Fig. 5-5). Therefore the increase in channel activity by Njun required the specific native amino acid sequence in the N-terminal 22 residues of junctin.

In the second control experiment, Njun was added to the luminal side of purified RyR1 or RyR2. This also tested whether the activation of RyRs by FLjun (Chapter 3.3.4) was due to a luminal action of the N-terminal domain of the full-length protein. Addition of 213 nM *trans* Njun had no effect on channel open probability of either RyR1 or RyR2 (P_o from 0.233 ± 0.038 ; to 0.246 ± 0.049 in RyR1 and from 0.073 ± 0.029 to 0.076 ± 0.032 in RyR2; Fig. 5-6C). This was reflected by a lack of changes in channel T_o and T_c (Fig. 5-6D&E). The results demonstrate that Njun regulates the RyR only from the cytoplasmic side.

Taken together, these data strongly suggest that the effects of Njun peptide on purified RyR1 and RyR2 are specific and only occur cytoplasmically.

5.3.4 No effect of Njun on native RyR1 or RyR2

As endogenous junctin is presumably absent in purified RyRs, it is important to determine whether the Njun interaction occurs with endogenous junctin and thus likely to have a physiological significance. To investigate this, both lipid bilayer experiments and calcium

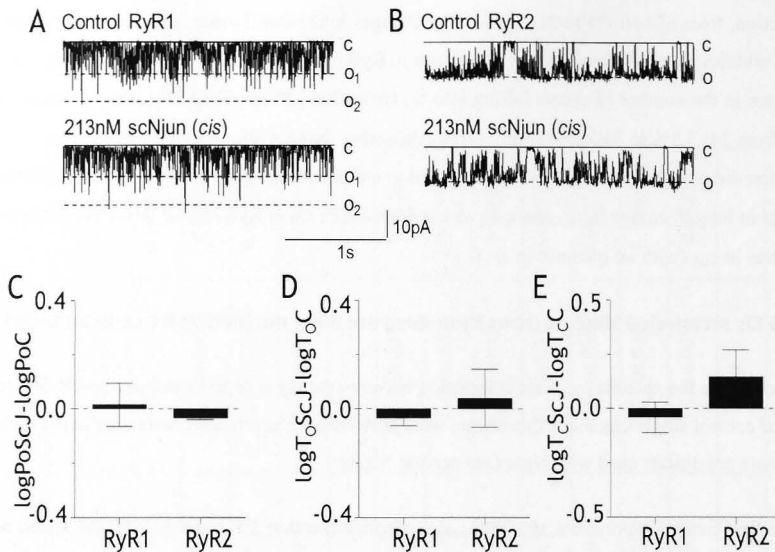


Figure 5-5 Addition of 213 nM scrambled Njun (Njun_{scrambled}) peptide (*cis*) to purified RyRs does not alter channel activity. (A)-(B) Records of 3 s of single channel activity at -40 mV. Single channel opening is downward from zero current (continuous line, c) to maximum open conductance for one channel opening (broken line, o or o₁) or two channels opening simultaneously (o₂). The upper trace in each panel shows control activity and the lower trace shows activity after adding 213 nM Njun_{scrambled} to the cytoplasmic solution bathing RyR1 (A) or RyR2 (B). (C)-(E) average data for relative open probability ($\log P_{oJ} - \log P_{oC}$, C), mean open time ($\log T_{oJ} - \log T_{oC}$, D) and mean closed time ($\log T_{cJ} - \log T_{cC}$, E), determined for individual channel for RyR1 (n=12-16) and RyR2 (n=8). No significant differences found with Njun_{scrambled} before and after peptide addition ($P > 0.05$ Student's *t*-test, paired).

release spectrophotometric assay were carried out using native RyR channels with endogenous junctin still attached. It was expected Njun would not be able to bind or activate the native channels if the site in native RyRs was occupied by the N-terminal domain of endogenous junctin.

5.3.4.1 No effect of cytoplasmic addition of Njun on native RyR1/2 activity

In this set of experiments, single channel recordings were conducted as described in section 2.9.2-2.9.4. Native skeletal or cardiac SR vesicles were incorporated into bilayers with the usual resting (1mM) *trans* [Ca²⁺] and 1 μM *cis* [Ca²⁺]. As with *cis* Njun_{scrambled} and *trans* Njun added to purified RyRs, the addition of 213 nM Njun into the *cis* solution had no significant effect on open probability of either native RyR1 or RyR2 (P_o was 0.066 ± 0.001 before and 0.067 ± 0.011 after *cis* Njun addition in RyR 1, while 0.109 ± 0.021 before and 0.124 ± 0.028 after peptide addition in RyR2; Fig. 5-7A). Likewise, no overall changes in T_o and T_c were observed (Fig. 5-7B&C).

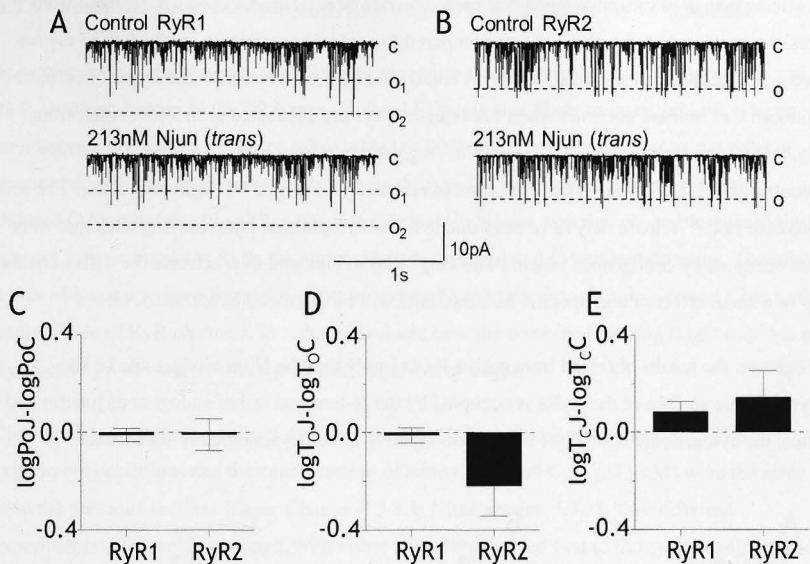


Figure 5-6 Purified RyRs remain unaffected by the addition of 213 nM Njun to the *trans* chamber. (A)-(B) Records of 3 s of single channel activity at -40 mV. Single channel opening is downward from zero current (c, continuous line) to maximum open conductance for one channel opening (broken line, o or o₁) or two channels opening simultaneously (o₂). The upper trace in each panel shows control activity and the lower trace shows activity after adding 213 nM Njun to the luminal side of RyR1 (A) or RyR2 (B). (C)-(E) average data for relative open probability (logP_{oJ}-logP_{oC}, C), mean open time (logT_{oJ}-logT_{oC}, D) and mean closed time (logT_{cJ}-logT_{cC}, E). No significant differences found before and after luminal Njun addition (P>0.05 Student's *t*-test, paired, n=8-14 for RyR1 and n=8-9 for RyR2).

5.3.4.2 Effect of Njun on Ca²⁺ release from SR vesicles

To further examine the effects of Njun on native RyRs channel activity in a more intact setting, its ability to release Ca²⁺ from SR vesicles was determined. The Ca²⁺ release spectrophotometric assay was performed in two ways as described in section 2.10 and 5.2.5.

In the first, Njun was added to a solution containing RyR1 or RyR2 channels in SR vesicles to see if it would stimulate Ca²⁺ release (section 2.10.1 and 5.2.5.1). In control experiments, MilliQ-water was used. Addition of peptide caused a small increase in the rate of Ca²⁺ release from RyR2-containing vesicles (from 4.76±0.45 in the absence of Njun in control experiment, to 5.10±0.44 nmol Ca²⁺/mg protein/min) (Fig. 5-7D 2nd black bin). There was no significant change in Ca²⁺ release from vesicles containing RyR1 (Fig. 5-7D 1st black bin).

In the second experiment, the vesicles were pre-incubated with Njun for 20 min prior to the experiment to provide sufficient time for any RyR-Njun interaction to be fully established.

Caffeine was used to stimulate Ca^{2+} release. The rate of caffeine-induced Ca^{2+} release from vesicles pre-incubated with Njun was compared to control experiments in which the vesicles were pre-incubated with MilliQ-water. A small but significant increase in the rate of caffeine-induced Ca^{2+} release occurred when SR vesicles were pre-incubated with 5 μM Njun, from 64.4 ± 7.10 (control) to 73.3 ± 8.23 nmol Ca^{2+} /mg protein/min in RyR1, and from 28.3 ± 7.09 (control) to 31.7 ± 7.97 nmol Ca^{2+} /mg protein/min in RyR2 (Fig. 5-7D light grey bins). The small increase in Ca^{2+} release may have been due to a few cytoplasmic Njun binding sites that were not occupied by endogenous junctin, allowing Njun to bind and thus activate the native channels or to a small effect of non-specific binding. This will be discussed in section 5.4.2.

Together, the results obtained from native RyRs imply that the Njun binding site on the cytoplasmic surface of the RyRs is occupied by the N-terminal tail of endogenous junctin and thus, the cytoplasmic Njun-RyR interaction is likely to be physiologically significant.

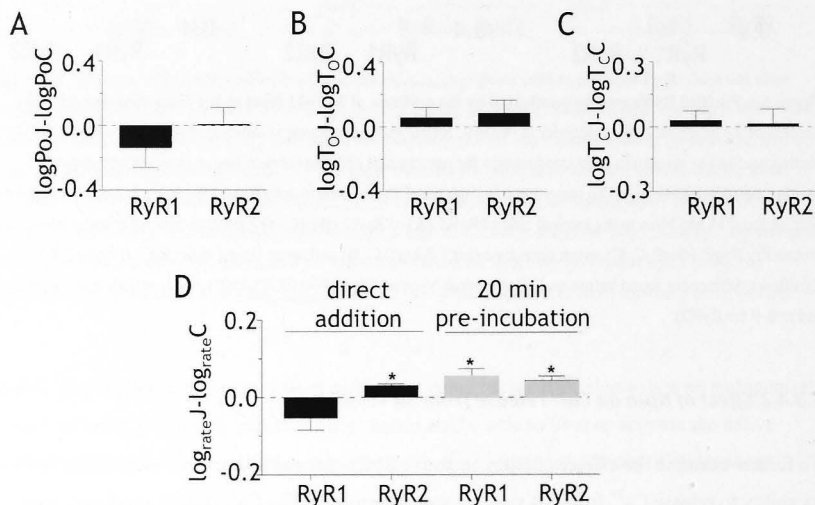


Figure 5-7 Njun has minimal effect on native RyRs containing endogenous junctin. (A)-(C) Addition of 213 nM Njun to the cytoplasmic side of native RyRs. Average data for relative open probability ($\log P_{oJ}$ - $\log P_{oC}$, **A**), mean open ($\log T_{oJ}$ - $\log T_{oC}$, **B**) and closed ($\log T_{cJ}$ - $\log T_{cC}$, **C**) times, for RyR1 (left) and RyR2 (right). No significant difference found before and after cytoplasmic addition of Njun to native RyRs ($P > 0.05$ Student's *t*-test, paired, $n = 12-14$ for RyR1 and $n = 11-13$ for RyR2). (D) The rate of Ca^{2+} release from SR vesicles after adding 5 μM Njun to the extravesicular solution. Addition of Njun produced an immediate small increase in the rate of Ca^{2+} release from cardiac SR through RyR2 ($n = 3$), but not from skeletal SR ($n = 4$) through RyR1 (black bins). Preincubation in 5 μM Njun produced a significant increase in the rate of caffeine induced Ca^{2+} release through RyR1 ($n = 12$) and RyR2 ($n = 7$) (light grey bins). Asterisks (*) indicate the average values significantly different from the control ($P < 0.05$ Student's *t*-test, paired).

5.3.5 Combined effects of Cjun and Njun on purified RyR1 and RyR2 channels

In vivo, junctin is inserted into the SR membrane with its N-terminal tail in the cytoplasm and its C-terminal domain in the SR lumen. Isolated FLjun is also likely to insert into the bilayer membrane in the same orientation when added to the luminal (*trans*) solution, as the short N-terminal domain would be more likely to pass through the bilayer than the bulky, highly charged C-terminal domain. Thus it is possible that, in bilayer experiments and in the cellular context, junctin regulates RyRs through both its N-terminal and C-terminal domains. Therefore it was of interest to investigate the effect of adding Njun to the cytoplasmic side and Cjun to the luminal side of RyR channels, in order to evaluate how the combined binding might impinge on RyR activity and whether this reproduced the effect of FLjun.

Cjun and Njun were reassociated with the reconstituted purified RyR sequentially. The experiment conditions and the concentration of added Njun and Cjun (213 nM) were the same as in the previous sections (Cjun: Chapter 4.3.3.1; Njun: section 5.3.2). Two different experimental protocols were used, with either Njun being added first to the cytoplasmic solution and then Cjun added to the luminal solution, or Cjun being added first to the luminal solution and then Njun added to the cytoplasmic solution. In the first case (Fig. 5-8A&C), after the typical increase in RyR1 and RyR2 activity with cytoplasmic Njun was established (Fig. 5-8A&C, middle traces; and Fig. 5-9A black bins, ~5-fold rise in P_o of RyR1 (from 0.016 ± 0.004 to 0.063 ± 0.03) and RyR2 channels (from 0.05 ± 0.02 to 0.21 ± 0.07)), Cjun was added to luminal side of the Njun-regulated RyRs. The Njun-induced channel activation was attenuated after luminal Cjun addition (Fig. 5-8A&C, bottom traces), with a significant reduction in channel activity by $37 \pm 9.7\%$ and $26 \pm 8.1\%$ in P_o compared with the activity of Njun-activated RyR1s and RyR2s respectively (Fig. 5-9A cross hatched bins; P_o 0.029 ± 0.008 for RyR1, 0.185 ± 0.08 for RyR2). Notably, P_o remained higher than control activity. For comparison, the effect of FLjun alone (data from Fig. 3-9C-E, Chapter 3) is included in Fig. 5-10. As described previously (section 5.3.2), the increase in activity produced by cytoplasmic Njun alone was significantly greater than that when FLjun was added to the luminal solution. Notably, the levels of activity following the subsequent luminal addition of Cjun were not significantly different from those seen with luminal FLjun (Fig. 5-10A&B 3rd black bins and 1st light stippled bins).

Njun and Cjun were then added in the reverse order, i.e. Cjun was added first to the luminal solution and then Njun added to the cytoplasmic solution (Fig. 5-8B&D). There were the usual decreases in the open probability of RyR1 and RyR2 channels ($66 \pm 14.3\%$ and $43 \pm 4.9\%$ decrease respectively; P_o fell from 0.168 ± 0.04 to 0.06 ± 0.04 for RyR1 and from 0.30 ± 0.076 to 0.17 ± 0.04 for RyR2) when Cjun was added first to the luminal solution, which once again confirms that Cjun inhibits RyRs (Fig. 5-8B&D, middle traces; Fig. 5-9B black bins; for comparison, see Chapter 4, Fig. 4-3). Subsequent cytoplasmic addition of Njun caused a ~2 fold

increase in the open probability (Fig. 5-8, bottom traces; Fig. 5-9B, cross-hatched bins; P_o 0.093±0.065 for RyR1, 0.29±0.069 for RyR2). However, the activity remained lower than control and was thus in marked contrast to the activation when cytoplasmic Njun was added alone (compare with Fig. 5-3). The channel activity when Cjun was added to the luminal solution, followed by Njun to the cytoplasmic solution was close to initial control level in RyR2 and ~50% of control level in RyR1, and this is also very different from the activation seen when FLjun was added luminally (Fig. 5-10A&B last grey stippled bins comparing to 1st light stippled bins). It appears that when Cjun is associated first with the luminal domain of RyR, the ability of Njun to activate the channel is abolished.

The effects of these additions on channel gating properties, T_o and T_c , were also examined. A decrease in T_c after addition of Njun (Fig. 5-11C&D 2nd black bins) was consistent with the results presented in section 5.3.2 (Fig. 5-3E). Upon Cjun reassociation with the RyR/Njun complex, T_c was significantly increased in RyR1 causing the suppression of channel activity and was not altered in RyR2 (Fig. 5-11C&D 3rd black bins). Despite the prolongation in T_c , the mean closed time remained significantly shorter (40±12.7% and 62±5.0% less) than the purified RyR1 and RyR2 control respectively (Fig. 5-11C&D 3rd black bins). This indicates that channel closures with the Njun-RyR-Cjun combination are shorter than closures of purified RyRs alone (control). It is notable that the levels of T_c were then not significantly different from those seen with luminal FLjun (Fig. 5-11C&D 1st light stippled bins). There was no significant change in T_o in this set of experiments, although there was a trend towards higher T_o values (Fig. 5-11A&B black bins). Therefore, the changes in relative open probability with FLjun or with Njun (*cis*) followed by Cjun (*trans*) were mainly due to significant changes in T_c in both RyR1 and RyR2 channels.

By contrast, in the second experiment where Cjun was added first to the luminal solution and then Njun added to the cytoplasmic solution, T_o decreased by 45±12.1% in RyR1 and 46±18.9% in RyR2 with the luminal addition of Cjun, then increased after the cytoplasmic addition of Njun, but only to control levels (Fig. 5-11A&B last two grey stippled bins). In addition, luminal Cjun evoked a marked increase in average T_c (~8-fold in RyR2, ~12-fold in RyR1). Subsequent addition of Njun reduced T_c to control levels in RyR2 but had no effect on RyR1 (Fig. 5-11C&D last two grey stippled bins). These changes in T_o and T_c with Cjun (*trans*) followed by Njun (*cis*) were again very different from the changes induced by luminal FLjun (Fig. 5-11A-D 1st light stippled bins).

To summarize, the results indicate that the increase in RyR channel activity seen when FLjun is added to the luminal solution may depend on the cytoplasmic tail binding to the RyR first and then the luminal domains of the proteins interacting.

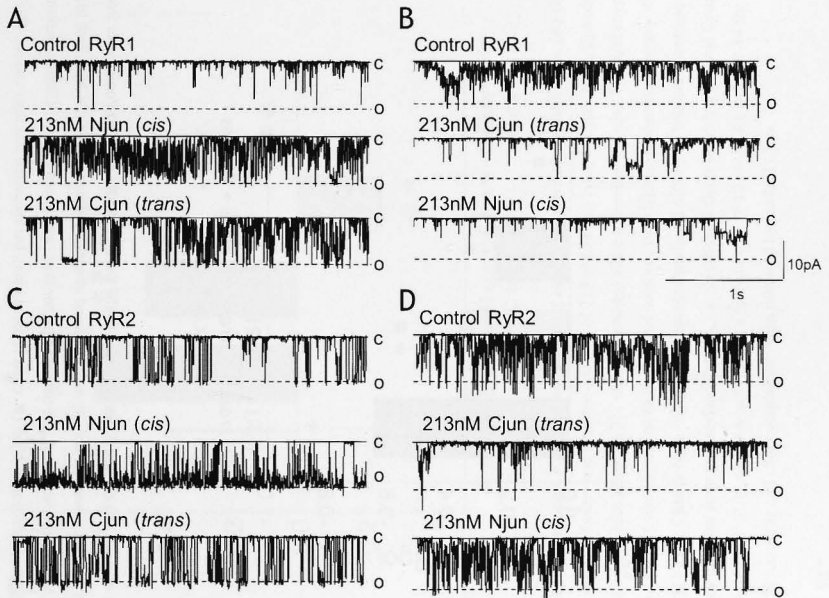


Figure 5-8 Sequential addition of Njun to the cytoplasmic solution and Cjun to the luminal solution of purified RyRs at 1 mM *trans* Ca²⁺. (A)-(D) Records of 3 s of single channel activity at -40 mV showing the sequential addition of either Njun *cis* 1st, Cjun *trans* 2nd (A&C) or Cjun *trans* 1st and then Njun *cis* to purified RyR1 (A&B) or RyR2 (C&D). Single channel opening is downward from zero current (continuous line, c) to maximum open conductance (broken line, o). The top traces show purified RyR control activity at 1 mM *trans* Ca²⁺; the middle traces show activity after adding 213 nM of either Njun to *cis* chamber (A&C) or Cjun to *trans* chamber (B&D); and the bottom traces show activity after addition of either 213 nM Cjun luminally (A&C) or 213 nM Njun cytoplasmically (B&D). Two types of regulation of the RyR are demonstrated in the two sets of experiments: 1) adding 213 nM Njun first to the cytoplasmic solution induced a dramatic increase in channel activity, which was attenuated by the following luminal Cjun addition, but remained higher than control (A&C); 2) luminal addition of 213 nM Cjun inhibited channel activity, the following addition of Njun cytoplasmically increased channel activity, but remained less than control (B&D).

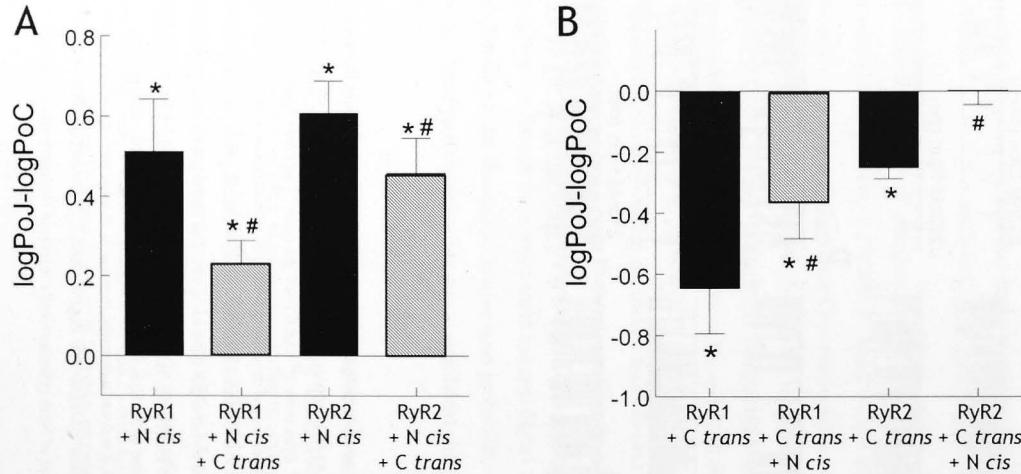


Figure 5-9 Summarised data of relative open probability for the effect of sequential addition of Njun (N) *cis* and Cjun (C) *trans* to the purified RyRs. (A)-(B) Pooled data from +40 mV and -40 mV for relative open probability ($\log P_{o,J} - \log P_{o,C}$) for experiments as illustrated in Fig. 5-8. Channels activity was increased after the addition of 213 nM Njun first to the cytoplasmic solution (**A**, black bins), and was attenuated by the following luminal Cjun addition (**A**, cross hatched bins), but remained higher than control activity. (**B**) Channel activity was decreased with the luminal addition of 213 nM Cjun (**B**, black bins), then increased after the cytoplasmic addition of Njun (**B**, cross hatched bins), but remained less than control. (*): significant differences between control and with 213 nM Njun or Cjun. (#): data value significantly different from the previous channel activity ($P < 0.05$, Student's paired *t*-test, $n = 10$ for RyR1 and $n = 8-10$ for RyR2).

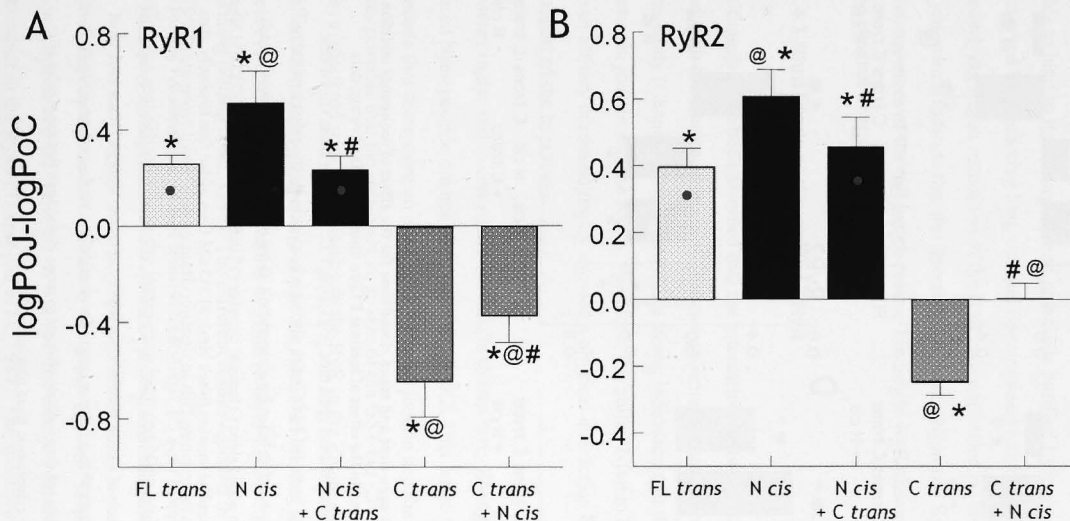


Figure 5- 10 Channel activity of purified RyRs after sequential addition of Njun (N) to the *cis* chamber, then Cjun (C) *trans*, reflects activity seen with luminal FLjun. (A)-(B) Average data for relative open probability ($\log P_{oJ} - \log P_{oC}$) for pooled data from both +40 mV and -40 mV, before and after the addition of 213 nM FLjun, Njun or Cjun (Njun, Cjun data are from Fig. 5-9, FLjun data are from Fig. 3-9 and included for comparison). Three experiments are shown in each panel: 1) 213 nM FLjun added alone to luminal chamber (1st light stippled bins); 2) 213 nM Njun added first to the cytoplasmic solution, then Cjun luminally (black bins); 3) 213 nM Cjun added first to the luminal solution, then Njun cytoplasmically (grey stippled bins). The asterisk (*) indicates significant differences between control parameters and with 213 nM FLjun, Cjun or Njun. The at (@) denotes significant difference between parameters with luminal FLjun and cytoplasmic Njun or luminal Cjun. The hash (#) indicates data value significantly different from the previous data set, i.e. significant effects of adding luminal Cjun with cytoplasmic Njun (3rd black bin), or of adding cytoplasmic Njun with luminal Cjun (5th grey stippled bin) ($P < 0.05$ ANOVA and Student's paired *t*-test, $n = 10$ for RyR1 and $n = 8-14$ for RyR2). The red dots indicate changes in open probability that are similar after luminal addition of FLjun alone and after cytoplasmic Njun followed by luminal Cjun.

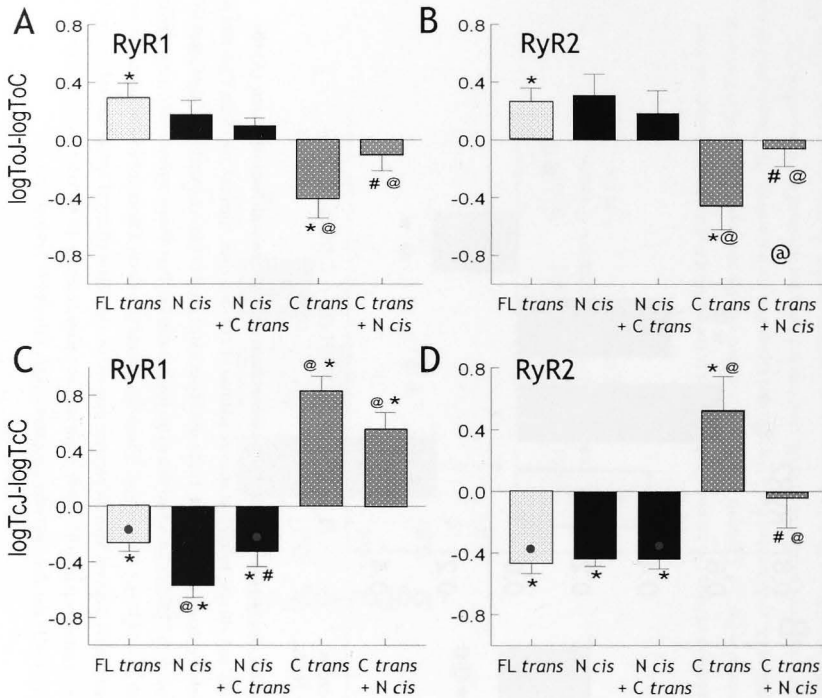


Figure 5-11 Summary of relative mean open time and mean closed time for the effect of sequential addition of Njun (N) cis and Cjun (C) trans, compared to the effect of luminal FLjun alone. (A)–(D) Average data (combined data for +40 and –40mV) for relative mean open time ($\log T_{oJ} - \log T_{oC}$, **A&B**), or mean closed time ($\log T_{cJ} - \log T_{cC}$, **C&D**) before and after the addition of 213 nM FLjun, Njun or Cjun to purified RyR1 (**A&C**) or RyR2 (**B&D**) (FLjun data are from Fig. 3-9 and included for comparison). Three experiments are shown in each panel, from left to right: 1) 213 nM FLjun added alone to luminal chamber (1st light stippled bins); 2) 213 nM Njun added cytoplasmically, then Cjun to the luminal solution (black bins); 3) 213 nM Cjun added first luminally, then Njun to the cytoplasmic solution (grey stippled bins). (*): significant differences from control parameters induced by 213 nM FLjun, Cjun or Njun. (@): significant difference between parameters with luminal FLjun and cytoplasmic Njun or luminal Cjun. (#): significant effects of adding luminal Cjun with cytoplasmic Njun (3rd black bin), or of adding cytoplasmic Njun with luminal Cjun (5th light grey stippled bin) ($P < 0.05$ ANOVA and Student's paired *t*-test, $n = 6-9$ for RyR1 and $n = 7-14$ for RyR2). The red dots indicate changes in mean closed time that are similar after luminal addition of FLjun alone and after cytoplasmic Njun plus luminal Cjun.

5.4 Discussion

The results of the physical interaction and functional regulation of the purified RyRs by the N-terminal tail of junctin (Njun) are described in this chapter, for the first time in either skeletal or cardiac muscle. The effects of *cis* Njun in conjunction with *trans* Cjun on RyRs were also explored at resting (1mM) luminal $[Ca^{2+}]$. The novel results clearly demonstrate that Njun is able to bind to RyRs directly and potentiate purified RyR channel activity *in vitro*, the latter is achieved by promoting long channel openings and reducing long channel closures. Mechanisms underlying FLjun regulation of the RyRs were revealed by the combined actions of Njun and Cjun, which indicate that the interaction between Njun and RyR dictates the functional consequences of the full length protein binding to RyR channels, and allows Cjun to modulate the channel *in vivo*.

5.4.1 Njun binds to the purified RyR

Although it has been assumed that the interactions between junctin and the RyRs occurred only between the luminal domains of the two proteins as mentioned in Chapter 4, results obtained in this study (Chapter 3 and 4) provide a strong indication that there are additional interactions between junctin and the RyRs. Therefore, the ability Njun to bind to the RyRs was tested. Data from affinity chromatography showed a physical interaction between Njun and the RyRs, in support of the hypothesis.

Interestingly, and in contrast to the results shown here, Zhang et al. (1997) reported that GST-fused Njun peptide did not bind to cardiac RyR2. This led to the general belief over the last decade that there were no interaction between junctin and the RyR on the cytoplasmic side. It was possible that the relatively large size of the GST tag (26 kDa vs. ~2.2 kDa (Njun)) might have interfered with Njun binding to the RyR in the Zhang study (Zhang et al., 1997). This is different from the small size of the biotin tag (244 Da) used in this study. In addition, the time delay (2-3 min) for full activation by Njun (section 5.3.2) might contribute to a failure to detect binding (Zhang et al., 1997). The different results reported in this study and by Zhang et al. (1997) are most likely due to methodological differences between laboratories rather than reflecting real differences in the interaction between Njun and the RyR.

Given that Njun is a short, relatively charged peptide, it was possible that the binding between Njun peptide and the RyRs was a non-specific charge interactions since charged residues are abundant in the RyRs (Takeshima et al., 1989). The specificity of Njun effects was examined using an Njun_{scrambled} peptide. The physical association with the RyRs was greatly reduced although still present when the original Njun sequence was scrambled (Fig. 5-2). This was considered to be non-specific binding as the scrambled peptide did not affect channel activity

(Fig. 5-5). Overall, the greater binding of Njun (than Njun_{scrambled}) to the RyRs suggests that a specific sequence of Njun is important for this physical interaction.

5.4.2 Cytoplasmic Njun modulates purified RyR1 and RyR2 channel activity

Despite the long-standing assumption that the functional effect of junctin on RyRs depends on luminal interactions between the proteins, the results obtained in previous chapters (Chapter 3 and 4) indicate that the cytoplasmic N-terminal domain of junctin may play a part in regulation of the RyRs by the whole junctin (FLjun) protein. In support of this hypothesis, the direct cytoplasmic Njun/RyR association led to a dramatic increase in channel activity of both RyR isoforms at the resting luminal Ca^{2+} concentration (1 mM), to levels significantly greater than the increase induced by luminal FLjun. This was in marked contrast to the inhibition of RyR1 by N-terminal triadin residues (Groh et al., 1999). A series of control experiments were conducted to ensure the functional Njun interaction was not a non-specific effect of the peptide. Firstly, the scrambled Njun peptide added to cytoplasmic solutions did not activate the channels, reinforcing that the specific sequence is critical for Njun activity. Secondly, there was no interaction between Njun and the luminal domain of the RyR since *trans* addition of Njun caused no effect on channel activity, suggesting that activation by *cis* Njun was not due to its crossing the membrane and the action of Njun on the cytoplasmic domain of the RyRs was a specific effect.

In addition to specificity, it was equally important to determine the possible physiological significance of the cytoplasmic Njun-RyR interaction. Native RyRs in SR vesicles containing endogenous junctin provided as a useful tool in this case since, if the cytoplasmic interaction occurred in the cell, the cytoplasmic junctin binding site would be occupied by endogenous junctin, hence exogenous Njun would not exert its usual effect. Indeed, addition of Njun to native RyRs in lipid bilayers resulted in no change in channel activity. The lack of an effect of Njun on native RyRs suggests that a cytoplasmic binding site for Njun in RyRs does exist and that this cytoplasmic interaction is physiologically relevant. This is further supported by the observation that Njun added to the cytoplasmic side of SR vesicles after ~30 min had only a minimal effect on Ca^{2+} release. The small increase in Ca^{2+} release could be due to Njun binding to a few cytoplasmic junctin binding sites that were not occupied by endogenous junctin. Indeed, Zhang et al. (1997) found that only a fraction of cardiac RyR2s were bound to junctin in the detergent extract. This was attributed by the authors to some RyR2s being bound to triadin and occluding junctin binding sites, or other unknown factors. Therefore, if the cytoplasmic, N-terminal tail of triadin did bind to the cytoplasmic domain of RyR in SR vesicles, and if this site were the same as or similar to Njun binding site as the N-terminal domains of junctin and triadin share certain sequence similarity (an example shown in Fig. 5-12), then it is possible that the added Njun peptide would compete with triadin for those binding sites. In addition, it has been

shown that cytoplasmic domain of skeletal triadin binding to the cytoplasmic domain of RyR1 inhibited the channel (Groh et al., 1999; Ohkura et al., 1998). Accordingly, it was possible that Njun could displace triadin and cause some activation, as seen here in this study. On the other hand, the small increase was not observed in lipid bilayer experiments and this could be attributed to: 1) much fewer RyRs in SR vesicles being exposed to Njun in bilayer studies than that in Ca^{2+} release assays, since the latter would allow all RyRs contained in the membrane vesicles to be accessible to Njun thus increase the chance of Njun to either compete with triadin or to associate with the unoccupied binding sites in some RyRs; 2) a relatively brief exposure (<15 min) of channels to Njun in comparison with the longer incubation of vesicles with Njun (~30 min) in Ca^{2+} release assay; 3) the higher concentration of Njun used in the vesicle studies. Together, the weak effect of Njun on the cytoplasmic side of native RyRs indicates that the cytoplasmic interaction is established *in vivo* and thus likely to be physiologically significant.

In conclusion, the results provide the first evidence for an interaction between the cytoplasmic domains of junctin and RyR. Njun positively regulates the RyR channels from cytoplasmic side in a specific manner that is likely to be physiologically relevant.

```

N-trad_rs/c      MTEITAEGNASTTTTVIDSKNGSVPKSPGKVLKRTVTEDLVTTTFSSP 47
N-jun_cc        MAEETKHGGHK-----NGRKGGLS---GSS----- 22
*: * * . * . . . . . : : : * : . . . * .

```

Figure 5-12 Cytoplasmic N-terminal domains of triadin and junctin sequence alignment and similarity. N-terminal sequence alignment of sequences corresponding to rabbit skeletal triadin (residues 1-47; NCBI accession number NP_001076212) or rabbit cardiac triadin 1 (residues 1-47; NCBI accession number AAC48496) (rs/c), and canine cardiac (cc) junctin (residues 1-22; NCBI accession number NP_001003196). The aligned residues are either identical (*), similar (:), weakly similar (.) or dissimilar. Alignment and similarity was determined using a CLUSTALW multiple sequence alignment (Combet et al., 2000).

5.4.3 Njun plays a dominant role in FLjun regulation of the RyR

Based on the data showing that cytoplasmic Njun activates RyRs (this chapter, Fig. 5-13B), luminal Cjun inhibits RyRs (Chapter 4, Fig. 5-13C) and FLjun moderately activates RyRs (Chapter 3, Fig. 5-13A), it was possible that *cis* Njun in conjunction with *trans* Cjun would affect RyR channel activity in a similar way to FLjun. Indeed, the excess activation induced by Njun being added first to the cytoplasmic solution was subsequently attenuated by the luminal addition of Cjun, and the resultant moderate activation remarkably resembles the effect of luminal FLjun. However, when Cjun was first associated with RyR luminally, cytoplasmic addition of Njun no longer activated the channel. This was in marked contrast to the FLjun effect and was completely unexpected. The results suggest that when FLjun is added to the luminal side of the RyR channels, its N-terminal tail and C-terminal tail may associate with the RyR in a sequential manner, and that the cytoplasmic interaction must be established before any

luminal binding in order to achieve the normal modulation of RyR channels displayed by full length junctin. This also suggests that *in vivo*, the cytoplasmic interaction may first anchor junctin to the RyR, following which the luminal interaction is able to proceed. The hypothetical mechanism of junctin regulation of RyR at 1 mM luminal Ca^{2+} is illustrated in Fig. 5-13D.

A model for junctin regulation of RyR activity

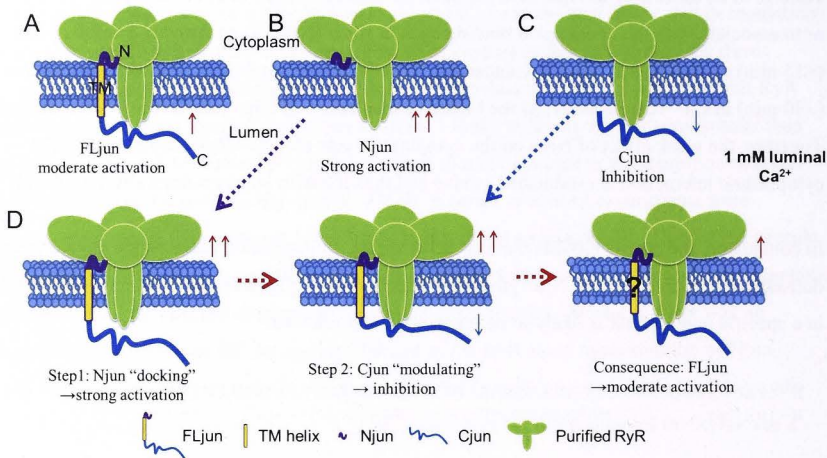


Figure 5-13 A hypothetical model of dual junctin/RyR interaction sites at resting 1 mM $[\text{Ca}^{2+}]$. (A)-(C) Interactions between junctin and RyR at 1 mM resting *trans* $[\text{Ca}^{2+}]$ after addition of FLjun (*trans*, **A**), Njun (*cis*, **B**) or Cjun (*trans*, **C**) to purified RyRs. (**D**) The hypothetical mechanism of junctin modulation of RyR at 1 mM luminal $[\text{Ca}^{2+}]$ may proceed as follows: 1) the interaction between the cytoplasmic domain of junctin and RyR occurs first, which anchors junctin to the RyR and induces strong activation of the channels (left); 2) the luminal modulation of RyR by the C-terminal domain of junctin is then allowed to take place, which evokes a small inhibition (middle); 3) the combined actions of Njun and Cjun results in moderate activation of the RyR channel (right). Solid red upward arrows indicate activating effects on the RyR, while green downward arrows denote inhibition. Double red arrows indicate strong activation. Question marks indicate effects or interactions that have not thus far been determined.

It should be kept in mind that post-translational modifications were missing in both the Cjun and Njun used in this study, since the Cjun was expressed in *E.coli* and the Njun was chemically synthesized. Such modifications may exist in endogenous junctin, such as phosphorylation (e.g., 9 residues have been predicted as potential phosphorylation sites using *KinasePhos*, Fig. 5-14), although to date no studies have reported or specifically investigated this. It should be noted that there is also a possibility of interactions between the transmembrane domains of junctin and the RyR (Figure 5-13, with question mark), which was not tested in this study as the peptide would be very hydrophobic and difficult to purify, probably insoluble. Regardless, the











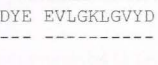
CANINEJUNCTIN						
Locations (AA)	Phosphorylated Sites	HMM Bit Score	E-value	Catalytic Kinases	Predictive Models	
					HMMs	Logo
19	KGGLSGSSF	-3.8	13	<u>ATM</u>	<u>HMM</u>	
87	AKRRTKAKV	-0.4	3.2	<u>PKC</u>	<u>HMM</u>	
87	AKRRTKAKV	-4.6	12	<u>PKA</u>	<u>HMM</u>	
95	VKELTKEEL	2.0	0.83	<u>CKII</u>	<u>HMM</u>	
106	EKEKTESRK	-2.8	12	<u>PKC</u>	<u>HMM</u>	
143	SRKESPKGK	-2.5	5.8	<u>PKG</u>	<u>HMM</u>	
143	SRKESPKGK	-0.5	5	<u>cdc2</u>	<u>HMM</u>	
166	KAKESRKKS	-2.1	4.8	<u>PKG</u>	<u>HMM</u>	
170	SRKKS ^T NVK	-0.7	2.8	<u>PKG</u>	<u>HMM</u>	
171	RKKS ^T NVKD	-1.1	2.8	<u>PKA</u>	<u>HMM</u>	
178	KDASSKTAS	-0.3	2.9	<u>CKI</u>	<u>HMM</u>	
MAEETKHGGH KNGRKGGL ^S G SSFPTWFMVI ALLGVWTSVA VVWF ^D LDVDE EVLGLG ^V YVD 60 -----S----- ATM ADGDGDFD ^V D DAKV ^L LEGGP GVAKRRT ^T KAK VKEL ^T KEELK KEKEK ^T ESRK ENKNEERRK 120 -----T----- PKC -----T----- PKA -----T----- CKII -----T----- PKC KKEKEDERK ^D KKIADADIS ^R KES ^P KGK ^K DR EKENVGLDKS AKAKE ^S RKKS ^T NVKDASSKT 180 -----S----- PKG -----S----- cdc2 -----S----- PKG -----S----- PKG -----T----- PKA -----S----- CKI ASRD ^K DDTKE GKTSSKH ^T HS AKGNNQ ^R RKN 210						

Figure 5-14 Potential phosphorylation sites in canine cardiac junctin (accession number: NP_001003196.1). Phosphorylation sites are predicted using online analysis tool *KinasePhos* (<http://kinasephos.mbc.nctu.edu.tw/>) (Huang et al., 2005).

reproduction of luminal FLjun (isolated from muscle) activity by addition of cytoplasmic Njun followed by addition of luminal Cjun indicates that a) any post-translational modifications of the N- and C-terminal domains of junctin and b) interactions between the transmembrane domains of the two proteins are probably not important for RyR activation by luminal FLjun *in vitro*. Nevertheless, it remains possible that potential modifications of junctin and/or transmembrane domain of junctin interaction with the RyR may play roles in its interaction with other proteins and/or its function in the SR *in vivo*.

5.4.4 Conclusion

The results presented so far in this thesis provide novel insight into the complex mechanisms underlying the regulatory effects of FLjun on RyR channel activity. Junctin regulates both RyR1 and RyR2 via two distinct interactions, involving both cytoplasmic and SR luminal domains. The interaction between the cytoplasmic domains of junctin and the RyR appears to dictate the functional consequences of the full length protein binding to RyR channels, followed by a modulation through luminal domain interaction. However, it remains unknown exactly which residues in junctin interact with the RyRs to achieve the functional effects. Therefore, the localization of the RyR-binding sites on junctin was investigated in order to gain a deeper understanding of the interaction between junctin and the RyRs, as well as a fuller picture of the junctin regulatory mechanism. The results are described in the final chapter of this thesis.

Chapter 6 Localization and characterization of a RyR interacting domain in junctin

6.1 Introduction

Inter-protein interactions constitute one of the most important aspects of protein function. Fundamental to protein-protein interactions are the specific domains within proteins which physically interact with one another in order to accomplish specific functional effects. Therefore, locating the domains of two different proteins which interact provides a global view of the protein interaction network, and possibly gives clues to overall protein functions.

The interacting regions between junctin and RyR are less well defined than those of triadin and RyR1. With triadin, it has been suggested that only three acidic residues – D⁴⁸⁷⁸, D⁴⁹⁰⁷ and E⁴⁹⁰⁸ –flanking the pore loop in RyR1, and residues 200-232 with the presence of a KEKE motif in Trisk 95 are critical for triadin-RyR1 interaction (Goonasekera et al., 2007; Lee et al., 2004). A similar binding site for triadin on RyR2 has also been proposed (Dulhunty et al., 2012). It has been demonstrated that junctin and triadin interact with different sites of RyR1, since 1) disrupting the putative triadin binding sites on RyR1 does not alter junctin binding (Goonasekera et al., 2007) and 2) junctin and triadin activate skeletal RyR1 in an additive fashion (Wei et al., 2009a). A recent study by Altschafel et al. (2011) identified two distinct domains of junctin that bind to two different luminal domains of RyR2 (see Chapter 1, section 1.9.6.1), which again contrasts with the single triadin-RyR binding site. Notably, junctin binds to the pore loop of RyR2 (residues 4789-4846), a highly conserved domain rich in charged amino acids (Nakai et al., 1990), and the same region that triadin binds to. Overall, these observations suggest that multiple binding sites are required for the junctin-RyR interaction.

KEKE motifs (for definition, refer to (Realini et al., 1994)) have been proposed to facilitate protein-protein associations by acting as polar zippers (Perutz, 1994; Realini and Rechsteiner, 1995; West et al., 2000). Junctin contains multiple KEKE motifs in its luminal C-terminal domain, with one qualifying as a “true” KEKE motif according to Realini’s criteria (Realini et al., 1994) (e.g., ⁸⁵KRKTKAKVKELTKEELKKEKEK¹⁰⁶ in human short isoform) and other KEKE-like motifs. It has been suggested that KEKE motifs in junctin potentially bind to the pore loop of the RyRs (Zhang et al., 1997). The observation that the full fragment of a junctin luminal domain (residues 78-210) but not smaller fragments containing KEKE-like domains, binds to RyR2 pore loop indicates that multiple KEKE motifs are likely required for this interaction. On the other hand, deletion of residues 86-102 in human junctin isoform, which contains >70% of the “true” KEKE motif of junctin, prevents junctin localization to the junctional SR, suggesting that this KEKE motif is likely to be involved in proper junctin

targeting (Rossi et al., 2013). To date, however, the role of KEKE motifs, if any, in the interaction between junctin and the RyR has not been investigated. Therefore, interactions between junctin KEKE motif and RyRs isolated from the heart and skeletal muscle were investigated.

Aim:

In this chapter, experiments were performed to determine (a) RyR binding residues in junctin luminal domain, in particular the KEKE motif, and (b) potential functional effect of the KEKE motif of junctin on the RyR channel activity.

6.2 Materials and Methods

6.2.1 Methods overview

Affinity chromatography was utilized to assess the ability of junctin KEKE motif peptide to bind to RyR1 and RyR2; single channel recordings were conducted to explore the direct regulation of both RyR isoforms by this junctin KEKE motif.

6.2.2 RyR preparation

Recombinant RyR1 and RyR2 were used for affinity chromatography to assess binding between Jun_{KEKEcanine} peptide and the RyR as that used for Njun (Chapter 5). The recombinant RyR1 and RyR2 were expressed and purified from HEK293 cells as detailed in section 2.4 and 5.2.2.

For lipid bilayer experiments, RyR1 and RyR2 were solubilized and purified from SR as described in section 2.3.2.

6.2.3 Affinity chromatography

Affinity chromatography assays were performed as described in section 2.8.2 to determine the physical interaction between Jun_{KEKEcanine} peptide and RyR1 and RyR2. The assay involved binding the biotinylated Jun_{KEKEcanine} peptide to agarose using neutravidin covered resin. Then pre-cleared RyR constructs were incubated with the peptide-bound resin. The RyRs bound to the resin by interaction with the peptide were assessed using SDS-PAGE and immunoblot.

6.2.4 Single channel recording and analysis

Single channel recording was conducted and analyzed as described in section 2.9. Prior to addition of Jun_{KEKE} peptide the *cis* and *trans* chambers consisted of: *cis* solution (230 mM

CsCH₃O₃S, 20 mM CsCl, 10mM TES and 1 μM free Ca²⁺, pH 7.4) and *trans* solution (230 mM CsCH₃O₃S, 20 mM CsCl, 10mM TES and 1 mM CaCl₂, pH 7.4).

6.3 Results

6.3.1 Identification of RyR1 binding residues in Cjun

The pore loop of RyR1 and RyR2 is a region of high charge density and influences the gating and conductance of the channel. This region has been shown to bind to a KEKE motif (residues 200-232, Fig. 6-2A) in triadin (Goonasekera et al., 2007; Wium et al., 2012). Furthermore, addition of this triadin KEKE motif peptide to the luminal side of purified RyR1 produces a significant increase in channel activity (Wium et al., 2012). Since the C-terminal domain of junctin binds to this pore loop of RyR2 (Altschaffl et al., 2011) and probably of RyR1, and a similar KEKE motif also exist in this domain (residues 85-106 in human junctin isoform, Fig. 6-2A), it was interesting to investigate whether this region interacts with the RyRs. Therefore, peptides corresponding to this KEKE motif of two junctin isoforms (Jun_{KEKE}^{rabbit} and Cjun_{KEKE}^{canine}) were synthesized (section 2.1.2) and binding and functional interactions of the peptides with the RyRs were examined.

6.3.1.1 Physical interaction between KEKE motif and RyR1/2

NeutrAvidin agarose affinity chromatography was performed as described in section 2.8.2 and 6.2.3 to determine whether the Jun_{KEKE}^{canine} peptide bound to RyR1 or RyR2. Recombinant RyR1 and RyR2 were used in this study as for Njun (Chapter 5, section 5.2.2 and 5.2.3), which were shown not to bind to the agarose (see Fig. 5-2B lane1&4, Chapter 5). The final NeutrAvidin agarose attachments (biotinylated Jun_{KEKE}^{canine} peptide + RyRs) were subjected to gel electrophoresis and immunoblot. Probing the immunoblot with anti-RyR 34C antibody and StrepTactin-HRP conjugate revealed the presence of the RyR1 and RyR2 resolving at > 250 kDa and the peptide at ~10 kDa (Fig. 6-1 lane1&2 respectively). Therefore, there is a strong

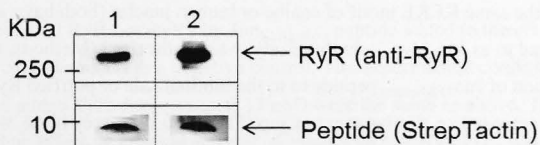


Figure 6-1 A region of junctin that binds to RyRs. Immunoblot showing the association of recombinant RyR1 and RyR2 with the biotinylated Jun_{KEKE}^{canine} peptide coupled to neutravidin agarose (Lane 1 and 2, respectively, n=3 for RyR1 and n=3 for RyR2). The upper half of the membrane was probed with anti-RyR 34C antibody, and the lower half was probed with Streptactin-HRP conjugate to identify the biotin tagged peptides. Positions of molecular weight marker are shown to the left of lanes.

association between the junctin KEKE peptide and RyR1 or RyR2 at least *in vitro*. This was in contrast to a study by Altschaf et al. (2011) where blot overlay assays did not detect a binding of a recombinant junctin fragment (residues 76-161, human isoform), which contains the KEKE motif, to RyR2.

6.3.3.2 Functional effect of Jun_{KEKE} on purified RyR1 and RyR2 (luminal)

Since the junctin KEKE motif peptide binds to the RyRs, the functional consequences of this interaction were tested using single channel recording with standard *cis* and *trans* solutions as described in section 2.9.3 and 2.9.4. Purified RyR1 or RyR2 was reconstituted into planar lipid bilayers and channel activity was recorded under symmetrical (Cs^+) conditions (section 2.9.4). The cytoplasmic (*cis*) $[\text{Ca}^{2+}]$ was $1 \mu\text{M}$, and the luminal (*trans*) $[\text{Ca}^{2+}]$ 1mM . 213 nM Jun_{KEKE}_{rabbit} peptide was added to the *trans* chamber.

A strong inhibition in channel activity of both RyR1 and RyR2 was apparent with the presence of luminal Jun_{KEKE}_{rabbit} peptide (Fig. 6-2B&C). There was a $54 \pm 8.7\%$ decrease in activity of RyR1 channels (P_o fell from 0.16 ± 0.036 to 0.09 ± 0.038) and a $55 \pm 4.8\%$ reduction in average P_o (from 0.35 ± 0.065 to 0.16 ± 0.038) in RyR2 (Fig. 6-2D black bins). This decrease in open probability could be attributed to a significant prolongation of mean closed time T_c (4.08 ± 0.368 -fold increase in RyR1 and 2.38 ± 0.334 -fold in RyR2) with abbreviation of mean open times T_o ($38 \pm 10.0\%$ decrease in RyR1 and $30 \pm 8.3\%$ in RyR2) (Fig. 6-2E&F black bins). Interestingly, the inhibition induced by KEKE peptides added to the luminal solution was similar to that seen with luminal whole Cjun construct (see Chapter 4, Fig. 4-3), suggesting that residues of the junctin KEKE peptide is likely to be involved in the specific inhibitory interaction between luminal Cjun and RyR1 or RyR2.

It should be noted that there is a two-residue difference in junctin KEKE motif between rabbit and canine/human isoforms (Fig. 6-2A, residues highlighted in red). In order to determine whether the inhibitory effect seen with Jun_{KEKE}_{rabbit} was species specific, a peptide corresponding to the same KEKE motif of canine or human junctin (both have identical sequences), referred to as Jun_{KEKE}_{canine} in this study, was synthesized (Methods, section 2.1.2 and Fig. 6-2A). Addition of Jun_{KEKE}_{canine} peptide to the luminal side of purified RyRs also inhibited channel activity in a similar way to Cjun (Fig. 6-2D light grey bins), with a trend towards a longer mean closed time and a shorter mean open time (Fig. 6-2E&F light grey bins). The results suggest that there is no species difference with respect to the effect of Jun_{KEKE} motif peptide on RyRs and that the two residues that differ between canine/human and rabbit are not important in the ability of Jun_{KEKE} peptide to regulate RyR activity.

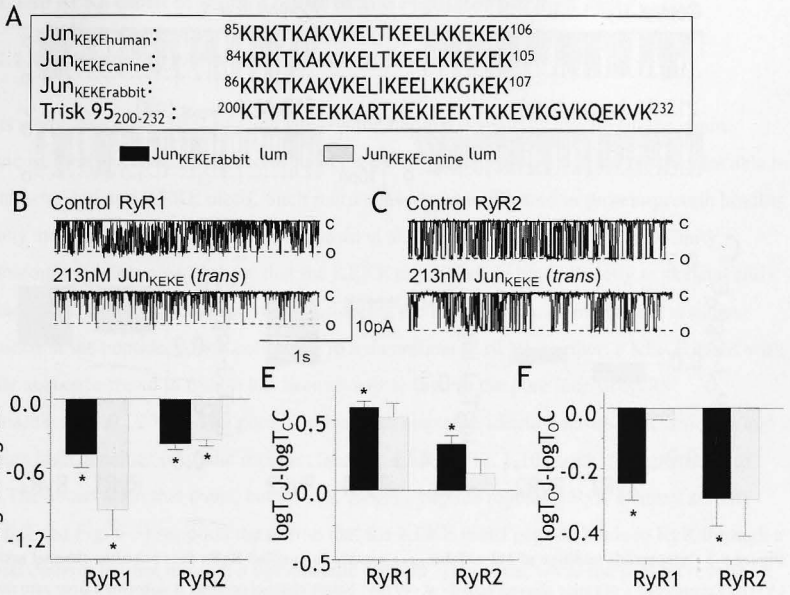


Figure 6-2 Addition of junctin KEKE peptide (Jun_{KEKE}) to the *trans* chamber inhibits purified RyR channel activity. (A) Conservation of the sequence of the KEKE motif in human, dog and rabbit junctin and comparison with the active KEKE motif in the luminal domain of skeletal triadin. (B)-(C) Records of 3 s of single channel activity, at -40 mV. Single channel opening is downward from zero current (c, continuous line) to maximum open conductance (o, broken lines). The top recording in each panel shows control channel activity and the lower trace shows activity in the same channel after addition of 213 nM Jun_{KEKE} to the luminal solution. (D)-(F) Average pooled data from both -40 mV and +40 mV for relative open probability (logP_{oJ}-logP_{oC}, D), mean closed time (logT_{oJ}-logT_{oC}, E), and mean open time (logT_{oJ}-logT_{oC}, F). Data are shown for effects of the rabbit KEKE peptide on the luminal side of RyR1 (n=10-12) and RyR2 (n=12-16) (black bins). Some experiments were also performed with luminal addition of the canine KEKE peptide (as Cjun was derived from the full length canine junctin (Methods, section 2.5.3)) with similar results in RyR21 (n=2-4) and RyR2 (n=4) (light grey bins). The asterisk (*) indicates average values significantly different from the control (P<0.05 Student's *t*-test, paired).

Regulation of purified RyR1 or RyR2 by Jun_{KEKE}Rabbit peptide added to the *cis* side of the channel was finally examined as a negative control. The experimental conditions and the concentration of added Cjun Jun_{KEKE}Rabbit (213 nM) were the same as above. The presence of Jun_{KEKE}Rabbit had no effect on channel activity of either RyR1 or RyR2 (P_o was 0.16 ± 0.035 before and 0.18 ± 0.035 after *cis* Jun_{KEKE}Rabbit addition in RyR1, while 0.28 ± 0.033 before and 0.31 ± 0.045 after peptide addition in RyR2; Fig. 6-3). This lack of overall regulatory effect on the RyR indicates the KEKE motif peptide of junctin can regulate the RyR only from the SR lumen. This was in contrast to the weak inhibition imposed by cytoplasmic Cjun under the same conditions (Chapter 4, Fig. 4-5).

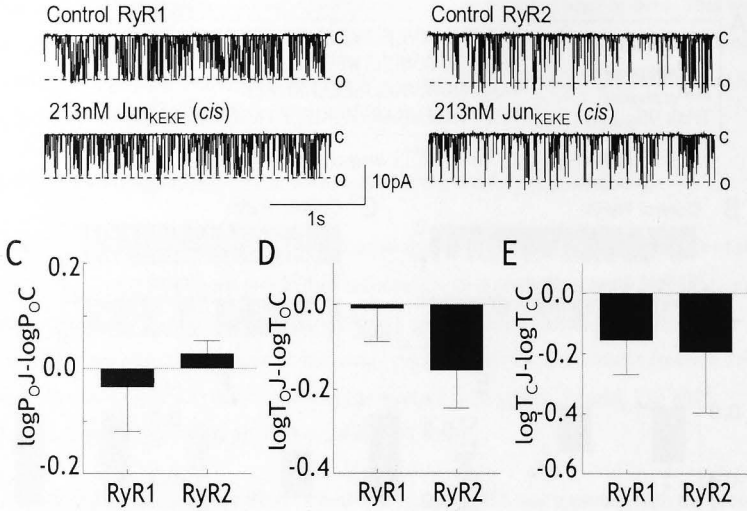


Figure 6-3 Cytoplasmic addition of 213 nM Jun_{KEKE} peptide to purified RyRs does not alter channel activity. (A)-(B) Records of 3 s of single channel activity at -40 mV. Single channel opening is downward from zero current (c, continuous line) to maximum open conductance (broken line, o). The upper trace in each panel shows control activity and the lower trace shows activity after adding 213 nM Jun_{KEKE} to the cytoplasmic solution bathing RyR1 (A) or RyR2 (B). (C)-(E) average data for relative open probability ($\log P_{oJ} - \log P_{oC}$, C), mean open time ($\log T_{oJ} - \log T_{oC}$, D) and mean closed time ($\log T_{cJ} - \log T_{cC}$, E), determined for individual channel for RyR1 (n=7-8) and RyR2 (n=5-8). No significant differences found with Jun_{KEKE} before and after peptide addition ($P > 0.05$ Student's *t*-test, paired).

Taken together, the results in Fig. 6-2 and Fig. 6-3 show that the KEKE motif between junctin residues 85 and 110 can bind to RyR1 and RyR2 directly and by itself can reproduce the functional effects of full Cjun construct on the luminal side of the channels.

6.4 Discussion

In order to fully elucidate junctin-RyR interaction, it is important to determine their interacting regions. However, only one study has addressed the specific binding domains in RyR and junctin in cardiac muscle (Altschafel et al., 2011). In the present study, the interaction between a potential RyR-binding site of junctin and the RyR was investigated. One of the RyR-binding sites of junctin has been mapped to a KEKE motif (residues 86-107 in rabbit cardiac junctin and 84-105 in canine cardiac junctin), and for the first time the KEKE motif has been shown to regulate RyR1 and RyR2 channel activity with a similar inhibitory effect to that of luminal Cjun (for Cjun data, see Chapter 4).

6.4.1 The KEKE motif of junctin binds to and regulates purified RyR

6.4.1.1 A RyR-binding site on junctin – the KEKE motif

In this study, one of the RyR binding sites on the luminal domain of junctin (in the canine cardiac isoform) has been localized to residues 84-105, a region with a primary structure able to be characterized as a KEKE motif. Such motifs have been implicated in protein-protein binding in many studies (Jones et al., 1995; Kobayashi et al., 2000; Zhang et al., 1997). Affinity chromatography data clearly show that the KEKE motif peptide binds directly to skeletal and cardiac RyRs. This was not surprising considering the high abundance of charged residues contained in the peptide, which contribute to a theoretical pI of 10. Further, a KEKE motif with similar sequence found in triadin has been shown to bind to the pore loop of RyR1 (Goonasekera et al., 2007). The pore loop has high sequence identity across RyR isoforms and it contains high densities of acidic residues (section 1.6.3.2, Fig. 1-10), with a calculated pI of 3.96. The observation that *trans*, but not *cis*, Jun_{KEKE} peptide regulates RyR channel activity (Fig. 6-2 and Fig. 6-3) supports the notion that the KEKE motif peptide binds to RyR through a luminal domain but not through a cytoplasmic domain. Therefore, while the present results are not sufficient to draw any firm conclusions, it is plausible that this KEKE motif in junctin would interact directly with charged residues in the pore loop of the RyR, and thus supports Cjun's binding to the pore loop of RyR2 (Altschafel et al., 2011) and probably of RyR1.

Curiously, a recombinant junctin peptide (residues 78-161) containing the 84-105 KEKE motif has been shown in blot overlay assays to bind to neither the M5-M6 linker nor the pore loop of RyR2; however, the full length of a luminal domain fragment (residues 78-210) binds to the pore loop, again suggesting that multiple KEKE motifs are required for the interaction between the pore loop and junctin (Altschafel et al., 2011). This to some extent, contradicts our speculation, since our results show that the KEKE motif alone can pull down both RyR isoforms. The reason for this disparity is unclear and may be due to methodological differences between laboratories. However, it should be kept in mind that the binding regions on the RyR for its direct interactions with the junctin KEKE motif have not been located and it therefore remains possible that junctin's KEKE motif binds to regions other than the pore loop on the luminal domain of the RyR. Binding assays using the junctin-derived KEKE motif peptide along with the isolated pore loop of the RyR may shed light on whether there is indeed a direct physical association between the two, but due to time and technical constraints this avenue was not further pursued in this study.

6.4.1.2 KEKE motif exerts an inhibitory effect on purified RyR, similar to that seen in Cjun luminal effect.

The functional consequences of such a physical link between the KEKE peptide of junctin and the RyRs were revealed in lipid bilayers. A significant reduction in channel open probability of both purified skeletal and cardiac RyRs was observed upon addition of the KEKE motif peptide to the *trans* chamber, accompanied by abbreviated mean open times and prolonged mean closed times. It appears, therefore, that the KEKE motif is a potent luminal RyR inhibitor. Depressed channel activity by the KEKE peptide is reminiscent of the action of luminal Cjun, which imposes a similar inhibition on both RyR1 and RyR2 (for Cjun data, see Chapter 4, Fig. 4-3). Thus, it is likely that the KEKE motif in Cjun participates in the full Cjun construct regulation of RyR1 and RyR2. It would be interesting to see how the KEKE motif peptide cooperates with other parts of junctin to exert the full Cjun or FLjun effect. Also it would be interesting to know whether this KEKE motif peptide is involved in conveying CSQ1 signal to RyR1 (Wei et al., 2009a) as it has been shown that junctin binds to CSQ2 through multiple KEKE motifs (Kobayashi et al., 2000). However, due to time limits no further specific testing of the KEKE peptide function was carried out for this thesis. Interestingly, the junctin KEKE peptide-induced channel inhibition was very different from the significant increase produced by the luminal triadin KEKE₂₀₀₋₂₃₂ peptide (Wium et al., 2012), notwithstanding a similar KEKE content between the two (Fig. 6-2A). Significantly, neither peptide affects the channel from the cytoplasmic side (Fig. 6-7 and (Wium et al., 2012)).

6.4.1.3 Species-independence of junctin KEKE motif regulation of the RyRs

Despite the high sequence similarity (>90%) of the junctin KEKE motif peptide across species (Fig. 6-2A), it was argued that the minor difference (2 out of 22 residues, see Fig. 6-2A, residues highlighted in red) implied that the KEKE motif may be unimportant in the function of junctin (Wetzel et al., 2000). To resolve this problem, peptides corresponding to the KEKE motif of both rabbit cardiac and canine/human cardiac isoforms were applied in lipid bilayers. No differences were observed in the regulatory effect of either peptide (referred to as Jun_{KEKE}^{rabbit} and Jun_{KEKE}^{canine}), suggesting that the KEKE motif may not be as unimportant as suggested (Wetzel et al., 2000), but rather that the two residues play a negligible role in the overall regulation of RyR channel activity by the KEKE motif peptides. This also implies that the effect of the KEKE peptide on RyRs is species-independent.

6.4.2 Rationale for using the KEKE motif peptide from different species

It should be noted that the KEKE peptide used in this study was either rabbit cardiac isoform or canine cardiac isoform due to multiple reasons. Firstly, the FLjun applied in lipid bilayer studies was the rabbit skeletal isoform. To compare the FLjun and the KEKE peptide effect, it was necessary to use constructs of the same isoform. However, sequence of rabbit skeletal junctin is currently unavailable, whereas the cardiac isoform from the same species has been partially

deduced (NCBI accession number: AAF37204.1 and (Wetzel et al., 2000)). Since the same isoform of junctin is expressed in skeletal and cardiac muscle (Jones et al., 1995), a KEKE peptide corresponding to rabbit cardiac junctin isoform was thus used. Secondly, addition of Jun_{KEKE^{rabbit}} to luminal side of the RyRs inhibits channel activity in the same way as luminal Cjun, which was constructed from the canine cardiac DNA. Thus, it was interesting to know whether the KEKE peptide from the same origin (canine) would have a similar effect. This would also help answer whether species differences exist and whether the two unconserved residues would make any difference as mentioned in section 6.4.1.3. Therefore, the functional effect of Jun_{KEKE^{canine}} was also tested. Finally, investigation of the binding of the junctin fragment containing the KEKE motif to the RyR was conducted previously on human cardiac junctin isoform (Altschafel et al., 2011). For the sake of comparison, the KEKE peptide of canine cardiac junctin was employed in affinity chromatography, since there is no difference between the canine and human sequences (Fig. 6-2A). This also complemented the functional studies.

6.4.3 Limitations

One of the limitations of this study is a lack of negative controls. Apart from the buffer control (i.e., MilliQ-water added to RyR channels, see Chapter 3, Fig. 3-8), the only negative control in the experiments in this chapter was the addition of the KEKE peptide to cytoplasmic solution which produced no effect (Fig. 6-7), suggesting the KEKE peptide can only regulate the channels through luminal interaction. Nevertheless, no further controls were conducted to confirm the specificity of the KEKE motif-RyR interaction. Scrambled peptides were not considered due to the high content of K and E residues that would be preserved in any scrambled sequences. An alternative would be to introduce alanine mutations into the native junctin KEKE peptide sequence; this would also allow assessment of which residues within this sequence are potentially important for its binding to RyR as well as its functional effect on channel activity. In addition, control with native RyR channels should also be considered. As it would be expected that the KEKE motif peptide would not be able to bind or inhibit the native channels if the site in native RyRs is occupied by the KEKE motif of endogenous junctin. However, due to time constraints, the experiments could not be conducted.

6.4.4 Conclusion

In this study, one RyR (both RyR1 and RyR2) binding site in junctin has been located to a KEKE motif (residues 84-105), therefore together with Chapter 5, at least two RyR-binding sites in junctin have been determined in this study – the junctin N-terminal domain and the C-terminal domain KEKE motif. In addition, we provide the first evidence that the KEKE motif of junctin alone reproduces the functional effects of full Cjun construct on the luminal side of the channels, suggesting its involvement in Cjun regulation of the RyR. Altogether, multiple

interacting domains between junctin and the RyR indicate the complexity of junctin-RyR interaction as suggested for RyR2 regulation by junctin (detailed in Chapter 1.9.6 and (Altschaff et al., 2011)).

Chapter 7 General Discussion

This thesis describes an in-depth investigation of the molecular interactions between junctin and RyR isolated from skeletal and cardiac muscle. The direct regulation of the RyR by the full length junctin protein is described as well as the separate roles of junctin's luminal C-terminal domain and cytoplasmic N-terminal tail, and their combined actions in modulating RyR activity. In addition the interacting domains between junctin and the RyR are described. Overall the results suggest that junctin modulates RyR activity directly, and that this regulation is through both cytoplasmic and luminal domain-domain interactions between the two proteins. The principal individual findings of this study are as follows:

- 1) Full length junctin (FLjun) alters cardiac RyR2 gating directly when the resting luminal $[Ca^{2+}]$ is 1 mM. FLjun in the luminal, but not cytoplasmic, solution enhances channel activity, mainly due to a re-distribution of opening and closing events, with more long open events and fewer long closure events. Similar findings were obtained in junctin regulating skeletal RyR. The increased RyR1 activity by junctin is consistent with that reported by Wei et al. (2009a).
- 2) The luminal C-terminal domain of junctin (Cjun) interacts with the RyR. The physical association of Cjun and the RyR results in an unexpected inhibition of channel activity in lipid bilayers which is in contrast to the activation by FLjun.
- 3) The cytoplasmic N-terminal tail of junctin (Njun) was for the first time shown to interact directly with the RyR and to have a significant effect on channel gating. The cytoplasmic interaction between Njun and the RyR leads to a dramatic increase in channel activity to a much greater level than that seen with FLjun.
- 4) FLjun activation of RyR depends on both cytoplasmic and luminal interactions between the two proteins, where the cytoplasmic interaction plays a dominant role. For the FLjun effect to occur, the cytoplasmic interaction must be established before the luminal binding, indicative of the fine-tuning of RyR activity by junctin.
- 5) A RyR-binding site on the luminal domain of junctin was located at a KEKE motif (residues 86-107 of rabbit cardiac isoform, or 84-105 of canine cardiac isoform). The KEKE motif peptide alone was shown to inhibit RyR in the same way as full Cjun construct. This result suggests the involvement of the KEKE motif in overall regulation of RyR by junctin.
- 6) Substantial differences between junctin and triadin interactions with RyRs were shown in this study. First, the multiple binding sites for junctin determined here (cytoplasmic and luminal domains) and by Altschafel et al. (2011) are in contrast to the single triadin binding site in the pore loop (Goonasekera et al., 2007). Second, on the cytoplasmic side, the N-terminal tail of

junctin enhances RyR1 and RyR2 activity, in contrast to the inhibition of RyR1 by triadin N-terminal domain (Groh et al., 1999). Third, for the luminal interaction, the KEKE motif of junctin (residues 86-107) inhibits RyR channels, whereas a corresponding region of triadin activates RyR1 (residues 200-232) (Wium et al., 2012). The differences support the idea that junctin and triadin serve distinct functions as suggested by Wei et al. (2009a).

7) All junctin constructs in this study were found to regulate RyR1 and RyR2 in a very similar fashion, suggesting that conserved regions in the two proteins may be responsible for their binding to junctin.

7.1 Distinct functional consequences of Njun and Cjun association with RyRs

7.1.1 The significance of Njun interaction with RyRs

It was surprising that the N-terminal residues of junctin not only bound to RyRs but also caused a substantial enhancement in channel activity (Chapter 5). Preliminary data by Dr. Shamaruh Mirza from the Muscle Research Group suggest that the binding site for Njun resides in residues 183-2156 of RyR1, and the Njun-binding site in RyR2 is likely to be similar to that in RyR1 but requires further exploration (personal communication with Prof. Angela Dulhunty). These findings are in contrast to a previous report proposing that junctin interacts with the RyR only through luminal domains because Njun binding to RyR2 was not detected, whereas Cjun bound to RyR2 (Zhang et al., 1997). Nevertheless, N-terminal binding is not unprecedented. The cytoplasmic N-terminal residues of the structurally similar protein triadin (aa18-46) in the *cis* solution inhibits RyR1 activity and binds directly to RyR1 (Groh et al., 1999), although other studies failed to detect a physical interaction between the cytoplasmic domain of triadin and the RyR1 (Caswell et al., 1999; Guo and Campbell, 1995). Reasons for this discrepancy remain unclear, but the possibility that there is a cytoplasmic interaction between RyR and triadin *in vivo* cannot be excluded. Similarly, it is plausible that the cytoplasmic Njun-RyR interaction exists *in vivo*. Indeed, preliminary findings by Dr. Shamaruh Mirza indicate less association of the triadin-binding deficient mutant (Goonasekera et al., 2007) with Cjun than with FLjun, consistent with binding of FLjun to the RyR at both cytoplasmic and luminal sites, although this could also be explained by a second luminal site. Furthermore, the activating effect on RyRs imposed by cytoplasmic Njun and luminal FLjun in contrast to the inhibition by luminal Cjun indicates that the N-terminal tail of junctin may play a significant role in FLjun regulation of the RyRs. This is further supported by the combined actions of Njun and Cjun where adding Njun cytoplasmically, followed by Cjun lumenally, but not in the reverse order, reproduced the FLjun effect. That the cytoplasmic interaction must be established first suggests that this interaction may anchor junctin to the RyRs and dictate the functional consequences of the full length

protein binding to RyR channels. The luminal modulation of RyR by the C-terminal domain of junctin is then allowed to take place *in vivo*. The physiological relevance of the cytoplasmic interaction between junctin and RyR is further strengthened by an absence of the strong activating effect of cytoplasmic Njun on native RyRs containing endogenous junctin, in contrast to the effect that was seen with purified RyRs.

7.1.2 Implication of Cjun as a channel inhibitor

It was unexpected that Cjun would impose an inhibitory effect on channel activity, rather than the activation seen with FLjun (Chapter 4). That said, Cjun acting as a channel inhibitor on isolated RyR2 in bilayers may help explain the negative regulatory role of junctin derived from most transgenic studies in cardiac system (detailed in Chapter 1.9.4.1). The depressed contractility of heart and reduced Ca^{2+} release in junctin overexpression models may be partly attributed to an accumulation of free junctin in the SR lumen, since the availability of SR membrane structures is limited. In addition, it might be less likely for a correct stoichiometric ratio of junctin to RyR to occur when the excess junctin is competing for space in the membrane. Thus, the inhibitory effect of the C-terminal domain of junctin may outweigh the activating effect of FLjun (Chapter 3 and (Gyorke et al., 2004a)) or FLjun in conjunction with CSQ2 (as suggested in (Wei et al., 2009b)). However, the question remains as to why junctin ablation would lead to enhanced contractility and augmented Ca^{2+} transients, especially in the cases where junctin was completely absent (Altschafel et al., 2011; Yuan et al., 2007). A possible explanation is that the changes may be caused by an increased SR Ca^{2+} load accompanying junctin reduction; alternatively, or in addition, altered luminal Ca^{2+} sensitivity of RyR2 possibly caused by an impaired physical interaction between the RyR and CSQ2 with junctin removal or other luminal proteins *in vivo*. Whatever the explanation, the results indicate that the loss of FLjun-specific activation of RyR2 plays only a small part in the response to junctin ablation.

7.2 Similar actions of junctin on RyR1 and RyR2

It is noteworthy that all junctin constructs used in this study—FLjun, Cjun, Njun and the KEKE motif peptide—bound to skeletal and cardiac RyRs in similar amounts. It is also worth noting that each construct regulated RyR1 and RyR2 channels in remarkably similar ways, whether added to the cytoplasmic or luminal solution. This is not surprising since the same junctin isoform is expressed in skeletal and cardiac muscle. On the other hand, despite a high level of identity between the RyR1 and RyR2 isoforms (>60%, Chapter 1.6.1), there is still considerable sequence diversity. Therefore, the similar actions of junctin and its fragments on RyR1 and RyR2 activity indicate that the binding sites for junctin are possibly in regions where the sequences are homologous in the two RyR isoforms. Preliminary results obtained by Dr. Shamaruh Mirza show that Cjun binds to the same luminal loops—the M5-M6 linker and the

pore loop—in both RyR1 and RyR2, although this requires further confirmation, in particular with the M5-M6 linker (for explanations, see below). These results further support the likely homology of junctin binding sites. The pore loop between RyR isoforms has a high sequence identity and influences the gating and conductance of the channel. Notably, it contains high densities of acidic residues at the mouth of the pore (Fig. 1-9, and also section 1.6.3.2, Fig. 1-10) which, it has been suggested, are important in ion handling and gating characteristic in RyR2 (Mead-Savery et al., 2009). As a Cjun fragment (residues 78-210) containing the junctin KEKE motif region binds to the RyR2 pore loop (Altschafel et al., 2011), and full Cjun (residues 45-210) binds to RyR1 pore loop (as mentioned above), it is likely that the junctin KEKE motif region binds to the pore loop, possibly through a direct interaction with the charged residues at the luminal end of the pore. On the other hand, the M5-M6 linker is less homologous compared to the pore loop in RyR1 and RyR2, particularly in its C-terminal region. Nevertheless, the N-terminal residues in M5-M6 linker in RyR1 and RyR2 do share certain similarities (⁴⁵⁸²VSDSPPE⁴⁵⁸⁹ and ⁴⁵²³VSTSSVVE⁴⁵³⁰ in rabbit RyR1 and RyR2 respectively). Thus, if Cjun does bind to the M5-M6 linker, then the similar residues in the N-terminal region in M5-M6 linker are likely to support its binding to junctin (e.g., residues 47-47 in (Altschafel et al., 2011)), and the C-terminal region in M5-M6 linker may not contribute to the binding. However, there is also possibility that Cjun does not bind to the M5-M6 linker in RyR1 considering the sequence differences between the two isoforms. To reiterate, the results obtained with Cjun binding to luminal loops in RyR1 so far are rather tentative and more testing is needed.

7.2.1 Implication of the similar actions in CSQ/junctin/RyR interaction

It has been previously shown that CSQ1 inhibits RyR1 via junctin (Wei et al., 2009a), while CSQ2 activates RyR2 (with junctin and triadin associated) in the presence of 1 mM luminal Ca²⁺ (Wei et al., 2009b). If CSQ2 activation is also through junctin, then either different conformational alterations in junctin occur upon binding to CSQ1 and CSQ2 owing to the difference between the two CSQ isoforms, or changes in the conformation of junctin are similar but junctin interacts in different ways with RyR1 and RyR2 upon CSQ binding. Indeed, CSQ1 imposes opposite effects on RyR1 and RyR2 activity, where it inhibits native RyR1 but activates native RyR2 when both contain endogenous junctin (Wei et al., 2009b). Thus the CSQ1/junctin complex must interact differently with RyR1 and RyR2, possibly through sequence diversity between RyR1 and RyR2 in the way in which binding is communicated to channel gating mechanism. Although the precise pathways remain to be elucidated, it is very likely that the sequence difference between CSQ1 and CSQ2 and between RyR1 and RyR2 would have a profound impact on the overall functional consequences of the interaction among CSQ, junctin and the RyR (Fig. 7-1).

7.3 Implications of multiple interacting domains between RyRs and junctin

The distinct regulatory modes of RyR regulation by luminal Cjun and cytoplasmic Njun suggest a presence of both cytoplasmic and luminal interacting sites on RyR for junctin. In support of this, biochemical experiments using Njun, Cjun or Jun_{KEKE} and RyR1 or RyR2, together with the preliminary findings mentioned in section 7.1.1 and 7.2, indicate that at least two or three distinct domains of RyR1 interact with junctin, including luminal domains binding to Cjun and a cytoplasmic region binding to Njun. This was further strengthened by the observation that both FLjun (Goonasekera et al., 2007) and Cjun (mentioned in section 7.1.1, work by Dr. Shamaruh Mirza) retained their ability to bind to RyR1 after mutating three residues in the pore loop that are critical for triadin binding. Two luminal binding sites for junctin on RyR2 have also been demonstrated (Altschafel et al., 2011). Although a binding site for Njun on cytoplasmic domain of RyR2 remains to be determined, it is clear that such a cytoplasmic interaction does exist at least *in vitro* and the Njun-binding region of RyR2 is expected to be similar to that of RyR1 as discussed in section 7.1.1. Therefore, junctin can potentially interact with RyR through at least two or three distinct domains to influence channel activity (illustrated in Fig. 7-1). In this case, cytoplasmic and luminal factors may impose a fine modification of the overall regulation of RyRs by junctin through these different regulatory modes.

The KEKE motifs in junctin and triadin have long been presumed to be involved in their interactions with RyR as well as CSQ (Jones et al., 1995; Kobayashi et al., 2000; Zhang et al., 1997). Indeed, it is suggested that multiple KEKE motifs in junctin are involved in its binding to CSQ (Kobayashi et al., 2000), as well as multiple binding sites between junctin and RyR (this study and (Altschafel et al., 2011)). These properties distinguish junctin from triadin. The KEKE motif in triadin is critical for its binding to RyR and is thought to be the same as the site responsible for CSQ binding (Dulhunty et al., 2009; Kobayashi et al., 2000; Lee et al., 2004). Thus the question arises whether triadin can bind to RyR and CSQ at the same time. An inability to bind both simultaneously would provide a structural basis for the inability of triadin to convey signals from CSQ1 to RyR1 as CSQ1 binding to triadin may alter its binding to RyR1 ((Wei et al., 2009a); illustrated in Fig. 7-1, under section 7.4). In contrast, junctin can mediate signalling between CSQ1 and RyR1 (Wei et al., 2009a), hence it can presumably bind to CSQ1 and RyR1 simultaneously through its multiple binding sites for CSQ and for RyR as mentioned above. When CSQ1 binds to RyR1-associated junctin, the additional binding sites between RyR1 and junctin would keep junctin anchored to RyR1, allowing the information of CSQ to be communicated via junctin to RyR1 and thus to influence channel activity ((Wei et al., 2009a); Fig. 7-1 B&D). Furthermore, if CSQ binds to the same KEKE motif in junctin that is presumably bound to the RyR pore loop, the connection between junctin and the pore loop of

RyR would be interrupted (Fig. 7-1 C&E). In this case, the functional consequences of CSQ1 binding may depend on removal of the KEKE motif inhibitory effect (Chapter 6) on RyRs and reveal the effects of junctin binding to the M5-M6 linker of RyR which are likely to be different between RyR1 and RyR2 since there is very low sequence similarity in the C-terminal region of the M5-M6 linker between the two, this is based on the assumption that junctin binds to the M5-M6 linker of RyR1 as seen that with RyR2 (Altschafli et al., 2011). On the other hand, it is also possible that junctin does not bind to M5-M6 linker in RyR1 (see section 7.2), which would again differ from that with RyR2. And such difference would similarly be revealed as a consequence of CSQ1 binding as discussed above. This may also provide some basis for the mechanism underlying the inhibition of RyR1 but activation of RyR2 by CSQ1 under the same conditions (Wei et al., 2009b).

7.4 Interplay between triadin/junctin/CSQ/RyR in skeletal and cardiac muscle

In the skeletal system, separate roles of junctin and triadin have been also been indicated in intact myotubes. Studies in dyspedic myotubes (Goonasekera et al., 2007) and in C2C12 cells (Wang et al., 2009) suggest that triadin facilitates depolarization-induced Ca^{2+} release and so is more involved in EC coupling, while junctin plays a major role in SR Ca^{2+} load and supports Ca^{2+} homeostasis and the resting activity of RyR channels, consistent with junctin mediating Ca^{2+} -dependent signals between CSQ1 and RyR1 (Wei et al., 2009a). However, recent mouse models with either junctin knockout or triadin knockout or junctin/triadin double knockout suggest that the disruption of triadin/CSQ1 link has a more profound impact on myoplasmic Ca^{2+} regulation than disruption of junctin/CSQ1 association (Boncompagni et al., 2012). Nevertheless, knocking out the triadin/junctin is accompanied by changes in junctional SR structure and CSQ1 expression and perhaps expression of other junctional proteins (Boncompagni et al., 2012), all of which would complicate the transgenic results and prevent a clear assessment of alterations directly attributable to a disrupted triadin/CSQ1 or junctin/CSQ1 complex. Therefore, the precise roles of triadin and junctin in SR Ca^{2+} regulation in skeletal muscle remain to be clearly elucidated.

In the cardiac system, the separate roles of junctin-CSQ2 and triadin-CSQ2 are yet to be addressed. There are only two studies directly testing the action of combined junctin and triadin in transmitting CSQ2 signal to RyR2 (Gyorke et al., 2004a; Wei et al., 2009b), with disparate results. In one study, addition of CSQ2 to the reconstituted RyR2/triadin/junctin complex inhibits canine RyR2 and allows SR luminal Ca^{2+} regulation of the channel (Gyorke et al., 2004a). In contrast, the other study with sheep RyR2 under different conditions shows that CSQ2 activates (does not inhibit) the CSQ-devoid native RyR2 (containing endogenous junctin

and triadin) (Wei et al., 2009b). Undoubtedly, species- and experimental condition-differences require further clarification, for example, the presence or absence of cytosolic Mg^{2+} and ATP, as it has been demonstrated that CSQ2 decreased or increased RyR2 channel activity when cytosolic MgATP was present or absent respectively (see (Chen et al., 2013) and Chapter 1.7.3.3), and it remains possible that there is also interaction between CSQ2 and other luminal proteins *in vivo* and the effects of which may impinge on the effects mediated through the CSQ2/triadin/junctin/RyR2 complex. The relative ratios of junctin/CSQ2 and triadin/CSQ2 may also account for the disparities between the two studies—5 $\mu\text{g/ml}$ of junctin, triadin and CSQ2 in (Gyorke et al., 2004a), while 16 $\mu\text{g/ml}$ of CSQ2 with endogenous junctin and triadin (concentrations unknown) in (Wei et al., 2009b). It has been shown junctin-CSQ2 ratios have a great impact on reversible CSQ2 polymerization and depolymerization, which may further affect CSQ2 sensing luminal $[Ca^{2+}]$ and its influence on RyR2 activity (Lee et al., 2012). The triadin-CSQ2 ratio being a critical modulator of the SR Ca^{2+} signalling has also been suggested in ventricular myocytes (Kucerova et al., 2012). So far, no studies have further characterized the specific effect of junctin or triadin alone on CSQ2 regulation of RyR2.

A hypothetical mechanism of the potential interplay between junctin/triadin/CSQ/RyR in skeletal and cardiac muscle is illustrated in Fig. 7-1. This model ties together previously published results (Altschafel et al., 2011; Goonasekera et al., 2007; Gyorke et al., 2004a; Wei et al., 2009a; Wei et al., 2009b) with the findings and speculations of this study (under Discussion section 7.2-7.4). This model is based on the following assumptions: 1) the single KEKE motif binding site in triadin is unable to bind to RyR and CSQ simultaneously, thus binding of CSQ to triadin results in disruption of triadin binding to RyR, 2) the junctin (possibly the “true” KEKE motif)-binding site in RyR pore loop is a separate site from that of triadin. Multiple binding sites on junctin and RyR for the junctin-RyR interaction are shown in this model (those interactions not been clearly defined yet are indicated with question marks in Fig. 7-1), supporting the notion that junctin can bind to RyR and CSQ at the same time thus is able to convey signals from CSQ to RyR.

Despite the numerous gaps that remain in the CSQ-junctin/triadin-RyR story, it is clear that a complex integration of signals arising from the interactions between these proteins regulates Ca^{2+} homeostasis in skeletal and cardiac muscle. There is still a long way to go before we grasp the whole picture of the interactions between the proteins, including the influence of each on the expression of the others. However, knowledge of the basic elements of these interactions is essential for building an understanding of the whole process.

A model of potential interplay between junctin/triadin/CSQ/RyR in skeletal and cardiac muscle

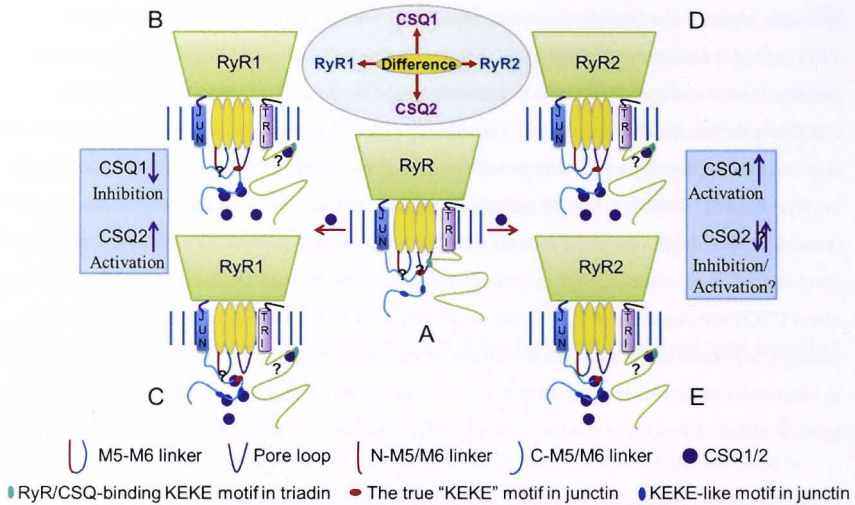


Figure 7-1 A schematic model for potential interplay between CSQ/junctin/RyR/triadin in skeletal and cardiac muscle. (A) Cartoon of RyRs associated with junctin (JUN) and triadin (TRI) before CSQ addition. (B) & (C) Interaction between CSQ (CSQ1/CSQ2), junctin, skeletal triadin and RyR1. (D) & (E) interaction between CSQ (CSQ1/2), junctin, cardiac triadin and RyR2. Triadin is shown to bind to a separate RyR site in the pore loop from that of junctin. The quaternary CSQ-junctin-RyR-triadin interaction tethers CSQ close to the release channel pore. CSQ binding to triadin results in disruption of triadin binding to RyR. There are two possibilities for CSQ binding to junctin when the same CSQ isoform was added: 1) CSQ binds to junctin through different sites from that of RyR to junctin, differences between RyR1 and RyR2 results in different changes in RyR channel activity upon CSQ addition (B&D); 2) CSQ binds to junctin through the same KEKE motif in junctin that is presumably bound to the RyR pore loop, therefore binding of CSQ to junctin results in removal of the KEKE motif inhibitory effect on RyRs and reveals the effects of junctin binding to the M5-M6 linker of RyR (C&E). The effects are likely to be different between RyR1 and RyR2 (activation or inhibition as indicated by purple arrows) which is due to the possibility that either (a) there is low sequence similarity in the C-terminal region of the M5-M6 linker (C-M5/M6 linker) if junctin does binds to this region in RyR1; or (b) junctin binds to the M5-M6 linker in RyR2 but not in RyR1. The difference between CSQ1 and CSQ2 may account for their different effects on the overall functional consequences of the interaction between CSQ, junctin and the RyR isoform channel (e.g., RyR1 is inhibited by CSQ1 but activated by CSQ2, indicated in the light blue box). Solid purple downward arrows indicate inhibitory effects on the RyR, while upward arrows denote activation. Question marks indicate interactions/effects that have not thus far been definitely determined.

7.5 Conclusion

In conclusion, this research has provided novel information on the molecular mechanism underlying junctin regulating the RyR Ca^{2+} release channel in skeletal and cardiac muscle. Of particular importance are the new details of the effects of the cytoplasmic N-terminal domain of junctin on RyRs. The results have shed important light on the complex regulation of the RyR from both its cytoplasmic and luminal side by junctin and provide an explanation of the mechanism for CSQ1/RyR/junctin complex interactions.

7.6 Future directions

The work presented in this thesis has advanced our knowledge of junctin-RyR interaction; however there are still many unknowns in the junctin-related regulatory effects on RyR Ca^{2+} release that remain to be resolved and may be included in future research plans.

- In the present study it has been established that there are RyR1-junctin interacting sites on the cytoplasmic and luminal domains of the proteins, however the actual binding sites remains to be precisely located. The Njun-binding site in RyR1 has been localized in the cytoplasmic domain (residues 183-2156, work by Dr. Shamaruh Mirza). An aim of future research would be to identify the binding region in RyR1 for Njun. The identification of the precise location of the Njun binding site in RyR2 is of equal importance. Regarding Cjun-binding site in RyR1, further examinations are required. Site-directed mutagenesis in the M5-M6 linker and the pore loop of the RyR1 and/or RyR2 may provide valuable insight into residues that are critical for Cjun binding. Overall, the information yielded from these studies will help us better understand the Njun “docking” and Cjun “modulating” theory.
- Biochemical and functional studies demonstrated that the one “true” KEKE motif (for definition, see Chapter 6.1 and (Realini et al., 1994)) in junctin is able to bind to and inhibit RyRs. In order to obtain a more complete understanding of the role of this KEKE motif in the binding and inhibition of RyRs, mutation and knock out in either the FLjun or the Cjun should be performed, with binding and RyR activity studies. In addition, a reconstitution of mutated FLjun, CSQ1 and RyR1 in lipid bilayer system may provide some insight into whether junctin’s KEKE motif is involved in junctin relaying CSQ1 signal to RyR1. Further investigations also need to be carried out to identify the precise binding site for the KEKE motif in RyR. Likewise, mutations could be carried out in the pore loop of RyR which is speculated above to be the KEKE motif-binding site. Similar studies could be performed on other sites if new binding domains other than the pore loop in RyR for the KEKE motif are identified. The ability of the KEKE motif peptide to modulate the mutated RyRs could be assessed in lipid bilayers.

- In addition to the “true” KEKE motif, there are other KEKE-like motifs in junctin (e.g., ¹¹³ESKHEERKRGKKEK¹²⁶, ¹⁴⁹KKSKEKEKAESA KTKENRKK¹⁶⁸ in rabbit cardiac isoform). Questions as to whether they can interact with the RyR directly and modulate channel activity and whether they are involved in RyR/CSQ/triadin/junctin interactions remain to be answered.
- In this study, it has been demonstrated that Njun and Cjun have distinct roles in junctin regulating RyRs: dictator and modulator, respectively. As junctin can convey CSQ1 signal to RyR1, it is an interesting question that which domain (s) of junctin is/are responsible for junctin as a transmitter. This project is currently underway. The investigation of the contributions of Njun and Cjun in transmitting signals between CSQ1 and RyR1 will give valuable insight into junctin/CSQ1/RyR1 interaction.
- Junctin-CSQ2 molar ratios have been shown to be important in Ca²⁺-dependent CSQ depolymerization. A ratio of ~1 results in the most CSQ2 depolymerization, whereas either higher or lower ratios cause less depolymerization, indicating the importance of a stoichiometric interaction of junctin and CSQ2 in CSQ2 depolymerization (Lee et al., 2012). Therefore, it would be interesting to test what the functional consequences of different ratios of junctin-CSQ2 on RyR2 activity at different luminal Ca²⁺ concentrations. Knowledge of this may provide valuable insight into the observed alterations in transgenic studies or in some heart failure conditions where CSQ2 or junctin levels are significantly changed.
- The results presented in this thesis were exclusively obtained from *in vitro* studies. Thus, it will be necessary to test the interactions identified here in an *in vivo* setting in order to validate their physiological relevance. This includes confirmation of Njun interaction with RyRs, the significance of which has been tested in several ways with native RyRs *in vitro*. For example a mice model could be engineered that expresses only Cjun but not FLjun, since Cjun has been shown to be able to target to jSR by itself (Rossi et al., 2013). In this case, expression levels of RyR, CSQ and triadin or other Ca²⁺ handling proteins in the SR would also need to be assessed. The model may shed some light on the contribution of Cjun and Njun to the formation of the quaternary protein complex (RyR/CSQ/triadin/junctin), and to regulating RyR Ca²⁺ release and contraction in the heart and in skeletal muscle.

References

- Ahern, G.P., Junankar, P.R., and Dulhunty, A.F. (1994). Single channel activity of the ryanodine receptor calcium release channel is modulated by FK-506. *FEBS Lett* 352, 369-374.
- Ahern, G.P., Junankar, P.R., and Dulhunty, A.F. (1997). Subconductance states in single-channel activity of skeletal muscle ryanodine receptors after removal of FKBP12. *Biophys J* 72, 146-162.
- Altschafll, B.A., Arvanitis, D.A., Fuentes, O., Yuan, Q., Kranias, E.G., and Valdivia, H.H. (2011). Dual role of junctin in the regulation of ryanodine receptors and calcium release in cardiac ventricular myocytes. *J Physiol* 589, 6063-6080.
- Amador, F.J., Liu, S., Ishiyama, N., Plevin, M.J., Wilson, A., MacLennan, D.H., and Ikura, M. (2009). Crystal structure of type I ryanodine receptor amino-terminal beta-trefoil domain reveals a disease-associated mutation "hot spot" loop. *P Natl Acad Sci USA* 106, 11040-11044.
- Anderson, K., Lai, F.A., Liu, Q.Y., Rousseau, E., Erickson, H.P., and Meissner, G. (1989). Structural and functional characterization of the purified cardiac ryanodine receptor-Ca²⁺ release channel complex. *J Biol Chem* 264, 1329-1335.
- Arvanitis, D.A., Vafiadaki, E., Fan, G.C., Mitton, B.A., Gregory, K.N., Del Monte, F., Kontogianni-Konstantopoulos, A., Sanoudou, D., and Kranias, E.G. (2007). Histidine-rich Ca-binding protein interacts with sarcoplasmic reticulum Ca-ATPase. *Am J Physiol Heart Circ Physiol* 293, H1581-1589.
- Ashley, R.H., and Williams, A.J. (1990). Divalent cation activation and inhibition of single calcium release channels from sheep cardiac sarcoplasmic reticulum. *J Gen Physiol* 95, 981-1005.
- Baker, R.T., Catanzariti, A.M., Karunasekara, Y., Soboleva, T.A., Sharwood, R., Whitney, S., and Board, P.G. (2005). Using deubiquitylating enzymes as research tools. *Methods in Enzymology* 398, 540-554.
- Bal, N.C., Sharon, A., Gupta, S.C., Jena, N., Shaikh, S., Gyorko, S., and Periasamy, M. (2010). The catecholaminergic polymorphic ventricular tachycardia mutation R33Q disrupts the N-terminal structural motif that regulates reversible calsequestrin polymerization. *J Biol Chem* 285, 17188-17196.
- Balshaw, D., Gao, L., and Meissner, G. (1999). Luminal loop of the ryanodine receptor: a pore-forming segment? *Proc Natl Acad Sci U S A* 96, 3345-3347.
- Bannwarth, M., and Schulz, G.E. (2003). The expression of outer membrane proteins for crystallization. *Bba-Biomembranes* 1610, 37-45.
- Barg, S., Copello, J.A., and Fleischer, S. (1997). Different interactions of cardiac and skeletal muscle ryanodine receptors with FK-506 binding protein isoforms. *Am J Physiol* 272, C1726-1733.
- Bauerova-Hlinkova, V., Bauer, J., Hostinova, E., Gasperik, J., Beck, K., Borko, L., Faltinova, A., Zahradnikova, A., and Sevcik, J. (2011). Bioinformatics Domain Structure Prediction and Homology Modeling of Human Ryanodine Receptor 2. 325-352.
- Bauerova-Hlinkova, V., Hostinova, E., Gasperik, J., Beck, K., Borko, L., Lai, F.A., Zahradnikova, A., and Sevcik, J. (2010). Bioinformatic mapping and production of recombinant N-terminal domains of human cardiac ryanodine receptor 2. *Protein Expr Purif* 71, 33-41.

- Beard, N.A., Casarotto, M.G., Wei, L., Varsanyi, M., Laver, D.R., and Dulhunty, A.F. (2005). Regulation of ryanodine receptors by calsequestrin: effect of high luminal Ca²⁺ and phosphorylation. *Biophys J* 88, 3444-3454.
- Beard, N.A., Laver, D.R., and Dulhunty, A.F. (2004). Calsequestrin and the calcium release channel of skeletal and cardiac muscle. *Prog Biophys Mol Biol* 85, 33-69.
- Beard, N.A., Sakowska, M.M., Dulhunty, A.F., and Laver, D.R. (2002). Calsequestrin is an inhibitor of skeletal muscle ryanodine receptor calcium release channels. *Biophys J* 82, 310-320.
- Beard, N.A., Wei, L., Cheung, S.N., Kimura, T., Varsanyi, M., and Dulhunty, A.F. (2008). Phosphorylation of skeletal muscle calsequestrin enhances its Ca²⁺ binding capacity and promotes its association with junctin. *Cell Calcium* 44, 363-373.
- Beard, N.A., Wei, L., and Dulhunty, A.F. (2009). Ca²⁺ signaling in striated muscle: the elusive roles of triadin, junctin, and calsequestrin. *Eur Biophys J* 39, 27-36.
- Benacquista, B.L., Sharma, M.R., Samsó, M., Zorzato, F., Treves, S., and Wagenknecht, T. (2000). Amino acid residues 4425-4621 localized on the three-dimensional structure of the skeletal muscle ryanodine receptor. *Biophysical Journal* 78, 1349-1358.
- Berridge, M.J., Lipp, P., and Bootman, M.D. (2000). The versatility and universality of calcium signalling. *Nature reviews Molecular cell biology* 1, 11-21.
- Bers, D.M. (2001). *Excitation-contraction coupling and cardiac contractile force*, 2nd edn (Dordrecht ; Boston: Kluwer Academic Publishers).
- Bers, D.M. (2002). Cardiac excitation-contraction coupling. *Nature* 415, 198-205.
- Bers, D.M. (2004). Macromolecular complexes regulating cardiac ryanodine receptor function. *J Mol Cell Cardiol* 37, 417-429.
- Bhat, M.B., Zhao, J., Takeshima, H., and Ma, J. (1997). Functional calcium release channel formed by the carboxyl-terminal portion of ryanodine receptor. *Biophys J* 73, 1329-1336.
- Block, B.A., Imagawa, T., Campbell, K.P., and Franzini-Armstrong, C. (1988). Structural evidence for direct interaction between the molecular components of the transverse tubule/sarcoplasmic reticulum junction in skeletal muscle. *J Cell Biol* 107, 2587-2600.
- Boncompagni, S., Rossi, A.E., Micaroni, M., Beznoussenko, G.V., Polishchuk, R.S., Dirksen, R.T., and Protasi, F. (2009). Mitochondria are linked to calcium stores in striated muscle by developmentally regulated tethering structures. *Molecular biology of the cell* 20, 1058-1067.
- Boncompagni, S., Thomas, M., Lopez, J.R., Allen, P.D., Yuan, Q., Kranias, E.G., Franzini-Armstrong, C., and Perez, C.F. (2012). Triadin/Junctin double null mouse reveals a differential role for Triadin and Junctin in anchoring CASQ to the jSR and regulating Ca²⁺ homeostasis. *PLoS One* 7, e39962.
- Brandt, N.R., Caswell, A.H., Brandt, T., Brew, K., and Mellgren, R.L. (1992). Mapping of the calpain proteolysis products of the junctional foot protein of the skeletal muscle triad junction. *The Journal of membrane biology* 127, 35-47.
- Brandt, N.R., Caswell, A.H., Carl, S.A., Ferguson, D.G., Brandt, T., Brunschwig, J.P., and Bassett, A.L. (1993). Detection and localization of triadin in rat ventricular muscle. *J Membr Biol* 131, 219-228.
- Brandt, N.R., Caswell, A.H., Wen, S.R., and Talvenheimo, J.A. (1990). Molecular interactions of the junctional foot protein and dihydropyridine receptor in skeletal muscle triads. *J Membr Biol* 113, 237-251.

- Brette, F., and Orchard, C. (2003). T-tubule function in mammalian cardiac myocytes. *Circ Res* 92, 1182-1192.
- Brillantes, A.B., Ondrias, K., Scott, A., Kobrinisky, E., Ondriasova, E., Moschella, M.C., Jayaraman, T., Landers, M., Ehrlich, B.E., and Marks, A.R. (1994). Stabilization of calcium release channel (ryanodine receptor) function by FK506-binding protein. *Cell* 77, 513-523.
- Brooks, S.P., and Storey, K.B. (1992). Bound and determined: a computer program for making buffers of defined ion concentrations. *Anal Biochem* 201, 119-126.
- Bull, R., and Marengo, J.J. (1993). Sarcoplasmic reticulum release channels from frog skeletal muscle display two types of calcium dependence. *FEBS letters* 331, 223-227.
- Cai, W.F., Pritchard, T., Florea, S., Lam, C.K., Han, P., Zhou, X., Yuan, Q., Lehnart, S.E., Allen, P.D., and Kranias, E.G. (2012). Ablation of junctin or triadin is associated with increased cardiac injury following ischaemia/reperfusion. *Cardiovasc Res* 94, 333-341.
- Campbell, K.P., MacLennan, D.H., Jorgensen, A.O., and Mintzer, M.C. (1983). Purification and Characterization of Calsequestrin from Canine Cardiac Sarcoplasmic-Reticulum and Identification of the 53,000 Dalton Glycoprotein. *Journal of Biological Chemistry* 258, 1197-1204.
- Canato, M., Scorzeto, M., Giacomello, M., Protasi, F., Reggiani, C., and Stienen, G.J.M. (2010). Massive alterations of sarcoplasmic reticulum free calcium in skeletal muscle fibers lacking calsequestrin revealed by a genetically encoded probe. *P Natl Acad Sci USA* 107, 22326-22331.
- Capes, E.M., Loaiza, R., and Valdivia, H.H. (2011). Ryanodine receptors. *Skeletal muscle* 1, 18.
- Capote, J., Bolanos, P., Schuhmeier, R.P., Melzer, W., and Caputo, C. (2005). Calcium transients in developing mouse skeletal muscle fibres. *J Physiol* 564, 451-464.
- Carl, S.L., Felix, K., Caswell, A.H., Brandt, N.R., Ball, W.J., Jr., Vaghy, P.L., Meissner, G., and Ferguson, D.G. (1995). Immunolocalization of sarcolemmal dihydropyridine receptor and sarcoplasmic reticular triadin and ryanodine receptor in rabbit ventricle and atrium. *J Cell Biol* 129, 673-682.
- Carraro, U., Rizzi, C., and Sandri, M. (1991). Effective recovery by KCl precipitation of highly diluted muscle proteins solubilized with sodium dodecyl sulfate. *Electrophoresis* 12, 1005-1010.
- Caswell, A.H., and Brandt, N.R. (2002). Membrane topography of cardiac triadin. *Arch Biochem Biophys* 398, 61-72.
- Caswell, A.H., Brandt, N.R., Brunschwig, J.P., and Purkerson, S. (1991). Localization and partial characterization of the oligomeric disulfide-linked molecular weight 95,000 protein (triadin) which binds the ryanodine and dihydropyridine receptors in skeletal muscle triadic vesicles. *Biochemistry* 30, 7507-7513.
- Caswell, A.H., Motoike, H.K., Fan, H., and Brandt, N.R. (1999). Location of ryanodine receptor binding site on skeletal muscle triadin. *Biochemistry* 38, 90-97.
- Catanzariti, A.M., Soboleva, T.A., Jans, D.A., Board, P.G., and Baker, R.T. (2004a). An efficient system for high-level expression and easy purification of authentic recombinant proteins. *Protein science : a publication of the Protein Society* 13, 1331-1339.
- Catanzariti, A.M., Soboleva, T.A., Jans, D.A., Board, P.G., and Baker, R.T. (2004b). An efficient system for high-level expression and easy purification of authentic recombinant proteins. *Protein Sci* 13, 1331-1339.

- Chamberlain, B.K., and Fleischer, S. (1988). Isolation of canine cardiac sarcoplasmic reticulum. *Methods Enzymol* 157, 91-99.
- Chen, H., Valle, G., Furlan, S., Nani, A., Gyorke, S., Fill, M., and Volpe, P. (2013). Mechanism of calsequestrin regulation of single cardiac ryanodine receptor in normal and pathological conditions. *The Journal of general physiology*.
- Chen, S.R., Li, X., Ebisawa, K., and Zhang, L. (1997). Functional characterization of the recombinant type 3 Ca²⁺ release channel (ryanodine receptor) expressed in HEK293 cells. *The Journal of biological chemistry* 272, 24234-24246.
- Chen, S.R., Zhang, L., and MacLennan, D.H. (1992). Characterization of a Ca²⁺ binding and regulatory site in the Ca²⁺ release channel (ryanodine receptor) of rabbit skeletal muscle sarcoplasmic reticulum. *J Biol Chem* 267, 23318-23326.
- Chen, W., Steenbergen, C., Levy, L.A., Vance, J., London, R.E., and Murphy, E. (1996). Measurement of free Ca²⁺ in sarcoplasmic reticulum in perfused rabbit heart loaded with 1,2-bis(2-amino-5,6-difluorophenoxy)ethane-N,N,N',N'-tetraacetic acid by ¹⁹F NMR. *J Biol Chem* 271, 7398-7403.
- Ching, L.L., Williams, A.J., and Sitsapesan, R. (2000). Evidence for Ca(2+) activation and inactivation sites on the luminal side of the cardiac ryanodine receptor complex. *Circulation research* 87, 201-206.
- Cho, J.H., Oh, Y.S., Park, K.W., Yu, J., Choi, K.Y., Shin, J.Y., Kim, D.H., Park, W.J., Hamada, T., Kagawa, H., et al. (2000). Calsequestrin, a calcium sequestering protein localized at the sarcoplasmic reticulum, is not essential for body-wall muscle function in *Caenorhabditis elegans*. *J Cell Sci* 113 (Pt 22), 3947-3958.
- Chopra, N., Kannankeril, P.J., Yang, T., Hlaing, T., Holinstat, I.A., Etensohn, K., Pfeifer, K., Akin, B., Jones, L.R., Franzini-Armstrong, C., et al. (2007). Reduction of cardiac calsequestrin increases sarcoplasmic reticulum Ca²⁺-Leak independent of luminal Ca²⁺ and triggers ventricular Arrhythmias in mice. *Circulation* 116, 153-153.
- Chopra, N., and Knollmann, B.C. (2009). Cardiac Calsequestrin: The New Kid on the Block in Arrhythmias. *J Cardiovasc Electr* 20, 1179-1185.
- Chopra, N., and Knollmann, B.C. (2013). Triadin regulates cardiac muscle couplon structure and microdomain Ca(2+) signalling: a path towards ventricular arrhythmias. *Cardiovasc Res* 98, 187-191.
- Chopra, N., Yang, T., Asghari, P., Moore, E.D., Huke, S., Akin, B., Cattolica, R.A., Perez, C.F., Hlaing, T., Knollmann-Ritschel, B.E., et al. (2009). Ablation of triadin causes loss of cardiac Ca²⁺ release units, impaired excitation-contraction coupling, and cardiac arrhythmias. *Proc Natl Acad Sci U S A* 106, 7636-7641.
- Chu, A., Dixon, M.C., Saito, A., Seiler, S., and Fleischer, S. (1988). [4] Isolation of sarcoplasmic reticulum fractions referable to longitudinal tubules and functional terminal cisternae from rabbit skeletal muscle. In *Methods in Enzymology*, B.F. Sidney Fleischer, ed. (Academic Press), pp. 36-46.
- Chu, A., Fill, M., Stefani, E., and Entman, M.L. (1993). Cytoplasmic Ca²⁺ does not inhibit the cardiac muscle sarcoplasmic reticulum ryanodine receptor Ca²⁺ channel, although Ca(2+)-induced Ca²⁺ inactivation of Ca²⁺ release is observed in native vesicles. *The Journal of membrane biology* 135, 49-59.
- Colpo, P., Nori, A., Sacchetto, R., Damiani, E., and Margreth, A. (2001). Phosphorylation of the triadin cytoplasmic domain by CaM protein kinase in rabbit fast-twitch muscle sarcoplasmic reticulum. *Mol Cell Biochem* 223, 139-145.
- Combet, C., Blanchet, C., Geourjon, C., and Deleage, G. (2000). NPS@: network protein sequence analysis. *Trends in biochemical sciences* 25, 147-150.

- Copello, J.A., Barg, S., Onoue, H., and Fleischer, S. (1997). Heterogeneity of Ca²⁺ gating of skeletal muscle and cardiac ryanodine receptors. *Biophys J* 73, 141-156.
- Costello, B., Chadwick, C., Saito, A., Chu, A., Maurer, A., and Fleischer, S. (1986). Characterization of the Junctional Face Membrane from Terminal Cisternae of Sarcoplasmic-Reticulum. *Journal of Cell Biology* 103, 741-753.
- Cozens, B., and Reithmeier, R.A. (1984). Size and shape of rabbit skeletal muscle calsequestrin. *J Biol Chem* 259, 6248-6252.
- Cukierman, S., Yellen, G., and Miller, C. (1985). The K⁺ channel of sarcoplasmic reticulum. A new look at Cs⁺ block. *Biophysical Journal* 48, 477-484.
- Dainese, M., Quarta, M., Lyfenko, A.D., Paolini, C., Canato, M., Reggiani, C., Dirksen, R.T., and Protasi, F. (2009). Anesthetic- and heat-induced sudden death in calsequestrin-1 knockout mice. *FASEB Journal* 23, 1710-1720.
- Damiani, E., Picello, E., Saggini, L., and Margreth, A. (1995). Identification of triadin and of histidine-rich Ca(2+)-binding protein as substrates of 60 kDa calmodulin-dependent protein kinase in junctional terminal cisternae of sarcoplasmic reticulum of rabbit fast muscle. *Biochem Biophys Res Commun* 209, 457-465.
- Das, S.K., Chu, W., Zhang, Z., Hasstedt, S.J., and Elbein, S.C. (2004). Calsequestrin 1 (CASQ1) gene polymorphisms under chromosome 1q21 linkage peak are associated with type 2 diabetes in Northern European Caucasians. *Diabetes* 53, 3300-3306.
- Denegri, M., Avelino-Cruz, J.E., Boncompagni, S., De Simone, S.A., Auricchio, A., Villani, L., Volpe, P., Protasi, F., Napolitano, C., and Priori, S.G. (2012). Viral gene transfer rescues arrhythmogenic phenotype and ultrastructural abnormalities in adult calsequestrin-null mice with inherited arrhythmias. *Circ Res* 110, 663-668.
- Di Blasi, C., Blasevich, F., Bellafiore, E., Mottarelli, E., Gibertini, S., Zanotti, S., Saredi, S., Mantegazza, R., Morandi, L., and Mora, M. (2010). Calsequestrin and junctin immunoreactivity in hexagonally cross-linked tubular arrays myopathy. *Neuromuscular disorders* : NMD 20, 326-329.
- Dinchuk, J.E., Henderson, N.L., Burn, T.C., Huber, R., Ho, S.P., Link, J., O'Neil, K.T., Focht, R.J., Scully, M.S., Hollis, J.M., et al. (2000). Aspartyl beta -hydroxylase (Asph) and an evolutionarily conserved isoform of Asph missing the catalytic domain share exons with junctin. *The Journal of biological chemistry* 275, 39543-39554.
- Donoso, P., Prieto, H., and Hidalgo, C. (1995). Luminal calcium regulates calcium release in triads isolated from frog and rabbit skeletal muscle. *Biophys J* 68, 507-515.
- Doyle, D.A., Morais Cabral, J., Pfuetzner, R.A., Kuo, A., Gulbis, J.M., Cohen, S.L., Chait, B.T., and MacKinnon, R. (1998). The structure of the potassium channel: molecular basis of K⁺ conduction and selectivity. *Science* 280, 69-77.
- Du, G.G., Avila, G., Sharma, P., Khanna, V.K., Dirksen, R.T., and MacLennan, D.H. (2004). Role of the sequence surrounding predicted transmembrane helix M4 in membrane association and function of the Ca(2+) release channel of skeletal muscle sarcoplasmic reticulum (ryanodine receptor isoform 1). *J Biol Chem* 279, 37566-37574.
- Du, G.G., Guo, X., Khanna, V.K., and MacLennan, D.H. (2001). Functional characterization of mutants in the predicted pore region of the rabbit cardiac muscle Ca(2+) release channel (ryanodine receptor isoform 2). *The Journal of biological chemistry* 276, 31760-31771.
- Du, G.G., Khanna, V.K., and MacLennan, D.H. (2000). Mutation of divergent region 1 alters caffeine and Ca(2+) sensitivity of the skeletal muscle Ca(2+) release channel (ryanodine receptor). *J Biol Chem* 275, 11778-11783.

- Du, G.G., Sandhu, B., Khanna, V.K., Guo, X.H., and MacLennan, D.H. (2002). Topology of the Ca²⁺ release channel of skeletal muscle sarcoplasmic reticulum (RyR1). *Proc Natl Acad Sci U S A* 99, 16725-16730.
- Dulhunty, A., Gage, P., Curtis, S., Chelvanayagam, G., and Board, P. (2001a). The glutathione transferase structural family includes a nuclear chloride channel and a ryanodine receptor calcium release channel modulator. *J Biol Chem* 276, 3319-3323.
- Dulhunty, A., Wei, L., and Beard, N. (2009). Junctin - the quiet achiever. *J Physiol* 587, 3135-3137.
- Dulhunty, A.F. (2006). Excitation-contraction coupling from the 1950s into the new millennium. *Clinical and Experimental Pharmacology and Physiology* 33, 763-772.
- Dulhunty, A.F., Beard, N.A., Pouliquin, P., and Kimura, T. (2006). Novel regulators of RyR Ca²⁺ release channels: insight into molecular changes in genetically-linked myopathies. *J Muscle Res Cell Motil* 27, 351-365.
- Dulhunty, A.F., Junankar, P.R., Eager, K.R., Ahern, G.P., and Laver, D.R. (1996). Ion channels in the sarcoplasmic reticulum of striated muscle. *Acta physiologica Scandinavica* 156, 375-385.
- Dulhunty, A.F., Laver, D.R., Curtis, S.M., Pace, S., Haarmann, C., and Gallant, E.M. (2001b). Characteristics of irreversible ATP activation suggest that native skeletal ryanodine receptors can be phosphorylated via an endogenous CaMKII. *Biophys J* 81, 3240-3252.
- Dulhunty, A.F., Laver, D.R., Gallant, E.M., Casarotto, M.G., Pace, S.M., and Curtis, S. (1999). Activation and inhibition of skeletal RyR channels by a part of the skeletal DHPR II-III loop: effects of DHPR Ser687 and FKBP12. *Biophysical Journal* 77, 189-203.
- Dulhunty, A.F., and Pouliquin, P. (2003). What we don't know about the structure of ryanodine receptor calcium release channels. *Clinical and experimental pharmacology & physiology* 30, 713-723.
- Dulhunty, A.F., Wium, E., Li, L., Hanna, A.D., Mirza, S., Talukder, S., Ghazali, N.A., and Beard, N.A. (2012). Proteins within the intracellular calcium store determine cardiac RyR channel activity and cardiac output. *Clinical and experimental pharmacology & physiology* 39, 477-484.
- Eager, K.R., and Dulhunty, A.F. (1999). Cardiac ryanodine receptor activity is altered by oxidizing reagents in either the luminal or cytoplasmic solution. *The Journal of membrane biology* 167, 205-214.
- Eltit, J.M., Feng, W., Lopez, J.R., Padilla, I.T., Pessah, I.N., Molinski, T.F., Fruen, B.R., Allen, P.D., and Perez, C.F. (2010). Ablation of skeletal muscle triadin impairs FKBP12/RyR1 channel interactions essential for maintaining resting cytoplasmic Ca²⁺. *J Biol Chem* 285, 38453-38462.
- Eltit, J.M., Szpyt, J., Li, H., Allen, P.D., and Perez, C.F. (2011). Reduced gain of excitation-contraction coupling in triadin-null myotubes is mediated by the disruption of FKBP12/RyR1 interaction. *Cell Calcium* 49, 128-135.
- Engelhardt, S., Boknik, P., Keller, U., Neumann, J., Lohse, M.J., and Hein, L. (2001). Early impairment of calcium handling and altered expression of junctin in hearts of mice overexpressing the beta1-adrenergic receptor. *FASEB J* 15, 2718-2720.
- Euden, J., Mason, S.A., and Williams, A.J. (2013). Functional characterization of the cardiac ryanodine receptor pore-forming region. *PLoS One* 8, e66542.
- Fabiato, A. (1985). Time and calcium dependence of activation and inactivation of calcium-induced release of calcium from the sarcoplasmic reticulum of a skinned canine cardiac Purkinje cell. *The Journal of general physiology* 85, 247-289.

- Faggioni, M., and Knollmann, B.C. (2012). Calsequestrin 2 and arrhythmias. *Am J Physiol Heart Circ Physiol* 302, H1250-1260.
- Fan, G.C., Yuan, Q., and Kranias, E.G. (2008). Regulatory roles of junctin in sarcoplasmic reticulum calcium cycling and myocardial function. *Trends Cardiovasc Med* 18, 1-5.
- Fan, G.C., Yuan, Q.Y., Zhao, W., Chu, G.X., and Kranias, E.G. (2007). Junctin is a prominent regulator of contractility in cardiomyocytes. *Biochemical and Biophysical Research Communications* 352, 617-622.
- Fan, H., Brandt, N.R., and Caswell, A.H. (1995). Disulfide bonds, N-glycosylation and transmembrane topology of skeletal muscle triadin. *Biochemistry* 34, 14902-14908.
- Feriotto, G., Finotti, A., Volpe, P., Treves, S., Ferrari, S., Angelelli, C., Zorzato, F., and Gambari, R. (2005). Myocyte enhancer factor 2 activates promoter sequences of the human AbetaH-J-J locus, encoding aspartyl-beta-hydroxylase, junctin, and junctate. *Mol Cell Biol* 25, 3261-3275.
- Field, A.C., Hill, C., and Lamb, G.D. (1988). Asymmetric charge movement and calcium currents in ventricular myocytes of neonatal rat. *J Physiol* 406, 277-297.
- Fieni, F., Bae Lee, S., Jan, Y.N., and Kirichok, Y. (2012). Activity of the mitochondrial calcium uniporter varies greatly between tissues. *Nat Commun* 3, 1317.
- Fill, M., and Copello, J.A. (2002). Ryanodine receptor calcium release channels. *Physiological reviews* 82, 893-922.
- Fill, M., Coronado, R., Mickelson, J.R., Vilven, J., Ma, J.J., Jacobson, B.A., and Louis, C.F. (1990). Abnormal ryanodine receptor channels in malignant hyperthermia. *Biophysical Journal* 57, 471-475.
- Fleischer, S., Ogunbunmi, E.M., Dixon, M.C., and Fleer, E.A. (1985). Localization of Ca²⁺ release channels with ryanodine in junctional terminal cisternae of sarcoplasmic reticulum of fast skeletal muscle. *P Natl Acad Sci USA* 82, 7256-7259.
- Fliegel, L., Newton, E., Burns, K., and Michalak, M. (1990). Molecular cloning of cDNA encoding a 55-kDa multifunctional thyroid hormone binding protein of skeletal muscle sarcoplasmic reticulum. *J Biol Chem* 265, 15496-15502.
- Fodor, J., Gonczi, M., Sztretye, M., Dienes, B., Olah, T., Szabo, L., Csoma, E., Szentesi, P., Szigeti, G.P., Marty, I., et al. (2008). Altered expression of triadin 95 causes parallel changes in localized Ca²⁺ release events and global Ca²⁺ signals in skeletal muscle cells in culture. *J Physiol* 586, 5803-5818.
- Foskett, J.K., White, C., Cheung, K.H., and Mak, D.O. (2007). Inositol trisphosphate receptor Ca²⁺ release channels. *Physiol Rev* 87, 593-658.
- Franzini-Armstrong, C. (1970). STUDIES OF THE TRIAD : I. Structure of the Junction in Frog Twitch Fibers. *The Journal of cell biology* 47, 488-499.
- Franzini-Armstrong, C. (2009). Architecture and regulation of the Ca²⁺ delivery system in muscle cells. *Applied physiology, nutrition, and metabolism = Physiologie appliquee, nutrition et metabolisme* 34, 323-327.
- Franzini-Armstrong, C., Kenney, L.J., and Varriano-Marston, E. (1987). The structure of calsequestrin in triads of vertebrate skeletal muscle: a deep-etch study. *J Cell Biol* 105, 49-56.
- Franzini-Armstrong, C., and Nunzi, G. (1983). Junctional feet and particles in the triads of a fast-twitch muscle fibre. *J Muscle Res Cell Motil* 4, 233-252.
- Franzini-Armstrong, C., and Protasi, F. (1997). Ryanodine receptors of striated muscles: a complex channel capable of multiple interactions. *Physiological reviews* 77, 699-729.

- Franzini-Armstrong, C., Protasi, F., and Ramesh, V. (1998). Comparative ultrastructure of Ca²⁺ release units in skeletal and cardiac muscle. *Ann N Y Acad Sci* 853, 20-30.
- Franzini-Armstrong, C., Protasi, F., and Ramesh, V. (1999). Shape, size, and distribution of Ca(2+) release units and couplons in skeletal and cardiac muscles. *Biophys J* 77, 1528-1539.
- Franzini-Armstrong, C., Protasi, F., and Tijssens, P. (2005). The assembly of calcium release units in cardiac muscle. *Ann N Y Acad Sci* 1047, 76-85.
- Froemming, G.R., Murray, B.E., and Ohlendieck, K. (1999). Self-aggregation of triadin in the sarcoplasmic reticulum of rabbit skeletal muscle. *Biochimica et biophysica acta* 1418, 197-205.
- Fryer, M.W., and Stephenson, D.G. (1996). Total and sarcoplasmic reticulum calcium contents of skinned fibres from rat skeletal muscle. *J Physiol* 493 (Pt 2), 357-370.
- Fu, M., Damcott, C.M., Sabra, M., Pollin, T.I., Ott, S.H., Wang, J., Garant, M.J., O'Connell, J.R., Mitchell, B.D., and Shuldiner, A.R. (2004). Polymorphism in the calsequestrin 1 (CASQ1) gene on chromosome 1q21 is associated with type 2 diabetes in the old order Amish. *Diabetes* 53, 3292-3299.
- Furuichi, T., Furutama, D., Hakamata, Y., Nakai, J., Takeshima, H., and Mikoshiba, K. (1994). Multiple types of ryanodine receptor/Ca²⁺ release channels are differentially expressed in rabbit brain. *The Journal of neuroscience : the official journal of the Society for Neuroscience* 14, 4794-4805.
- Gatti, G., Trifari, S., Mesaeli, N., Parker, J.M., Michalak, M., and Meldolesi, J. (2001). Head-to-tail oligomerization of calsequestrin: a novel mechanism for heterogeneous distribution of endoplasmic reticulum luminal proteins. *J Cell Biol* 154, 525-534.
- Gergs, U., Berndt, T., Buskase, J., Jones, L.R., Kirchhefer, U., Muller, F.U., Schluter, K.D., Schmitz, W., and Neumann, J. (2007). On the role of junctin in cardiac Ca²⁺ handling, contractility, and heart failure. *Am J Physiol Heart Circ Physiol* 293, H728-734.
- Gergs, U., Kirchhefer, U., Buskase, J., Kiele-Dunsche, K., Buchwalow, I.B., Jones, L.R., Schmitz, W., Traub, O., and Neumann, J. (2011). Sarcoplasmic reticulum Ca²⁺ release in neonatal rat cardiac myocytes. *J Mol Cell Cardiol* 51, 682-688.
- Giannini, G., Conti, A., Mammarella, S., Scrobogna, M., and Sorrentino, V. (1995). The ryanodine receptor/calcium channel genes are widely and differentially expressed in murine brain and peripheral tissues. *J Cell Biol* 128, 893-904.
- Gilchrist, J.S., Belcastro, A.N., and Katz, S. (1992). Intraluminal Ca²⁺ dependence of Ca²⁺ and ryanodine-mediated regulation of skeletal muscle sarcoplasmic reticulum Ca²⁺ release. *J Biol Chem* 267, 20850-20856.
- Ginsburg, K.S., Weber, C.R., and Bers, D.M. (1998). Control of Maximum Sarcoplasmic Reticulum Ca Load in Intact Ferret Ventricular Myocytes: Effects of Thapsigargin and Isoproterenol. *The Journal of General Physiology* 111, 491-504.
- Glover, L., Culligan, K., Cala, S., Mulvey, C., and Ohlendieck, K. (2001). Calsequestrin binds to monomeric and complexed forms of key calcium-handling proteins in native sarcoplasmic reticulum membranes from rabbit skeletal muscle. *Biochimica et biophysica acta* 1515, 120-132.
- Godt, R.E., and Maughan, D.W. (1988). On the composition of the cytosol of relaxed skeletal muscle of the frog. *Am J Physiol* 254, C591-604.
- Goonasekera, S.A., Beard, N.A., Groom, L., Kimura, T., Lyfenko, A.D., Rosenfeld, A., Marty, I., Dulhunty, A.F., and Dirksen, R.T. (2007). Triadin binding to the C-terminal luminal

- loop of the ryanodine receptor is important for skeletal muscle excitation contraction coupling. *J Gen Physiol* 130, 365-378.
- Groh, S., Marty, I., Ottolia, M., Prestipino, G., Chapel, A., Villaz, M., and Ronjat, M. (1999). Functional interaction of the cytoplasmic domain of triadin with the skeletal ryanodine receptor. *J Biol Chem* 274, 12278-12283.
- Grunwald, R., and Meissner, G. (1995). Lumenal sites and C terminus accessibility of the skeletal muscle calcium release channel (ryanodine receptor). *The Journal of biological chemistry* 270, 11338-11347.
- Guo, W., and Campbell, K.P. (1995). Association of triadin with the ryanodine receptor and calsequestrin in the lumen of the sarcoplasmic reticulum. *J Biol Chem* 270, 9027-9030.
- Guo, W., Jorgensen, A.O., and Campbell, K.P. (1996a). Triadin, a linker for calsequestrin and the ryanodine receptor. *Society of General Physiologists series* 51, 19-28.
- Guo, W., Jorgensen, A.O., Jones, L.R., and Campbell, K.P. (1996b). Biochemical characterization and molecular cloning of cardiac triadin. *J Biol Chem* 271, 458-465.
- Guyton, A.C., and Hall, J.E. (2006). *Textbook of Medical Physiology*, 11 edn (Philadelphia: Elsevier).
- Gyorke, I., and Gyorke, S. (1998). Regulation of the cardiac ryanodine receptor channel by luminal Ca^{2+} involves luminal Ca^{2+} sensing sites. *Biophys J* 75, 2801-2810.
- Gyorke, I., Hester, N., Jones, L.R., and Gyorke, S. (2004a). The role of calsequestrin, triadin, and junctin in conferring cardiac ryanodine receptor responsiveness to luminal calcium. *Biophys J* 86, 2121-2128.
- Gyorke, S., Gyorke, I., Lukyanenko, V., Terentyev, D., Viatchenko-Karpinski, S., and Wiesner, T.F. (2002). Regulation of sarcoplasmic reticulum calcium release by luminal calcium in cardiac muscle. *Front Biosci* 7, d1454-1463.
- Gyorke, S., Gyorke, I., Terentyev, D., Viatchenko-Karpinski, S., and Williams, S.C. (2004b). Modulation of sarcoplasmic reticulum calcium release by calsequestrin in cardiac myocytes. *Biol Res* 37, 603-607.
- Gyorke, S., Stevens, S.C., and Terentyev, D. (2009). Cardiac calsequestrin: quest inside the SR. *J Physiol* 587, 3091-3094.
- Gyorke, S., and Terentyev, D. (2008). Modulation of ryanodine receptor by luminal calcium and accessory proteins in health and cardiac disease. *Cardiovasc Res* 77, 245-255.
- Hain, J., Onoue, H., Mayrleitner, M., Fleischer, S., and Schindler, H. (1995). Phosphorylation modulates the function of the calcium release channel of sarcoplasmic reticulum from cardiac muscle. *J Biol Chem* 270, 2074-2081.
- Hakamata, Y., Nakai, J., Takeshima, H., and Imoto, K. (1992). Primary structure and distribution of a novel ryanodine receptor/calcium release channel from rabbit brain. *FEBS letters* 312, 229-235.
- Hanna, A.D., Janczura, M., Cho, E., Dulhunty, A.F., and Beard, N.A. (2011). Multiple actions of the anthracycline daunorubicin on cardiac ryanodine receptors. *Mol Pharmacol* 80, 538-549.
- Hayek, S.M., Zhao, J., Bhat, M., Xu, X., Nagaraj, R., Pan, Z., Takeshima, H., and Ma, J. (1999). A negatively charged region of the skeletal muscle ryanodine receptor is involved in Ca^{2+} -dependent regulation of the Ca^{2+} release channel. *FEBS letters* 461, 157-164.
- He, Z., Dunker, A.K., Wesson, C.R., and Trumble, W.R. (1993). Ca^{2+} -induced folding and aggregation of skeletal muscle sarcoplasmic reticulum calsequestrin. The involvement of the trifluoperazine-binding site. *J Biol Chem* 268, 24635-24641.

- Herrmann-Frank, A., and Lehmann-Horn, F. (1996). Regulation of the purified Ca²⁺ release channel/ryanodine receptor complex of skeletal muscle sarcoplasmic reticulum by luminal calcium. *Pflügers Archiv : European journal of physiology* 432, 155-157.
- Hohenegger, M., Herrmann-Frank, A., Richter, M., and Lehmann-Horn, F. (1995). Activation and labelling of the purified skeletal muscle ryanodine receptor by an oxidized ATP analogue. *The Biochemical journal* 308 (Pt 1), 119-125.
- Hollingworth, S., Zhao, M., and Baylor, S.M. (1996). The amplitude and time course of the myoplasmic free [Ca²⁺] transient in fast-twitch fibers of mouse muscle. *The Journal of general physiology* 108, 455-469.
- Holloway, P.W. (1973). A simple procedure for removal of triton X-100 from protein samples. *Analytical Biochemistry* 53, 304-308.
- Holmberg, S.R., and Williams, A.J. (1989). Single channel recordings from human cardiac sarcoplasmic reticulum. *Circ Res* 65, 1445-1449.
- Hong, C.S., Cho, M.C., Kwak, Y.G., Song, C.H., Lee, Y.H., Lim, J.S., Kwon, Y.K., Chae, S.W., and Kim, D.H. (2002). Cardiac remodeling and atrial fibrillation in transgenic mice overexpressing junctin. *FASEB J* 16, 1310-1312.
- Hong, C.S., Ji, J.H., Kim, J.P., Jung, D.H., and Kim, D.H. (2001). Molecular cloning and characterization of mouse cardiac triadin isoforms. *Gene* 278, 193-199.
- Houle, T.D., Ram, M.L., and Cala, S.E. (2004). Calsequestrin mutant D307H exhibits depressed binding to its protein targets and a depressed response to calcium. *Cardiovasc Res* 64, 227-233.
- Howarth, F.C., Glover, L., Culligan, K., Qureshi, M.A., and Ohlendieck, K. (2002). Calsequestrin expression and calcium binding is increased in streptozotocin-induced diabetic rat skeletal muscle though not in cardiac muscle. *Pflügers Archiv : European journal of physiology* 444, 52-58.
- Huang, H.D., Lee, T.Y., Tzeng, S.W., and Horng, J.T. (2005). KinasePhos: a web tool for identifying protein kinase-specific phosphorylation sites. *Nucleic acids research* 33, W226-229.
- Hymel, L., Inui, M., Fleischer, S., and Schindler, H. (1988). Purified ryanodine receptor of skeletal muscle sarcoplasmic reticulum forms Ca²⁺-activated oligomeric Ca²⁺ channels in planar bilayers. *Proc Natl Acad Sci U S A* 85, 441-445.
- Ikemoto, N., Bhatnagar, G.M., Nagy, B., and Gergely, J. (1972). Interaction of divalent cations with the 55,000-dalton protein component of the sarcoplasmic reticulum. Studies of fluorescence and circular dichroism. *J Biol Chem* 247, 7835-7837.
- Ikemoto, N., Nagy, B., Bhatnagar, G.M., and Gergely, J. (1974). Studies on a metal-binding protein of the sarcoplasmic reticulum. *J Biol Chem* 249, 2357-2365.
- Inui, M., Saito, A., and Fleischer, S. (1987a). Isolation of the ryanodine receptor from cardiac sarcoplasmic reticulum and identity with the feet structures. *J Biol Chem* 262, 15637-15642.
- Inui, M., Saito, A., and Fleischer, S. (1987b). Purification of the ryanodine receptor and identity with feet structures of junctional terminal cisternae of sarcoplasmic reticulum from fast skeletal muscle. *The Journal of biological chemistry* 262, 1740-1747.
- Jalilian, C., Gallant, E.M., Board, P.G., and Dulhunty, A.F. (2008). Redox potential and the response of cardiac ryanodine receptors to CLIC-2, a member of the glutathione S-transferase structural family. *Antioxid Redox Signal* 10, 1675-1686.
- Janowski, E., Cleemann, L., Sasse, P., and Morad, M. (2006). Diversity of Ca²⁺ signaling in developing cardiac cells. *Interactive and Integrative Cardiology* 1080, 154-164.

- Jayaraman, T., Brillantes, A.M., Timerman, A.P., Fleischer, S., Erdjument-Bromage, H., Tempst, P., and Marks, A.R. (1992). FK506 binding protein associated with the calcium release channel (ryanodine receptor). *J Biol Chem* 267, 9474-9477.
- Jenny, R.J., Mann, K.G., and Lundblad, R.L. (2003). A critical review of the methods for cleavage of fusion proteins with thrombin and factor Xa. *Protein Expr Purif* 31, 1-11.
- Jeyakumar, L.H., Copello, J.A., O'Malley, A.M., Wu, G.M., Grassucci, R., Wagenknecht, T., and Fleischer, S. (1998). Purification and characterization of ryanodine receptor 3 from mammalian tissue. *The Journal of biological chemistry* 273, 16011-16020.
- Jones, L.R., Suzuki, Y.J., Wang, W., Kobayashi, Y.M., Ramesh, V., Franzini-Armstrong, C., Cleemann, L., and Morad, M. (1998). Regulation of Ca²⁺ signaling in transgenic mouse cardiac myocytes overexpressing calsequestrin. *The Journal of clinical investigation* 101, 1385-1393.
- Jones, L.R., Zhang, L., Sanborn, K., Jorgensen, A.O., and Kelley, J. (1995). Purification, primary structure, and immunological characterization of the 26-kDa calsequestrin binding protein (junctin) from cardiac junctional sarcoplasmic reticulum. *J Biol Chem* 270, 30787-30796.
- Jung, D.H., Lee, C.J., Suh, C.K., You, H.J., and Kim, D.H. (2005). Molecular properties of excitation-contraction coupling proteins in infant and adult human heart tissues. *Mol Cells* 20, 51-56.
- Kaftan, E., Marks, A.R., and Ehrlich, B.E. (1996). Effects of rapamycin on ryanodine receptor/Ca(2+)-release channels from cardiac muscle. *Circ Res* 78, 990-997.
- Kagari, T., Yamaguchi, N., and Kasai, M. (1996). Biochemical characterization of calsequestrin-binding 30-kDa protein in sarcoplasmic reticulum of skeletal muscle. *Biochem Biophys Res Commun* 227, 700-706.
- Kermode, H., Williams, A.J., and Sitsapesan, R. (1998). The interactions of ATP, ADP, and inorganic phosphate with the sheep cardiac ryanodine receptor. *Biophysical Journal* 74, 1296-1304.
- Kim, E., Youn, B., Kemper, L., Campbell, C., Milting, H., Varsanyi, M., and Kang, C. (2007). Characterization of human cardiac calsequestrin and its deleterious mutants. *J Mol Biol* 373, 1047-1057.
- Kim, K.C., Caswell, A.H., Brunschwig, J.P., and Brandt, N.R. (1990a). Identification of a new subpopulation of triad junctions isolated from skeletal muscle; morphological correlations with intact muscle. *J Membr Biol* 113, 221-235.
- Kim, K.C., Caswell, A.H., Talvenheimo, J.A., and Brandt, N.R. (1990b). Isolation of a Terminal Cisterna Protein Which May Link the Dihydropyridine Receptor to the Junctional Foot Protein in Skeletal-Muscle. *Biochemistry* 29, 9281-9289.
- Kirchhefer, U., Baba, H.A., Hanske, G., Jones, L.R., Kirchhof, P., Schmitz, W., and Neumann, J. (2004a). Age-dependent biochemical and contractile properties in atrium of transgenic mice overexpressing junctin. *Am J Physiol Heart Circ Physiol* 287, H2216-2225.
- Kirchhefer, U., Hanske, G., Jones, L.R., Justus, I., Kaestner, L., Lipp, P., Schmitz, W., and Neumann, J. (2006). Overexpression of junctin causes adaptive changes in cardiac myocyte Ca(2+) signaling. *Cell Calcium* 39, 131-142.
- Kirchhefer, U., Jones, L.R., Begrow, F., Boknik, P., Hein, L., Lohse, M.J., Riemann, B., Schmitz, W., Stypmann, J., and Neumann, J. (2004b). Transgenic triadin 1 overexpression alters SR Ca²⁺ handling and leads to a blunted contractile response to beta-adrenergic agonists. *Cardiovasc Res* 62, 122-134.

- Kirchhefer, U., Klimas, J., Baba, H.A., Buchwalow, I.B., Fabritz, L., Huls, M., Matus, M., Muller, F.U., Schmitz, W., and Neumann, J. (2007). Triadin is a critical determinant of cellular Ca cycling and contractility in the heart. *Am J Physiol Heart Circ Physiol* 293, H3165-3174.
- Kirchhefer, U., Neumann, J., Baba, H.A., Begrow, F., Kobayashi, Y.M., Reinke, U., Schmitz, W., and Jones, L.R. (2001). Cardiac hypertrophy and impaired relaxation in transgenic mice overexpressing triadin 1. *J Biol Chem* 276, 4142-4149.
- Kirchhefer, U., Neumann, J., Bers, D.M., Buchwalow, I.B., Fabritz, L., Hanske, G., Justus, I., Riemann, B., Schmitz, W., and Jones, L.R. (2003). Impaired relaxation in transgenic mice overexpressing junctin. *Cardiovascular Research* 59, 369-379.
- Kirchhof, P., Klimas, J., Fabritz, L., Zwiener, M., Jones, L.R., Schafers, M., Hermann, S., Boknik, P., Schmitz, W., Breithardt, G., et al. (2007). Stress and high heart rate provoke ventricular tachycardia in mice expressing triadin. *J Mol Cell Cardiol* 42, 962-971.
- Knollmann, B.C. (2009). New roles of calsequestrin and triadin in cardiac muscle. *J Physiol* 587, 3081-3087.
- Knollmann, B.C., Chopra, N., Hlaing, T., Akin, B., Yang, T., Etensohn, K., Knollmann, B.E., Horton, K.D., Weissman, N.J., Holinstat, I., et al. (2006). Casq2 deletion causes sarcoplasmic reticulum volume increase, premature Ca²⁺ release, and catecholaminergic polymorphic ventricular tachycardia. *J Clin Invest* 116, 2510-2520.
- Knollmann, B.C., Knollmann-Ritschel, B.E., Weissman, N.J., Jones, L.R., and Morad, M. (2000). Remodelling of ionic currents in hypertrophied and failing hearts of transgenic mice overexpressing calsequestrin. *J Physiol* 525 Pt 2, 483-498.
- Knudson, C.M., Stang, K.K., Moomaw, C.R., Slaughter, C.A., and Campbell, K.P. (1993). Primary structure and topological analysis of a skeletal muscle-specific junctional sarcoplasmic reticulum glycoprotein (triadin). *J Biol Chem* 268, 12646-12654.
- Kobayashi, Y.M., Alseikhan, B.A., and Jones, L.R. (2000). Localization and characterization of the calsequestrin-binding domain of triadin 1. Evidence for a charged beta-strand in mediating the protein-protein interaction. *J Biol Chem* 275, 17639-17646.
- Kobayashi, Y.M., and Jones, L.R. (1999). Identification of triadin 1 as the predominant triadin isoform expressed in mammalian myocardium. *J Biol Chem* 274, 28660-28668.
- Kong, H., Wang, R., Chen, W., Zhang, L., Chen, K., Shimoni, Y., Duff, H.J., and Chen, S.R. (2007). Skeletal and cardiac ryanodine receptors exhibit different responses to Ca²⁺ overload and luminal Ca²⁺. *Biophysical Journal* 92, 2757-2770.
- Koop, A., Goldmann, P., Chen, S.R., Thieleczek, R., and Varsanyi, M. (2008). ARVC-related mutations in divergent region 3 alter functional properties of the cardiac ryanodine receptor. *Biophysical Journal* 94, 4668-4677.
- Korneyev, D., Petrosky, A.D., Zepeda, B., Ferreira, M., Knollmann, B., and Escobar, A.L. (2012). Calsequestrin 2 deletion shortens the refractoriness of Ca(2)(+) release and reduces rate-dependent Ca(2)(+)-alternans in intact mouse hearts. *J Mol Cell Cardiol* 52, 21-31.
- Krause, K.H., Chou, M., Thomas, M.A., Sjolund, R.D., and Campbell, K.P. (1989). Plant cells contain calsequestrin. *J Biol Chem* 264, 4269-4272.
- Kucerova, D., Baba, H.A., Boknik, P., Fabritz, L., Heinick, A., Mat'us, M., Muller, F.U., Neumann, J., Schmitz, W., and Kirchhefer, U. (2012). Modulation of SR Ca²⁺ release by the triadin-to-calsequestrin ratio in ventricular myocytes. *Am J Physiol Heart Circ Physiol* 302, H2008-2017.

- Kuwajima, G., Futatsugi, A., Niinobe, M., Nakanishi, S., and Mikoshiba, K. (1992). Two types of ryanodine receptors in mouse brain: skeletal muscle type exclusively in Purkinje cells and cardiac muscle type in various neurons. *Neuron* 9, 1133-1142.
- Laemmli, U.K. (1970). Cleavage of structural proteins during the assembly of the head of bacteriophage T4. *Nature* 227, 680-685.
- Lahat, H., Pras, E., Olender, T., Avidan, N., Ben-Asher, E., Man, O., Levy-Nissenbaum, E., Khoury, A., Lorber, A., Goldman, B., et al. (2001). A missense mutation in a highly conserved region of CASQ2 is associated with autosomal recessive catecholamine-induced polymorphic ventricular tachycardia in Bedouin families from Israel. *Am J Hum Genet* 69, 1378-1384.
- Lai, F.A., Dent, M., Wickenden, C., Xu, L., Kumari, G., Misra, M., Lee, H.B., Sar, M., and Meissner, G. (1992). Expression of a cardiac Ca²⁺-release channel isoform in mammalian brain. *Biochem J* 288 (Pt 2), 553-564.
- Lai, F.A., Erickson, H.P., Rousseau, E., Liu, Q.Y., and Meissner, G. (1988). Purification and reconstitution of the calcium release channel from skeletal muscle. *Nature* 331, 315-319.
- Lam, E., Martin, M.M., Timerman, A.P., Sabers, C., Fleischer, S., Lukas, T., Abraham, R.T., O'Keefe, S.J., O'Neill, E.A., and Wiederrecht, G.J. (1995). A novel FK506 binding protein can mediate the immunosuppressive effects of FK506 and is associated with the cardiac ryanodine receptor. *J Biol Chem* 270, 26511-26522.
- Lamb, G.D. (1993). Ca²⁺ inactivation, Mg²⁺ inhibition and malignant hyperthermia. *J Muscle Res Cell Motil* 14, 554-556.
- Lamb, G.D., Cellini, M.A., and Stephenson, D.G. (2001). Different Ca²⁺ releasing action of caffeine and depolarisation in skeletal muscle fibres of the rat. *J Physiol* 531, 715-728.
- Lamb, G.D., and Stephenson, D.G. (1991). Effect of Mg²⁺ on the control of Ca²⁺ release in skeletal muscle fibres of the toad. *J Physiol* 434, 507-528.
- Lamb, G.D., and Walsh, T. (1987). Calcium currents, charge movement and dihydropyridine binding in fast- and slow-twitch muscles of rat and rabbit. *J Physiol* 393, 595-617.
- Lanner, J.T., Georgiou, D.K., Joshi, A.D., and Hamilton, S.L. (2010). Ryanodine receptors: structure, expression, molecular details, and function in calcium release. *Cold Spring Harb Perspect Biol* 2, a003996.
- Laver, D. (2001). The power of single channel recording and analysis: its application to ryanodine receptors in lipid bilayers. *Clinical and experimental pharmacology & physiology* 28, 675-686.
- Laver, D.R. (2007). Ca²⁺ stores regulate ryanodine receptor Ca²⁺ release channels via luminal and cytosolic Ca²⁺ sites. *Biophysical Journal* 92, 3541-3555.
- Laver, D.R. (2010). Regulation of RyR Channel Gating by Ca²⁺, Mg²⁺ and ATP. *Curr Top Membr* 66, 69-89.
- Laver, D.R., Baynes, T.M., and Dulhunty, A.F. (1997a). Magnesium inhibition of ryanodine-receptor calcium channels: evidence for two independent mechanisms. *J Membr Biol* 156, 213-229.
- Laver, D.R., and Honen, B.N. (2008). Luminal Mg²⁺, a key factor controlling RYR2-mediated Ca²⁺ release: cytoplasmic and luminal regulation modeled in a tetrameric channel. *J Gen Physiol* 132, 429-446.
- Laver, D.R., Kong, C.H.T., Intiaz, M.S., and Cannell, M.B. (2013). Termination of calcium-induced calcium release by induction decay: An emergent property of stochastic

- channel gating and molecular scale architecture. *Journal of Molecular and Cellular Cardiology* 54, 98-100.
- Laver, D.R., Lenz, G.K., and Lamb, G.D. (2001). Regulation of the calcium release channel from rabbit skeletal muscle by the nucleotides ATP, AMP, IMP and adenosine. *The Journal of Physiology* 537, 763-778.
- Laver, D.R., O'Neill, E.R., and Lamb, G.D. (2004). Luminal Ca²⁺-regulated Mg²⁺ inhibition of skeletal RyRs reconstituted as isolated channels or coupled clusters. *J Gen Physiol* 124, 741-758.
- Laver, D.R., Owen, V.J., Junankar, P.R., Taske, N.L., Dulhunty, A.F., and Lamb, G.D. (1997b). Reduced inhibitory effect of Mg²⁺ on ryanodine receptor-Ca²⁺ release channels in malignant hyperthermia. *Biophysical Journal* 73, 1913-1924.
- Laver, D.R., Roden, L.D., Ahern, G.P., Eager, K.R., Junankar, P.R., and Dulhunty, A.F. (1995). Cytoplasmic Ca²⁺ inhibits the ryanodine receptor from cardiac muscle. *J Membr Biol* 147, 7-22.
- Lee, B.S., Sessanna, S., Laychock, S.G., and Rubin, R.P. (2002). Expression and cellular localization of a modified type 1 ryanodine receptor and L-type channel proteins in non-muscle cells. *J Membr Biol* 189, 181-190.
- Lee, E.H., Song, D.W., Lee, J.M., Meissner, G., Allen, P.D., and Kim do, H. (2006). Occurrence of atypical Ca²⁺ transients in triadin-binding deficient-RYR1 mutants. *Biochem Biophys Res Commun* 351, 909-914.
- Lee, H.B., Xu, L., and Meissner, G. (1994). Reconstitution of the skeletal muscle ryanodine receptor-Ca²⁺ release channel protein complex into proteoliposomes. *J Biol Chem* 269, 13305-13312.
- Lee, H.G., Kang, H., Kim, D.H., and Park, W.J. (2001). Interaction of HRC (histidine-rich Ca(2+)-binding protein) and triadin in the lumen of sarcoplasmic reticulum. *J Biol Chem* 276, 39533-39538.
- Lee, J.M., Rho, S.H., Shin, D.W., Cho, C., Park, W.J., Eom, S.H., Ma, J., and Kim, D.H. (2004). Negatively charged amino acids within the intraluminal loop of ryanodine receptor are involved in the interaction with triadin. *J Biol Chem* 279, 6994-7000.
- Lee, K.W., Maeng, J.S., Choi, J.Y., Lee, Y.R., Hwang, C.Y., Park, S.S., Park, H.K., Chung, B.H., Lee, S.G., Kim, Y.S., et al. (2012). Role of Junctin Protein Interactions in Cellular Dynamics of Calsequestrin Polymer upon Calcium Perturbation. *Journal of Biological Chemistry* 287, 1679-1687.
- Lim, K.Y., Hong, C.S., and Kim, D.H. (2000). cDNA cloning and characterization of human cardiac junctin. *Gene* 255, 35-42.
- Lindsay, A.R., and Williams, A.J. (1991). Functional characterisation of the ryanodine receptor purified from sheep cardiac muscle sarcoplasmic reticulum. *Biochimica et biophysica acta* 1064, 89-102.
- Liu, Q.Y., Lai, F.A., Rousseau, E., Jones, R.V., and Meissner, G. (1989). Multiple conductance states of the purified calcium release channel complex from skeletal sarcoplasmic reticulum. *Biophysical Journal* 55, 415-424.
- Liu, Z., Zhang, J., Li, P., Chen, S.R., and Wagenknecht, T. (2002). Three-dimensional reconstruction of the recombinant type 2 ryanodine receptor and localization of its divergent region 1. *The Journal of biological chemistry* 277, 46712-46719.
- Liu, Z., Zhang, J., Sharma, M.R., Li, P., Chen, S.R., and Wagenknecht, T. (2001). Three-dimensional reconstruction of the recombinant type 3 ryanodine receptor and localization of its amino terminus. *P Natl Acad Sci USA* 98, 6104-6109.

- Liu, Z., Zhang, J., Wang, R., Wayne Chen, S.R., and Wagenknecht, T. (2004). Location of divergent region 2 on the three-dimensional structure of cardiac muscle ryanodine receptor/calcium release channel. *J Mol Biol* 338, 533-545.
- Lobo, P.A., and Van Petegem, F. (2009). Crystal structures of the N-terminal domains of cardiac and skeletal muscle ryanodine receptors: insights into disease mutations. *Structure* 17, 1505-1514.
- Lopez, J.R., Contreras, J., Linares, N., and Allen, P.D. (2000). Hypersensitivity of malignant hyperthermia-susceptible swine skeletal muscle to caffeine is mediated by high resting myoplasmic $[Ca^{2+}]$. *Anesthesiology* 92, 1799-1806.
- Ludtke, S.J., Serysheva, I., Hamilton, S.L., and Chiu, W. (2005). The pore structure of the closed RyR1 channel. *Structure* 13, 1203-1211.
- Luft, J.H. (1971). Ruthenium red and violet. I. Chemistry, purification, methods of use for electron microscopy and mechanism of action. *Anat Rec* 171, 347-368.
- Lukyanenko, V., Gyorke, I., and Gyorke, S. (1996). Regulation of calcium release by calcium inside the sarcoplasmic reticulum in ventricular myocytes. *Pflug Arch Eur J Phys* 432, 1047-1054.
- Lukyanenko, V., Subramanian, S., Gyorke, I., Wiesner, T.F., and Gyorke, S. (1999). The role of luminal Ca^{2+} in the generation of Ca^{2+} waves in rat ventricular myocytes. *J Physiol* 518 (Pt 1), 173-186.
- Lukyanenko, V., Viatchenko-Karpinski, S., Smirnov, A., Wiesner, T.F., and Gyorke, S. (2001). Dynamic regulation of sarcoplasmic reticulum Ca^{2+} content and release by luminal Ca^{2+} -sensitive leak in rat ventricular myocytes. *Biophysical Journal* 81, 785-798.
- Lynch, P.J., Tong, J., Lehane, M., Mallet, A., Giblin, L., Heffron, J.J., Vaughan, P., Zafr, G., MacLennan, D.H., and McCarthy, T.V. (1999). A mutation in the transmembrane/luminal domain of the ryanodine receptor is associated with abnormal Ca^{2+} release channel function and severe central core disease. *P Natl Acad Sci USA* 96, 4164-4169.
- Ma, J. (1993). Block by ruthenium red of the ryanodine-activated calcium release channel of skeletal muscle. *J Gen Physiol* 102, 1031-1056.
- Ma, J. (1995). Desensitization of the skeletal muscle ryanodine receptor: evidence for heterogeneity of calcium release channels. *Biophysical Journal* 68, 893-899.
- Ma, J., Fill, M., Knudson, C.M., Campbell, K.P., and Coronado, R. (1988). Ryanodine receptor of skeletal muscle is a gap junction-type channel. *Science* 242, 99-102.
- MacLennan, D.H., and Wong, P.T. (1971). Isolation of a calcium-sequestering protein from sarcoplasmic reticulum. *Proceedings of the National Academy of Sciences of the United States of America* 68, 1231-1235.
- MacMillan, D. (2013). FK506 binding proteins: Cellular regulators of intracellular Ca^{2+} signalling. *European Journal of Pharmacology* 700, 181-193.
- Mahony, L. (1996). Regulation of intracellular calcium concentration in the developing heart. *Cardiovasc Res* 31 Spec No, E61-67.
- Manunta, M., Rossi, D., Simeoni, I., Butelli, E., Romanin, C., Sorrentino, V., and Schindler, H. (2000). ATP-induced activation of expressed RyR3 at low free calcium. *FEBS Lett* 471, 256-260.
- Marengo, J.J., Hidalgo, C., and Bull, R. (1998). Sulfhydryl oxidation modifies the calcium dependence of ryanodine-sensitive calcium channels of excitable cells. *Biophys J* 74, 1263-1277.

- Marieb, E.N., and Hoehn, K. (2007). Human anatomy & physiology, 7th edn (San Francisco: Pearson Benjamin Cummings).
- Marty, I., Faure, J., Fourest-Lieuvain, A., Vassilopoulos, S., Oddoux, S., and Brocard, J. (2009). Triadin: what possible function 20 years later? *J Physiol* 587, 3117-3121.
- Marty, I., Robert, M., Ronjat, M., Bally, I., Arlaud, G., and Villaz, M. (1995). Localization of the N-terminal and C-terminal ends of triadin with respect to the sarcoplasmic reticulum membrane of rabbit skeletal muscle. *Biochem J* 307 (Pt 3), 769-774.
- Marty, I., Thevenon, D., Scotto, C., Groh, S., Sainnier, S., Robert, M., Grunwald, D., and Villaz, M. (2000). Cloning and characterization of a new isoform of skeletal muscle triadin. *J Biol Chem* 275, 8206-8212.
- Marty, I., Villaz, M., Arlaud, G., Bally, I., and Ronjat, M. (1994). Transmembrane orientation of the N-terminal and C-terminal ends of the ryanodine receptor in the sarcoplasmic reticulum of rabbit skeletal muscle. *The Biochemical journal* 298 Pt 3, 743-749.
- Mattei, M.G., Giannini, G., Moscatelli, F., and Sorrentino, V. (1994). Chromosomal localization of murine ryanodine receptor genes RYR1, RYR2, and RYR3 by in situ hybridization. *Genomics* 22, 202-204.
- Mayrleitner, M., Timerman, A.P., Wiederrecht, G., and Fleischer, S. (1994). The calcium release channel of sarcoplasmic reticulum is modulated by FK-506 binding protein: effect of FKBP-12 on single channel activity of the skeletal muscle ryanodine receptor. *Cell Calcium* 15, 99-108.
- Mead-Savery, F.C., Wang, R., Tanna-Topan, B., Chen, S.R., Welch, W., and Williams, A.J. (2009). Changes in negative charge at the luminal mouth of the pore alter ion handling and gating in the cardiac ryanodine-receptor. *Biophys J* 96, 1374-1387.
- Meissner, G. (1984). Adenine nucleotide stimulation of Ca²⁺-induced Ca²⁺ release in sarcoplasmic reticulum. *The Journal of biological chemistry* 259, 2365-2374.
- Meissner, G. (1994). Ryanodine receptor/Ca²⁺ release channels and their regulation by endogenous effectors. *Annu Rev Physiol* 56, 485-508.
- Meissner, G., Conner, G.E., and Fleischer, S. (1973). Isolation of sarcoplasmic reticulum by zonal centrifugation and purification of Ca²⁺-pump and Ca²⁺-binding proteins. *Biochimica et biophysica acta* 298, 246-269.
- Meissner, G., Darling, E., and Eveleth, J. (1986). Kinetics of rapid Ca²⁺ release by sarcoplasmic reticulum. Effects of Ca²⁺, Mg²⁺, and adenine nucleotides. *Biochemistry* 25, 236-244.
- Meissner, G., and Henderson, J.S. (1987). Rapid calcium release from cardiac sarcoplasmic reticulum vesicles is dependent on Ca²⁺ and is modulated by Mg²⁺, adenine nucleotide, and calmodulin. *The Journal of biological chemistry* 262, 3065-3073.
- Meissner, G., Rios, E., Tripathy, A., and Pasek, D.A. (1997). Regulation of skeletal muscle Ca²⁺ release channel (ryanodine receptor) by Ca²⁺ and monovalent cations and anions. *J Biol Chem* 272, 1628-1638.
- Michalak, M., Dupraz, P., and Shoshan-Barmatz, V. (1988). Ryanodine binding to sarcoplasmic reticulum membrane; comparison between cardiac and skeletal muscle. *Biochimica et biophysica acta* 939, 587-594.
- Miller, C., and Racker, E. (1976). Ca⁺⁺-induced fusion of fragmented sarcoplasmic reticulum with artificial planar bilayers. *J Membr Biol* 30, 283-300.
- Miller, M.S., Frieman, W.F., and Wetzel, G.T. (1997). Caffeine-induced contractions in developing rabbit heart. *Pediatric Research* 42, 287-292.

- Miller, S.L., Currie, S., Loughrey, C.M., Kettlewell, S., Seidler, T., Reynolds, D.F., Hasenfuss, G., and Smith, G.L. (2005). Effects of calsequestrin over-expression on excitation-contraction coupling in isolated rabbit cardiomyocytes. *Cardiovascular research* 67, 667-677.
- Milstein, M.L., McFarland, T.P., Marsh, J.D., and Cala, S.E. (2008). Inefficient glycosylation leads to high steady-state levels of actively degrading cardiac triadin-1. *J Biol Chem* 283, 1929-1935.
- Mitchell, R.D., Simmerman, H.K., and Jones, L.R. (1988). Ca²⁺ binding effects on protein conformation and protein interactions of canine cardiac calsequestrin. *J Biol Chem* 263, 1376-1381.
- Moorman, A.F., Vermeulen, J.L., Koban, M.U., Schwartz, K., Lamers, W.H., and Boheler, K.R. (1995). Patterns of expression of sarcoplasmic reticulum Ca(2+)-ATPase and phospholamban mRNAs during rat heart development. *Circ Res* 76, 616-625.
- Nakai, J., Imagawa, T., Hakamat, Y., Shigekawa, M., Takeshima, H., and Numa, S. (1990). Primary structure and functional expression from cDNA of the cardiac ryanodine receptor/calcium release channel. *FEBS letters* 271, 169-177.
- Nakanishi, S., Kuwajima, G., and Mikoshiba, K. (1992). Immunohistochemical localization of ryanodine receptors in mouse central nervous system. *Neuroscience research* 15, 130-142.
- Neylon, C.B., Richards, S.M., Larsen, M.A., Agrotis, A., and Bobik, A. (1995). Multiple types of ryanodine receptor/Ca²⁺ release channels are expressed in vascular smooth muscle. *Biochemical and Biophysical Research Communications* 215, 814-821.
- Novak, P., and Soukup, T. (2011). Calsequestrin distribution, structure and function, its role in normal and pathological situations and the effect of thyroid hormones. *Physiological research / Academia Scientiarum Bohemoslovaca* 60, 439-452.
- O'Brien, J., Valdivia, H.H., and Block, B.A. (1995). Physiological differences between the alpha and beta ryanodine receptors of fish skeletal muscle. *Biophysical Journal* 68, 471-482.
- Oddoux, S., Brocard, J., Schweitzer, A., Szentesi, P., Giannesini, B., Brocard, J., Faure, J., Pernet-Gallay, K., Bendahan, D., Lunardi, J., et al. (2009). Triadin deletion induces impaired skeletal muscle function. *J Biol Chem* [Epub ahead of print].
- Ogata, T., and Yamasaki, Y. (1987). High-resolution scanning electron-microscopic studies on the three-dimensional structure of mitochondria and sarcoplasmic reticulum in the different twitch muscle fibers of the frog. *Cell and tissue research* 250, 489-497.
- Ogawa, Y., Kurebayashi, N., and Murayama, T. (2000). Putative roles of type 3 ryanodine receptor isoforms (RyR3). *Trends in cardiovascular medicine* 10, 65-70.
- Ohkura, M., Furukawa, K., Fujimori, H., Kuruma, A., Kawano, S., Hiraoka, M., Kuniyasu, A., Nakayama, H., and Ohizumi, Y. (1998). Dual regulation of the skeletal muscle ryanodine receptor by triadin and calsequestrin. *Biochemistry* 37, 12987-12993.
- Ohnishi, M., and Reithmeier, R.A. (1987). Fragmentation of rabbit skeletal muscle calsequestrin: spectral and ion binding properties of the carboxyl-terminal region. *Biochemistry* 26, 7458-7465.
- Olson, R.D., Li, X., Palade, P., Shadle, S.E., Mushlin, P.S., Gambliel, H.A., Fill, M., Boucek, R.J., Jr., and Cusack, B.J. (2000). Sarcoplasmic reticulum calcium release is stimulated and inhibited by daunorubicin and daunorubicinol. *Toxicology and applied pharmacology* 169, 168-176.

- Ondrias, K., Brillantes, A.M., Scott, A., Ehrlich, B.E., and Marks, A.R. (1996). Single channel properties and calcium conductance of the cloned expressed ryanodine receptor/calcium-release channel. *Society of General Physiologists series* 51, 29-45.
- Orlova, E.V., Serysheva, II, van Heel, M., Hamilton, S.L., and Chiu, W. (1996). Two structural configurations of the skeletal muscle calcium release channel. *Nat Struct Biol* 3, 547-552.
- Ostwald, T.J., MacLennan, D.H., and Dorrington, K.J. (1974). Effects of cation binding on the conformation of calsequestrin and the high affinity calcium-binding protein of sarcoplasmic reticulum. *J Biol Chem* 249, 5867-5871.
- Otsu, K., Willard, H.F., Khanna, V.K., Zorzato, F., Green, N.M., and MacLennan, D.H. (1990). Molecular cloning of cDNA encoding the Ca²⁺ release channel (ryanodine receptor) of rabbit cardiac muscle sarcoplasmic reticulum. *The Journal of biological chemistry* 265, 13472-13483.
- Ottini, L., Marziali, G., Conti, A., Charlesworth, A., and Sorrentino, V. (1996). Alpha and beta isoforms of ryanodine receptor from chicken skeletal muscle are the homologues of mammalian RyR1 and RyR3. *The Biochemical journal* 315 (Pt 1), 207-216.
- Oyamada, H., Murayama, T., Takagi, T., Iino, M., Iwabe, N., Miyata, T., Ogawa, Y., and Endo, M. (1994). Primary structure and distribution of ryanodine-binding protein isoforms of the bullfrog skeletal muscle. *The Journal of biological chemistry* 269, 17206-17214.
- Page, E., and Buecker, J.L. (1981). Development of dyadic junctional complexes between sarcoplasmic reticulum and plasmalemma in rabbit left ventricular myocardial cells. *Morphometric analysis. Circ Res* 48, 519-522.
- Paolini, C., Protasi, F., and Franzini-Armstrong, C. (2004). The relative position of RyR feet and DHPR tetrads in skeletal muscle. *J Mol Biol* 342, 145-153.
- Paolini, C., Quarta, M., Nori, A., Boncompagni, S., Canato, M., Volpe, P., Allen, P.D., Reggiani, C., and Protasi, F. (2007). Reorganized stores and impaired calcium handling in skeletal muscle of mice lacking calsequestrin-1. *The Journal of Physiology* 583, 767-784.
- Park, H., Park, I.Y., Kim, E., Youn, B., Fields, K., Dunker, A.K., and Kang, C. (2004). Comparing skeletal and cardiac calsequestrin structures and their calcium binding: a proposed mechanism for coupled calcium binding and protein polymerization. *J Biol Chem* 279, 18026-18033.
- Park, H., Wu, S., Dunker, A.K., and Kang, C. (2003). Polymerization of calsequestrin. Implications for Ca²⁺ regulation. *J Biol Chem* 278, 16176-16182.
- Peng, M., Fan, H., Kirley, T.L., Caswell, A.H., and Schwartz, A. (1994). Structural diversity of triadin in skeletal muscle and evidence of its existence in heart. *FEBS Lett* 348, 17-20.
- Percival, A.L., Williams, A.J., Kenyon, J.L., Grinsell, M.M., Airey, J.A., and Sutko, J.L. (1994). Chicken skeletal muscle ryanodine receptor isoforms: ion channel properties. *Biophysical Journal* 67, 1834-1850.
- Perez, C.F., Lopez, J.R., and Allen, P.D. (2005). Expression levels of RyR1 and RyR3 control resting free Ca²⁺ in skeletal muscle. *American journal of physiology Cell physiology* 288, C640-649.
- Perez, C.F., Mukherjee, S., and Allen, P.D. (2003). Amino acids 1-1,680 of ryanodine receptor type 1 hold critical determinants of skeletal type for excitation-contraction coupling. Role of divergence domain D2. *The Journal of biological chemistry* 278, 39644-39652.
- Perutz, M. (1994). Polar zippers: their role in human disease. *Protein Sci* 3, 1629-1637.

- Popova, O.B., Baker, M.R., Tran, T.P., Le, T., and Serysheva, II (2012). Identification of ATP-binding regions in the RyR1 Ca(2)(+) release channel. *PLoS One* 7, e48725.
- Porta, M., Diaz-Sylvester, P.L., Neumann, J.T., Escobar, A.L., Fleischer, S., and Copello, J.A. (2012). Coupled gating of skeletal muscle ryanodine receptors is modulated by Ca²⁺, Mg²⁺, and ATP. *American journal of physiology Cell physiology* 303, C682-697.
- Postma, A.V., Denjoy, I., Hoorntje, T.M., Lupoglazoff, J.M., Da Costa, A., Sebillon, P., Mannens, M.M., Wilde, A.A., and Guicheney, P. (2002). Absence of calsequestrin 2 causes severe forms of catecholaminergic polymorphic ventricular tachycardia. *Circ Res* 91, e21-26.
- Priori, S.G., and Chen, S.R. (2011). Inherited dysfunction of sarcoplasmic reticulum Ca²⁺ handling and arrhythmogenesis. *Circ Res* 108, 871-883.
- Pritchard, T.J., and Kranias, E.G. (2009). Junctin and the histidine-rich Ca²⁺ binding protein: potential roles in heart failure and arrhythmogenesis. *J Physiol* 587, 3125-3133.
- Protasi, F., Paolini, C., Canato, M., Reggiani, C., and Quarta, M. (2011). Lessons from calsequestrin-1 ablation in vivo: much more than a Ca(2+) buffer after all. *J Muscle Res Cell Motil* 32, 257-270.
- Protasi, F., Paolini, C., and Dainese, M. (2009). Calsequestrin-1: a new candidate gene for malignant hyperthermia and exertional/environmental heat stroke. *J Physiol* 587, 3095-3100.
- Qi, Y., Ogunbunmi, E.M., Freund, E.A., Timerman, A.P., and Fleischer, S. (1998). FK-binding protein is associated with the ryanodine receptor of skeletal muscle in vertebrate animals. *J Biol Chem* 273, 34813-34819.
- Qin, J., Valle, G., Nani, A., Chen, H., Ramos-Franco, J., Nori, A., Volpe, P., and Fill, M. (2009). Ryanodine receptor luminal Ca²⁺ regulation: swapping calsequestrin and channel isoforms. *Biophys J* 97, 1961-1970.
- Qin, J., Valle, G., Nani, A., Nori, A., Rizzi, N., Priori, S.G., Volpe, P., and Fill, M. (2008). Luminal Ca²⁺ regulation of single cardiac ryanodine receptors: Insights provided by calsequestrin and its mutants. *Journal of General Physiology* 131, 325-334.
- Radermacher, M., Rao, V., Grassucci, R., Frank, J., Timerman, A.P., Fleischer, S., and Wagenknecht, T. (1994). Cryo-electron microscopy and three-dimensional reconstruction of the calcium release channel/ryanodine receptor from skeletal muscle. *The Journal of cell biology* 127, 411-423.
- Radermacher, M., Wagenknecht, T., Grassucci, R., Frank, J., Inui, M., Chadwick, C., and Fleischer, S. (1992). Cryo-EM of the native structure of the calcium release channel/ryanodine receptor from sarcoplasmic reticulum. *Biophysical Journal* 61, 936-940.
- Ramachandran, S., Chakraborty, A., Xu, L., Mei, Y., Samsó, M., Dokholyan, N.V., and Meissner, G. (2013). Structural determinants of skeletal muscle ryanodine receptor gating. *J Biol Chem* 288, 6154-6165.
- Ramachandran, S., Serohijos, A.W., Xu, L., Meissner, G., and Dokholyan, N.V. (2009). A structural model of the pore-forming region of the skeletal muscle ryanodine receptor (RyR1). *PLoS computational biology* 5, e1000367.
- Realini, C., and Rechsteiner, M. (1995). A proteasome activator subunit binds calcium. *The Journal of biological chemistry* 270, 29664-29667.
- Realini, C., Rogers, S.W., and Rechsteiner, M. (1994). KEKE motifs. Proposed roles in protein-protein association and presentation of peptides by MHC class I receptors. *FEBS Lett* 348, 109-113.

- Rezgui, S.S., Vassilopoulos, S., Brocard, J., Platel, J.C., Bouron, A., Arnoult, C., Oddoux, S., Garcia, L., De Waard, M., and Marty, I. (2005). Triadin (Trisk 95) overexpression blocks excitation-contraction coupling in rat skeletal myotubes. *J Biol Chem* 280, 39302-39308.
- Rios, E., and Brum, G. (1987). Involvement of dihydropyridine receptors in excitation-contraction coupling in skeletal muscle. *Nature* 325, 717-720.
- Rizzi, N., Liu, N., Napolitano, C., Nori, A., Turcato, F., Colombi, B., Bicciato, S., Arcelli, D., Spedito, A., Scelsi, M., et al. (2008). Unexpected structural and functional consequences of the R33Q homozygous mutation in cardiac calsequestrin: a complex arrhythmogenic cascade in a knock in mouse model. *Circ Res* 103, 298-306.
- Rossi, A.E., Boncompagni, S., Wei, L., Protasi, F., and Dirksen, R.T. (2011). Differential impact of mitochondrial positioning on mitochondrial Ca(2+) uptake and Ca(2+) spark suppression in skeletal muscle. *Am J Physiol Cell Physiol* 301, C1128-1139.
- Rossi, D., Lorenzini, S., Scarcella, A.M., and Sorrentino, V. (2013). The Intraluminal Domain of Junctin Contains Junctional Sarcoplasmic Reticulum Targeting Sequences. *Biophysical Journal* 104, 203a-203a.
- Rousseau, E., and Pinkos, J. (1990). pH modulates conducting and gating behaviour of single calcium release channels. *Pflugers Archiv : European journal of physiology* 415, 645-647.
- Rousseau, E., Smith, J.S., Henderson, J.S., and Meissner, G. (1986). Single channel and 45Ca²⁺ flux measurements of the cardiac sarcoplasmic reticulum calcium channel. *Biophys J* 50, 1009-1014.
- Roux-Buisson, N., Cacheux, M., Fourest-Lieuvin, A., Fauconnier, J., Brocard, J., Denjoy, I., Durand, P., Guicheney, P., Kyndt, F., Leenhardt, A., et al. (2012). Absence of triadin, a protein of the calcium release complex, is responsible for cardiac arrhythmia with sudden death in human. *Human Molecular Genetics* 21, 2759-2767.
- Royer, L., Sztretze, M., Manno, C., Pouvreau, S., Zhou, J., Knollmann, B.C., Protasi, F., Allen, P.D., and Rios, E. (2010). Paradoxical buffering of calcium by calsequestrin demonstrated for the calcium store of skeletal muscle. *J Gen Physiol* 136, 325-338.
- Rubtsov, A.M., and Batrukova, M.A. (1997). Ca-release channels (ryanodine receptors) of sarcoplasmic reticulum: structure and properties. A review. *Biochemistry Biokhimiia* 62, 933-945.
- Sacchetto, R., Damiani, E., Turcato, F., Nori, A., and Margreth, A. (2001). Ca(2+)-dependent interaction of triadin with histidine-rich Ca(2+)-binding protein carboxyl-terminal region. *Biochem Biophys Res Commun* 289, 1125-1134.
- Sacchetto, R., Turcato, F., Damiani, E., and Margreth, A. (1999). Interaction of triadin with histidine-rich Ca(2+)-binding protein at the triadic junction in skeletal muscle fibers. *J Muscle Res Cell Motil* 20, 403-415.
- Sagara, Y., and Inesi, G. (1991). Inhibition of the sarcoplasmic reticulum Ca²⁺ transport ATPase by thapsigargin at subnanomolar concentrations. *The Journal of biological chemistry* 266, 13503-13506.
- Saito, A., Seiler, S., Chu, A., and Fleischer, S. (1984). Preparation and morphology of sarcoplasmic reticulum terminal cisternae from rabbit skeletal muscle. *The Journal of cell biology* 99, 875-885.
- Samso, M., Feng, W., Pessah, I.N., and Allen, P.D. (2009). Coordinated movement of cytoplasmic and transmembrane domains of RyR1 upon gating. *PLoS Biol* 7, e85.

- Samso, M., and Wagenknecht, T. (1998). Contributions of electron microscopy and single-particle techniques to the determination of the ryanodine receptor three-dimensional structure. *J Struct Biol* 121, 172-180.
- Samso, M., Wagenknecht, T., and Allen, P.D. (2005). Internal structure and visualization of transmembrane domains of the RyR1 calcium release channel by cryo-EM. *Nat Struct Mol Biol* 12, 539-544.
- Sato, Y., Ferguson, D.G., Sako, H., Dorn, G.W., 2nd, Kadambi, V.J., Yatani, A., Hoit, B.D., Walsh, R.A., and Kranias, E.G. (1998). Cardiac-specific overexpression of mouse cardiac calsequestrin is associated with depressed cardiovascular function and hypertrophy in transgenic mice. *The Journal of biological chemistry* 273, 28470-28477.
- Schneider, M.F., and Chandler, W.K. (1973). Voltage dependent charge movement of skeletal muscle: a possible step in excitation-contraction coupling. *Nature* 242, 244-246.
- Scott, B.T., Simmerman, H.K., Collins, J.H., Nadal-Ginard, B., and Jones, L.R. (1988). Complete amino acid sequence of canine cardiac calsequestrin deduced by cDNA cloning. *J Biol Chem* 263, 8958-8964.
- Serysheva, I., Hamilton, S.L., Chiu, W., and Ludtke, S.J. (2005). Structure of Ca²⁺ release channel at 14 Å resolution. *J Mol Biol* 345, 427-431.
- Serysheva, I., Ludtke, S.J., Baker, M.L., Cong, Y., Topf, M., Eramian, D., Sali, A., Hamilton, S.L., and Chiu, W. (2008). Subnanometer-resolution electron cryomicroscopy-based domain models for the cytoplasmic region of skeletal muscle RyR channel. *P Natl Acad Sci USA* 105, 9610-9615.
- Serysheva, I., Orlova, E.V., Chiu, W., Sherman, M.B., Hamilton, S.L., and van Heel, M. (1995). Electron cryomicroscopy and angular reconstitution used to visualize the skeletal muscle calcium release channel. *Nat Struct Biol* 2, 18-24.
- Serysheva, I., Schatz, M., van Heel, M., Chiu, W., and Hamilton, S.L. (1999). Structure of the skeletal muscle calcium release channel activated with Ca²⁺ and AMP-PCP. *Biophysical Journal* 77, 1936-1944.
- Shannon, T.R., Ginsburg, K.S., and Bers, D.M. (2002). Quantitative assessment of the SR Ca²⁺ leak-load relationship. *Circulation Research* 91, 594-600.
- Shannon, T.R., Guo, T., and Bers, D.M. (2003). Ca²⁺ scraps: local depletions of free [Ca²⁺] in cardiac sarcoplasmic reticulum during contractions leave substantial Ca²⁺ reserve. *Circ Res* 93, 40-45.
- Sharma, M.R., Jeyakumar, L.H., Fleischer, S., and Wagenknecht, T. (2000). Three-dimensional structure of ryanodine receptor isoform three in two conformational states as visualized by cryo-electron microscopy. *The Journal of biological chemistry* 275, 9485-9491.
- Sharma, M.R., Penczek, P., Grassucci, R., Xin, H.B., Fleischer, S., and Wagenknecht, T. (1998). Cryoelectron microscopy and image analysis of the cardiac ryanodine receptor. *The Journal of biological chemistry* 273, 18429-18434.
- Shen, X., Franzini-Armstrong, C., Lopez, J.R., Jones, L.R., Kobayashi, Y.M., Wang, Y., Kerrick, W.G., Caswell, A.H., Potter, J.D., Miller, T., et al. (2007). Triadins modulate intracellular Ca²⁺ homeostasis but are not essential for excitation-contraction coupling in skeletal muscle. *J Biol Chem* 282, 37864-37874.
- Shin, D.W., Ma, J., and Kim, D.H. (2000). The asp-rich region at the carboxyl-terminus of calsequestrin binds to Ca²⁺ and interacts with triadin. *FEBS Lett* 486, 178-182.
- Shin, D.W., Pan, Z., Kim, E.K., Lee, J.M., Bhat, M.B., Parness, J., Kim, D.H., and Ma, J. (2003). A retrograde signal from calsequestrin for the regulation of store-operated Ca²⁺ entry in skeletal muscle. *The Journal of biological chemistry* 278, 3286-3292.

- Shkryl, V.M., and Shirokova, N. (2006). Transfer and tunneling of Ca²⁺ from sarcoplasmic reticulum to mitochondria in skeletal muscle. *J Biol Chem* 281, 1547-1554.
- Shou, W., Aghdasi, B., Armstrong, D.L., Guo, Q., Bao, S., Charng, M.J., Mathews, L.M., Schneider, M.D., Hamilton, S.L., and Matzuk, M.M. (1998). Cardiac defects and altered ryanodine receptor function in mice lacking FKBP12. *Nature* 391, 489-492.
- Sigworth, F.J., and Sine, S.M. (1987). Data transformations for improved display and fitting of single-channel dwell time histograms. *Biophys J* 52, 1047-1054.
- Sitsapasan, R., Montgomery, R.A., MacLeod, K.T., and Williams, A.J. (1991). Sheep cardiac sarcoplasmic reticulum calcium-release channels: modification of conductance and gating by temperature. *J Physiol* 434, 469-488.
- Sitsapasan, R., and Williams, A.J. (1994a). Gating of the native and purified cardiac SR Ca(2+)-release channel with monovalent cations as permeant species. *Biophysical Journal* 67, 1484-1494.
- Sitsapasan, R., and Williams, A.J. (1994b). Regulation of the gating of the sheep cardiac sarcoplasmic reticulum Ca(2+)-release channel by luminal Ca²⁺. *The Journal of membrane biology* 137, 215-226.
- Sitsapasan, R., and Williams, A.J. (1995). The gating of the sheep skeletal sarcoplasmic reticulum Ca(2+)-release channel is regulated by luminal Ca²⁺. *The Journal of membrane biology* 146, 133-144.
- Sitsapasan, R., and Williams, A.J. (1997). Regulation of current flow through ryanodine receptors by luminal Ca²⁺. *J Membr Biol* 159, 179-185.
- Slupsky, J.R., Ohnishi, M., Carpenter, M.R., and Reithmeier, R.A. (1987). Characterization of cardiac calsequestrin. *Biochemistry* 26, 6539-6544.
- Smith, J.S., Coronado, R., and Meissner, G. (1985). Sarcoplasmic reticulum contains adenine nucleotide-activated calcium channels. *Nature* 316, 446-449.
- Smith, J.S., Coronado, R., and Meissner, G. (1986). Single channel measurements of the calcium release channel from skeletal muscle sarcoplasmic reticulum. Activation by Ca²⁺ and ATP and modulation by Mg²⁺. *The Journal of general physiology* 88, 573-588.
- Smith, J.S., Imagawa, T., Ma, J., Fill, M., Campbell, K.P., and Coronado, R. (1988). Purified ryanodine receptor from rabbit skeletal muscle is the calcium-release channel of sarcoplasmic reticulum. *The Journal of general physiology* 92, 1-26.
- Sommer, J.R., T. High, P. Ingram, R. Nassar, I. Taylor, and D. Kopf. (1998). Couplings and couplons. *J Gen Physiol* 112, 14a (Abstr.).
- Sonnleitner, A., Fleischer, S., and Schindler, H. (1997). Gating of the skeletal calcium release channel by ATP is inhibited by protein phosphatase 1 but not by Mg²⁺. *Cell Calcium* 21, 283-290.
- Sridhar, P., Awasthi, A.K., Azim, C.A., Burma, S., Habib, S., Jain, A., Mukherjee, B., Ranjan, A., and Hasnain, S.E. (1994). Baculovirus Vector-Mediated Expression of Heterologous Genes in Insect Cells. *J Bioscience* 19, 603-614.
- Sun, X.H., Protasi, F., Takahashi, M., Takeshima, H., Ferguson, D.G., and Franzini-Armstrong, C. (1995). Molecular architecture of membranes involved in excitation-contraction coupling of cardiac muscle. *J Cell Biol* 129, 659-671.
- Szegedi, C., Sarkozi, S., Herzog, A., Jona, I., and Varsanyi, M. (1999). Calsequestrin: more than 'only' a luminal Ca²⁺ buffer inside the sarcoplasmic reticulum. *Biochem J* 337 (Pt 1), 19-22.

- Szent-Gyorgyi, A.G. (1975). Calcium regulation of muscle contraction. *Biophys J* 15, 707-723.
- Tae, H.S., Cui, Y., Karunasekara, Y., Board, P.G., Dulhunty, A.F., and Casarotto, M.G. (2011). Cyclization of the intrinsically disordered alpha1S dihydropyridine receptor II-III loop enhances secondary structure and in vitro function. *J Biol Chem* 286, 22589-22599.
- Takekura, H., Bennett, L., Tanabe, T., Beam, K.G., and Franzini-Armstrong, C. (1994). Restoration of junctional tetrads in dysgenic myotubes by dihydropyridine receptor cDNA. *Biophys J* 67, 793-803.
- Takeshima, H., Nishimura, S., Matsumoto, T., Ishida, H., Kangawa, K., Minamino, N., Matsuo, H., Ueda, M., Hanaoka, M., Hirose, T., et al. (1989). Primary structure and expression from complementary DNA of skeletal muscle ryanodine receptor. *Nature* 339, 439-445.
- Tanabe, T., Beam, K.G., Powell, J.A., and Numa, S. (1988). Restoration of excitation-contraction coupling and slow calcium current in dysgenic muscle by dihydropyridine receptor complementary DNA. *Nature* 336, 134-139.
- Taske, N.L., Eyre, H.J., O'Brien, R.O., Sutherland, G.R., Denborough, M.A., and Foster, P.S. (1995). Molecular cloning of the cDNA encoding human skeletal muscle triadin and its localisation to chromosome 6q22-6q23. *European journal of biochemistry / FEBS* 233, 258-265.
- Tencerova, B., Zahradnikova, A., Gaburjakova, J., and Gaburjakova, M. (2012). Luminal Ca²⁺ controls activation of the cardiac ryanodine receptor by ATP. *The Journal of general physiology* 140, 93-108.
- Terentyev, D., Cala, S.E., Houle, T.D., Viatchenko-Karpinski, S., Gyorke, I., Terentyeva, R., Williams, S.C., and Gyorke, S. (2005). Triadin overexpression stimulates excitation-contraction coupling and increases predisposition to cellular arrhythmia in cardiac myocytes. *Circ Res* 96, 651-658.
- Terentyev, D., Nori, A., Santoro, M., Viatchenko-Karpinski, S., Kubalova, Z., Gyorke, I., Terentyeva, R., Vedamoorthyrao, S., Blom, N.A., Valle, G., et al. (2006). Abnormal interactions of calsequestrin with the ryanodine receptor calcium release channel complex linked to exercise-induced sudden cardiac death. *Circ Res* 98, 1151-1158.
- Terentyev, D., Viatchenko-Karpinski, S., Gyorke, I., Volpe, P., Williams, S.C., and Gyorke, S. (2003). Calsequestrin determines the functional size and stability of cardiac intracellular calcium stores: Mechanism for hereditary arrhythmia. *Proc Natl Acad Sci U S A* 100, 11759-11764.
- Terentyev, D., Viatchenko-Karpinski, S., Valdivia, H.H., Escobar, A.L., and Gyorke, S. (2002). Luminal Ca²⁺ controls termination and refractory behavior of Ca²⁺-induced Ca²⁺ release in cardiac myocytes. *Circ Res* 91, 414-420.
- Terentyev, D., Viatchenko-Karpinski, S., Vedamoorthyrao, S., Oduru, S., Gyorke, I., Williams, S.C., and Gyorke, S. (2007). Protein-protein interactions between triadin and calsequestrin are involved in modulation of sarcoplasmic reticulum calcium release in cardiac myocytes. *J Physiol-London* 583, 71-80.
- Thevenon, D., Smida-Rezgui, S., Chevessier, F., Groh, S., Henry-Berger, J., Beatriz Romero, N., Villaz, M., DeWaard, M., and Marty, I. (2003). Human skeletal muscle triadin: gene organization and cloning of the major isoform, Trisk 51. *Biochem Biophys Res Commun* 303, 669-675.
- Tijksens, P., Jones, L.R., and Franzini-Armstrong, C. (2003). Junctin and calsequestrin overexpression in cardiac muscle: the role of junctin and the synthetic and delivery pathways for the two proteins. *J Mol Cell Cardiol* 35, 961-974.

- Tiller, G.E., Mueller, T.J., Dockter, M.E., and Struve, W.G. (1984). Hydrogenation of Triton X-100 Eliminates Its Fluorescence and Ultraviolet-Light Absorption While Preserving Its Detergent Properties. *Analytical Biochemistry* 141, 262-266.
- Timerman, A.P., Ogunbumni, E., Freund, E., Wiederrecht, G., Marks, A.R., and Fleischer, S. (1993). The calcium release channel of sarcoplasmic reticulum is modulated by FK-506-binding protein. Dissociation and reconstitution of FKBP-12 to the calcium release channel of skeletal muscle sarcoplasmic reticulum. *J Biol Chem* 268, 22992-22999.
- Timerman, A.P., Onoue, H., Xin, H.B., Barg, S., Copello, J., Wiederrecht, G., and Fleischer, S. (1996). Selective binding of FKBP12.6 by the cardiac ryanodine receptor. *J Biol Chem* 271, 20385-20391.
- Tinker, A., Lindsay, A.R., and Williams, A.J. (1992a). Block of the sheep cardiac sarcoplasmic reticulum Ca(2+)-release channel by tetra-alkyl ammonium cations. *J Membr Biol* 127, 149-159.
- Tinker, A., Lindsay, A.R., and Williams, A.J. (1992b). A model for ionic conduction in the ryanodine receptor channel of sheep cardiac muscle sarcoplasmic reticulum. *J Gen Physiol* 100, 495-517.
- Tinker, A., and Williams, A.J. (1992). Divalent cation conduction in the ryanodine receptor channel of sheep cardiac muscle sarcoplasmic reticulum. *J Gen Physiol* 100, 479-493.
- Tinker, A., and Williams, A.J. (1993). Probing the structure of the conduction pathway of the sheep cardiac sarcoplasmic reticulum calcium-release channel with permeant and impermeant organic cations. *J Gen Physiol* 102, 1107-1129.
- Tinker, A., and Williams, A.J. (1995). Measuring the length of the pore of the sheep cardiac sarcoplasmic reticulum calcium-release channel using related trimethylammonium ions as molecular calipers. *Biophys J* 68, 111-120.
- Tomasi, M., Canato, M., Paolini, C., Dainese, M., Reggiani, C., Volpe, P., Protasi, F., and Nori, A. (2012). Calsequestrin (CASQ1) rescues function and structure of calcium release units in skeletal muscles of CASQ1-null mice. *Am J Physiol Cell Physiol* 302, C575-586.
- Towbin, H., Staehelin, T., and Gordon, J. (1979). Electrophoretic transfer of proteins from polyacrylamide gels to nitrocellulose sheets: procedure and some applications. *P Natl Acad Sci USA* 76, 4350-4354.
- Toyoshima, C., and Inesi, G. (2004). Structural basis of ion pumping by CA(2+)-ATPase of the sarcoplasmic reticulum. *Annu Rev Biochem* 73, 269-292.
- Treves, S., Feriotto, G., Moccagatta, L., Gambari, R., and Zorzato, F. (2000). Molecular cloning, expression, functional characterization, chromosomal localization, and gene structure of junctate, a novel integral calcium binding protein of sarco(endo)plasmic reticulum membrane. *The Journal of biological chemistry* 275, 39555-39568.
- Treves, S., Pouliquin, R., Moccagatta, L., and Zorzato, F. (2002). Functional properties of EGFP-tagged skeletal muscle calcium-release channel (ryanodine receptor) expressed in COS-7 cells: sensitivity to caffeine and 4-chloro-m-cresol. *Cell Calcium* 31, 1-12.
- Treves, S., Vukcevic, M., Maj, M., Thurnheer, R., Mosca, B., and Zorzato, F. (2009). Minor sarcoplasmic reticulum membrane components that modulate excitation-contraction coupling in striated muscles. *The Journal of Physiology* 587, 3071-3079.
- Tripathy, A., and Meissner, G. (1996). Sarcoplasmic reticulum lumenal Ca²⁺ has access to cytosolic activation and inactivation sites of skeletal muscle Ca²⁺ release channel. *Biophys J* 70, 2600-2615.

- Tu, Q., Velez, P., Brodwick, M., and Fill, M. (1994a). Streaming potentials reveal a short ryanodine-sensitive selectivity filter in cardiac Ca²⁺ release channel. *Biophys J* 67, 2280-2285.
- Tu, Q., Velez, P., Cortes-Gutierrez, M., and Fill, M. (1994b). Surface charge potentiates conduction through the cardiac ryanodine receptor channel. *J Gen Physiol* 103, 853-867.
- Tung, C.C., Lobo, P.A., Kimlicka, L., and Van Petegem, F. (2010). The amino-terminal disease hotspot of ryanodine receptors forms a cytoplasmic vestibule. *Nature* 468, 585-588.
- Tunwell, R.E., Wickenden, C., Bertrand, B.M., Shevchenko, V.I., Walsh, M.B., Allen, P.D., and Lai, F.A. (1996). The human cardiac muscle ryanodine receptor-calcium release channel: identification, primary structure and topological analysis. *The Biochemical journal* 318 (Pt 2), 477-487.
- Van Petegem, F. (2012). Ryanodine receptors: structure and function. *J Biol Chem* 287, 31624-31632.
- Vassilopoulos, S., Brocard, J., Garcia, L., Marty, I., and Bouron, A. (2007). Retrograde regulation of store-operated calcium channels by the ryanodine receptor-associated protein triadin 95 in rat skeletal myotubes. *Cell Calcium* 41, 179-185.
- Vassilopoulos, S., Oddoux, S., Groh, S., Cacheux, M., Faure, J., Brocard, J., Campbell, K.P., and Marty, I. (2010). Caveolin 3 is associated with the calcium release complex and is modified via in vivo triadin modification. *Biochemistry* 49, 6130-6135.
- Vassilopoulos, S., Thevenon, D., Rezgui, S.S., Brocard, J., Chapel, A., Lacampagne, A., Lunardi, J., Dewaard, M., and Marty, I. (2005). Triadins are not triad-specific proteins: two new skeletal muscle triadins possibly involved in the architecture of sarcoplasmic reticulum. *J Biol Chem* 280, 28601-28609.
- Vetter, R., Studer, R., Reinecke, H., Kolar, F., Ostadalova, I., and Drexler, H. (1995). Reciprocal changes in the postnatal expression of the sarcolemmal Na⁺-Ca²⁺-exchanger and SERCA2 in rat heart. *J Mol Cell Cardiol* 27, 1689-1701.
- Volpe, P., Alderson-Lang, B.H., Madeddu, L., Damiani, E., Collins, J.H., and Margreth, A. (1990). Calsequestrin, a component of the inositol 1,4,5-trisphosphate-sensitive Ca²⁺ store of chicken cerebellum. *Neuron* 5, 713-721.
- Volpe, P., Martini, A., Furlan, S., and Meldolesi, J. (1994). Calsequestrin is a component of smooth muscles: the skeletal- and cardiac-muscle isoforms are both present, although in highly variable amounts and ratios. *Biochem J* 301 (Pt 2), 465-469.
- Vukcevic, M., Broman, M., Islander, G., Bodelsson, M., Ranklev-Twetman, E., Muller, C.R., and Treves, S. (2010). Functional properties of RYR1 mutations identified in Swedish patients with malignant hyperthermia and central core disease. *Anesthesia and analgesia* 111, 185-190.
- Wagenknecht, T., Grassucci, R., Frank, J., Saito, A., Inui, M., and Fleischer, S. (1989). Three-dimensional architecture of the calcium channel/foot structure of sarcoplasmic reticulum. *Nature* 338, 167-170.
- Wagenknecht, T., and Radermacher, M. (1995). Three-dimensional architecture of the skeletal muscle ryanodine receptor. *FEBS letters* 369, 43-46.
- Wagenknecht, T., and Radermacher, M. (1997). Ryanodine receptors: structure and macromolecular interactions. *Current opinion in structural biology* 7, 258-265.
- Wagenknecht, T., and Samso, M. (2002). Three-dimensional reconstruction of ryanodine receptors. *Frontiers in bioscience : a journal and virtual library* 7, d1464-1474.

- Wang, J.P., Needleman, D.H., Seryshev, A.B., Aghdasi, B., Slavik, K.J., Liu, S.Q., Pedersen, S.E., and Hamilton, S.L. (1996). Interaction between ryanodine and neomycin binding sites on Ca²⁺ release channel from skeletal muscle sarcoplasmic reticulum. *J Biol Chem* 271, 8387-8393.
- Wang, S., Trumble, W.R., Liao, H., Wesson, C.R., Dunker, A.K., and Kang, C.H. (1998). Crystal structure of calsequestrin from rabbit skeletal muscle sarcoplasmic reticulum. *Nat Struct Biol* 5, 476-483.
- Wang, W., Cleemann, L., Jones, L.R., and Morad, M. (2000). Modulation of focal and global Ca²⁺ release in calsequestrin-overexpressing mouse cardiomyocytes. *The Journal of Physiology* 524 Pt 2, 399-414.
- Wang, Y., Li, X., Duan, H., Fulton, T.R., Eu, J.P., and Meissner, G. (2009). Altered stored calcium release in skeletal myotubes deficient of triadin and junctin. *Cell Calcium* 45, 29-37.
- Wang, Y., Xu, L., Duan, H., Pasek, D.A., Eu, J.P., and Meissner, G. (2006). Knocking down type 2 but not type 1 calsequestrin reduces calcium sequestration and release in C2C12 skeletal muscle myotubes. *J Biol Chem* 281, 15572-15581.
- Wehrens, X.H., Lehnart, S.E., Huang, F., Vest, J.A., Reiken, S.R., Mohler, P.J., Sun, J., Guatimosim, S., Song, L.S., Rosembly, N., et al. (2003). FKBP12.6 deficiency and defective calcium release channel (ryanodine receptor) function linked to exercise-induced sudden cardiac death. *Cell* 113, 829-840.
- Wei, L. (2008). How calsequestrin governs the intracellular calcium store of skeletal muscle. In John Curtin School of Medical Research (the Australian National University).
- Wei, L., Abdellatif, Y.A., Liu, D., Kimura, T., Coggan, M., Gallant, E.M., Beard, N.A., Board, P.G., and Dulhunty, A.F. (2008). Muscle-specific GSTM2-2 on the luminal side of the sarcoplasmic reticulum modifies RyR ion channel activity. *Int J Biochem Cell Biol* 40, 1616-1628.
- Wei, L., Gallant, E.M., Dulhunty, A.F., and Beard, N.A. (2009a). Junctin and triadin each activate skeletal ryanodine receptors but junctin alone mediates functional interactions with calsequestrin. *International Journal of Biochemistry & Cell Biology* 41, 2214-2224.
- Wei, L., Hanna, A.D., Beard, N.A., and Dulhunty, A.F. (2009b). Unique isoform-specific properties of calsequestrin in the heart and skeletal muscle. *Cell Calcium* 45, 474-484.
- Wei, L., Varsanyi, M., Dulhunty, A.F., and Beard, N.A. (2006). The conformation of calsequestrin determines its ability to regulate skeletal ryanodine receptors. *Biophys J* 91, 1288-1301.
- Welch, W., Rheault, S., West, D.J., and Williams, A.J. (2004). A model of the putative pore region of the cardiac ryanodine receptor channel. *Biophysical Journal* 87, 2335-2351.
- West, R.W., Jr., Kruger, B., Thomas, S., Ma, J., and Milgrom, E. (2000). RLR1 (THO2), required for expressing lacZ fusions in yeast, is conserved from yeast to humans and is a suppressor of SIN4. *Gene* 243, 195-205.
- Wetzel, G.T., Ding, S., and Chen, F. (2000). Molecular cloning of junctin from human and developing rabbit heart. *Mol Genet Metab* 69, 252-258.
- Williams, A.J. (1992). Ion conduction and discrimination in the sarcoplasmic reticulum ryanodine receptor/calcium-release channel. *J Muscle Res Cell Motil* 13, 7-26.
- Williams, A.J., West, D.J., and Sitsapesan, R. (2001). Light at the end of the Ca²⁺-release channel tunnel: structures and mechanisms involved in ion translocation in ryanodine receptor channels. *Quarterly Reviews of Biophysics* 34, 61-104.

- Wium, E., Dulhunty, A.F., and Beard, N.A. (2012). A skeletal muscle ryanodine receptor interaction domain in triadin. *PLoS One* 7, e43817.
- Xiao, R.P., Valdivia, H.H., Bogdanov, K., Valdivia, C., Lakatta, E.G., and Cheng, H. (1997). The immunophilin FK506-binding protein modulates Ca²⁺ release channel closure in rat heart. *J Physiol* 500 (Pt 2), 343-354.
- Xu, L., Mann, G., and Meissner, G. (1996a). Regulation of cardiac Ca²⁺ release channel (ryanodine receptor) by Ca²⁺, H⁺, Mg²⁺, and adenine nucleotides under normal and simulated ischemic conditions. *Circulation Research* 79, 1100-1109.
- Xu, L., Mann, G., and Meissner, G. (1996b). Regulation of cardiac SR Ca²⁺ release channel by luminal and cytosolic Ca²⁺ and pH. *Biophysical Journal* 70, Tup32-Tup32.
- Xu, L., and Meissner, G. (1998). Regulation of cardiac muscle Ca²⁺ release channel by sarcoplasmic reticulum luminal Ca²⁺. *Biophys J* 75, 2302-2312.
- Xu, L., Tripathy, A., Pasek, D.A., and Meissner, G. (1999). Ruthenium red modifies the cardiac and skeletal muscle Ca(2+) release channels (ryanodine receptors) by multiple mechanisms. *The Journal of biological chemistry* 274, 32680-32691.
- Yamaguchi, N., Kagari, T., and Kasai, M. (1999). Inhibition of the ryanodine receptor calcium channel in the sarcoplasmic reticulum of skeletal muscle by an ADP/ATP translocase inhibitor, atractyloside. *Biochem Biophys Res Commun* 258, 247-251.
- Yamaguchi, N., and Kasai, M. (1998). Identification of 30 kDa calsequestrin-binding protein, which regulates calcium release from sarcoplasmic reticulum of rabbit skeletal muscle. *Biochemical Journal* 335, 541-547.
- Yazaki, P.J., Salvatori, S., Sabbadini, R.A., and Dahms, A.S. (1990). Calsequestrin, an intracellular calcium-binding protein of skeletal muscle sarcoplasmic reticulum, is homologous to aspartactin, a putative laminin-binding protein of the extracellular matrix. *Biochem Biophys Res Commun* 166, 898-903.
- Yildirim, S.S., Akman, D., Catalucci, D., and Turan, B. (2013). Relationship Between Downregulation of miRNAs and Increase of Oxidative Stress in the Development of Diabetic Cardiac Dysfunction: Junctin as a Target Protein of miR-1. *Cell Biochem Biophys*.
- Yin, J.C., Li, G.X., Ren, X.F., and Herrler, G. (2007). Select what you need: A comparative evaluation of the advantages and limitations of frequently used expression systems for foreign genes. *J Biotechnol* 127, 335-347.
- Yuan, Q., Fan, G.C., Dong, M., Altschaf, B., Diwan, A., Ren, X., Hahn, H.H., Zhao, W., Waggoner, J.R., Jones, L.R., et al. (2007). Sarcoplasmic reticulum calcium overloading in junctin deficiency enhances cardiac contractility but increases ventricular automaticity. *Circulation* 115, 300-309.
- Yuan, Q., Han, P., Dong, M., Ren, X., Zhou, X., Chen, S., Jones, W.K., Chu, G., Wang, H.S., and Kranias, E.G. (2009). Partial downregulation of junctin enhances cardiac calcium cycling without eliciting ventricular arrhythmias in mice. *Am J Physiol Heart Circ Physiol* 296, H1484-1490.
- Zhang, J., Liu, Z., Masumiya, H., Wang, R., Jiang, D., Li, F., Wagenknecht, T., and Chen, S.R. (2003). Three-dimensional localization of divergent region 3 of the ryanodine receptor to the clamp-shaped structures adjacent to the FKBP binding sites. *The Journal of biological chemistry* 278, 14211-14218.
- Zhang, L., Franzini-Armstrong, C., Ramesh, V., and Jones, L.R. (2001). Structural alterations in cardiac calcium release units resulting from overexpression of junctin. *J Mol Cell Cardiol* 33, 233-247.

- Zhang, L., Kelley, J., Schmeisser, G., Kobayashi, Y.M., and Jones, L.R. (1997). Complex formation between junctin, triadin, calsequestrin, and the ryanodine receptor. Proteins of the cardiac junctional sarcoplasmic reticulum membrane. *J Biol Chem* 272, 23389-23397.
- Zhao, M., Li, P., Li, X., Zhang, L., Winkfein, R.J., and Chen, S.R. (1999). Molecular identification of the ryanodine receptor pore-forming segment. *The Journal of biological chemistry* 274, 25971-25974.
- Zhao, X., Min, C.K., Ko, J.K., Parness, J., Kim do, H., Weisleder, N., and Ma, J. (2010). Increased store-operated Ca^{2+} entry in skeletal muscle with reduced calsequestrin-1 expression. *Biophys J* 99, 1556-1564.
- Zimanyi, I., and Pessah, I.N. (1991). Comparison of [3H]ryanodine receptors and Ca^{++} release from rat cardiac and rabbit skeletal muscle sarcoplasmic reticulum. *J Pharmacol Exp Ther* 256, 938-946.
- Zissimopoulos, S., and Lai, F.A. (2007). Ryanodine receptor structure, function and pathophysiology. In *Calcium: a matter of life or death*, J. Krebs, and M. Michalak, eds. (Elsevier), pp. 287-342.
- Zorzato F, F.J., Otsu K, Phillips M, Green NM, Lai FA, Meissner G, MacLennan DH (1990). Molecular cloning of cDNA encoding human and rabbit forms of the Ca^{2+} release channel (ryanodine receptor) of skeletal muscle sarcoplasmic reticulum. *Journal of Biological Chemistry* 265, 2244-2256.
- Zorzato, F., Fujii, J., Otsu, K., Phillips, M., Green, N.M., Lai, F.A., Meissner, G., and MacLennan, D.H. (1990). Molecular cloning of cDNA encoding human and rabbit forms of the Ca^{2+} release channel (ryanodine receptor) of skeletal muscle sarcoplasmic reticulum. *The Journal of biological chemistry* 265, 2244-2256.
- Zucchi, R., and Ronca-Testoni, S. (1997). The sarcoplasmic reticulum Ca^{2+} channel/ryanodine receptor: modulation by endogenous effectors, drugs and disease states. *Pharmacol Rev* 49, 1-51.